

Dissertation

Metallosupramolecular complexes with *d*-block metals
as highly effective and selective catalytic systems

Kompleksy metalosupramolekularne z metalami *d*-elektronowymi
jako wysoce efektywne i selektywne systemy katalityczne

M.Sc. Gracjan Kurpik

Supervision: Prof. dr hab. Artur R. Stefankiewicz



The work was carried out in the Laboratory of Functional Nanostructures
Center for Advanced Technologies/Faculty of Chemistry
Adam Mickiewicz University in Poznań.

The doctoral dissertation is presented as a series of thematically coherent scientific articles,
published in peer-reviewed journals within the field of Science, specifically in the discipline of
Chemical Science.

Poznań, 2024

„I've always believed that if you put in the work, the results will come. I don't do things half-heartedly. Because I know if I do, then I can expect half-hearted results.”

Michael Jordan

Acknowledgements

First and foremost, I would like to express my deepest gratitude to my supervisor – **Professor Artur Stefankiewicz**, who opened doors for me to opportunities that I had never even dreamed of. It was he who, during the laboratory classes in 2015, noticed the potential in a young and insecure student. Since then, I have started my journey full of challenges, discoveries, and development. I am grateful for every expression of trust he has placed in me, for his boundless faith in my abilities, and for introducing me to the fascinating world of science, where each step has been not only a lesson but also an inspiration for further self-improvement.

I would like to thank **the entire team of the Laboratory of Functional Nanostructures** – Ania, Wojtek, Grzegorz, Filip, Wiktoria, Weronika, Ada, Agnieszka, Mateusz, Igor, Zuzia, Venky, Sidharth, as well as its former members. Thank you all for years of fruitful collaboration, immense support, and the great atmosphere in the lab.

I would like to thank **Dr. Paweł Dydio** from the University of Cambridge for the opportunity to collaborate on my recent project. It was both a considerable challenge and an extremely rewarding experience. I also extend my gratitude to **Prof. Marc Taillefer** and **Prof. Florian Monnier** from the Institute Charles Gerhardt Montpellier for their supervision during my research internship.

Thank you to everyone I have met along this scientific journey who has helped me to become not only a better chemist but also a better person. I appreciate every collaboration, as each one has been a valuable lesson for me.

I would also like to thank my family and friends for being with me throughout this time.

The research presented in this thesis was supported by funds from the National Science Centre:

- grant SONATA BIS no. 2018/30/E/ST5/00032,
- grant PRELUDIUM no. 2022/45/N/ST4/00518,

and by „The Excellence Initiative – Research University” program – grant no. 017/02/SNŚ/0006.

The research was conducted using the infrastructure available at the Center for Advanced Technologies in Poznań.



NATIONAL SCIENCE CENTRE
POLAND



Table of contents

Résumé	11
Abstract	17
Streszczenie.....	18
1. Introduction.....	19
1.1. Ligands.....	19
1.1.1. β -Diketonate ligands	19
1.1.2. Pyridine ligands.....	21
1.1.3. Pyridyl- β -diketonate ligands.....	23
1.2. Nanostructures based on pyridyl- β -diketones.....	26
1.2.1. Mono- and polynuclear complexes.....	26
1.2.2. Metallocycles	27
1.2.3. Metallocages	27
1.2.4. Coordination polymers and MOFs.....	28
1.3. Application potential of the coordination architectures based on pyridyl- β -diketones	30
1.3.1. Catalysis	30
1.3.2. Host-guest chemistry and sensing	31
1.3.3. Magnetism	32
1.3.4. Energy transfer	32
2. Research objectives.....	33
3. Discussion of the research.....	35
PUBLICATION A1	35
PUBLICATION A2	39
PUBLICATION A3	45
PUBLICATION A4	50
PUBLICATION A5	53
PUBLICATION A6	58
4. Summary.....	64
References	66

Reprints of publications.....	73
PUBLICATION A1.....	74
PUBLICATION A2.....	81
PUBLICATION A3.....	92
PUBLICATION A4.....	100
PUBLICATION A5.....	107
PUBLICATION A6.....	114
Declaration letters of co-authors.....	124

Personal data

Name and surname Gracjan Kurpik
Date of birth 20th August 1995
Place of birth Września

Education

since 10/2019 Doctoral School of Exact Sciences, Adam Mickiewicz University
PhD Studies, Chemical Sciences

2017 – 2019 Faculty of Chemistry, Adam Mickiewicz University
Master's Studies, General Chemistry
Highly efficient Cu^I catalyst system based on ambidentate ligands in amination reaction of aryl halides
Supervision: Prof. dr hab. Artur R. Stefankiewicz

2014 – 2017 Faculty of Chemistry, Adam Mickiewicz University
Bachelor's Studies, General Chemistry
Synthesis of novel metallosupramolecular polymers with Cu^{II} ions
Supervision: Prof. dr hab. Artur R. Stefankiewicz

The list of published articles

- 1) L. Pagès, [#] **G. Kurpik**,[#] R. Mollfulleda, R. A. A. Abdine, A. Walczak, F. Monnier, M. Swart, A. R. Stefankiewicz, M. Taillefer
Copper-catalyzed synthesis of (E)-allylic organophosphorus derivatives: a low toxic, mild, economical, and ligand-free method
ChemSusChem **2024**, e202401450; DOI: 10.1002/cssc.202401450
IF = 7.500; 95th percentile
- 2) **G. Kurpik**, A. Walczak, P. Dydio, A. R. Stefankiewicz
Multi-stimuli-responsive network of multicatalytic reactions using a single palladium/platinum catalyst
Angewandte Chemie International Edition **2024**, *63*, e202404684; DOI: 10.1002/anie.202404684
IF = 16.600; 96th percentile

- 3) **G. Kurpik**, A. Walczak, I. Łukasik, Z. Matela, A. R. Stefankiewicz
Crafting versatile modes of Pt^I complexes with flexidentate pyridyl-β-diketones: synthesis, structural characterization, and catalytic behavior in olefin hydrosilylation
 ChemCatChem **2023**, *16*, e202301465; DOI: 10.1002/cctc.202301465
 IF = 4.500; 92nd percentile

- 4) **G. Kurpik**, A. Walczak, G. Markiewicz, J. Harrowfield, A. R. Stefankiewicz
Enhanced catalytic performance derived from coordination-driven structural switching between homometallic complexes and heterometallic polymeric materials
 Nanoscale **2023**, *15*, 9543–9550; DOI: 10.1039/D3NR01298K
 IF = 7.300; 90th percentile

- 5) **G. Kurpik**, A. Walczak, M. Goldyn, J. Harrowfield, A. R. Stefankiewicz
Pd^I complexes with pyridine ligands: substituent effects on the NMR Data, crystal structures, and catalytic activity
 Inorganic Chemistry **2022**, *61*, 14019–14029; DOI: 10.1021/acs.inorgchem.2c01996
 IF = 4.600; 89th percentile

- 6) **G. Kurpik**, A. Walczak, M. Gilski, J. Harrowfield, A. R. Stefankiewicz
Effect of the nuclearity on the catalytic performance of a series of Pd^I complexes in the Suzuki-Miyaura reaction
 Journal of Catalysis **2022**, *411*, 193–199; DOI: 10.1016/j.jcat.2022.05.021
 IF = 7.300; 93rd percentile

- 7) A. Walczak, **G. Kurpik**, M. Zaranek, P. Pawluć, A. R. Stefankiewicz
C(sp³),N palladacyclic complexes bearing flexidentate ligands as efficient (pre)catalysts for Heck olefination of aryl halides
 Journal of Catalysis **2022**, *405*, 84–90; DOI: 10.1016/j.jcat.2021.11.033
 IF = 7.300; 93rd percentile

- 8) M. Kołodziejski, A. J. Brock, **G. Kurpik**, A. Walczak, F. Li, J. K. Clegg, A. R. Stefankiewicz
Charge neutral [Cu₂L₂] and [Pd₂L₂] metallocycles: self-assembly, aggregation, and catalysis
 Inorganic Chemistry **2021**, *60*, 9673–9679; DOI: 10.1021/acs.inorgchem.1c00967
 IF = 5.436; 89th percentile

- 9) A. Walczak,[#] **G. Kurpik**,[#] A. R. Stefankiewicz
Intrinsic effect of pyridine-N-position on structural properties of Cu-based low-dimensional coordination frameworks
 International Journal of Molecular Sciences **2020**, *21*, 6171; DOI: 10.3390/ijms21176171
 IF = 5.924; 90th percentile

- 10) R. A. A. Abdine, **G. Kurpiak**, A. Walczak, S. A. A. Aesh, A. R. Stefankiewicz, F. Monnier, M. Taillefer
Mild temperature amination of aryl iodides and aryl bromides with aqueous ammonia in the presence of CuBr and pyridyldiketone ligands
 Journal of Catalysis **2019**, 376, 119–122; DOI: 10.1016/j.jcat.2019.06.020
 IF = 7.888; 93rd percentile
- 11) A. Walczak, H. Stachowiak, **G. Kurpiak**, J. Kaźmierczak, G. Hreczycho, A. R. Stefankiewicz
High catalytic activity and selectivity in hydrosilylation of new Pt^{II} metallocupramolecular complexes based on ambidentate ligands
 Journal of Catalysis **2019**, 373, 139–146; DOI: 10.1016/j.jcat.2019.03.041
 IF = 7.888; 93rd percentile

These authors contributed equally to the work.

Impact factor (IF) from the year of publishing; source: *Journal Citation Reports*.

Contribution to scientific grants

- 1) Principal Investigator in: PRELUDIUM no. 2022/45/N/ST4/00518
Metallocupramolecular architectures based on flexidentate pyridyl- β -diketonate ligands – synthesis, properties, and catalytic applications
 Funding: National Science Centre
- 2) Principal Investigator in: Minigrant for PhD students no. 017/02/SNŚ/0006
Topology vs. catalytic activity – synthesis, physico-chemical properties, and functions of metallocupramolecular complexes based on d-block metals
 Funding: The Excellence Initiative – Research University (IDUB)
- 3) Investigator in: SONATA BIS no. 2018/30/E/ST5/00032
Self-assembled porous capsules as multifunctional nanomaterials
 Funding: National Science Centre
 Principal Investigator: Prof. dr hab. Artur R. Stefankiewicz
- 4) Investigator in: LIDER no. 024/391/L-5/13/NCBR/2014
Synthesis, physicochemical properties, and application of dynamic metal-organic framework materials
 Funding: National Centre for Research and Development
 Principal Investigator: Prof. dr hab. Artur R. Stefankiewicz

Internships

- 1) Institute Charles Gerhardt, Montpellier (France); February 2022 – April 2022 (3 months)
Copper-catalyzed hydrophosphorylation reaction of N-allenyl derivatives
Supervision: Prof. Marc Taillefer
- 2) Institute of Bioorganic Chemistry, Polish Academy of Sciences, Poznań (Poland); July 2019 – August 2019 (2 months)
Structural studies of oligonucleotides using NMR methods
Supervision: Prof. dr hab. Zofia Gdaniec
- 3) École Nationale Supérieure de Chimie, Montpellier (France); September 2018 – October 2018 (2 months)
Amination of aryl halides with aqueous ammonia catalyzed by copper/pyridyldiketone systems
Supervision: Prof. Florian Monnier

The list of international conferences

Oral communications

- 1) **G. Kurpik**, A. R. Stefankiewicz
Stimuli-responsive supramolecular transformations between homometallic complexes and heterometallic polymeric materials
2nd French-Polish Chemistry Congress, 28-31 August 2023, Montpellier (France)
- 2) **G. Kurpik**, A. R. Stefankiewicz
Metallosupramolecular assemblies – from simple complexes to functional nanostructures
„Solutions in Chemistry” Conference, 8-11 November 2022, Sveti Martin na Muri (Croatia)

Poster presentations

- 1) **G. Kurpik**, A. R. Stefankiewicz
Unlocking the potential of pyridyl- β -diketonate ligands for constructing functional coordination nanostructures with applications in catalysis
17th International Seminar on Inclusion Compounds and Porous Materials, 2-6 September 2024, Poznań (Poland)
- 2) **G. Kurpik**, A. R. Stefankiewicz
Unlocking the potential of pyridyl- β -diketonate ligands for constructing sophisticated coordination nanostructures with prospective applications
18th International Symposium on Macrocyclic and Supramolecular Chemistry, 6-10 May 2024, Hangzhou (China)

- 3) **G. Kurpiak**, A. Walczak, G. Markiewicz, J. Harrowfield, A. R. Stefankiewicz
Enhanced catalytic performance derived from stimuli-responsive supramolecular transformations between homometallic complexes and heterometallic polymeric materials
SupraChem 2024, 25-27 February 2024, Ulm (Germany)
- 4) **G. Kurpiak**, A. Walczak, G. Markiewicz, J. Harrowfield, A. R. Stefankiewicz
Coordination-driven switching from simple complexes to functional nanostructures
49th IUPAC World Chemistry Congress, 20-25 August 2023, Hague (Netherlands)
- 5) **G. Kurpiak**, A. Walczak, G. Markiewicz, J. Harrowfield, A. R. Stefankiewicz
Coordination-driven structural switching from simple Ag^I, Pd^{II}, and Pt^{II} complexes to functional heterometallic nanomaterials
17th International Symposium on Macrocyclic and Supramolecular Chemistry, 25-29 June 2023, Reykjavik (Iceland)
- 6) **G. Kurpiak**, A. Walczak, G. Markiewicz, J. Harrowfield, A. R. Stefankiewicz
Coordination-driven structural switching from simple Ag^I, Pd^{II}, and Pt^{II} complexes to heterometallic polymeric materials
44th International Conference on Coordination Chemistry, 28 August – 2 September 2022, Rimini (Italy)
- 7) **G. Kurpiak**, A. Walczak, M. Gilski, J. Harrowfield, A. R. Stefankiewicz
The effects of the local concentration and distribution of Pd-centres on the catalytic activity in Suzuki-Miyaura reaction
19th International Symposium on Novel Aromatic Compounds, 3-8 July 2022, Warsaw (Poland)
- 8) **G. Kurpiak**, A. Walczak, M. Gilski, J. Harrowfield, A. R. Stefankiewicz
The effects of the local concentration and distribution of Pd-centres on the catalytic activity in Suzuki-Miyaura reaction
22nd Tetrahedron Symposium 2022, 28 June – 1 July 2022, Lisbon (Portugal)
- 9) **G. Kurpiak**, A. Walczak, M. Gilski, J. Harrowfield, A. R. Stefankiewicz
Effect of the nuclearity on the catalytic performance of a series of Pd^{II} complexes in the Suzuki-Miyaura reaction
12th NanoTech Poland 2022, 1-3 June 2022, Poznań (Poland)
- 10) **G. Kurpiak**, A. Walczak, R. A. A. Abdine, S. A. A. Aesh, F. Monnier, M. Taillefer, A. R. Stefankiewicz
Highly efficient Cu^I catalyst system based on ambidentate ligands in amination reaction of aryl halides
French-Polish Chemistry Congress, 4-6 July 2019, Paris (France)

Awards

- 1) Scholarship of the Adam Mickiewicz University Foundation (FUAM) for the academic year 2023/2024
- 2) Rector's scholarship for PhD students for outstanding publication achievements (2022)
- 3) Rector's team award of 1st degree for exceptional scientific achievements (2020)
- 4) Laureate of 8 competitions organized within „The Excellence Initiative – Research University” program (2021-2024)
- 5) *Maxima Cum Laude Diploma* – Dean's award for the best graduates (2019)

Abstract

Metallosupramolecular complexes, owing to their fascinating coordination geometries, diverse topologies, unique physicochemical properties, and remarkable versatility, have long been the subject of intensive research and significant interest within the scientific community. Such systems, examined within a broader context, have exhibited a wide range of applications, contributing to ongoing advancements in the domain of coordination and metallosupramolecular chemistry. With the fundamentals of rational design and the established strategies for the synthesis of coordination architectures with tailored properties, the prospects for generating novel nanomaterials with specific functionalities remain wide open. This dissertation presents the characterization of three classes of building blocks utilized in the construction of coordination assemblies, namely β -diketonate and pyridine ligands, as well as ambidentate pyridyl- β -diketonates, which incorporate two distinct donor groups within their structures. The structural diversity of these ligands, combined with multiple metal centers, has led to the creation of a variety of coordination architectures with exceptional physicochemical properties. Through insights from recent advances, the avenues for harnessing these nanostructures as functional materials have been discussed, emphasizing their extensive applicability across different areas, such as catalysis, host-guest chemistry, sensing, magnetism, and energy transfer. Nevertheless, despite promising perspectives, this potential remains largely unexplored in many cases.

Hence, in the experimental section of this work, a new generation of metallosupramolecular complexes is presented, obtained using the aforementioned ligands and selected *d*-electron metal ions, specifically Ag^I, Pd^{II}, and Pt^{II}. A series of thematically coherent articles (**A1–A6**) details the design, synthesis, spectro-structural characterization, and functionality of these systems, *i.e.*, mono- and polynuclear complexes as well as heterometallic coordination polymers. The structures of all obtained compounds were precisely determined both in solution and in the solid state *via* various analytical techniques. Due to their intrinsic structural characteristics and functional capabilities, these assemblies were employed as effective and selective catalyst precursors in a range of organic transformations, including cross-couplings, substitutions, hydroadditions, and reductions. Furthermore, extensive investigations allowed for the identification of structural factors, such as the coordination mode of the central ions, the nuclearity of the complexes, the nature of pyridine ring substituents, and the complex topology, which enabled the determination of their impact on catalytic performance in specific processes and the enhancement of the catalytic activity of the given assemblies. Thus, it has been demonstrated that the ligand structure plays a key role not only in defining the overall topology of the coordination architecture but also affects physicochemical properties, thereby tailoring the resulting functionality.

Streszczenie

Kompleksy metalosupramolekularne, ze względu na imponującą różnorodność geometrii koordynacyjnych, fascynujące topologie, wyjątkowe właściwości fizykochemiczne oraz niezwykłą wszechstronność, od lat stanowią obiekt intensywnych badań i zainteresowania w środowisku naukowym. W szerszym kontekście układy te wykazały bogatą gamę zastosowań, napędzając ciągle postęp w chemii koordynacyjnej i metalosupramolekularnej. Dzięki podstawom racjonalnego projektowania i opracowanym strategiom syntezy złożonych architektur koordynacyjnych, perspektywy rozwoju innowacyjnych nanomateriałów o określonej funkcjonalności pozostają szeroko otwarte. Niniejsza rozprawa doktorska prezentuje charakterystykę trzech klas bloków budulcowych, które znalazły zastosowania w konstrukcji układów koordynacyjnych, a mianowicie ligandów β -diketonowych i pirydynowych, a także ambidentnych pirydylo- β -diketonów, zawierających w swojej strukturze dwie grupy donorowe o odmiennej naturze. Zróżnicowanie strukturalne tych ligandów organicznych, w zestawieniu z licznymi centrami metalicznymi, doprowadziło do syntezy rozmaitych architektur koordynacyjnych o nadzwyczajnych właściwościach. Analizując najnowsze doniesienia literaturowe, przedstawiono możliwości wszechstronnego wykorzystania tych materiałów, podkreślając ich potencjał aplikacyjny w takich obszarach jak kataliza, chemia gość-gospodarz, magnetyzm i transfer energii. Niemniej jednak, mimo obiecujących perspektyw, ten potencjał wciąż pozostaje w wielu przypadkach znacząco niewykorzystany.

W części eksperymentalnej niniejszej pracy zaprezentowano nową generację kompleksów metalosupramolekularnych, otrzymanych z wykorzystaniem wyżej wymienionych ligandów oraz wyselekcjonowanych jonów metali *d*-elektronowych (Ag^{I} , Pd^{II} , Pt^{II}). Seria tematycznie spójnych artykułów naukowych (**A1–A6**) szczegółowo opisuje projektowanie, syntezę, charakterystykę strukturalno-spektroskopową oraz funkcjonalność tych układów, *tj.* mono- i polinuklearnych związków kompleksowych, jak również heterometalicznych polimerów koordynacyjnych. Struktury uzyskanych związków zostały precyzyjnie określone zarówno w roztworze, jak i w ciele stałym przy użyciu różnych technik analitycznych. Ze względu na unikalne cechy strukturalne, wskazujące na ich znaczny potencjał aplikacyjny, otrzymane związki kompleksowe zostały zastosowane jako efektywne i selektywne katalizatory w szeregu reakcji organicznych, *m.in.* reakcji sprzęgania krzyżowego, substytucji, hydroaddycji i redukcji. Ponadto szeroko zakrojone badania pozwoliły na identyfikację czynników strukturalnych, takich jak tryb koordynacji jonu centralnego, liczba centrów metalicznych, natura podstawników pierścienia pirydynowego oraz topologia układu, które umożliwiły określenie ich wpływu na przebieg odpowiednich procesów katalitycznych i zwiększenie aktywności katalitycznej danych jednostek. W związku z tym wykazano, że struktura liganda definiuje nie tylko geometrię architektury koordynacyjnej, ale także wpływa na jej właściwości fizykochemiczne, a tym samym w istotny sposób determinuje jej funkcjonalność.

1. Introduction

Over the past few decades, substantial progress has been achieved in the design and synthesis of diverse coordination architectures with unique physicochemical properties.¹⁻⁶ The precise selection of organic ligands, combined with metal centers that exhibit defined coordination behavior enables the generation of complex systems with encoded structural features, such as tailored geometries, internal cavities, or flexible frameworks.^{7,8} Attributed to their well-defined structure and versatile functionalities, these architectures have attracted increasing attention in different areas, including catalysis, molecular recognition, host-guest chemistry, separation and magnetism, among others.^{3,9-15} The introduction section of this dissertation is intended to be a compendium of various organic ligands utilized as building blocks in the generation of diverse coordination assemblies. The discussion will focus on three types of organic ligands: β -diketonate and pyridine ligands, as well as ambidentate pyridyl- β -diketonates, which combine the characteristics of the former two. Since pyridyl- β -diketonates are a particular subject of interest in this thesis, an array of coordination architectures formed with them will be described in detail. Owing to their inherent structural features and functional capabilities,¹⁶ these complex systems are viable candidates for applications spanning different scientific domains, which will be presented in the final section of this introduction.

1.1. Ligands

1.1.1. β -Diketonate ligands

β -Diketonate compounds, with pentane-2,4-dione (commonly known as acetylacetone) as the simplest and most recognized example, represent a significant class of organic ligands extensively utilized in coordination and metallocsupramolecular chemistry for the construction of complex molecular architectures.¹⁷⁻²⁰ Such units are typically synthesized *via* Claisen condensation between appropriate ketones and esters, resulting in a product containing two carbonyl groups separated by a single carbon atom.²¹⁻²³ A characteristic feature of these compounds is keto-enol tautomerism, which refers to the equilibrium between their keto and enol forms (Figure 1).^{24,25} In the case of β -diketones, the equilibrium is significantly shifted toward the enol form, primarily due to the formation of an OH \cdots O hydrogen bond, which stabilizes a resonance structure with a six-

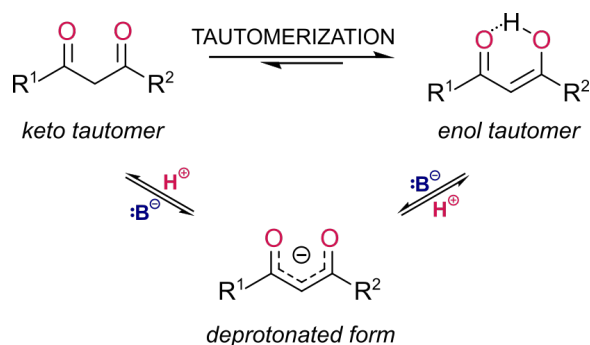


Figure 1. Keto-enol tautomerism in β -diketonate ligands.

membered ring.²⁶ Various factors can affect this keto-enol equilibrium, with solvent polarity, as well as the presence and nature of functional groups within the ligand structure being particularly influential.²⁷ For instance, the percentage of enol form in acetylacetone and hexafluoroacetylacetone is 85% and 100%, respectively, when measured neat at 33 °C.²⁸

The capacity to form stable coordination compounds with a diverse array of metal ions is directly attributed to the presence of β -diketonate ligands in their enol form. According to hard and soft acids and bases (HSAB) theory,^{29, 30} such ligands act as hard bases in complexation reactions, preferentially forming stable complexes with hard acids, *e.g.*, Mg^{II} , Fe^{III} , Al^{III} , Co^{III} , Cr^{III} ;³¹⁻³⁴ however, numerous combinations with metal ions classified as soft acids have also been reported.³⁵⁻³⁷ In a neutral environment or upon deprotonation under basic conditions, these ligands enable the coordination of metal centers as O,O' -chelates, resulting in the formation of six-membered rings (Figure 2a).³⁸⁻⁴⁰ Additionally, β -diketonates are highly effective bridging ligands.³⁸ Their ability to bridge metal ions arises from the use of only one lone pair of electrons *per* oxygen atom for primary bonding, with the remaining lone pairs available for secondary interactions. Consequently, oligomeric complexes can be generated, such as $[\text{Ni}(\text{acac})_2]_3$ and $[\text{Ba}_4(\text{tmhd})_8]$,^{41, 42} where acac and tmhd refer to acetylacetonate and 2,2,6,6-tetramethylheptane-3,5-dionate, respectively (Figure 2d). Furthermore, β -diketonate anions can also coordinate metal ions through the central carbon atom, leading to the generation of organometallic compounds (Figure 2c). Although this type of interaction is relatively rare with lighter metals, it is more common with metal ions from the second-row and especially third-row transition metals, *e.g.*, Pt^{II} and Ir^{III} .⁴³⁻⁴⁵

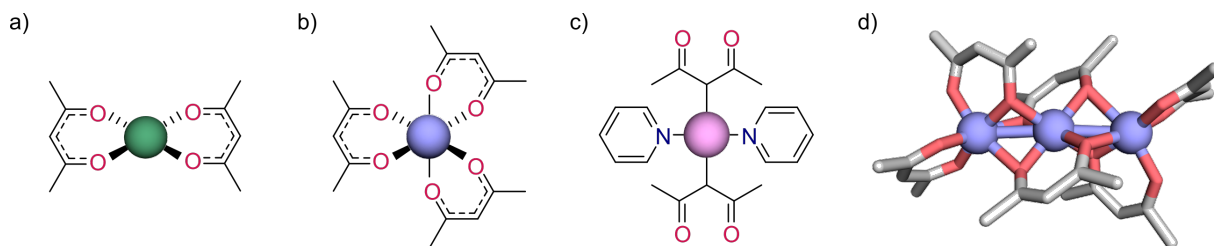


Figure 2. a) Structure of square planar complex $[\text{M}^{\text{II}}(\text{acac})_2]$. b) Structure of octahedral complex $[\text{M}^{\text{III}}(\text{acac})_3]$. c) Structure of $[\text{Pt}^{\text{II}}(\gamma\text{-acac})_2(\text{py})_2]$, with acac acting as a C-donor ligand.⁴⁵ d) Trimer structure of $[\text{Ni}(\text{acac})_2]_3$, with acac acting as a bridging ligand.⁴¹

Acetylacetonate anion, as a simple bidentate ligand, forms a number of complexes, with the most common being square planar $[\text{M}^{\text{II}}(\text{acac})_2]$ and octahedral $[\text{M}^{\text{III}}(\text{acac})_3]$ species, where M represents metal ion, and the geometry typically corresponds to the preferred coordination geometry of the metal center (Figure 2ab).^{32, 46-48} A variety of mixed-ligand compounds have also been reported, in which additional ligands, ranging from simple species such as H_2O , CO, and pyridine to more complex molecules, complete the coordination sphere of the metal center.⁴⁹⁻⁵¹ To date, the Cambridge Structural Database contains approximately 4,500 structures comprising M–acac bonding. In addition to simple acetylacetone, various structural modifications of this ligand have been developed through the introduction of different functional moieties or bulky substituents that replace the methyl groups.⁵²⁻⁵⁴ Such modifications enable precise tuning of the electronic density and steric hindrance of individual units, thereby facilitating the attainment of specific physicochemical properties. For instance, fluorinated analogues of acetylacetone can significantly

increase the volatility of coordination compounds, which is particularly useful in processes such as chemical vapor deposition, where volatile complexes are employed as metal precursors to deposit thin films of metals and metal oxides.^{55,56} In another example, sterically hindered β -diketonates with bulky moieties were used to prepare complexes that demonstrated higher efficiency and selectivity in catalyzed reactions compared to those catalyzed by simple metal acetylacetonates.⁵⁷⁻⁶¹ Thus, due to their potential for functionalization, β -diketonate ligands have become crucial for creating systems with properties tailored to specific utilities. Owing to their advantageous features, such as straightforward synthesis, high stability, and solubility in organic solvents, β -diketonate complexes have found applications in various fields, including catalysis, magnetism, analytical chemistry, and materials science.⁶²⁻⁶⁶

In addition to acetylacetonone and its bidentate derivatives, an important subclass includes oligo- β -diketonate ligands, which contain more than one β -diketonate group within a single molecule, allowing for simultaneous coordination with several metal centers.^{39, 47, 67-70} The incorporation of multiple coordination sites within a ligand structure enables the construction of metallosupramolecular architectures, both discrete and polymeric, with a diverse range of topologies and functionalities, which is particularly significant for their practical applications. For instance, Clegg *et al.* reported the synthesis of a tetrahedral coordination cage based on Fe^{III} ions and a bis- β -diketonate ligand (Figure 3a), which, due to its porosity, allowed for the encapsulation of THF molecules.⁷¹ As another example, a tris- β -diketonate ligand combined with Pd^{II} ions resulted in the formation of a branched polymer, which proved to be an efficient catalyst precursor in the Suzuki-Miyaura cross-coupling reaction (Figure 3b).⁷²

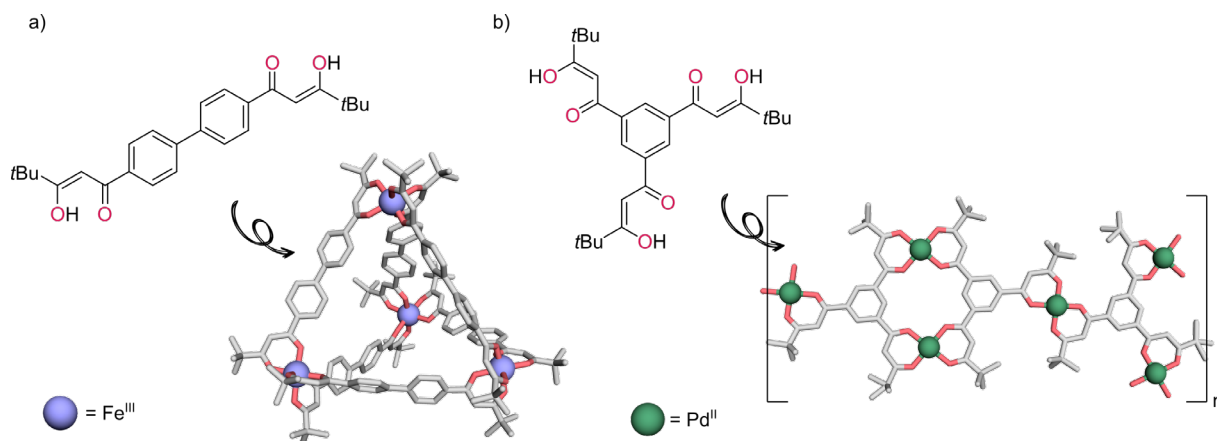


Figure 3. Metallosupramolecular architectures based on oligo- β -diketonate ligands: a) a coordination cage with Fe^{III} ions;⁷¹ b) a branched polymer with Pd^{II} ions.⁷²

1.1.2. Pyridine ligands

Since pyridine was discovered by Thomas Anderson in 1849, it has become one of the most extensively utilized heterocyclic compounds in chemistry. With its conjugated system of six π electrons delocalized over a planar ring, pyridine fulfills Hückel's criteria for aromatic systems. Although it exhibits numerous similarities to benzene, the incorporation of an electronegative N -atom into the aromatic ring leads to significant alterations in their physicochemical

properties.^{73,74} Due to the negative inductive effect of the *N*-atom, the electron density in the pyridine ring is non-uniformly distributed, resulting in a dipole moment and weaker resonance stabilization compared to benzene.⁷⁵ As an aromatic compound, pyridine is capable of undergoing both electrophilic and nucleophilic substitution reactions. In turn, the presence of a pair of non-bonding electrons in the valence shell of the *N*-atom determines its basic nature. In most reactions, pyridine acts as a typical tertiary amine, exhibiting susceptibility to protonation, alkylation, acetylation, and *N*-oxidation.^{76,77}

Given its electronic properties, pyridine is commonly utilized as a ligand, capable of generating a wide range of complexes. According to the HSAB theory, pyridine is classified as a borderline base, which allows to form stable combinations with both soft and hard acids.⁷⁸ While pyridine complexes with transition metals are the most common, compounds with metals from the *s*, *p*, and *f* blocks are also well-known.⁷⁹⁻⁸³ Pyridine, acting as a Lewis base, donates a lone pair of electrons to a Lewis acid, resulting in the formation of a coordination bond. In addition, the bonding between the metal center and pyridine can be strengthened through π back-donation. The anti-bonding π^* orbitals of the ligand are capable of accepting electron density from the *d π* orbitals of the metal ion (Figure 4). Moreover, in some cases, the π -electrons of the ring can also participate in bonding interactions with metal centers.⁷³

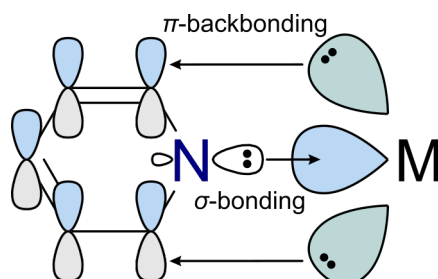


Figure 4. σ -Bonding and π -backbonding between the pyridine ligand and the metal center.

The pyridine ring is a prevalent structural motif in many ligands, including both monodentate and multidentate units. It offers almost unlimited potential for functionalization through the introduction of electron-donating or electron-withdrawing groups.⁸⁴⁻⁸⁹ Such structural and electronic adjustments of the heterocyclic ring allow for the generation of compounds with desired properties, expanding their range of applications. Pyridine-based complexes are of significant importance in both academic and industrial contexts, as demonstrated by their practical utility as catalysts, cytotoxic agents, chemosensors, or molecular magnets.⁹⁰⁻⁹⁵ For example, the complex $[\text{TiCl}_2(\text{py})_4]$ has been utilized in the catalytic polymerization of unsaturated hydrocarbons,⁷³ while $[\text{PdCl}_2(\text{py})_2]$ and its derivatives have shown potential in anticancer therapy.⁹⁶ The scope of pyridine-based complexes is vast, as reflected in the extensive literature in this field, and continues to expand with the development of new entities tailored for specific applications across various domains.

An important group of pyridine ligands that garners considerable interest comprises entities with multiple heterocyclic rings incorporated into a single structure. Starting with the pyridine ring, increasingly intricate systems can be designed, ranging from simple bipyridine ligands, such as 2,2'- and 4,4'-bipyridine, through 1,10-phenanthroline and terpyridine, to more sophisticated polycyclic

systems with multiple *N*-donors *per* molecule. These polydentate units can function as either chelating or bridging agents, interconnecting metal centers in well-defined spatial arrangements. For this reason, such ligands are employed as building blocks in the creation of metallosupramolecular architectures, including coordination polymers, metallocycles, and cages.⁹⁷⁻¹⁰⁵ To illustrate, 4,4'-bipyridine serves as an effective linker for transition metal ions in the synthesis of coordination polymers with various topologies, ranging from one-dimensional to three-dimensional structures (Figure 5). Due to their structural features, these polymers have found practical applications in gas sorption and catalysis.¹⁰⁶

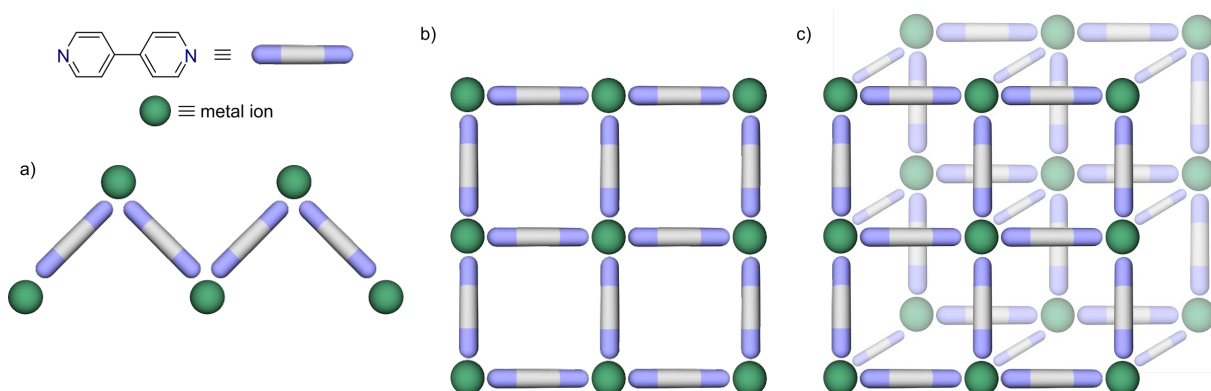


Figure 5. Coordination polymers formed with 4,4'-bipyridine: a) one-dimensional; b) two-dimensional; c) three-dimensional.

1.1.3. Pyridyl- β -diketonate ligands

The advancement of coordination supramolecular chemistry is driven by the design and synthesis of new families of sophisticated multi-donor ligands, among which important classes include the aforementioned multidentate acetylacetonate derivatives and polypyridine systems.¹⁰⁷⁻¹¹⁰ Although classical oligo- β -diketonates have long been demonstrated to be excellent chelating agents for a wide range of metal centers, as well as polypyridines have revealed high potential for the generation of intricate coordination assemblies, there are significantly fewer reports in the literature on pyridyl- β -diketonate ligands.¹⁶ Their advantage over the previously described species is their ambidentate character, which results in an ability to engage different metal ions and to construct a scope of heterometallic architectures. This feature is also extremely important from the application point of view, directly affecting the functionality of a given nanostructure, such as catalytic activity or magnetic properties.^{111, 112}

Pyridyl- β -diketonate compounds, analogous to classical β -diketonates, are synthesized *via* Claisen condensation between appropriate esters of carboxylic acids and ketones. Similar to acetylacetonate and its derivatives, these units exhibit keto-enol tautomerism, predominantly existing in the enol form.^{113, 114} As organic ligands, they are capable of binding metal centers in various ways through multiple donor-atom combinations. They can occur as neutral, anionic, or zwitterionic species, with each form demonstrating the ability to effectively coordinate with metal ions. Due to the presence of two coordination sites of distinct nature in their structure, specifically neutral pyridine and β -diketonate (in either its protonated or deprotonated state), these ligands are capable of binding

a wide range of metal centers, both hard and soft acids according to the HSAB classification (Figure 6a). In addition to the common coordination modes *via* O,O' -chelation or N -donation, some of them, depending on the relative position of the donor groups, can also create unconventional combinations, such as $N,C(sp^3)$ - and N,O -chelates (Figure 6b).¹¹⁵⁻¹¹⁷ As a consequence, the formation of specific coordination motifs is governed by several factors, with the most critical being the nature of the metal centers, the geometry of the ligand, and the reaction environment, particularly acid-base equilibria.

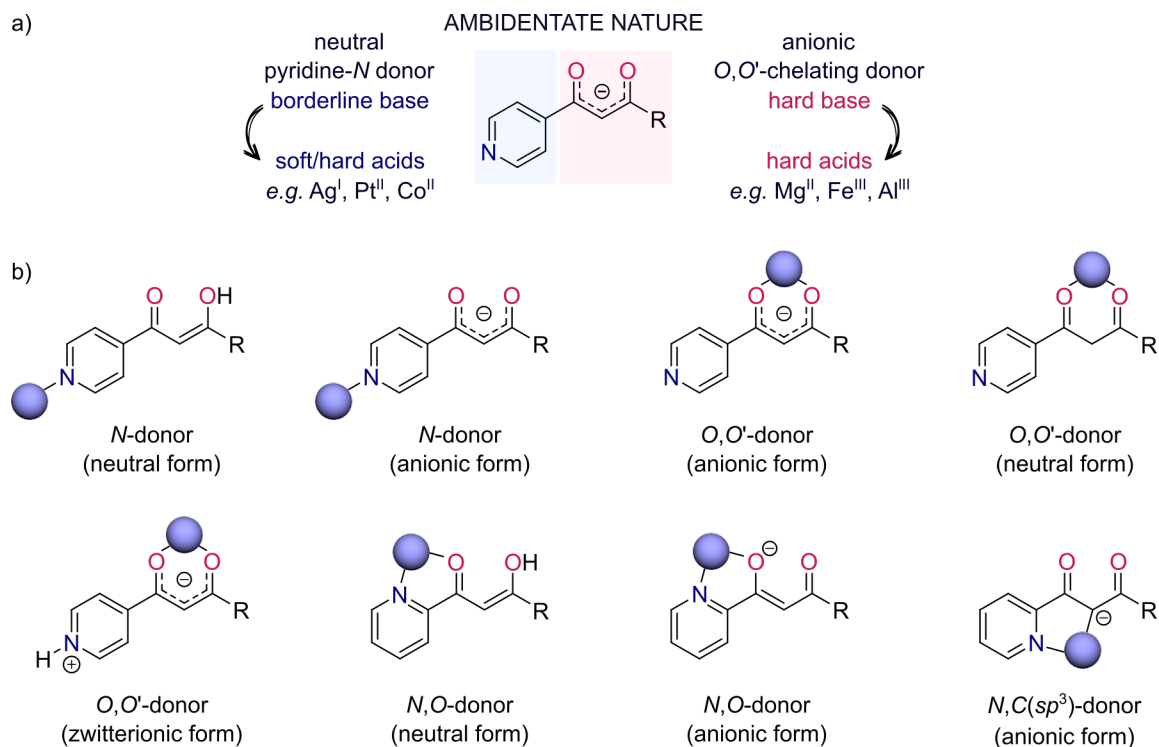
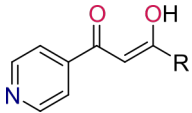
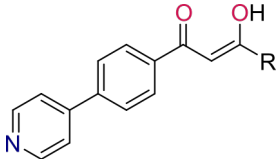
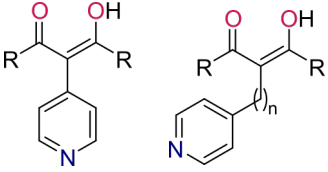
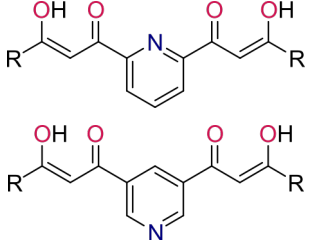
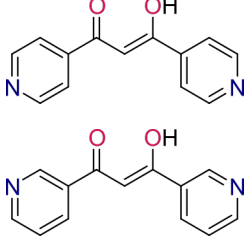
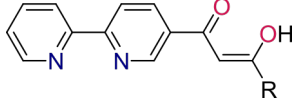
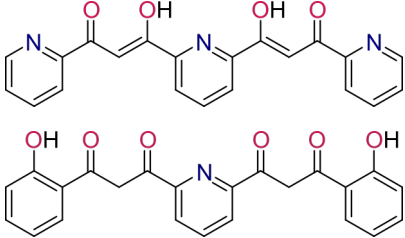


Figure 6. a) The distinct nature of the coordination sites in pyridyl- β -diketonate ligands. b) Various coordination modes of pyridyl- β -diketonates in their neutral, anionic, and zwitterionic forms.

The simplest representatives of this ligand family are entities consisting of a single β -diketonate moiety substituted by one pyridine ring. However, many more complex species that incorporate several β -diketonate and/or pyridine (or bipyridine) groups capable of binding several metal ions are known. Thus, the units classified within this ligand class exhibit diversity in numerous aspects, such as the number of coordination sites, the relative arrangement of donor groups, the position of the pyridine- N atom within the heterocyclic ring, and the presence of additional functional groups (Table 1). In contrast to mono- and poly- β -diketonates, pyridyl- β -diketonate ligands, due to the distinct character of their coordination sites as well as the ability to act as bridging species, have been widely employed to generate not only homometallic but also heterometallic systems, ranging from simple complexes through cages and macrocycles to larger architectures such as coordination polymers and metal-organic frameworks (MOFs).

Table 1. Examples of pyridyl- β -diketonate ligands and their use in the construction of coordination architectures.

No.	Ligand structure	R-groups	Architectures generated	References
1.	 <i>(including 2- and 3-substituted pyridine ring)</i>	-Me -CF ₃ -Et -iPr -tBu -Ph	mononuclear complexes polynuclear complexes cages polymers	113, 115, 116, 118- 134
2.		-Me -CF ₃	MOFs	135-137
3.		-Me	mononuclear complexes polynuclear complexes metallocycles cages polymers MOFs	138-158
4.		-Me -tBu	polynuclear complexes metallocycles cages polymers	159-170
5.	 <i>(including other N-atoms positions)</i>	-	mononuclear complexes metallocycles cages polymers MOFs	111, 112, 117, 127, 169, 171- 191
6.	 <i>(including other bipyridine substitution)</i>	-Me -CF ₃ -C ₂ F ₅	mononuclear complexes polynuclear complexes	192-194
7.		-	polynuclear complexes metallocycles cages	195-199

1.2. Nanostructures based on pyridyl- β -diketones

To date, a wide array of pyridyl- β -diketones has been utilized in the synthesis of structurally distinct coordination assemblies. Although the earliest publications on complexes with such ligands emerged in the second half of the 20th century,^{165, 200} substantial advancements in this area of chemistry have continued to the present day. This progress is reflected in the diverse range of nanostructures reported, with significant contributions from the research groups of Clegg, Lusby, Wang, Lindoy, and Stefankiewicz. As a consequence, effective strategies have been developed that employ these ligands as versatile building blocks for the design and controllable synthesis of novel coordination architectures with specific topologies and physicochemical properties. A brief overview of the current state of the art in this domain is provided ahead.

1.2.1. Mono- and polynuclear complexes

In the literature, a broad spectrum of mononuclear coordination compounds with ambidentate pyridyl- β -diketonate ligands has been reported. Among these complexes, both homo- and heteroleptic species can be distinguished, each exhibiting a variety of coordination geometries, with octahedral and square planar environments of the metal centers being the most common. Typically, metal ions within these structures are coordinated by either β -diketonate or pyridine-*N* donors, with one coordination site remaining non-coordinated (Figure 7). An array of complexes with ligands arranged as *O,O'*-chelates has been generated using a base for ligand deprotonation, encompassing a number of metal ions including Be^{II}, Cu^{II}, Pd^{II}, Cr^{III}, Co^{III}, Fe^{III}, Al^{III}, Ga^{III}, Dy^{III}, Tb^{III}, Ho^{III}, and Er^{III}.^{111-113, 115, 119, 138, 147, 148, 171, 183} In turn, *N*-donation has been confirmed in the structures of complexes with Ag^I, Ru^{II}, Os^{II}, Pd^{II}, and Pt^{II}.^{113, 118, 157} Additionally, other coordination modes have also been verified, such as *N,O*-chelation for Ru^{III}, Ir^{III}, and Pt^{II} ions,^{116, 187, 190} as well as *N,C(sp³)*-chelation for Au^{III}, Pd^{II}, and Pt^{II} ions.^{175, 201} Due to the presence of accessible coordination sites that can engage in further complexation reactions, most of these complexes can serve as metalloligands, capable of binding additional metal cations to form more intricate systems.

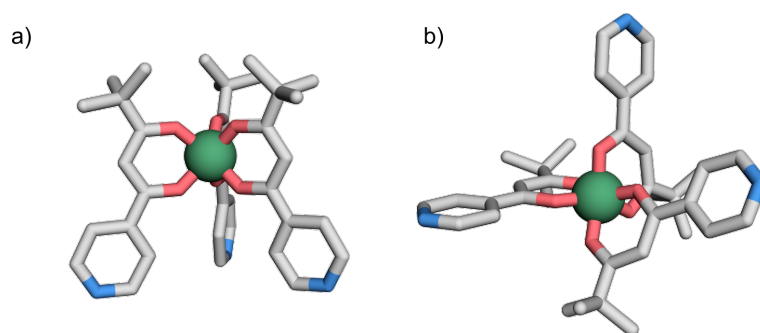


Figure 7. Octahedral Al^{III} complexes with pyridyl- β -diketonate ligand, existing in two isomeric forms: a) *fac* isomer; b) *mer* isomer.¹¹⁹ While the β -diketonate units are involved in coordination, the pyridine-*N* donors remain uncoordinated.

In addition to simple mononuclear coordination compounds, a variety of heteronuclear complexes have also been extensively reported. The heteroditopic nature of such ligands allows for the simultaneous coordination of multiple metal centers by a single ligand; however, the synthesis of

these species often requires the use of coligands to prevent polymerization reactions. Complexes with Fe^{III} and Re^{I} , Sc^{III} and Ru^{II} , Cr^{III} and Re^{I} , Cu^{II} and La^{III} , as well as Ni^{II} and Pb^{II} constitute prime examples, where the first metal center is coordinated as an O,O' -chelate and the second is coordinated by pyridine (or bipyridine) donors.^{145, 154, 161, 192, 193}

1.2.2. Metallochromes

Metallochromes represent another class of coordination assemblies formed with pyridyl- β -diketonate ligands. The literature reports examples of homonuclear metallochromes containing Cu^{II} , Ni^{II} , Pd^{II} , and Fe^{III} ions (Figure 8a), which are generated using ligands specifically designed to incorporate at least two β -diketonate moieties.^{165, 166, 168} In the structure of heteronuclear metallochromes, both O,O' -chelating and pyridine- N donors are involved in coordination, with a notable example being the mixed-metal $\text{Cu}^{\text{II}}/\text{Rh}^{\text{III}}$ metallochromes reported by Jin *et al.* (Figure 8b).^{169, 170}

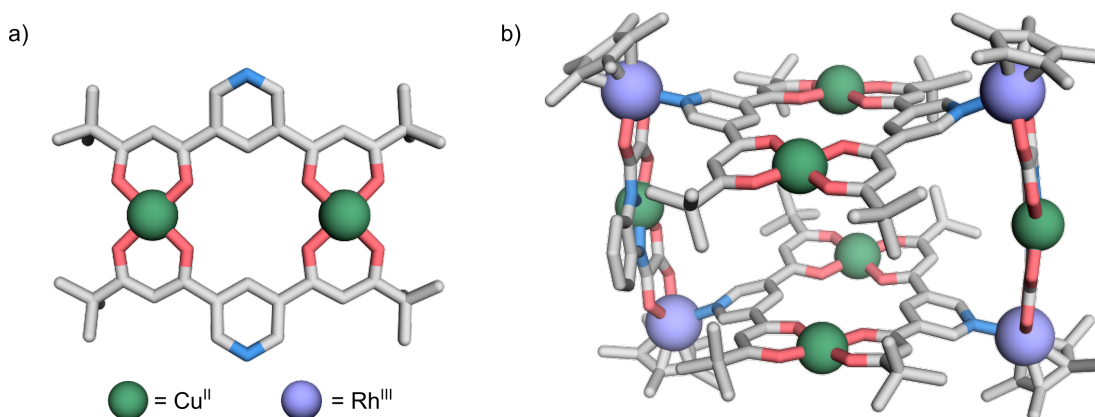


Figure 8. a) Structure of a dinuclear Cu^{II} metallochrom. b) Structure of a three-dimensional heteronuclear $\text{Cu}^{\text{II}}/\text{Rh}^{\text{III}}$ metallochrom.¹⁷⁰ H -atoms, counterions, and solvent molecules have been omitted for clarity.

1.2.3. Metallocages

Pyridyl- β -diketonate ligands have also been employed as linkers in the construction of coordination cages, which, due to their intriguing topologies and programmable properties, continue to attract great interest. The literature on metallocages incorporating pyridyl- β -diketonate ligands is fairly comprehensive, with notable contributions from Wang,^{126, 172} Brechin,¹²³ Lusby,^{120, 129, 130} Stang,^{119, 122} and their co-workers. Such architectures are generally synthesized through hierarchical self-assembly processes, with the first step involving the generation of tripodal metalloligands based on trivalent metal ions such as Al^{III} , Fe^{III} , and Cr^{III} . The cages are subsequently formed in complexation reactions with divalent metal ions, including Cu^{II} , Co^{II} , Zn^{II} , Ni^{II} , Pd^{II} , and Pt^{II} . The resulting heterometallic assemblies, with the most common formulas $[\text{M}_2^{\text{III}}\text{M}_3^{\text{II}}\text{L}_6]$ and $[\text{M}_8^{\text{III}}\text{M}_6^{\text{II}}\text{L}_{24}]$, where M denotes the metal ion and L denotes the ligand, predominantly adopt trigonal bipyramidal or cubic geometries (Figure 9). These geometries depend on the nature of specific metal centers and the reaction stoichiometry, while the volume of the internal cavities is determined by the ligand structure.

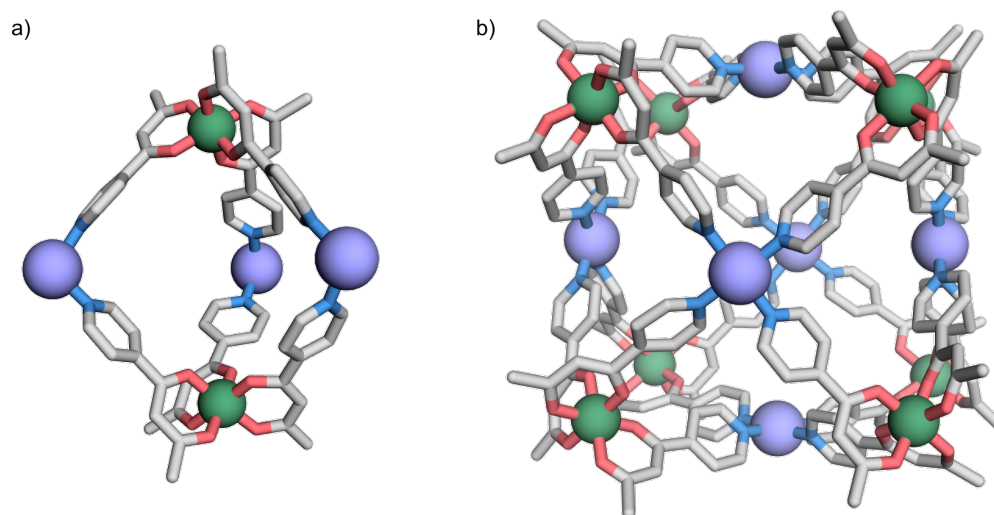


Figure 9. Heterometallic cages based on pyridyl- β -diketonate ligands with: a) trigonal bipyramidal geometry; b) cubic geometry. Blue and green spheres represent di- and trivalent metal ions, respectively. *H*-atoms, counterions, and solvent molecules have been omitted for clarity.

1.2.4. Coordination polymers and MOFs

Metallosupramolecular polymers based on pyridyl- β -diketones represent a subsequent class of coordination materials that have garnered significant attention. The ambidentate nature of these ligands enables the construction of extended networks with various dimensionalities and topologies. Homometallic polymers based on Cu^{II} ions, which exhibit characteristics intermediate between hard and soft acids, serve as a notable example, where coordination by structurally distinct ligands results in the formation of diverse coordination frameworks.^{115, 125, 134, 143, 158, 166} In these structures, octahedral Cu^{II} centers are coordinated as O,O' -chelates in a planar arrangement, with their coordination spheres completed by pyridine-*N* donors from other ligand molecules in the axial positions (Figure 10a). Another example of a homometallic aggregate was reported by Lindoy *et al.*, where the combination of pyridyl- β -diketone ligands with Zn^{II} ions led to the generation of a three-dimensional polymeric network.¹⁵⁸ Nevertheless, the scope of mixed-metal polymers is considerably broader due to the different preferences of metal centers for donors of distinct nature.^{139, 146, 147, 152, 153, 156, 171, 174, 181, 189} For instance, a heterometallic polymer reported by Domasevitch *et al.* comprises Fe^{III} ions coordinated as O,O' -chelates, while Cd^{II} centers are bound by pyridyl groups, forming one-dimensional chains.¹⁴⁴ Additionally, Wang *et al.* demonstrated the synthesis of three distinct coordination polymers using a tripodal metalloligand with Al^{III} ions. The reactions with Zn^{II} , Cd^{II} , and Hg^{II} ions resulted in the formation of materials with various topologies, *i.e.*, a one-dimensional ladder-like structure, a two-dimensional layer, and a helical arrangement, respectively (Figure 10bc).¹⁴⁹ Pyridyl- β -diketones can also serve as components in the generation of metal-organic frameworks (MOFs), which constitute a specific class of coordination polymers characterized by their porous, extended structures. Owing to the structural variety of ligands, numerous systems diversified in terms of composition, dimensionality, pore size, and other physicochemical features have been reported in the literature. These include homometallic architectures containing Cu^{II} , Mn^{II} , Co^{II} , and Zn^{II} centers,^{124, 135-137, 140, 173, 202} as well as mixed-metal-organic frameworks (MMOFs) with $\text{Al}^{\text{III}}/\text{Ag}^{\text{I}}$, $\text{Ga}^{\text{III}}/\text{Ag}^{\text{I}}$, $\text{Fe}^{\text{III}}/\text{Ag}^{\text{I}}$, and $\text{Cu}^{\text{II}}/\text{Cd}^{\text{II}}$ ions.^{150, 151, 173, 182}

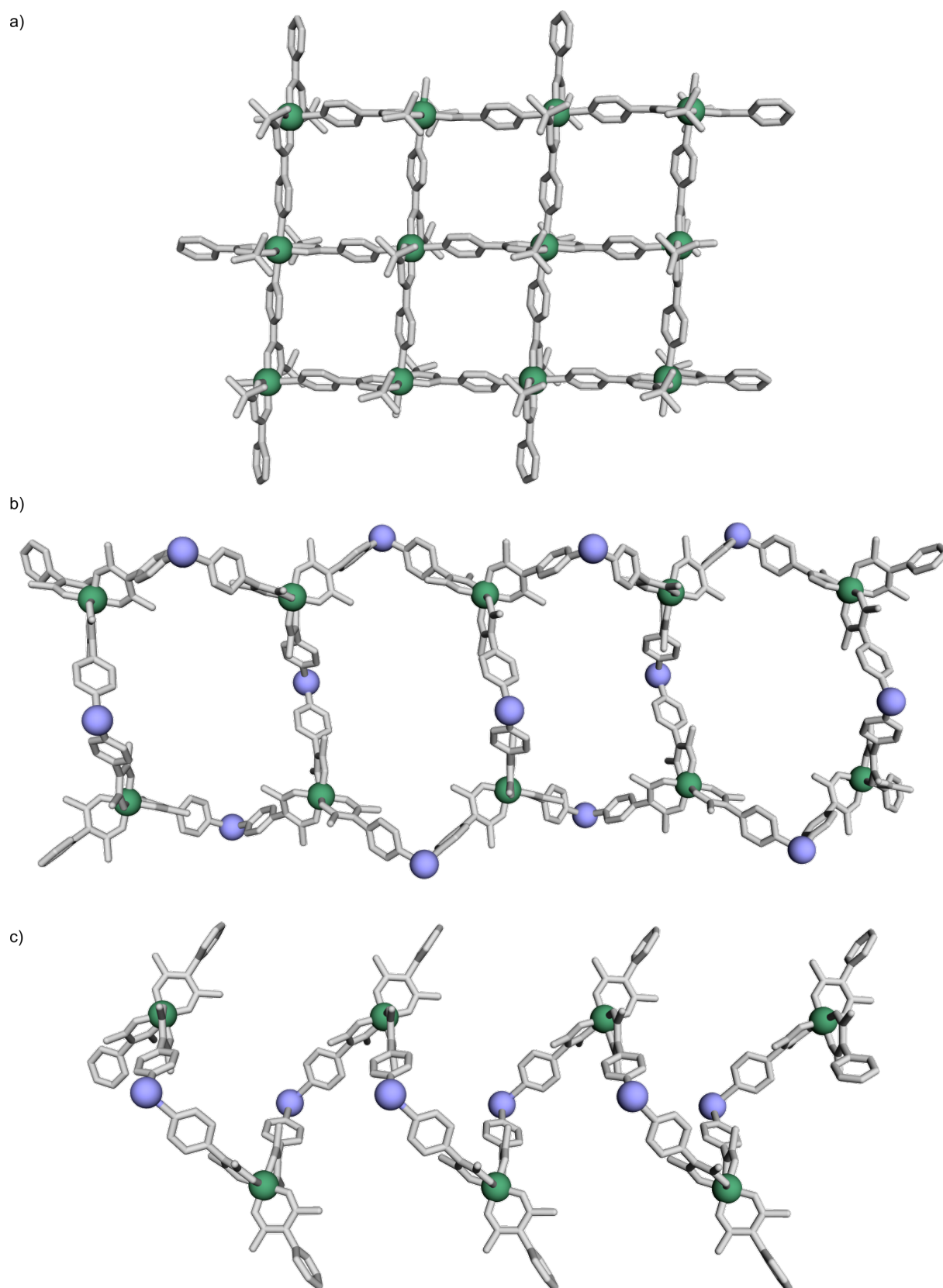


Figure 10. Examples of homo- and heterometallic coordination polymers based on pyridyl- β -diketonate ligands: a) two-dimensional sheet structure of the network with Cu^{II} ions;¹¹⁵ b) one-dimensional ladder-like structure of the $\text{Al}^{\text{III}}/\text{Zn}^{\text{II}}$ polymer;¹⁴⁹ c) helical structure of the $\text{Al}^{\text{III}}/\text{Hg}^{\text{II}}$ polymer.¹⁴⁹ *H*-atoms, counterions, and solvent molecules have been omitted for clarity.

1.3. Application potential of the coordination architectures based on pyridyl- β -diketones

Of the different ambidentate ligands showing promise as building blocks in coordination and metallosupramolecular chemistry, pyridyl- β -diketones have been recognized for their versatility in the development of functional nanostructures. The unique structure-dependent physicochemical properties of such architectures, *e.g.*, wide compositional diversity, permanent porosity, and exceptional stability, are of great importance due to their control of functionality. Although much of the literature concerns purely structural studies, the high application potential of the characterized molecules can be widely employed in various areas, such as catalysis, host-guest chemistry, sensing, energy transfer, and magnetism, as discussed below.

1.3.1. Catalysis

Metallosupramolecular architectures bearing pyridyl- β -diketonate ligands exhibit high potential for applications in catalysis, as demonstrated by various examples available in the literature. Their function is multifaceted, serving as key constituents in the construction of efficient catalytic systems that have found applications in a wide range of reactions, such as cross-coupling, amination, polymerization, or isomerization. Primarily, different types of coordination assemblies based on pyridyl- β -diketones, including homo- and heteronuclear complexes, polymers, MOFs, and cages, have been employed as conventional catalysts. In works published by Stefankiewicz *et al.*, the considerable potential of mononuclear Pd^{II} and Pt^{II} complexes was demonstrated in the Suzuki-Miyaura reaction and olefin hydrosilylation, respectively.^{113, 118} These studies emphasized the importance of ambidentate units within their structure, highlighting their enhanced efficiency compared to counterparts based on monofunctional ligands. Other notable examples include Fe^{III} complexes that efficiently catalyze the ring-opening polymerization of ϵ -caprolactone,¹¹¹ Au^{III} complexes used in cycloisomerization reactions,¹⁷⁵ and heterometallic polymers that facilitate the ring opening of epoxides with aromatic amines.²⁰³ Furthermore, pyridyl- β -diketonate ligands were utilized to create platforms for catalyst deposition, leading to efficient heterogeneous systems. For instance, a Mn^{II}-based MOF developed by Dong *et al.* served as an ideal platform to support Pd-Au alloy nanoparticles.¹³⁶ This composite system exhibited high activity as a heterogeneous catalyst for the one-pot tandem synthesis of imines from benzyl alcohols and anilines or benzylamines (Figure 11). As another example, a system consisting of a Cu^{II} MOF and Au nanoparticles was effectively employed in the synthesis of tricyanovinyl derivatives.¹³⁷ Additionally, pyridyl- β -diketones can function as auxiliary ligands in homogeneous catalytic systems, where the active form of catalyst is *in situ* generated in the reaction medium. Such examples were described by Taillefer and Chen, who developed catalytic systems based on Cu^I ions for C-N cross-coupling reactions of aryl halides with aqueous ammonia or *NH*-heterocycles.^{204, 205}

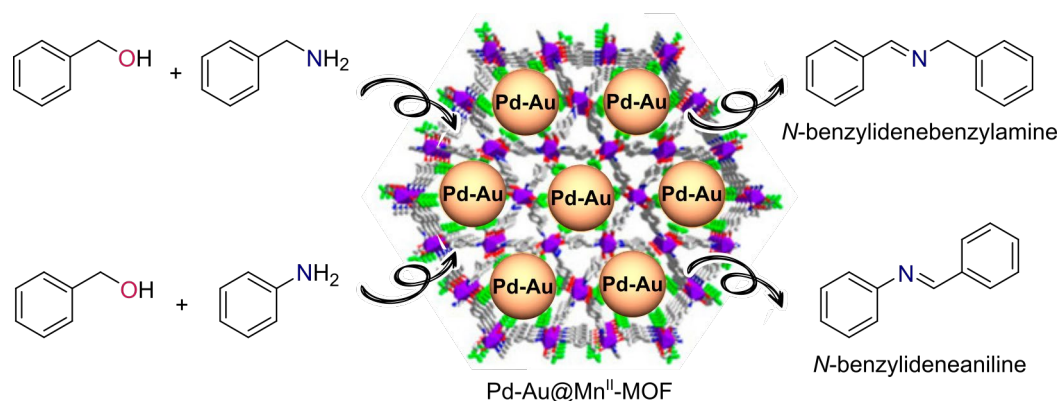


Figure 11. A heterogeneous system based on Mn^{II} MOF and Pd–Au alloy nanoparticles for the catalytic one-pot tandem synthesis of imines from alcohols and amines.¹³⁶

1.3.2. Host-guest chemistry and sensing

Given their structural versatility and superior binding properties, coordination assemblies based on pyridyl- β -diketonate ligands are becoming increasingly important in host-guest chemistry. The flexible framework of such architectures enables the creation of customizable internal cavities and channels, precisely designed to selectively recognize and encapsulate a range of guest molecules. Moreover, the intrinsic luminescent features of these ligands enhance their functionality, allowing for guest-driven luminescent responses that are particularly crucial for sensing and detection applications.²⁰⁶ An initial category of guest molecules suitable for such nanostructures serving as hosts includes anions. For instance, Aromi *et al.* reported $\text{Co}^{\text{II}}/\text{Co}^{\text{III}}$ clusters capable of trapping two CO_3^{2-} anions,¹⁹⁶ whereas Jin *et al.* demonstrated Ru^{II} metallocycles that effectively encapsulate counterions like OTf^- and PF_6^- .¹⁵⁵ As an example of cation encapsulation, Fe^{III} metallacryptands have shown high effectiveness as selective complexation agents for specific cations, particularly those from the alkaline, alkaline earth, and rare earth metal groups.^{164, 168} Furthermore, Dong *et al.* introduced two three-dimensional networks comprising Cu^{II} and Zn^{II} ions, which revealed their capacity to encapsulate larger entities, such as metal acetylacetonates, and exhibited the resultant guest-induced luminescent properties.¹³⁵ Owing to the presence of voids, porous architectures such as cages or MOFs can also be applied in gas sorption. This was exemplified by Hernández-

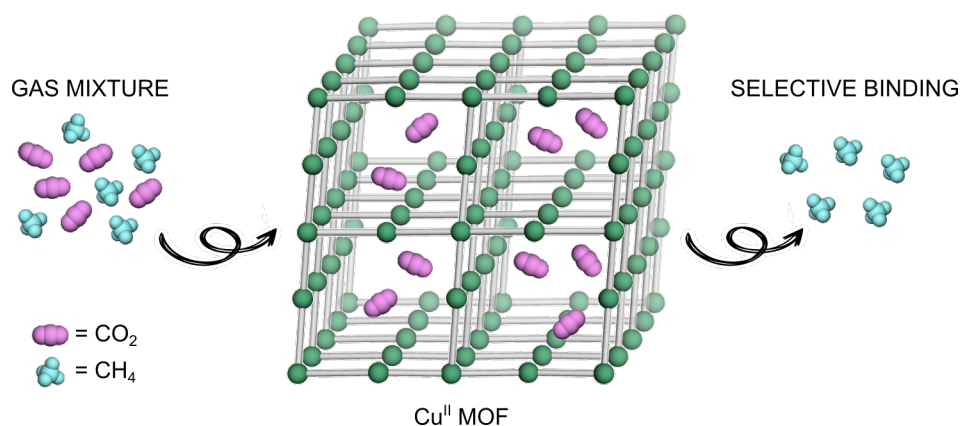


Figure 12. Schematic representation of the Cu^{II} MOF reported by Hernandez-Maldonado, illustrating the selective binding of CO_2 over CH_4 .¹⁴⁰

Maldonado *et al.*, who demonstrated a Cu^{II} MOF with one-dimensional pore channels that showed superior CO₂ selectivity over CH₄ (Figure 12).¹⁴⁰ Additionally, nanostructures with pyridyl- β -diketones, due to their encapsulation capabilities, have emerged as excellent candidates for use as sensors. For instance, Stang *et al.* developed Eu^{III} cages as efficient nanosensors for nitroaromatic compounds,¹²² while Liu and Zhou created dimeric and polymeric materials employing the same ions for the highly selective detection of Hg^{II} cations.¹²⁷

1.3.3. Magnetism

Pyridyl- β -diketonate complexes have also garnered significant attention due to their magnetic properties, acting as single-molecule toroids (SMTs), single-molecule magnets (SMMs), and molecular nanomagnets.^{162, 180} Such magnetic behavior can be finely tuned through various structural modifications of the ligands, since the type of magnetism revealed by these systems depends not only on the metal ion used but also on the coligands and the surrounding coordination environment. For instance, cluster systems with Ln^{III} ions, reported by Fuller *et al.*, have been presented as toroidal spin systems, indicating the important role of lanthanoid centers in the spin structure and the potential of pyridyl- β -diketonate ligands to support SMTs.¹⁸⁵ Le Guennic *et al.* demonstrated a Dy^{III} cubane complex that possesses a toroidal moment associated with a nonmagnetic ground state transposing this property to a tridimensional structure (3D-SMT).¹⁷⁸ In turn, Pliet *et al.* developed structurally diversified complexes based on Dy^{III}, for which magnetic measurements and *ab initio* calculations highlighted the SMM behavior.¹⁸³ In another example, Liu *et al.* reported a series of heterometallic molecular nanomagnets with varied magnetic relaxation behaviors by regulating the *N*-sites of β -diketonate ligands.¹¹² Studies in this field emphasize the crucial role of ligand environment and structural features in determining the magnetic properties of metal complexes, which can aid in designing species with tailored magnetic behavior, paving the way for advances in materials science and molecular magnetism.

1.3.4. Energy transfer

Apart from the aforementioned examples, complexes based on pyridyl- β -diketones have also found applications in the area of energy transfer. As exemplified by Huang *et al.*, these bridging ligands, incorporated in the structures of Ir^{III}/Eu^{III} bimetallic complexes, play an important role in the excitation energy transfer (EET) process. They were suitable to serve as efficient pathways for energy transfer, resulting in a systemic difference in the lowest triplet-state energy (T_1) of Ir^{III}, the EET efficiency from Ir^{III} to Eu^{III} ion, and a significant difference in the total luminescence quantum yields.¹⁹³ In turn, Chen *et al.* prepared a Eu^{III} complex functioning as an innovative model of energy-degeneracy-crossing-controlled photosensitized energy transfer (EnT). In this case, the pyridine ring, acting as a suitable electron acceptor added to the β -diketone moiety, creates a bright charge-transfer excitation state, promoting electron movement from the β -diketone unit to the substituted groups.¹³³ In other works, pyridyl- β -diketonate ligands were also applied to create coordination systems that facilitate photoinduced energy and electron-transfer processes within dynamic self-assembled donor-acceptor arrays.^{145, 154, 192}

2. Research objectives

Over the years, advancements in coordination chemistry have profoundly enhanced catalytic processes, while innovations in catalysis have reciprocally driven further progress in coordination chemistry. Since *d*-block metal complexes allow for the performance of reactions that are challenging to achieve with traditional methods and synthetic strategies based on functional group reactivity, they play a crucial role in modern catalysis. The design of organic ligands, which modulate the electron density and steric hindrance on the central atom, enables the synthesis of complexes with tailored properties for specific applications. Thus, the identification of structural and compositional factors that govern the catalytic activity of these systems is fundamental for developing novel catalysts to enhance their efficiency and selectivity.

In this doctoral dissertation, the main objective was to develop a new generation of coordination compounds aimed at applications in catalysis. To achieve this, a range of ligands based on pyridine and β -diketonate donors, as well as ambidentate species that incorporate these two distinct moieties within a single structure, were utilized as key components to construct new coordination assemblies. As a result of complexation reactions with a precisely selected set of metal centers, namely Ag^{I} , Pd^{II} , and Pt^{II} , a diverse array of coordination architectures was generated, including homo- and heteronuclear complexes as well as polymeric materials, all of which were characterized in depth using various analytical techniques. Given the structural and compositional features of the obtained systems, they were subsequently employed as catalyst precursors in multiple organic reactions to investigate their potential in this domain. Furthermore, extensive studies were conducted to identify the factors that enhance the catalytic activity of individual complexes, thereby indicating the most efficient and selective units for specific reactions. New approaches for the rational design of coordination compounds were developed with the aim of their application as catalytic systems.

Specific objectives were to:

- I. design and synthesize a new generation of homo- and heteronuclear coordination assemblies with Ag^{I} , Pd^{II} , and Pt^{II} ions using the aforementioned ligands (**A1–A6**);
- II. demonstrate the potential of ambidentate pyridyl- β -diketonate ligands to form various metallosupramolecular architectures, illustrating their flexibility and capability to adopt diverse coordination modes (**A3–A6**);
- III. investigate the coordination-driven structural switching processes triggered by external stimuli between different homo- and heterometallic complexes (**A2–A3, A5**);
- IV. determine the application potential of the obtained complexes as efficient and selective catalysts in organic reactions, including Pd-catalyzed cross-couplings and Pt-catalyzed hydrosilylation reactions (**A1–A6**);
- V. identify the factors that influence catalytic performance, such as the nuclearity of complexes or the coordination environment of metal centers, through comparative tests between individual complexes, and define the effects that lead to the enhancement in catalytic activity (**A1–A5**).

The presented doctoral dissertation is based on the following scientific reports:

- A1** **G. Kurpik**, A. Walczak, M. Gilski, J. Harrowfield, A. R. Stefankiewicz
Effect of the nuclearity on the catalytic performance of a series of Pd^I complexes in the Suzuki-Miyaura reaction
Journal of Catalysis **2022**, *411*, 193–199; DOI: 10.1016/j.jcat.2022.05.021
- A2** **G. Kurpik**, A. Walczak, M. Goldyn, J. Harrowfield, A. R. Stefankiewicz
Pd^I complexes with pyridine ligands: substituent effects on the NMR Data, crystal structures, and catalytic activity
Inorganic Chemistry **2022**, *61*, 14019–14029; DOI: 10.1021/acs.inorgchem.2c01996
- A3** **G. Kurpik**, A. Walczak, G. Markiewicz, J. Harrowfield, A. R. Stefankiewicz
Enhanced catalytic performance derived from coordination-driven structural switching between homometallic complexes and heterometallic polymeric materials
Nanoscale **2023**, *15*, 9543–9550; DOI: 10.1039/D3NR01298K
- A4** A. Walczak, **G. Kurpik**, M. Zaranek, P. Pawluć, A. R. Stefankiewicz
C(sp³),N palladacyclic complexes bearing flexidentate ligands as efficient (pre)catalysts for Heck olefination of aryl halides
Journal of Catalysis **2022**, *405*, 84–90; DOI: 10.1016/j.jcat.2021.11.033
- A5** **G. Kurpik**, A. Walczak, I. Łukasik, Z. Matela, A. R. Stefankiewicz
Crafting versatile modes of Pt^{II} complexes with flexidentate pyridyl-β-diketones: synthesis, structural characterization, and catalytic behavior in olefin hydrosilylation
ChemCatChem **2023**, *16*, e202301465; DOI: 10.1002/cctc.202301465
- A6** **G. Kurpik**, A. Walczak, P. Dydio, A. R. Stefankiewicz
Multi-stimuli-responsive network of multicatalytic reactions using a single palladium/platinum catalyst
Angewandte Chemie International Edition **2024**, *63*, e202404684; DOI: 10.1002/anie.202404684

3. Discussion of the research

PUBLICATION A1: Effect of the nuclearity on the catalytic performance of a series of Pd^{II} complexes in the Suzuki-Miyaura reaction.²⁰⁷

The development of polynuclear systems, which incorporate multiple densely packed catalytic sites within a single structure, presents a great opportunity to create novel catalysts or their precursors with enhanced activity. Due to the effect of nuclearity, also known as the effect of local concentrations, an increase in the number of catalytic centers within an individual molecule of the catalyst leads to higher reactivity, even while maintaining the same absolute concentration of metal ions.²⁰⁸⁻²¹² Therefore, a significant enhancement of catalytic activity can be achieved by embedding multiple metal centers on a precisely designed multifunctional core without increasing the catalyst loading. While homo- and heterometallic polymeric systems have been found to be efficient polynuclear catalysts across a broad range of organic reactions,²¹³⁻²¹⁶ the objective of the publication **A1** was to introduce a new family of oligonuclear complexes with high catalytic potential. As with larger species, *e.g.*, dendrimers and metallocupramolecular polymers, we hypothesized that the effect of nuclearity could be noteworthy for these relatively simpler coordination compounds as well. To explore this hypothesis, we designed a series of structurally related complexes, each comprising one, two, or three Pd^{II} centers *per* molecule. They were subsequently applied as catalysts in the model reaction of the Suzuki-Miyaura cross-coupling to examine the influence of increased nuclearity on their catalytic efficiency.

This study focused on a series of four metallocupramolecular Pd^{II} complexes, denoted as **C1–C4**, which are based on mono- and multidentate β -diketonate ligands: **HL1**, **H₂L2**, **H₂L3**, **H₃L4**, along with the 2,2'-bipyridine coligand (bpy). These ligands, recognized for their excellent chelating capabilities, served as scaffolds for Pd^{II} ions. The complexation reactions with a stoichiometric amount of [Pd(bpy)(NO₃)₂], used as a metal precursor, led to the formation of homometallic complexes, varying in the number of metal centers within the molecule (Figure 13).

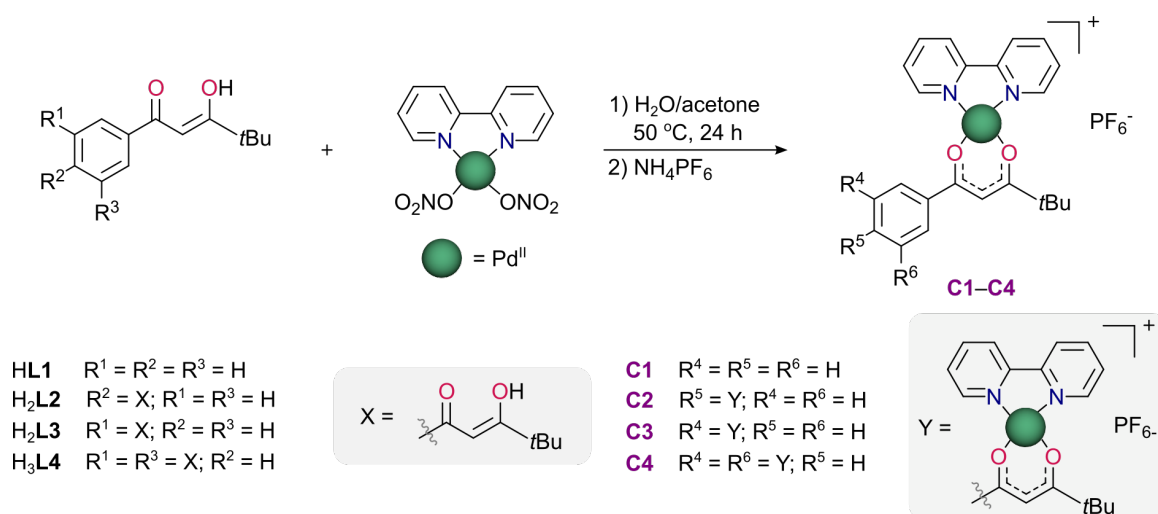


Figure 13. General reaction scheme for the synthesis of mono- and oligonuclear Pd^{II} complexes **C1–C4**.

The obtained complexes **C1–C4** were characterized in solution using NMR spectroscopy and mass spectrometry (ESI-MS), as well as in the solid state *via* X-ray diffraction. The ^1H NMR spectra recorded for the complexes **C1–C4** unequivocally confirmed the simultaneous involvement of both O,O' - and N,N' -chelates in the coordination of Pd^{II} ions. Using the complex **C4** as an example, the absence of enol proton signals near 16.5 ppm in the ^1H NMR, relative to the spectrum of H_3L_4 , shows complexation of Pd^{II} to have resulted in deprotonation of the β -diketonate moieties. In turn, the unsymmetrical structure of the bound β -diketonate entities is reflected in the loss of twofold symmetry of the signals attributed to the bpy coligands (Figure 14a). The successful formation of the desired complexes was also confirmed *via* ESI-MS analysis, as all identified signals were in good agreement with the calculated theoretical isotope distribution, thereby allowing the molecularity of **C1–C4** to be unambiguously established. Furthermore, the crystals obtained for the complexes **C1**, **C3**, and **C4** confirmed square planar geometry of Pd^{II} ions coordinated in a heteroleptic environment, where each Pd^{II} ion has an N_2O_2 coordination sphere, with chelation by both β -diketonate and bpy units (Figure 14b).

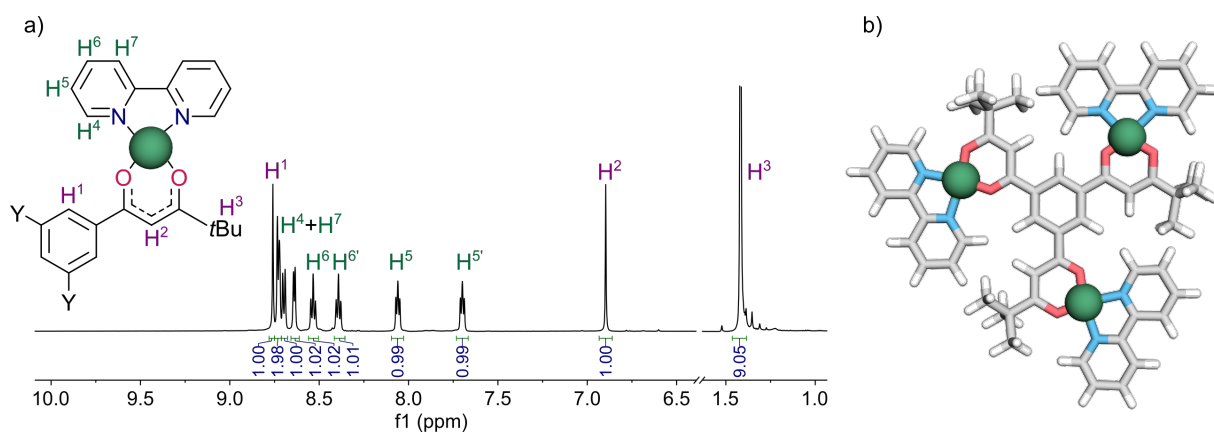


Figure 14. a) ^1H NMR spectrum (600 MHz, $\text{DMSO-}d_6$) of the complex **C4**. b) X-ray structure of **C4**.

To evaluate the impact of compositional differences on catalytic performance, the set of complexes **C1–C4** was applied as catalysts in the Suzuki-Miyaura cross-coupling, used as a model reaction. Initial studies utilized the mononuclear complex **C1** to identify optimal conditions for catalyzing the coupling between 4'-bromoacetophenone and phenylboronic acid. The highest catalytic activity was achieved in toluene at 80 °C, using K_2CO_3 as a base and a Pd loading of 0.1 mol%. Subsequently, a series of catalytic tests with structurally distinct aryl bromides and boronic acids were performed to explore the capabilities of the catalytic system and compare the efficiency of **C1–C4**. With the objective of demonstrating the influence of various nuclearity on catalytic activity, the same molar concentration of Pd^{II} centers was maintained in each catalytic reaction, ensuring that variations in reaction yields could not be ascribed to differences in Pd loadings. A number of reactions between functionalized substrates with electron-donating or electron-withdrawing groups was conducted under previously developed conditions and catalyzed by **C1–C4**. As determined *via* GC-MS analysis, most of the desired biphenyl derivatives **1–18** were obtained in good to excellent yields, depending on the catalyst used (Figure 15). Despite identical Pd loadings, comparative experiments showed that the trinuclear complex **C4** generally demonstrated the highest efficiency,

while the GC yields obtained for the mononuclear unit **C1** were the lowest. In turn, the results achieved with **C2** and **C3**, each comprising two catalytic sites in distinct locations, did not differ significantly. This allowed us to attribute the catalytic performance of **C1–C4** to the composition of these compounds, specifically to the number of Pd^{II} centers *per* complex molecule. A clear trend was observed, with catalytic activity increasing with the nuclearity of the complex.

Although a range of larger units, such as dendrimers and coordination polymers, have exhibited a positive effect of nuclearity in catalysis, systems based on oligonuclear complexes demonstrating this phenomenon are still very limited.²¹⁷⁻²¹⁹ While the origin of such reactivity enhancement is a subject of speculation, significant roles are attributed to increased local concentration, which allows for more efficient substrate binding, and to cooperative effects involving the assistance of nearby centers in catalytic cycles.^{208, 212, 220-222} Furthermore, an alternative explanation could be increased Lewis acidity of metal sites resulting from their proximity to each other. Consequently, polynuclear systems may possess more acidic catalytic centers compared to those with lower nuclearity, leading to enhanced binding of substrates, typically of a basic nature, and thereby favorably affecting the reaction course and the resulting yields.²²³⁻²²⁶

To conclude this part, a range of mono- and oligonuclear Pd^{II} complexes **C1–C4**, crafted with meticulously designed multitopic β -diketonate ligands and bpy coligand, has been introduced as a new class of catalysts for the Suzuki-Miyaura cross-coupling reaction. These units, diversified in terms of charge, composition, and morphology, demonstrated enhanced catalytic efficiency as the number of metal centers in the complex structure increased, while maintaining the same total Pd^{II} concentration. Therefore, this study presents a new example of the nuclearity effect on catalytic performance, specifically for relatively simple coordination compounds as opposed to macromolecular systems.

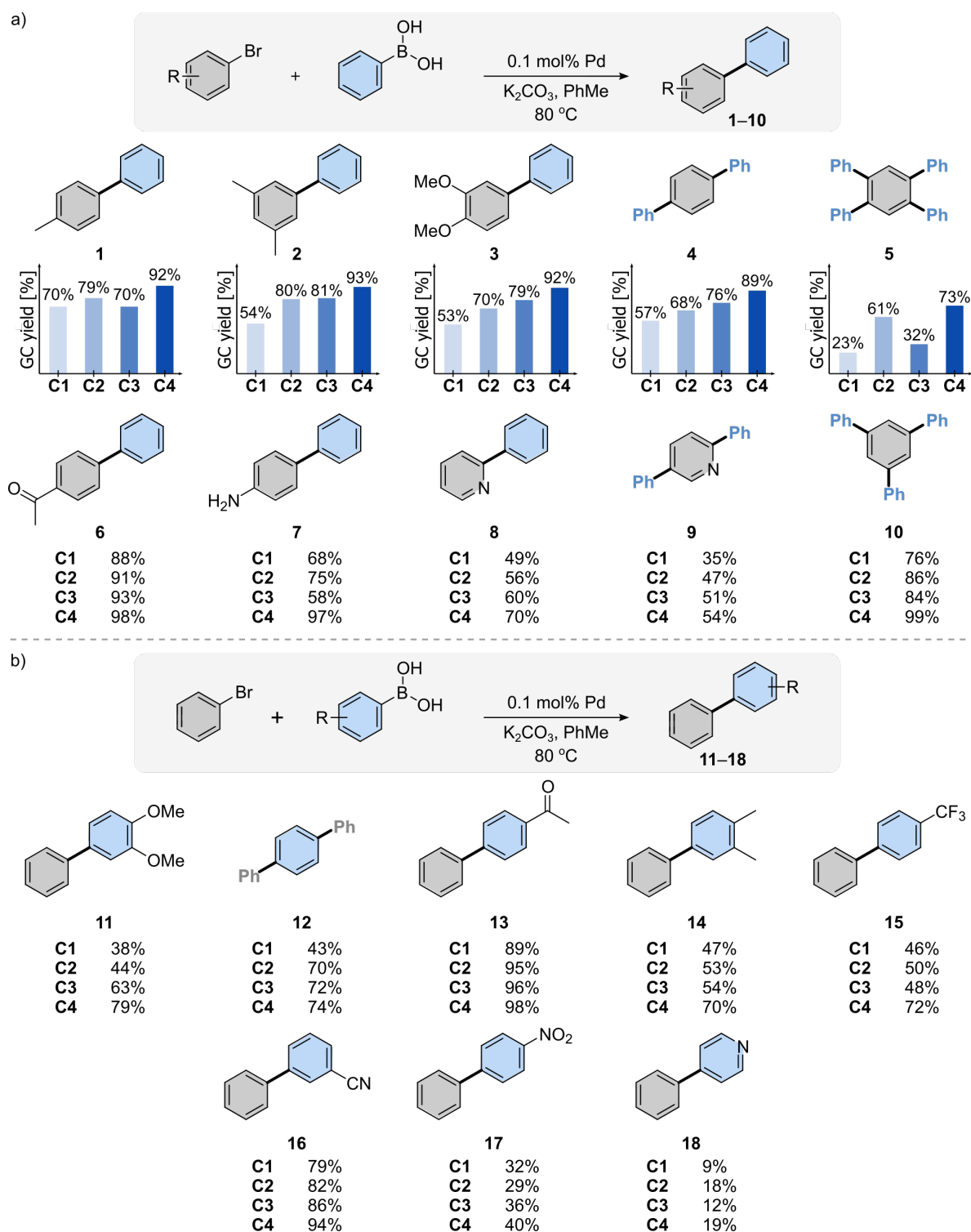


Figure 15. Scope of the Suzuki-Miyaura cross-coupling catalyzed by the complexes **C1–C4** between: a) structurally diverse aryl bromides and phenylboronic acid; b) bromobenzene and functionalized phenylboronic acids.

Reaction conditions: The reaction between ArBr (1.0 mmol) and ArB(OH)₂ (1.2 mmol) catalyzed by Pd^{II} complex (0.1 mol% Pd) was performed in the presence of K₂CO₃ (2.4 mmol) in toluene (10.0 mL) at 80 °C for 4–24 h. Yields determined by GC-MS analysis of aryl bromide decay.

* 0.5 mmol of ArBr was used (**4, 9**).

** 0.33 mmol of ArBr was used (**10**).

*** 0.25 mmol of ArBr was used (**5**).

**** 0.6 mmol of ArB(OH)₂ was used (**12**).

PUBLICATION A2: Pd^{II} complexes with pyridine ligands: substituent effects on the NMR data, crystal structures, and catalytic activity.²²⁷

As comprehensively described in the *Introduction* section, pyridine derivatives constitute a broad class of organic ligands for various transition metals. Structural modifications of the pyridine ring, achieved through functional groups incorporated as substituents, enable the modulation of the physicochemical properties of these ligands and, more importantly, the resulting coordination assemblies.^{84, 85} Accordingly, complexes with features tailored to specific applications can be generated. However, extensive investigations are still essential to provide a valuable guide for the rational design and synthesis of novel architectures with predictable structure-dependent properties.

Hence, in the work **A2**, an array of pyridine ligands was employed to create a wide variety of structurally distinct Pd^{II} complexes. We anticipated that the physicochemical properties of these coordination compounds could be tuned by the functionalization of ligand molecules with either electron-withdrawing or electron-donating groups. The in-depth structural characterization performed *via* ¹H NMR spectroscopy, ESI-MS analysis, and X-ray diffraction clearly indicated the dependence of certain features on the ligand basicity. While the Lewis basicity remains unmeasurable, the Brønsted basicity of pyridine derivatives, estimated as p*K*_a values, served as a convenient parameter to assess the effect of substituents on pyridine-*N* donor behavior.^{86, 228-230} Additionally, the factors that determine their catalytic performance in the Suzuki-Miyaura and Heck cross-coupling reactions were examined, leading to the identification of the most effective catalyst precursors for these processes.

A broad range of 4-substituted pyridine derivatives **L5–L16** was selected as building blocks for constructing Pd^{II} complexes with square planar geometry. The developed synthetic strategies, which are primarily diversified in terms of reaction stoichiometry but also consider factors such as solvent, temperature, and metal precursor, are detailed in Figure 16. Consequently, three families of compounds were obtained, *i.e.*, disubstituted species with the general formula *trans*-[PdL₂X₂], where X = Cl⁻ or NO₃⁻, and tetrasubstituted units [PdL₄](NO₃)₂. While a complete set of the compounds was obtained exclusively for the [PdL₂Cl₂] family, specific preferences related to the ligand basicity were noted in the formation of the other two classes of complexes. The equilibrium of complexation reactions appeared to be shifted toward the generation of [PdL₂(NO₃)₂] for the less basic ligands (**L12**, **L13**) and [PdL₄](NO₃)₂ for the strongly basic ligand (**L10**), which may explain why some species could not be isolated. In turn, the substituents of ligands **L14–L16** introduced additional donor groups that likely competed with nitrate counterions, leading to the formation of complexes **C14'–C16'** as inseparable mixtures. The structures of all the synthesized complexes were unambiguously determined in solution using ¹H NMR spectroscopy and ESI-MS analysis, as well as in the solid state by X-ray diffraction.

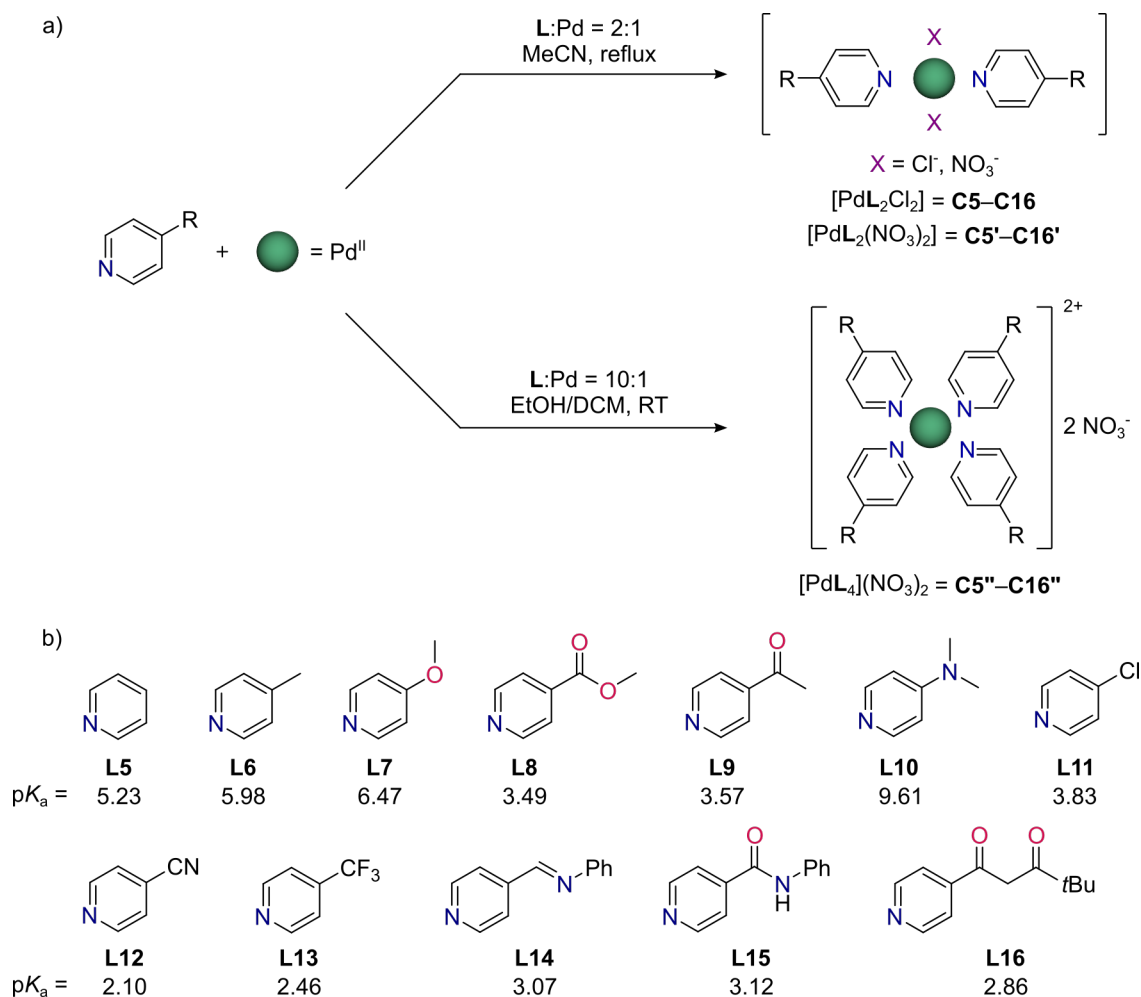


Figure 16. a) Synthesis of Pd^{II} complexes with pyridine ligands. b) Structures and the literature pK_a values^{84, 231, 232} of the ligands **L5–L16**.

Analysis of the ¹H NMR spectra of the complexes revealed a high degree of similarity, except for the signals corresponding to the different substituents. The data showed that the twofold symmetry of the pyridine derivatives was preserved, with all ligand molecules within a given compound being equivalent. More significant differences were observed in the chemical shifts, particularly for the H¹ protons on the carbon atoms adjacent to the pyridine-*N* donor atoms. Furthermore, in the ¹H NMR spectra of the [PdL₂(NO₃)₂] complexes, an additional set of signals was observed, attributed to the presence of minor amounts (<10%) of the *cis* isomer in solution. In comparison to the ¹H NMR spectra of the free ligands, the downfield chemical shifts in the spectra of the [PdL₂X₂] complexes clearly indicated the coordination of Pd^{II} ions, however, the most notable differences were seen for the tetrasubstituted units, with shifts of approximately 0.5–1.0 ppm. To explain the unprecedented chemical shifts, observed for analogous complexes with Pt^{II} ions as well,⁸⁴ it was suggested that the dominant effect may arise from ion pairing involving multiple stabilizing C–H¹⋯ONO₂ interactions, which were also noted in the solid state. Interestingly, the H¹ chemical shifts exhibited a nearly linear correlation with the pK_a values of the pyridine ligands, implying that the effects of substituents are still relevant, alongside any contributions from Pd^{II} coordination (Figure 17).

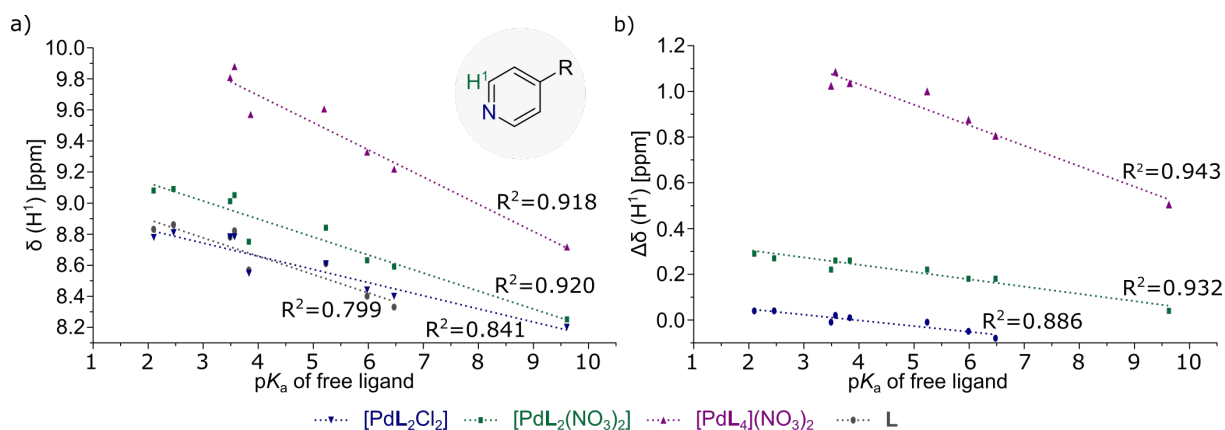


Figure 17. a) Relationships between the chemical shifts (δ , ppm) of the signal H^1 in the 1H NMR spectra (300 MHz, $CDCl_3$) and pK_a values of free ligands for the Pd^{II} complexes. b) Relationships between the chemical shift changes ($\Delta\delta$, ppm) of the signal H^1 in the 1H NMR spectra (300 MHz, $CDCl_3$) and pK_a values of free ligands for the Pd^{II} complexes.

X-ray diffraction analysis allowed for the establishment of the solid-state structures of thirteen complexes across three distinct classes, with representative structures based on the ligand **L11** shown in Figure 18. The structure determinations confirmed the unidentate *N*-coordination of the pyridine ligands in all cases, as well as the *trans* configuration of the disubstituted $[PdL_2X_2]$ species. The fundamental features, such as bond lengths and bond angles, were consistent with those of other Pd^{II} species reported in the literature. Additionally, X-ray diffraction provided insights into the weak interactions within the crystals, particularly those involving the substituents of the heterocyclic ring and the counterions.

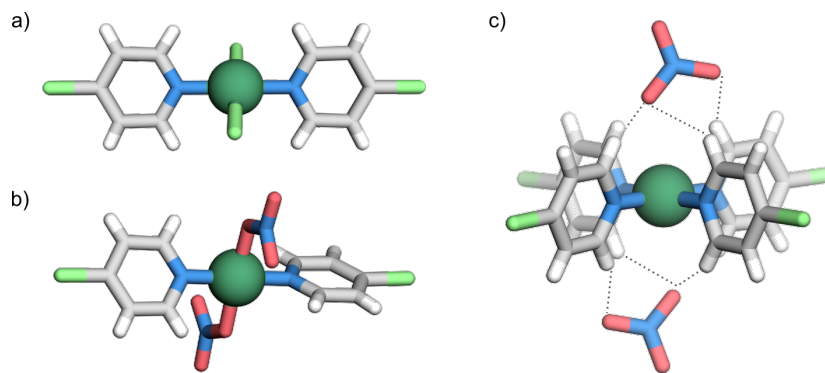


Figure 18. X-ray structures of the Pd^{II} complexes based on **L11**: a) $[Pd(L11)_2Cl_2]$ (**C11**); b) $[Pd(L11)_2(NO_3)_2]$ (**C11'**); c) $[Pd(L11)_4(NO_3)_2]$ (**C11''**). The solvent molecules were omitted for clarity.

As exemplified by the complexes **C6**, **C6'**, and **C6''** representing the three families, the complexes could be transformed into others under specific conditions. Titration experiments monitored by 1H NMR spectroscopy demonstrated that the complex **C6'** was irreversibly converted into **C6''** under basic conditions (Et_3N), while the addition of methanesulfonic acid (MSA) induced the transformation of **C6''** to **C6'**, a process that could be reversed upon neutralization. In contrast, titrations of **C6'** with MSA and **C6''** with Et_3N showed no significant changes, and **C6** was found to be completely insensitive in both the acidic and basic environments. Furthermore, the complex **C6''** was readily transferred into **C6** upon the addition of $Et_3N \cdot HCl$ as a source of chloride anions, highlighting the lability of the tetrasubstituted species.

In addition to the substituent effects on coordination behavior, NMR data, and crystal structures, we also hypothesized their impact on the functionality of the complexes. Therefore, we expanded our investigations by employing them as catalyst precursors in the Suzuki-Miyaura and Heck cross-coupling reactions, anticipating that the compositional and structural differences would be reflected in catalytic efficiency. The reaction conditions were initially developed using **C6''**, after which a diverse range of structurally distinct Pd^{II} complexes was tested under these optimized conditions.

Most of the Pd^{II} complexes exhibited high catalytic activity in the model reaction between 4'-bromoacetophenone and phenylboronic acid, resulting in the desired product in >90% yield. While only minor differences were observed between di- and tetrasubstituted compounds with the same ligand, leading to the conclusion that the nature of the complex does not significantly affect catalytic efficiency, more substantial disparities were noted depending on the type of substituent (Table 2). In some cases, particularly for the species based on **L8**, **L11**, **L12**, **L13**, and **L15**, the GC yields were lower, ranging from 64% to 87%. Although no straightforward correlation was observed between GC yields and the pK_a values of the pyridine ligands, Pd^{II} complexes with more basic ligands generally exhibited slightly higher catalytic activity. Furthermore, these Pd^{II} units demonstrated high efficiency in the Heck cross-coupling between styrene and iodobenzene, resulting in the formation of the expected *trans*-stilbene, in reaction yields predominantly exceeding 90% (Table 2). Despite the high GC yields in all cases, minor differences between the tetrasubstituted complexes and their disubstituted analogues were noted, with the latter generally showing slightly better performance, especially for the ligands **L7**, **L8**, **L11**, and **L16**. Nevertheless, the effect of any ring substituent was minimal, and no clear relationship was established between the ligand basicity and catalytic performance in this process as well.

Table 2. GC yields [%] in the Suzuki–Miyaura and Heck cross-coupling reactions catalyzed by Pd^{II} complexes based on the pyridine ligands **L5**–**L16**.

L	pK _a of L	GC yields [%] in Suzuki-Miyaura coupling ^a			GC yields [%] in Heck coupling ^b		
		PdL ₂ Cl ₂	PdL ₂ (NO ₃) ₂	[PdL ₄](NO ₃) ₂	PdL ₂ Cl ₂	PdL ₂ (NO ₃) ₂	[PdL ₄](NO ₃) ₂
L5	5.23	97	93	95	85	88	90
L6	5.98	93	92	98	90	91	94
L7	6.47	93	91	91	86	82	76
L8	3.49	78	72	64	89	92	79
L9	3.57	86	87	88	80	92	75
L10	9.61	93	-	90	86	-	83
L11	3.83	82	74	75	90	92	80
L12	2.10	88	66	-	91	93	-
L13	2.46	87	70	-	81	91	-
L14	3.07	98	-	90	93	-	88
L15	3.12	86	-	79	88	-	90
L16	2.86	83	-	92	92	-	77

^a Reaction conditions: The reaction between 4'-bromoacetophenone (0.2 mmol) and phenylboronic acid (0.24 mmol) catalyzed by Pd^{II} complex (0.1 mol%) was performed in the presence of K₃PO₄ (0.4 mmol) in toluene (2.0 mL) at 80 °C for 2 h. Yields determined by GC-MS analysis of 4'-bromoacetophenone decay.

^b Reaction conditions: The reaction between iodobenzene (0.2 mmol) and styrene (0.24 mmol) catalyzed by Pd^{II} complex (0.1 mol%) was performed in the presence of Et₃N (1.0 mmol) in DMSO (2.0 mL) at 120 °C for 2 h. Yields determined by GC-MS analysis of iodobenzene decay.

Complex **C6''**, a representative of the broad class of Pd^{II} compounds studied, was selected to explore the scope of both the Suzuki-Miyaura and Heck reactions. A series of experiments revealed high catalytic activity, regardless of the nature of the substrates functionalized with electron-withdrawing or electron-donating groups. As shown in Figure 19, a range of structurally distinct products **19–36**, including biphenyl, stilbene, and acrylate derivatives, were obtained in good to excellent yields. This clearly highlights significant versatility, indicating that complexes from this family could be effectively employed in other Pd-catalyzed processes.

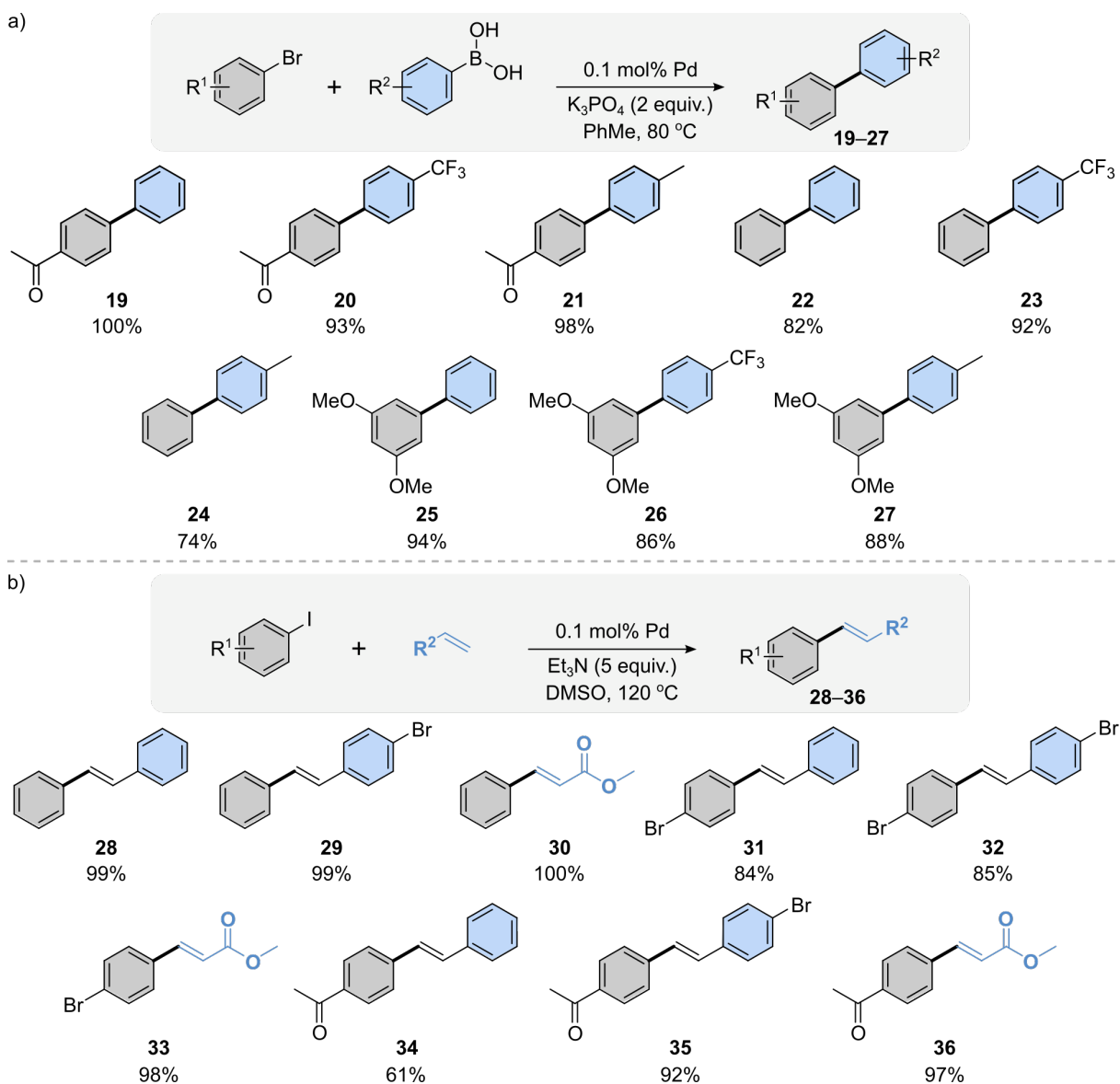


Figure 19. a) Scope of the Suzuki-Miyaura cross-coupling reaction catalyzed by the complex **C6''**. b) Scope of the Heck cross-coupling reaction catalyzed by the complex **C6''**.

Reaction conditions for the Suzuki-Miyaura coupling: The reaction between ArBr (1.0 mmol) and ArB(OH)₂ (1.2 mmol) catalyzed by **C6''** (0.1 mol% Pd) was performed in the presence of K₃PO₄ (2.4 mmol) in toluene (10.0 mL) at 80 °C for 2 h. Yields determined by GC-MS analysis of aryl bromide decay.

Reaction conditions for the Heck reaction: The reaction between ArI (1.0 mmol) and olefin (1.2 mmol) catalyzed by **C6''** (0.1 mol% Pd) was performed in the presence of Et₃N (2.4 mmol) in DMSO (10.0 mL) at 120 °C for 2 h. Yields determined by GC-MS analysis of aryl iodide decay.

In conclusion, a variety of Pd^{II} complexes based on multiple functionalized pyridine derivatives have been successfully synthesized and characterized both in solution and in the solid state. Their physicochemical properties were investigated in relation to ligand basicity, revealing the effects of substituents on spectroscopic and crystallographic data, and determining their functionality in catalysis. These systems have been demonstrated to serve as simple and efficient catalyst precursors for the Suzuki-Miyaura and Heck reactions within a diverse array of substrates under relatively mild conditions.

PUBLICATION A3: Enhanced catalytic performance derived from coordination-driven structural switching between homometallic complexes and heterometallic polymeric materials.²³³

While pyridyl- β -diketonate ligands were extensively discussed in the *Introduction*, a representative of this class, 4,4-dimethyl-1-(pyridin-4-yl)pentane-1,3-dione (**HL16**), was utilized in the publication **A3** to generate a series of homo- and heterometallic systems with Ag^I, Pd^{II}, and Pt^{II} ions. In this work, we focused on a unique feature of these assemblies, specifically their switchable character. The ambidentate nature of the ligand enabled numerous transformations between different coordination modes, triggered by various external stimuli such as metal salt addition or acid–base equilibria, which created a network of coordination-driven structural switching processes, ultimately resulting in the synthesis of new metallosupramolecular polymers. Additionally, we explored the application potential of these heterometallic aggregates, demonstrating their enhanced catalytic activity in the Heck cross-coupling reaction compared to their mononuclear constituents.

As illustrated in Figure 20, the pyridyl- β -diketonate ligand **HL16** was utilized in the synthesis of mononuclear complexes with Ag^I, Pd^{II}, and Pt^{II} ions, coordinated by either *N*-donors or *O,O'*-chelates depending on the reaction conditions. The reaction of **HL16** with Ag^I salt led to the formation of the disubstituted species [Ag(**HL16**)₂]₂NO₃ (**C17**), while previously reported procedures allowed for the preparation of the Pd^{II} and Pt^{II} complexes, specifically [Pd(**HL16**)₄](NO₃)₂ (**C19**), [Pt(**HL16**)₄](NO₃)₂ (**C20**), and [Pd(**L16**)₂] (**C22**).^{113, 118} In turn, using [Pd(en)(NO₃)₂] in the complexation reaction with **HL16** led to the synthesis of heteroleptic units, namely [Pd(en)(**HL16**)₂](NO₃)₂ (**C18**) and [Pd(en)(**L16**)]NO₃ (**C21**), in neutral or basic environments, respectively. The generation of all the complexes was successfully confirmed *via* ¹H NMR spectroscopy and ESI-MS analysis, and the structure of **C17** was established *via* X-ray diffraction. (*The crystal structures of C19, C20, and C22 were also determined in previous works.*^{113, 118})

Given the presence of free coordination sites and the different kinetic stability of **C17–C22**, we conducted extensive studies, followed by ¹H NMR titration experiments, to investigate coordination-driven structural switching between specific units (Figures 20–21). As described above, the reaction between **HL16** and Ag^I salt gave the complex **C17**, with β -diketonate moieties not involved in metal coordination. Whereas its use as a metalloligand in further complexation reactions would require deprotonation, this approach was excluded due to the decomposition of **C17** in a basic environment. However, the complex **C17** could be completely converted into **C19** and **C20** upon the addition of Pd(NO₃)₂ or Pt(NO₃)₂, respectively. A similar effect was achieved with [Pd(en)(NO₃)₂], resulting in the generation of the heteroleptic compound **C18**. The complexes **C18–C20** formed through metal ion exchange reactions, were subsequently exposed to the influence of a base (Et₃N). The addition of a base to a solution of **C19**, with coordination by four *N*-donors, induced a linkage rearrangement to *O,O'*-chelated forms and the creation of **C22**, a reaction that could be reversed by neutralization with MSA. Similarly, the titration of **C18** with Et₃N led to the formation of **C21**. In contrast, the Pt^{II} complex **C20** did not undergo any transformation in a basic environment, likely due to the greater kinetic inertness of Pt^{II} ions

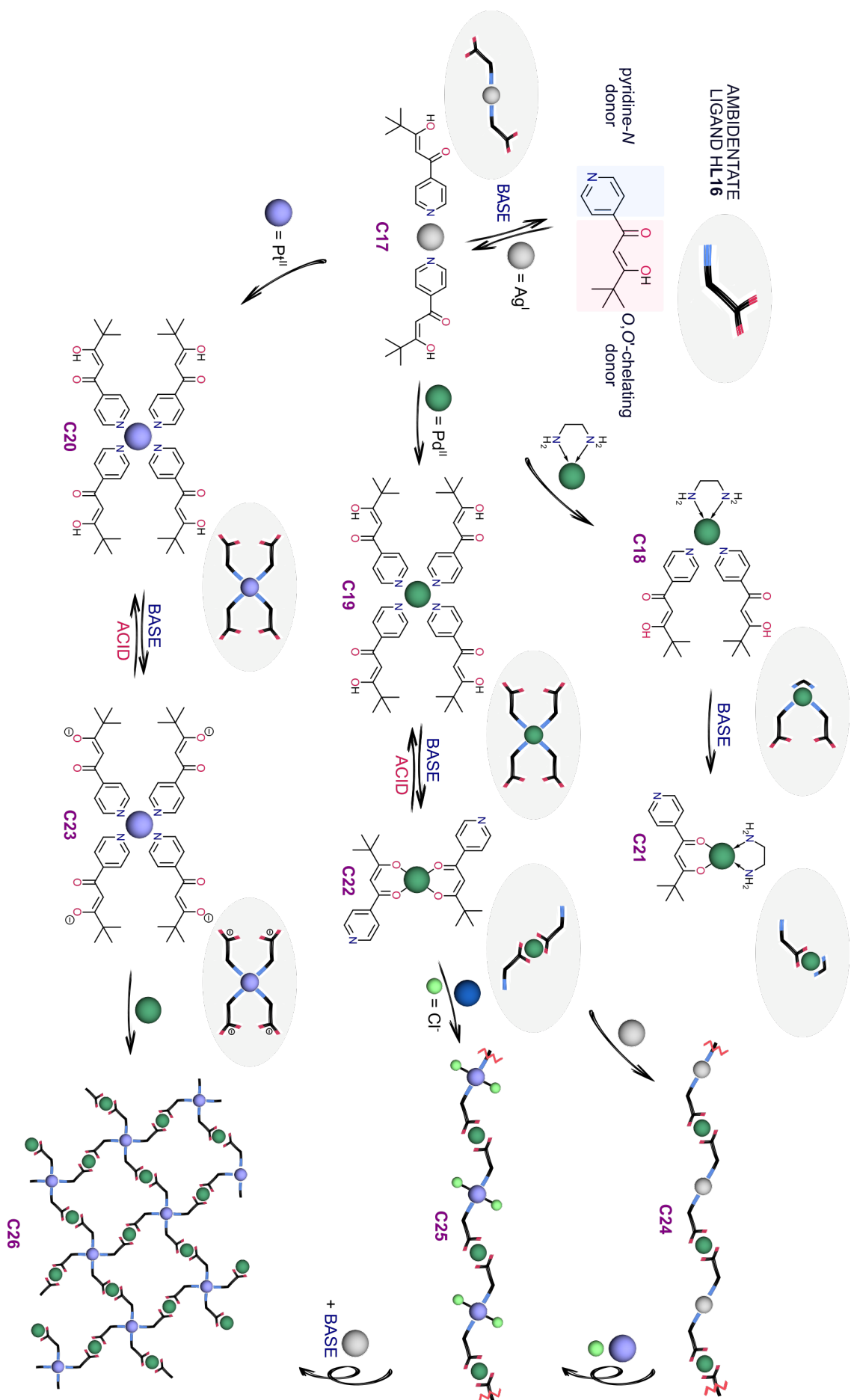


Figure 20. Stimuli-responsive supramolecular transformations within coordination-driven assemblies based on the pyridyl- β -diketonate ligand HL16.

compared to Pd^{II}. Under basic conditions, the uncoordinated β -diketonate moieties were deprotonated, while the complex structure remained intact. Additionally, the presence of accessible coordination sites in the structures of **C22** and **C23**, which are capable of reacting with additional metal centers, suggested their potential to function as metalloligands. Specifically, the reaction of **C22** with Ag^I or Pt^{II} salt led to the creation of new heterometallic aggregates **C24** and **C25**. While O,O'-chelation was preserved for Pd^{II} centers, Ag^I or Pt^{II} ions were bound by two pyridine-N donors, with the chloride ligands simultaneously retained in the coordination sphere of Pt^{II}. In turn, the ability of the enol units to be deprotonated without the complex decomposition enabled the generation of the branched polymer **C26** in the reaction of **C23** with Pd(NO₃)₂. The coordination-driven structural switching strategies developed for the complexes **C17**–**C23** were successfully

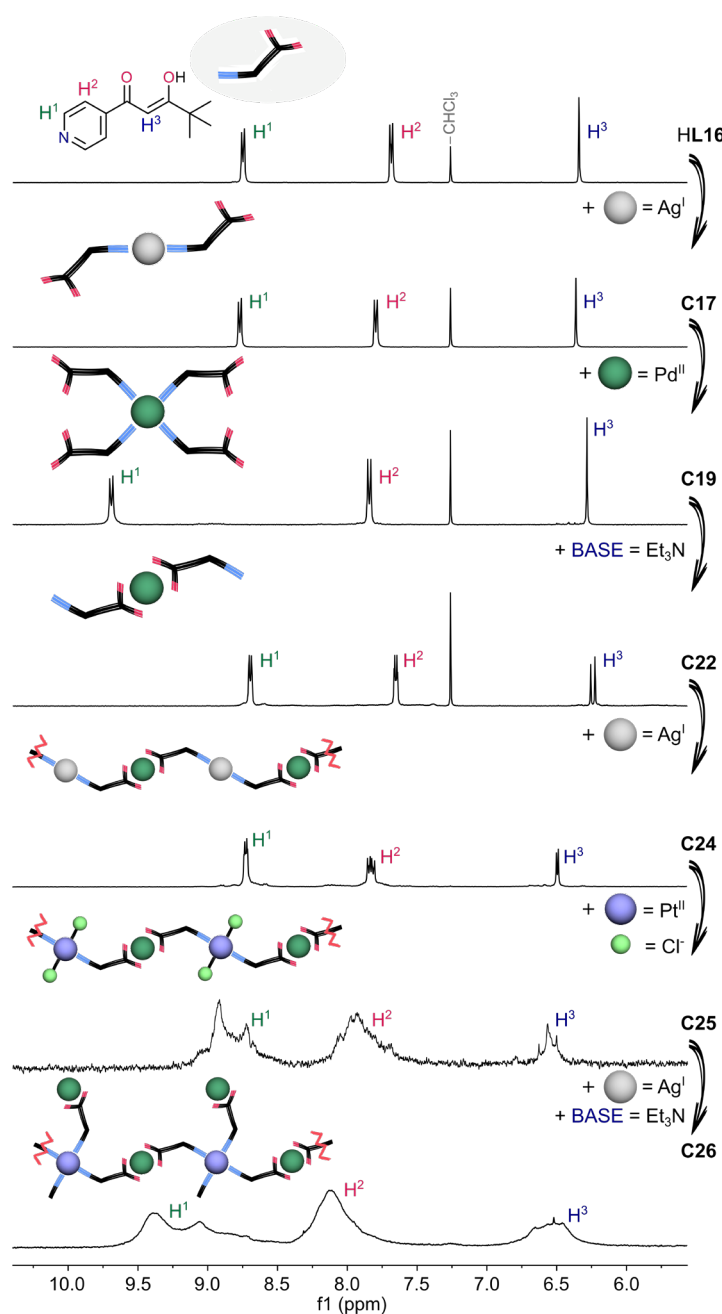


Figure 21. Parts of ¹H NMR spectra (600 MHz, CDCl₃ or DMSO-*d*₆ for **C24**–**C26**), illustrating the coordination-driven structural switching triggered by the addition of a metal salt or base.

applied in the transformations of coordination polymers **C24–C26**, allowing for the conversion of **C24** into **C25** upon the addition of PtCl_2 , and the transformation of **C25** into **C26** following the addition of AgNO_3 in the presence of a base (Figure 21).

The characterization of the heterometallic materials **C24–C26** was performed through the combination of analysis in solution with solid-state techniques. Although the ^1H NMR spectra recorded in $\text{DMSO-}d_6$ showed a set of broadened and overlapping signals that are not readily interpretable, their profiles are consistent with the generation of complex metalloaggregates (Figure 21). ESI-MS analysis confirmed the formation of the heterometallic assemblies, as the mass spectra revealed the presence of fragmentary constituents comprising chains of successive monomers linked by additional metal centers. XPS and ICP-MS analyses were performed to verify the presence of the expected metal pairs, identifying Ag and Pd in **C24**, and Pd and Pt in **C25** and **C26**. Moreover, the percentage contribution of individual metal ions, as determined by ICP-MS, corresponded well with the calculated values for each material. ATR-FTIR analysis confirmed the involvement of β -diketonate and pyridine-*N* donors in the coordination. The FTIR spectra demonstrated that the formation of the metalloaggregates resulted in red shifts of the bands associated with the $\nu(\text{C}=\text{O})$ and $\nu(\text{py})$ vibrations of the ligand functional groups. The polymers **C24–C26** were also analyzed using scanning electron microscopy (SEM) to determine their morphology. Depending on their one- or two-dimensional structures, the SEM images exhibited irregular clusters of various nanometer-scale sizes and quasi-spherical shapes. The SEM results were consistent with those from powder X-ray diffraction (pXRD), as the diffractograms for **C24–C26** confirmed their amorphous nature. In turn, EDS mapping demonstrated the topographic distribution of individual elements within the solids, revealing a uniform and consistent arrangement of the metal pairs in each sample. The stability of the polymers was investigated *via* thermogravimetric analysis (TGA). The stepwise decomposition led to the formation of mixtures of appropriate metal oxides as residue, with amounts corresponding to theoretical calculations.

Due to the presence of multiple Pd^{II} centers in the structures of the heterometallic polymers, they were considered excellent candidates to evaluate their catalytic activity. Among various Pd-catalyzed processes, the Heck cross-coupling was chosen as the model reaction. The conditions were optimized for the coupling of iodobenzene with styrene catalyzed by **C25**, resulting in the expected *trans*-stilbene in the highest yield, when the reaction was carried out in DMSO at 100 °C with Et_3N as the base and 0.05 mol% Pd.

At the next stage, a series of catalytic tests were conducted to investigate the effect of compositional differences on the catalytic performance of the heterometallic aggregates (Figure 22a). The same concentration of Pd was used in each reaction, and the catalyst loading for **C24–C26** was determined *via* ICP-MS analysis. As mentioned earlier, increased local concentrations of catalytic sites enhance the catalytic performance of polynuclear species,^{207, 208, 214} which was demonstrated by the high efficiency of **C24–C26**. In contrast, the mononuclear complex **C22**, as a building block of all the polymers, exhibited notably lower catalytic activity, likely due to the lack of cooperative effects from neighboring metal centers. Although the yields in the reactions catalyzed by **C24–C26** are generally approximate, the slightly lower efficiency of **C24** may be attributed to decreased

stability caused by labile Ag^{I} ions, while the reduced catalytic activity of **C26** may result from the limited accessibility of catalytic sites within its two-dimensional structure. Thus, **C25** was identified as the most efficient unit among those examined, and this system was subsequently utilized to explore the scope and limitations of the Heck cross-coupling between structurally distinct substrates (Figure 22b). In all cases, the desired products were obtained in high to excellent yields, ranging from 76% to 100%, regardless of the nature of the substituents. Noteworthy is the high selectivity for the (*E*)-configuration in the product formation, with (*Z*)-isomers constituting no more than 10%, as determined by GC-MS distribution.

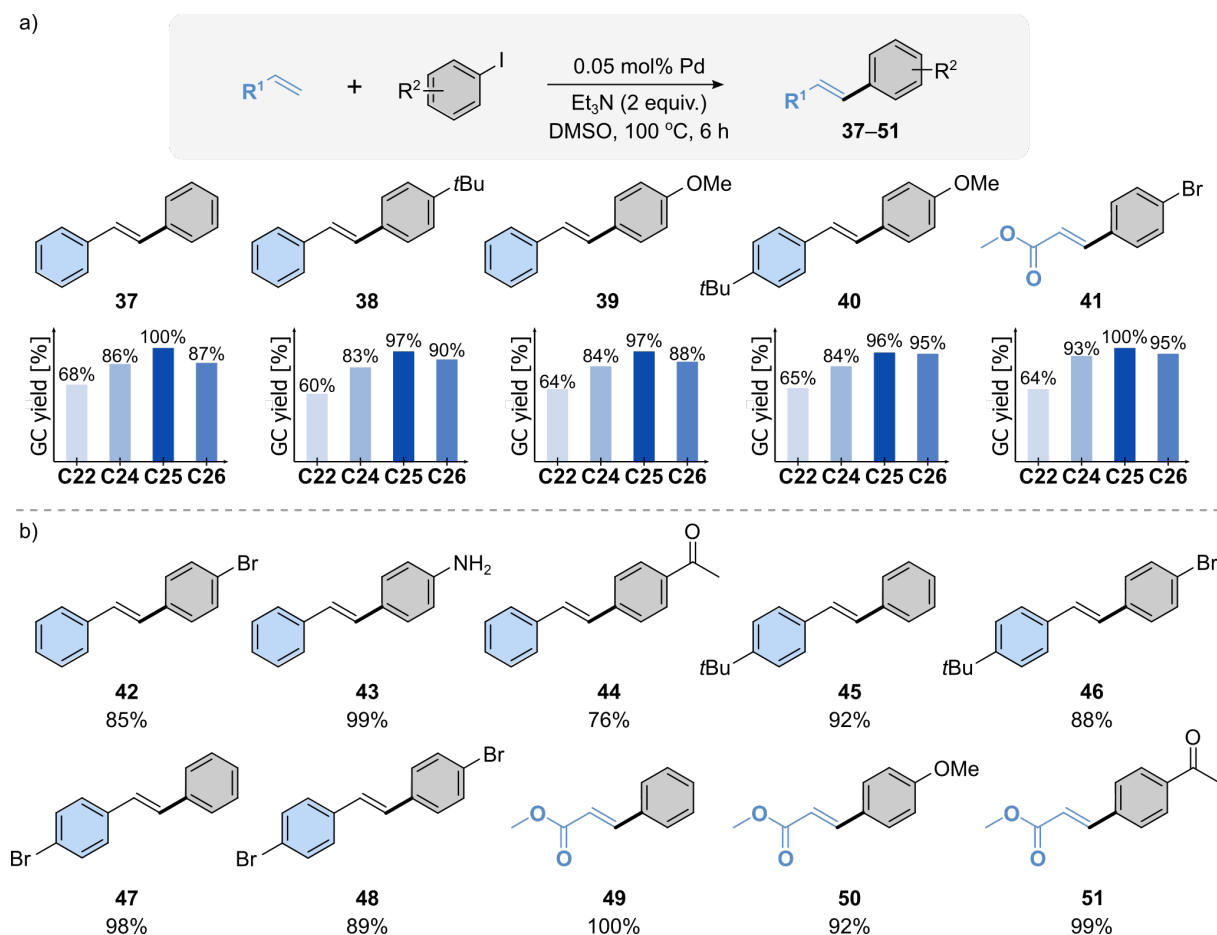


Figure 22. a) Different catalytic performance of the complex **C22** and the heterometallic polymers **C24–C26** in the Heck reaction. b) Scope of the Heck cross-coupling reaction catalyzed by **C25**.

Reaction conditions: The reaction between ArI (0.5 mmol) and olefin (0.5 mmol) catalyzed by Pd^{II} complex (0.05 mol% Pd) was performed in the presence of Et_3N (1.0 mmol) in DMSO (1.0 mL) at 100 °C for 6 h. Yields determined by GC-MS analysis of aryl iodide decay.

In summary, a diverse array of mono- and polynuclear systems based on the ambidentate pyridyl- β -diketonate ligand has been designed, synthesized, and comprehensively characterized. This work defines an efficient strategy for coordination-driven structural switching, as exemplified by the numerous supramolecular transformations between homometallic complexes and heterometallic polymeric materials. Our findings demonstrate that variations in nuclearity, composition, and morphology of the coordination assemblies significantly affect their catalytic performance in the Heck cross-coupling reaction.

PUBLICATION A4: $C(sp^3)$, N palladacyclic complexes bearing flexidentate ligands as efficient (pre)catalysts for Heck olefination of aryl halides.²³⁴

In a previous report from the Stefankiewicz group, pyridyl- β -diketonate ligands, specifically 2,2-dimethyl-5-(3- or 4-pyridyl)pentane-3,5-dione (HL16 and HL17), were utilized to form Pd^{II} complexes, which exhibited the typical O,O' -chelation of the β -diketone moiety or pyridine- N donation.¹¹³ In the publication **A4**, we employed the isomeric ligand, 2,2-dimethyl-5-(2-pyridyl)pentane-3,5-dione (HL18), where the donor atoms are arranged to function as an N,O -donor and, upon methylene deprotonation, as an N,C -donor. Thus, our efforts were directed toward determining the structure of Pd^{II} complexes bearing the pyridyl- β -diketonate ligand HL18. As a consequence, new organometallic species have been identified as geometric isomers with an unprecedented coordination mode, where one ligand molecule coordinates as an O,O' -chelate and another as an $N,C(sp^3)$ -chelate within a single complex. Given the broad potential applications of palladacyclic complexes as catalysts in cross-coupling reactions,²³⁵⁻²³⁷ their high catalytic activity was demonstrated in the Heck olefination reaction.

The reaction of the ligand HL18 with a Pd^{II} salt in a 2:1 molar ratio under basic conditions resulted in the generation of new organometallic complexes in the form of *cis* and *trans* isomers (Figure 23). While the *trans* isomer **C27** was isolated through selective crystallization, the *cis* isomer **C28** was separated from the mixture of both forms by mechanical selection. The structures of these compounds were established *via* X-ray diffraction measurements, which revealed a distorted pseudo-square planar geometry of the Pd^{II} ions with a CNO₂ coordination environment (Figure 24a). In their structure, the metal centers are coordinated by the β -diketonate moiety on one side and by the $N,C(sp^3)$ -donor on the other, resulting in the creation of stable five- or six-membered rings. The arrangement of the *tert*-butyl substituents determined their designation as *cis*

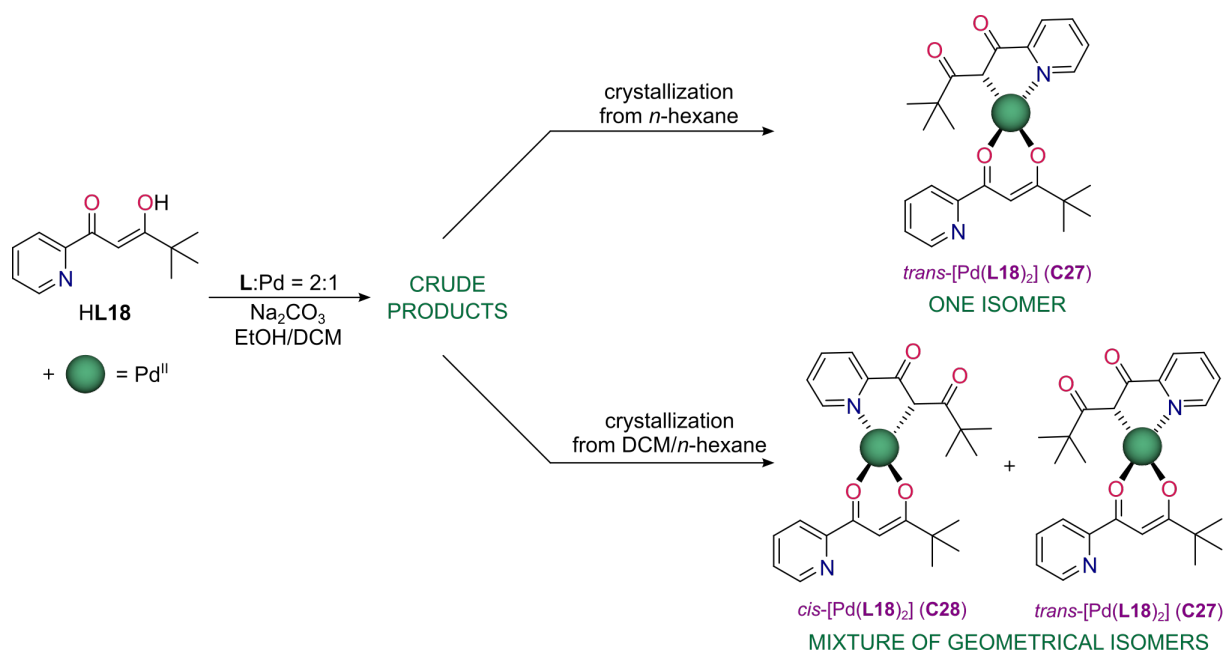


Figure 23. General reaction scheme for the synthesis of organometallic complexes **C27** and **C28**.

or *trans* isomers, based on their proximal or distal locations, respectively. It is also worth noting that the complexes exist as enantiomers, with both forms distributed in crystals.

In solution, the organometallic complexes were analyzed in two forms: as the pure *trans* isomer and as a mixture of *cis* and *trans* isomers, since the *cis* isomer was not isolated in sufficient quantities for complete characterization. The composition of **C27** and **C28** was unequivocally established *via* ESI-MS analysis, confirming the generation of compounds with the general formula $[\text{Pd}(\text{L18})_2]$. More detailed characterization was achieved using NMR measurements (Figure 24b). The ^1H NMR spectrum of **C27** clearly indicated that the solid-state structure is retained in solution, displaying duplicated signals consistent with the coordination of two ligand molecules as *O,O'*- and *N,C*-chelates. The *trans* geometry was verified based on 1D NOESY NMR analysis. In turn, the ^1H NMR spectrum recorded for the mixture of two geometric isomers revealed two sets of signals of approximately equal intensity, however, by subtracting the signals of the *trans* isomer, the signals corresponding to the *cis* isomer could be identified. Furthermore, *cis-trans* isomerization was followed *via* ^1H NMR spectroscopy as the chloroform solution of **C27** was heated from 25 to 60 °C. The percentage of the *cis* isomer increased with temperature, attaining a 2:3 molar ratio (*cis* to *trans*) at 60 °C, which remained unchanged upon cooling, even after several days.

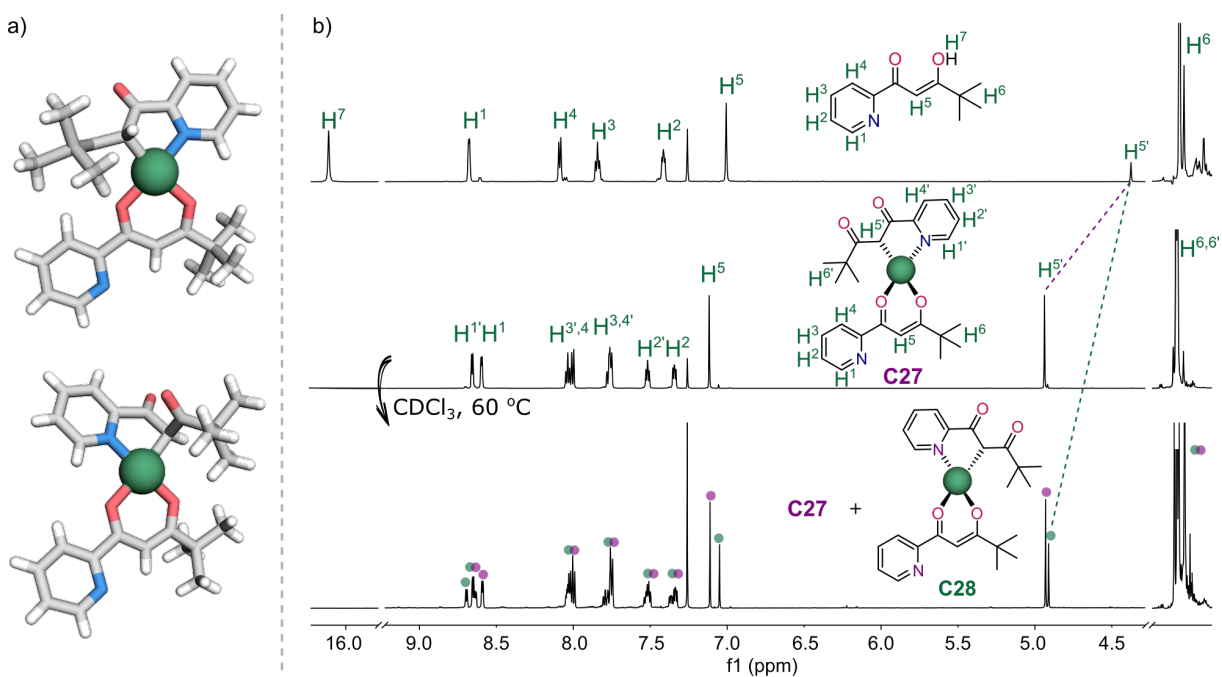


Figure 24. a) X-ray structures of two isomeric complexes: *cis*- and *trans*- $[\text{Pd}(\text{L18})_2]$. b) The stacked ^1H NMR spectra (600 MHz, CDCl_3) of **HL18**, the pure complex **C27**, and the mixture of isomers **C27**–**C28**.

In the context of catalytic studies, the stability of the complexes was investigated in a basic environment. Their structure remained essentially intact even after the addition of a sixfold excess of base (Et_3N), and no signs of decomposition or transformation were observed after heating and storing the samples for 7 days. Thus, the potential of these palladacyclic compounds as catalysts was evaluated in the Heck cross-coupling reaction, which was selected as the model system. Initial studies utilized the *trans* isomer **C27** to determine the optimal conditions for the coupling between 4-iodotoluene and styrene. The highest GC yields (>99%) and excellent selectivity toward the

formation of the *trans*-product were achieved in the reaction performed in DMF at 100 °C, using K_3PO_4 as the base and 0.5 mol% Pd. It was further established that the mixture of geometric isomers exhibited catalytic activity comparable to that of the pure *trans* isomer, consistent with the observed thermal equilibration between the two forms of the organometallic complex. Furthermore, under the conditions developed for **C27**, classical catalytic systems comprising either $Pd(dba)_2$ (0.5 mol%)/ PPh_3 (2 mol%) or $[PdCl_2(PPh_3)_2]$ (0.5 mol%) resulted in a maximum conversion of only 80%, thereby demonstrating the great performance of our system. With these results in hand, the scope of this method was investigated, involving a diverse range of functionalized aryl iodides and olefins. Numerous experiments confirmed the high efficiency of these new catalysts, as evidenced by good to excellent GC yields in most cases (Figure 25). In addition to its remarkable regioselectivity, the catalytic system also exhibited chemoselectivity for iodoarenes, with no cross-coupling involving bromoarene moieties observed.

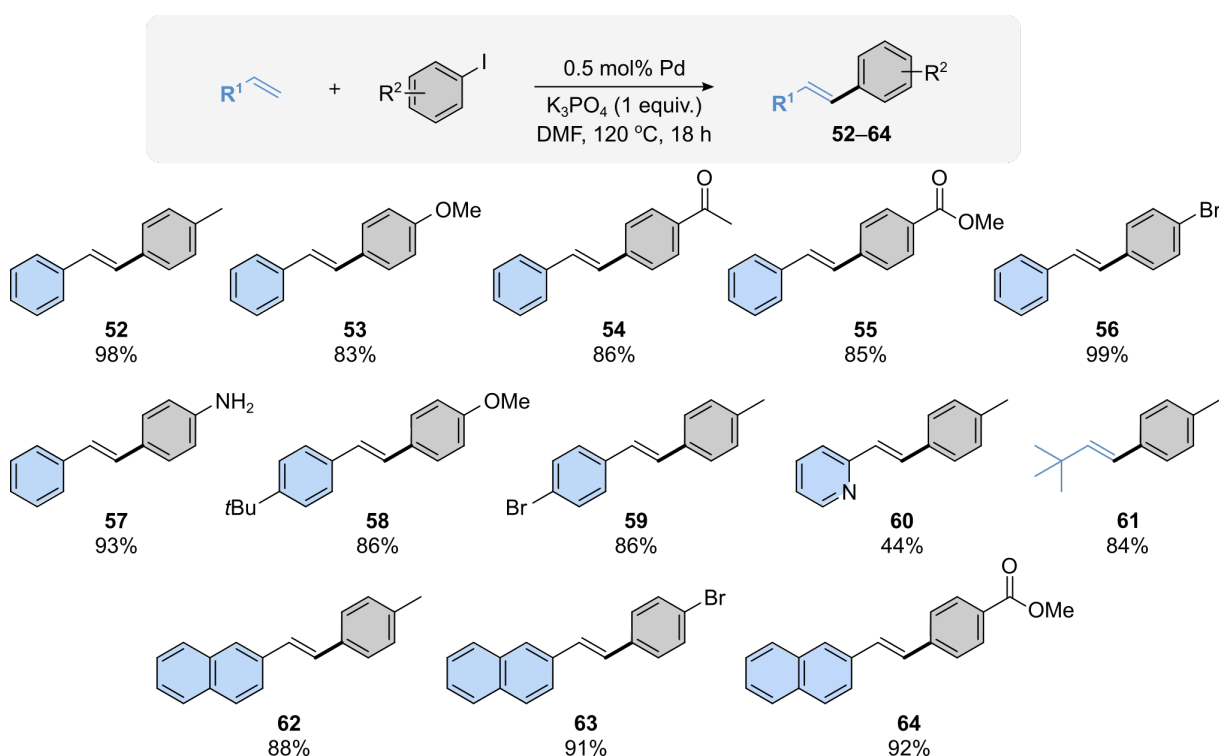


Figure 25. Scope of the Heck cross-coupling reaction catalyzed by the complexes **C27–C28**.

Reaction conditions: The reaction between ArI (1.0 mmol) and olefin (1.0 mmol) catalyzed by Pd^{II} complex (0.5 mol% Pd) was performed in the presence of K_3PO_4 (1.0 mmol) in DMF (1.0 mL) at 100 °C for 18 h. Yields determined by GC-MS analysis of aryl iodide decay.

In conclusion, new palladacyclic complexes were synthesized, with two molecules of a flexidentate pyridyl- β -diketonate ligand coordinated to the metal center *via* O,O' - and $N,C(sp^3)$ -chelates. The means of X-ray diffraction allowed the unambiguous establishment of the solid-state structures of both *cis* and *trans* isomers, which were further confirmed in solution. These organometallic compounds demonstrated exceptional stability in a basic environment, enabling their application as efficient and selective catalysts in the Heck cross-coupling reaction within a broad range of aryl iodides and olefins.

PUBLICATION A5: Crafting versatile modes of Pt^{II} complexes with flexidentate pyridyl- β -diketones: synthesis, structural characterization, and catalytic behavior in olefin hydrosilylation.²⁰¹

In the previous section, the intrinsic effect of the pyridine-*N* atom position on the complex structure has been demonstrated for a series of Pd^{II} species based on three isomeric pyridyl- β -diketonate ligands HL16–HL18.^{113, 234} As another example, structurally distinct assemblies with Cu^{II} ions were demonstrated by the Stefankiewicz group, including two-dimensional, topologically diverse coordination polymers for HL16 and HL17, as well as a mononuclear *O,O'*-chelated complex for HL18.¹¹⁵ In addition to differences in charge, composition, and dimensionality, variations in the location of the *N*-atom within the heterocyclic ring significantly affected the physicochemical properties, thereby influencing the functionality of the complexes in catalysis and gas sorption. Thus, in the work A5, a series of pyridyl- β -diketones HL16–HL18 was employed to examine their coordination behavior when combined with another metal center, specifically Pt^{II} ions, which often exhibit a preference for creating unconventional coordination motifs. The precise control of the synthetic reaction conditions led to the formation of distinct coordination species, with ligands arranged as simple pyridine-*N* donors, as well as unprecedented *N,C(sp³)*- and *N,O*-chelates. Finally, a new class of complexes was introduced as catalyst precursors for the olefin hydrosilylation reaction, demonstrating how enhanced catalytic performance can be achieved through the controlled manipulation of the coordination environment of central atoms.

The reactions of the ligands HL16–HL18 with a Pt^{II} salt led to the synthesis of a series of complexes C29–C34, each featuring a different coordination motif of the metal center (Figure 26). To achieve specific units, various synthetic strategies were utilized, with adjustments in stoichiometry, solvent, pH, and temperature. As a result of simple pyridine-*N* donation, the ligands HL16 and HL17 enabled the generation of di- and tetrasubstituted complexes with the general formulas [Pt(HL)₂Cl₂] (C29–C30) and [Pt(HL)₄](NO₃)₂ (C31–C32), analogous to those formed with Pd^{II} ions.^{113, 227} These species can be readily interconverted; specifically, the addition of an excess amount of free ligand to the disubstituted units in the presence of AgNO₃ results in the formation of tetrasubstituted species, which can be reverted to the disubstituted form by the introduction of chloride ions. Despite multiple efforts, the structures of the complexes generated in the reactions of HL16 or HL17 with PtCl₂ under basic conditions could not be determined, as the products appeared to form inseparable mixtures. While the ligands HL16 and HL17 exhibited the same behavior when reacted with Pt^{II} ions, the use of HL18 resulted in entirely distinct coordination modes. The complexes with the general formula [Pt(L18)₂] were synthesized after prior deprotonation of the ligand in the presence of a base (Na₂CO₃). Different reaction environments led to the formation of various coordination motifs, with *N,C(sp³)*- and *N,O*-chelation for complexes C33 and C34, respectively. Interestingly, the creation of five-membered chelate rings was preferred over the six-membered β -diketonate chelates, which had been observed previously for the Pd^{II} analogues.²³⁴

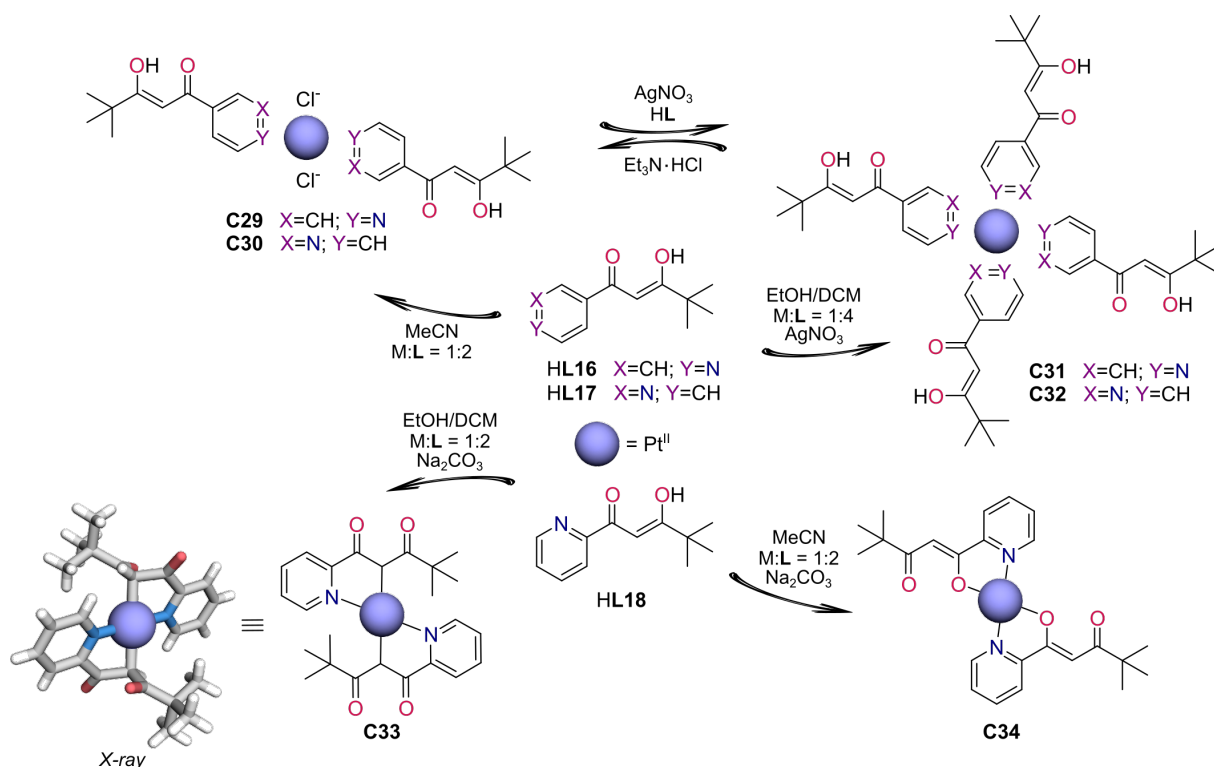


Figure 26. General reaction scheme for the synthesis of Pt^{II} complexes **C29–C34** based on isomeric pyridyl- β -diketonate ligands **HL16–HL18**.

The combination of various analytical techniques, such as X-ray diffraction, NMR spectroscopy, and ESI-MS, allowed for the in-depth characterization of the diverse coordination modes of Pt^{II} centers, thereby definitively confirming the complex structures. For **C33**, the structure was unambiguously established *via* X-ray diffraction, revealing a distorted square-planar geometry of the Pt^{II} ions with a C₂N₂ coordination environment. As opposed to the Pd^{II} analogues,²³⁴ the two ligand molecules are arranged in a *trans* configuration, each forming an N,C(*sp*³)-chelate ring. In turn, the crystal structure of **C32** was determined in a previous study.¹¹⁸ ESI-MS analysis confirmed the successful generation of the desired mononuclear species with the general formulas [Pt(HL)₂Cl₂] (**C29–C30**), [Pt(HL)₄](NO₃)₂ (**C31–C32**), and [Pt(L18)₂] (**C33–C34**), as all observed peaks were in good agreement with the theoretical isotope distribution. Furthermore, the complexes **C29–C34** were characterized in solution *via* ¹H NMR spectroscopy. The ¹H NMR spectra for the di- and tetrasubstituted species **C29–C32** were readily interpretable and consistent with the data for their Pd^{II} counterparts, while those for **C31–C32** aligned with previously reported results.¹¹⁸ As illustrated by the ¹H NMR spectra of the complexes **C29** and **C31** with the ligand **HL16** (Figure 27), the presence of signals from enol units indicated that the β -diketonate units were not involved in coordination. In comparison to the ¹H NMR spectrum of **HL16**, notable signal shifts in the aromatic region, particularly for the H¹ protons, confirmed coordination by pyridine-*N* donors. Similar effects were noted in the spectra of the complexes **C30** and **C32** based on the ligand **HL17**. As shown in the ¹H NMR spectrum of **C33**, its solid-state structure was retained in solution (Figure 28). The symmetrical arrangement of ligand molecules, consistent with the same coordination motif, was reflected in a single set of signals. Additionally, the significant shifts in the

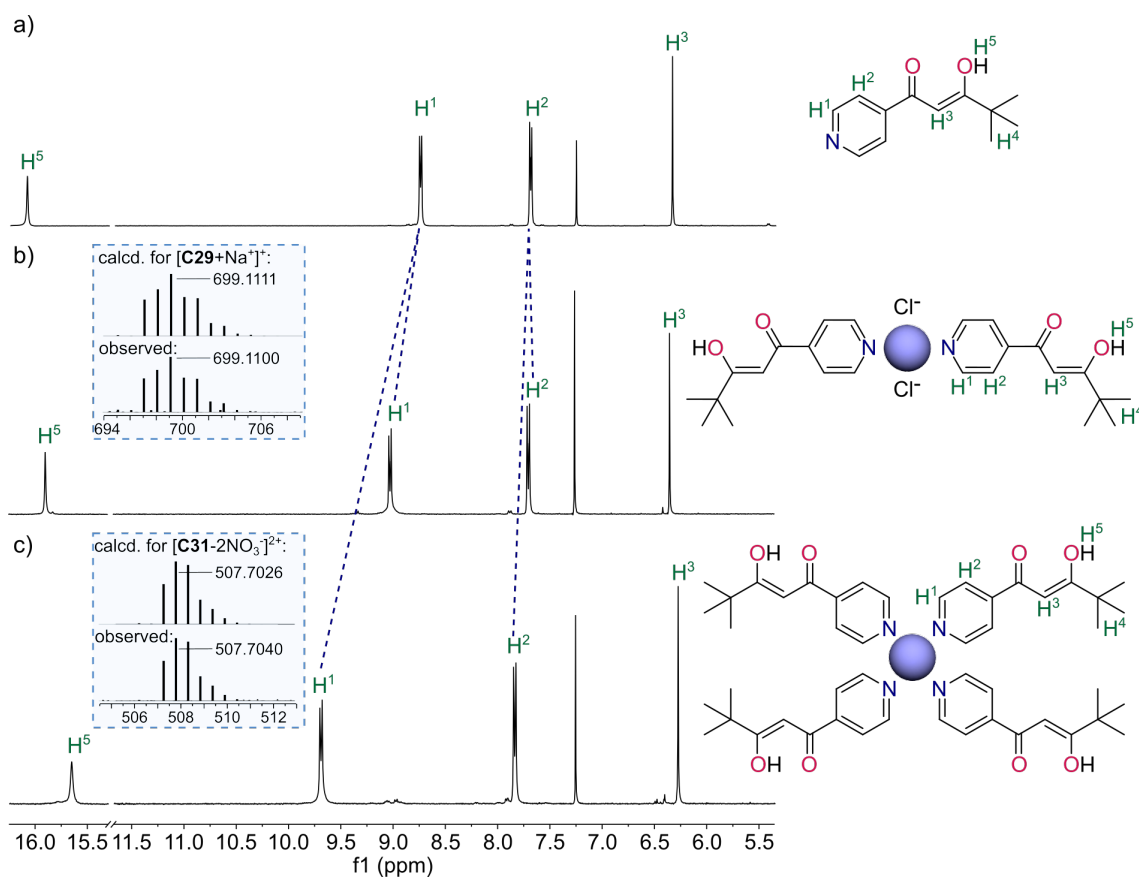


Figure 27. The stacked ^1H NMR spectra (600 MHz, CDCl_3) of: a) the ligand **HL16**; b) the complex **C29**; c) the complex **C31**. Inset: ESI-MS spectra of **C29** and **C31**, showing the calculated isotope model (top) and observed data (bottom).

relevant signals and the lack of the enol signal clearly indicated coordination by $N,C(sp^3)$ -chelates. In the ^1H NMR spectrum of **C34**, the notable downfield shift of the H^1 signal, along with the absence of the enol proton signal, were key factors that, considering the proximity of the β -diketonate moiety and pyridine- N donors, confirmed the coordination of Pt^{II} ions *via* N,O -chelates (Figure 28c).

Although the complexes **C31–C32** have been established as effective and selective catalyst precursors for hydrosilylation reactions,¹¹⁸ we aimed to investigate the catalytic activity of other Pt^{II} species, expecting that their structural and compositional diversity would be reflected in their catalytic performance. Therefore, the organometallic complex **C33** was chosen as the model catalyst for optimizing the conditions in the reaction between dimethylphenylsilane and 1-octene. The desired hydrosilylation product was obtained in the highest yield in the reaction performed in toluene at 80 °C, using 0.001 mol% Pt^{II} complex, and these conditions were selected for subsequent investigations. A series of catalytic reactions was carried out using 1-octene or styrene, representing aliphatic and aromatic olefins, respectively, along with structurally distinct hydrosilanes, employing **C29**, **C31**, **C33**, and **C34** as catalyst precursors. The results for **C30** were omitted due to its poor solubility, which led to significantly reduced reaction yields, while the results for **C32** were not included, as it exhibited comparable efficiency to the isomeric complex **C31**. Overall, a variety of hydrosilylation products was obtained in high yields, ranging from 74% to 100% (Figure 29).

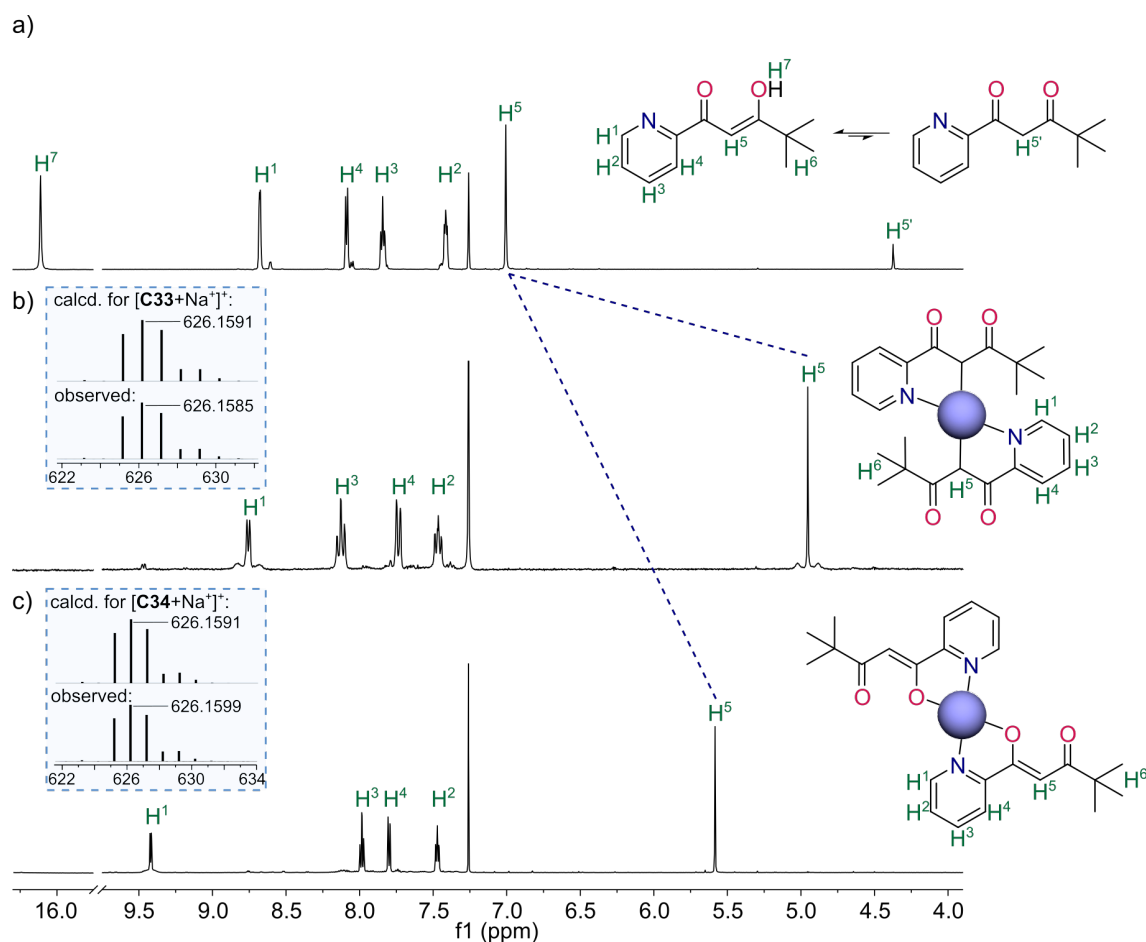


Figure 28. The stacked ^1H NMR spectra (600 MHz, CDCl_3) of: a) the ligand **HL18**; b) the complex **C33**; c) the complex **C34**. Inset: ESI-MS spectra of **C33** and **C34**, showing the calculated isotope model (top) and observed data (bottom).

Importantly, all the catalytic systems demonstrated high regioselectivity for the anti-Markovnikov addition. Although the reaction yields were generally high, variations among the individual systems were noted, with the organometallic complex **C33** exhibiting the highest efficiency. The slightly lower catalytic activity observed in reactions catalyzed by **C29** and **C31** can be attributed to the coordination of four ligands, which likely creates increased steric hindrance on the Pt^{II} ions. Furthermore, the electronic environment of the metal centers in **C33–C34** suggests that the direct involvement of β -diketonate moieties in coordination may positively contribute to catalytic efficiency. The electron density on the Pt^{II} centers increases significantly upon complexation with **HL18**, resulting in enhanced catalytic performance of **C33–C34**. In contrast, the β -diketonate units, as electron-withdrawing substituents on the pyridine rings in **C29–C32**, remain uncoordinated, thereby weakening the coordination bonds between the metal centers and the N -atom donors. The high catalytic activity of the complexes based on **HL18**, specifically **C33** and **C34**, which is comparable to that of the Karstedt's catalyst (Figure 29), underscores their considerable potential for widespread applications in olefin hydrosilylation.

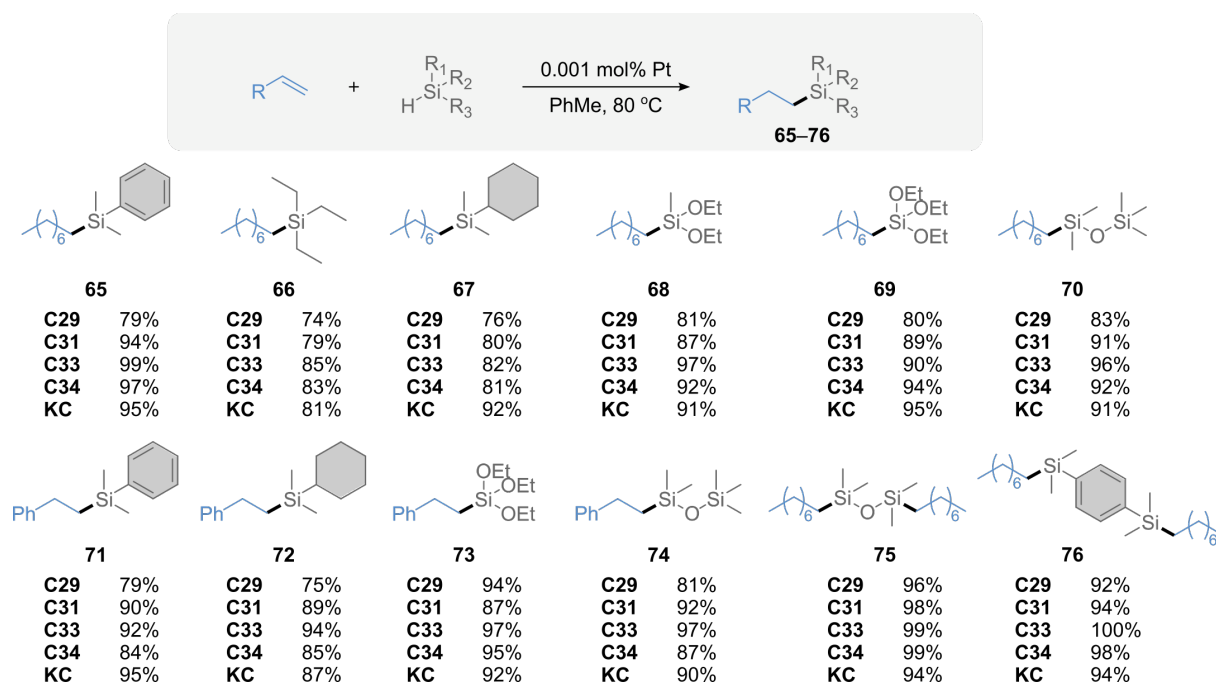


Figure 29. Scope of the hydrosilylation reaction catalyzed by the complexes **C29–C34** and the Karstedt's catalyst (**KC**).

Reaction conditions: The reaction between olefin (0.5 mmol) and hydrosilane (0.5 mmol) catalyzed by Pt^{II} complex (0.001 mol%) was performed in toluene (1.0 mL) at 80 °C for 1 h. Yields determined by GC-MS measurements or NMR spectroscopy using 1,3,5-trimethoxybenzene as internal standard.

* The reactions were performed for 6 h (**66**, **67**, **72**, **73**).

** 1.0 mmol of olefin was used (**75**, **76**).

In conclusion, a novel family of Pt^{II} complexes based on three isomeric pyridyl- β -diketones has been introduced, highlighting the influence of the position of *N*-donor atom within the ligand structure on the coordination mode adopted by the metal centers. As a result, three distinct types of coordination, *i.e.*, simple *N*-donation, *N,C(sp³)*-chelation, and *N,O*-chelation, were achieved, as unambiguously established *via* various analytical and spectroscopic methods. All of these species demonstrated remarkable efficiency and selectivity as catalyst precursors in hydrosilylation reactions within a broad range of structurally diverse reagents.

PUBLICATION A6: Multi-stimuli-responsive network of multicatalytic reactions using a single palladium/platinum catalyst.²³⁸

The incorporation of different metal centers with high catalytic activity into a single molecular structure offers an opportunity to create versatile catalysts with multifaceted performance.²³⁹ While Pd and Pt complexes are each capable of catalyzing a variety of reactions, integrating both metal ions into a single architecture significantly expands their potential applications in catalysis, encompassing a broad spectrum of cross-couplings, substitutions, additions, and reductions.²⁴⁰⁻²⁴⁴ In the publication A6, new heteronuclear complexes with Pd^{II} and Pt^{II} ions were introduced, engineered to provide cooperativity and compatibility between individual catalytic sites, and consequently to serve as multifunctional catalysts. Thus, an artificial system has been demonstrated that operates within an integrated network of multicatalytic reactions, effectively imitating the multi-stimuli-responsive systems found in nature.

A series of heteronuclear Pd^{II}/Pt^{II} complexes **C35–C38**, based on pyridyl- β -diketonate ligands **HL16–HL17** combined with coligands such as 2,2'-bipyridine (bpy) or ethylenediamine (en), has been designed and synthesized through hierarchical self-assembly. In each complex structure, the central Pt^{II} ion is coordinated *via* pyridine-*N* donors, while the four Pd^{II} ions are located in a heteroleptic environment, with *O,O'*-chelates on one side and *N,N'*-chelates on the other, as illustrated in Figure 30.

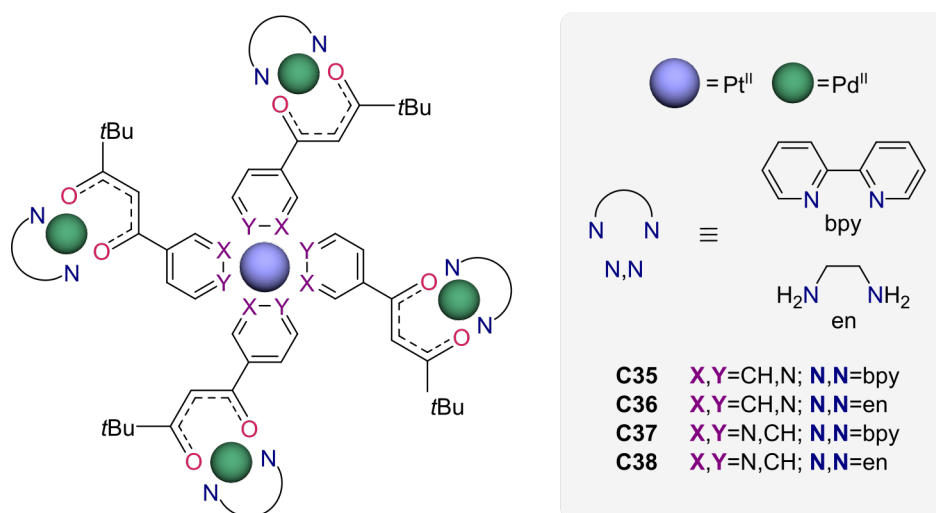


Figure 30. Structures of the heteronuclear Pd^{II}/Pt^{II} complexes **C35–C38**.

The generation and purity of the heterometallic assemblies **C35–C38** were verified in solution using NMR spectroscopy and mass spectrometry (ESI-MS). For example, the ¹H NMR spectrum of **C37** unequivocally confirmed the simultaneous involvement of β -diketonate moieties and *N*-donors from both pyridine and bipyridine units in coordination, as evidenced by the absence of the enol proton signal and the clearly downfield shifts of signals from protons adjacent to the *N*-atoms, compared to the ¹H NMR spectrum of **HL17** (Figure 31a). Additionally, all peaks in the ESI-MS spectra corresponded well with the calculated isotope distribution, confirming the successful formation of the desired heterometallic complexes (Figure 31b). Due to the low crystallinity in the

solid state, the crystal structures of the mononuclear constituents, namely $[\text{Pt}(\text{HL17})_4](\text{NO}_3)_2$ and $[\text{Pd}(\text{L17})(\text{bpy})]\text{PF}_6$, were used to model the heteronuclear structure of **C37**, as shown in Figure 31a.

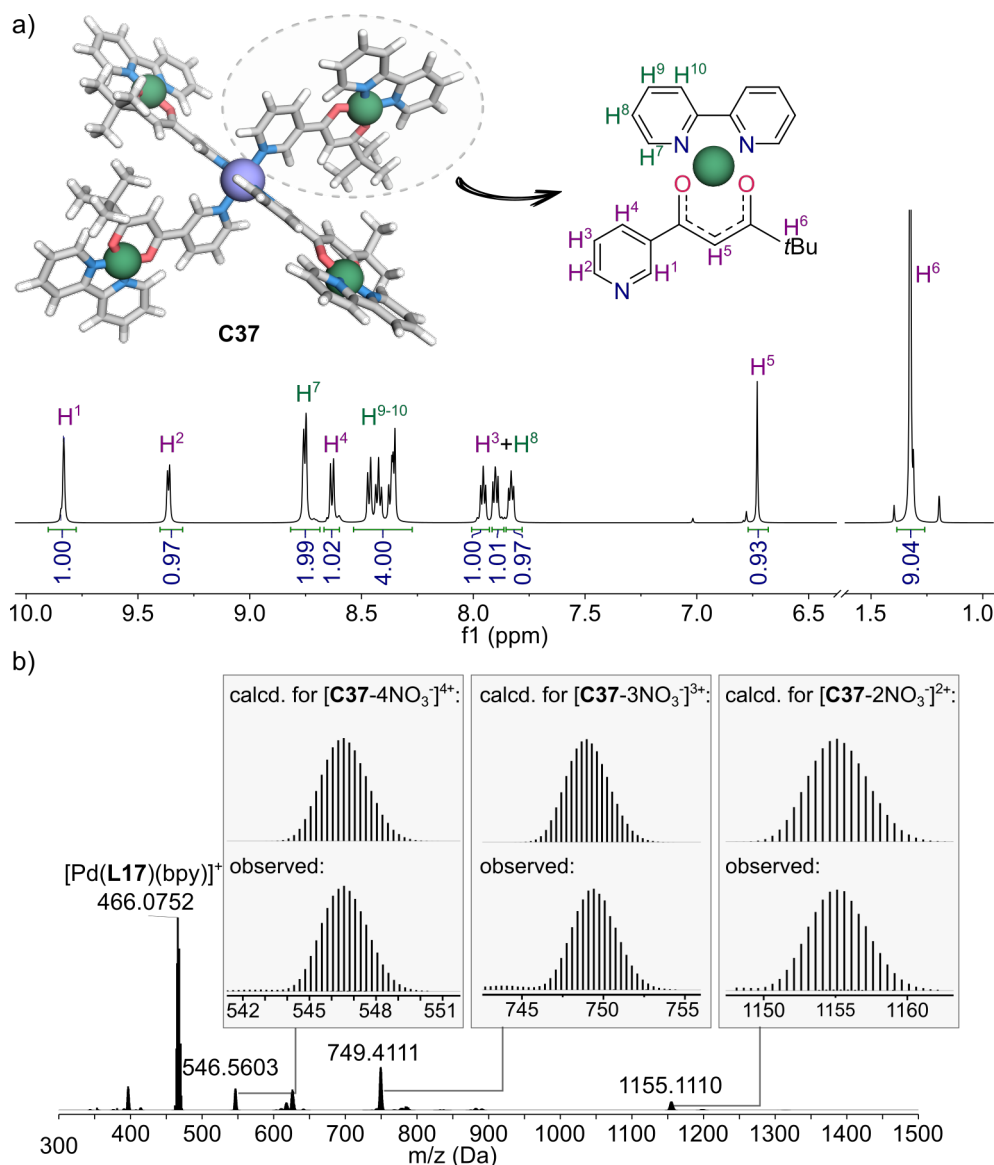


Figure 31. a) Part of the ^1H NMR spectrum (600 MHz, $\text{DMSO}-d_6$) of the heteronuclear complex **C37**. Inset: model structure of **C37**. b) ESI-MS spectrum of **C37**, showing the calculated isotope model (top) and the observed data (bottom).

The ability to combine two distinct, highly catalytically active metal ions within a single molecule rendered the heteronuclear complexes **C35–C38** of particular interest for evaluating their potential applications in multi-stage catalytic reactions. The extraordinary utility of Pd complexes in cross-coupling reactions,^{243, 245, 246} along with the high efficiency of Pt compounds in processes such as hydrosilylation and hydroformylation,^{242, 244} indicated that the resulting heterometallic assemblies could serve as multifunctional catalysts for a broad range of transformations. A set of simple reagents, *i.e.*, phenylacetylene **S1**, iodobenzene **S2**, and triethylsilane **S3**, was selected as model starting materials to assess their catalytic properties. It was anticipated that, in the presence of **C35–C38**, the substrates would undergo a series of sequential catalytic processes. As a consequence of multicatalytic reactions, a set of structurally distinct products **P1–P10** was formed, as depicted in

Figure 32. The topological analysis of the network of synthetic pathways exhibits three main branches (I–III), where the catalytic performance and selectivity of individual transformations are governed by sequences of various chemical and physical triggers, denoted as **T1–T9**. These simple additives and reaction conditions could be strategically employed in a controlled manner, functioning as external stimuli to direct the network toward specific products by promoting particular synthetic pathways, thereby reflecting the regulation of metabolic systems. Since the most efficient and selective synthetic pathways were observed with **C37** used as the catalyst, the following results are presented for this complex.

In branch I, all multi-stage transformations were initiated by the Sonogashira coupling between **S1** and **S2**. This reaction, performed in the presence of NaOH (**T1**) as a trigger and **C37** as the catalyst, led to the formation of **P1** in a quantitative yield (>99%). Subsequently, **P1** underwent various *in situ* transformations with **S3**, depending on the trigger applied, resulting in the selective generation of products **P2–P5**. In the absence of any additional trigger, the hydrosilylation reaction occurred, furnishing **P2** (98%). **P1** could also react with **S3** in semi-reductive processes triggered by DMSO (**T2**) or water (**T3**), leading to the formation of **P3** and **P4**, with overall yields of 90% and 62%, respectively. Additionally, thus-formed **P3** and **P4** were converted into one another when exposed to UV light (**T5**). TBAF (**T4**), identified as a consecutive trigger, enabled the conversion of **P2** into fully reduced **P5** (80%). Interestingly, some products in branch I could be formed through multiple pathways when additional triggers were introduced. Specifically, **P2** was transformed into a mixture of **P3** and **P4** upon the addition of DMSO (**T2**), with overall yields of 40% and 54%, respectively. In the presence of TBAF (**T4**), **P2** and **P4** were converted into **P5** (70% and 56%). Moreover, **P3** was transferred *in situ* into **P5** (64%) when exposed to H₂ and MeOH (**T6**).

In branch II, the reactions between **S1** and **S3** led to the generation of three new products **P6–P8**, two of which were capable of reacting with **S2** in subsequent transformations. The reaction of **S1** with **S3**, in the presence of NaOH (**T1**) and **C37**, gave the hydrosilylation product **P6** (97%). The same reaction, when triggered by DMSO (**T2**) or TBAF (**T4**), resulted in the formation of **P7** and **P8**, with overall yields of 95% and 97%, respectively. Thus-formed **P6** and **P7** could be further transformed into other products when additional triggers were employed. **P6** was converted *in situ* into **P7** (70%) or **P8** (75%) upon the addition of DMSO (**T2**) or TBAF (**T4**), respectively. Additionally, **P7** could be further transferred into **P8** (91%) after exposure to H₂ and MeOH (**T6**). The interconnection between branches I and II was established through the Hiyama and Heck cross-coupling reactions. **P6** and **P7** reacted with **S2** in processes triggered by either TBAF (**T4**) and temperature (**T9**) or Et₃N (**T7**), resulting in **P4** with overall yields of 31% and 67%, respectively.

Branch III involved two of the three substrates, specifically **S2** and **S3**. Their reaction in the presence of *t*BuONa (**T8**) and **C37** led to the generation of **P9** (80%). Conversely, the transformation performed in the absence of a base, however, at elevated temperature (**T9**), furnished **P10** (>99%). In contrast to branches I and II, branch III operates independently from the rest of the network.

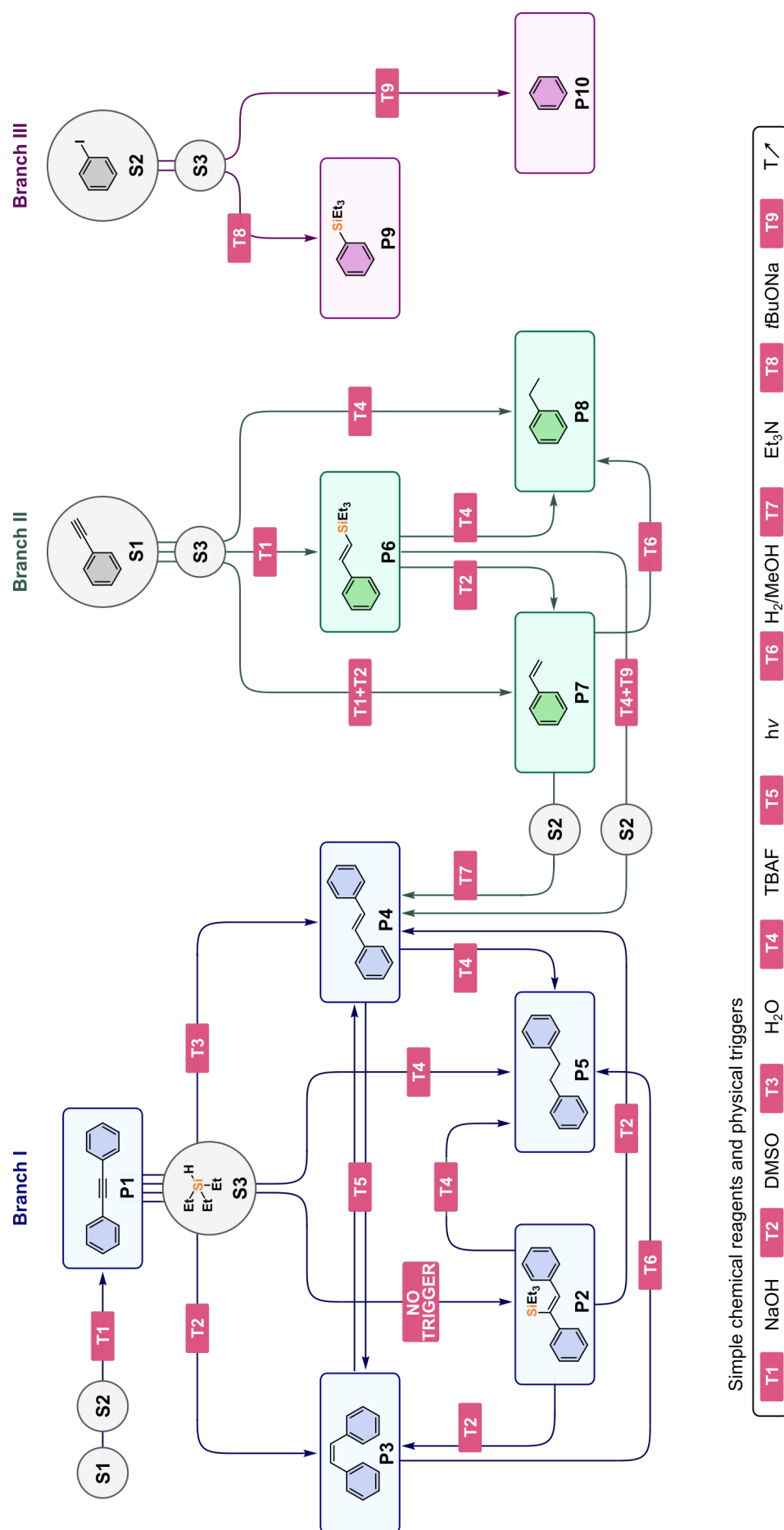
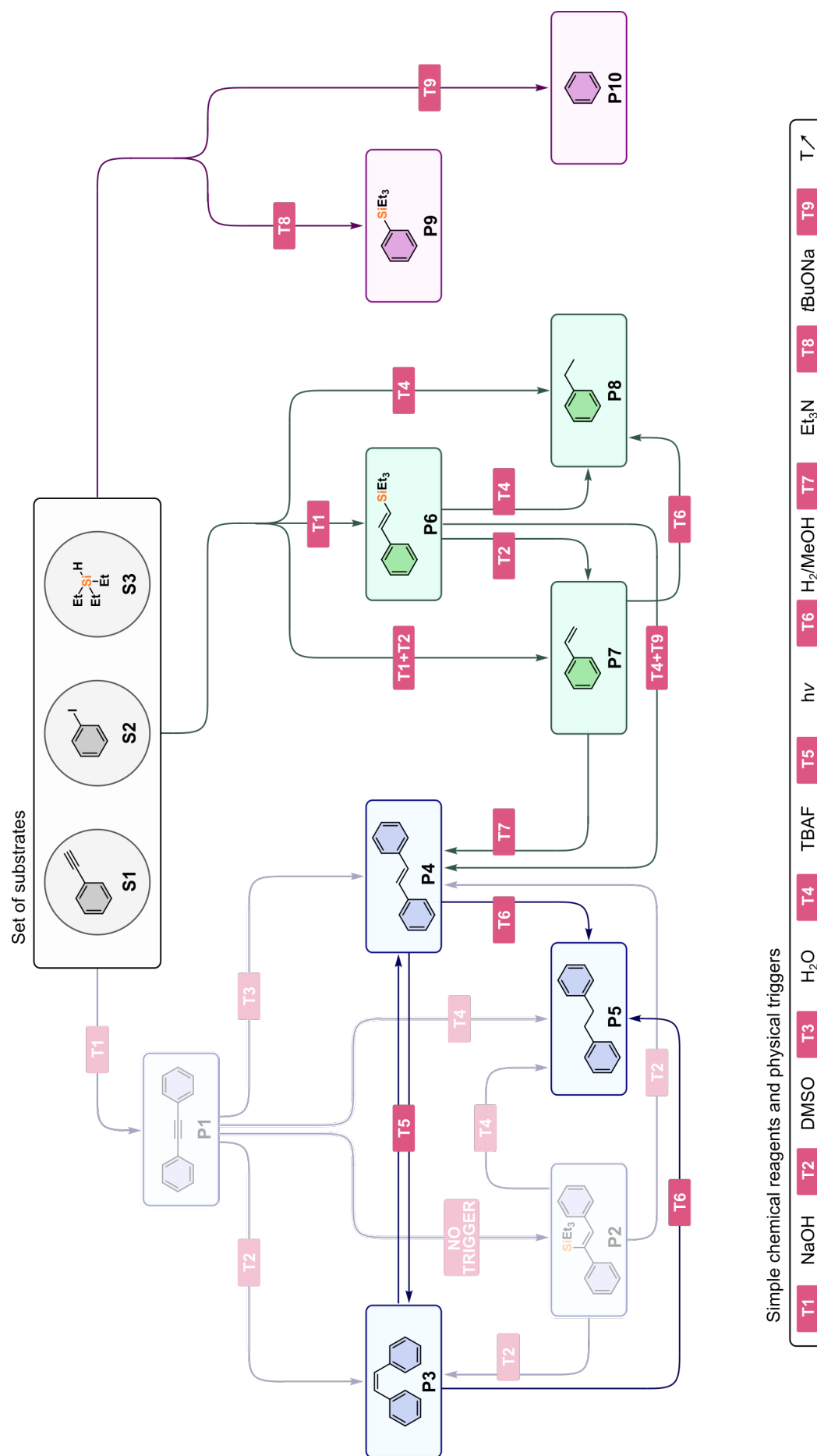


Figure 32. Stimuli-responsive network of multicatalytic reactions between **S1–S3**, catalyzed by the Pd^{II}/Pt^{II} complex **C37**.

At the next stage, we demonstrated that the network of multicatalytic reactions exhibits a significant degree of orthogonality between the individual pathways. In the experiments described above, the orthogonality of competitive synthetic routes catalyzed by **C37** was controlled by chemical and physical triggers (**T1–T9**), while the kinetic hierarchy was enhanced by the sequential introduction of substrates **S1–S3**. To evaluate the kinetic hierarchy and pathway orthogonality within this network, we investigated the performance of **C37** with all starting materials present in the system from the beginning (Figure 33). In branch I, the orthogonality was not fully achieved due to the kinetic preference for hydrosilylation and reduction reactions over the Sonogashira cross-coupling. Upon the formation of **P1**, the synthetic routes leading to **P2–P5** became entirely orthogonal. Nevertheless, the reaction between **S1**, **S2**, and **S3** in the presence of **T1** furnished **P6** (93%), which could be transformed *in situ* into **P7** (65%), **P8** (82%), or **P4** (23%) when triggered by **T2**, **T4**, or **T4** with **T9**, respectively, without the introduction of any additional reagents. When **S1**, **S2**, and **S3** were all reacted together in the presence of **T1** and **T2**, the semi-reduction reaction was favored, leading to **P7** (80%), which could then be converted into **P4** (68%) or **P8** (77%) upon the addition of **T7** or **T6**, respectively. Thus-formed **P4** was further transferred into **P3** (32%) or **P5** (56%) in processes triggered by **T5** or **T6**, respectively. As anticipated, the reaction between all the reagents, triggered by **T4**, resulted in **P8** (91%). Furthermore, both products of branch III, **P9** and **P10**, were generated in the presence of **S1**, **S2**, and **S3**, with overall yields of 52% and 93%, respectively, when triggered by **T8** or **T9**. As a consequence, all synthetic pathways in branches II and III can be considered as orthogonal, with the reactivity governed by the specific triggers applied.

To conclude, an artificial system inspired by the metabolic processes occurring in nature has been designed to respond to multiple external stimuli. This system operates within a network of mechanistically diverse reactions, including cross-couplings, reductions, substitutions, and additions, allowing for the efficient performance of multi-stage processes using three simple starting materials. Mimicking the stimuli-responsiveness of metabolic systems, all synthetic pathways were controlled by physical and chemical triggers and catalyzed by a multifunctional heteronuclear Pd^{II}/Pt^{II} complex, leading to the selective formation of ten distinct products.



4. Summary

This dissertation presents the design, synthesis, and spectro-structural characterization of a series of novel coordination assemblies, expanding the scope of complexes based on transition metals (Ag^{I} , Pd^{II} , Pt^{II}) and contributing to the development of new systems with high potential for applications in catalysis. An array of organic ligands incorporating β -diketonate units, pyridine donors, or a combination of both was effectively utilized as key constituents to construct structurally diverse compounds with various coordination arrangements, exhibiting intriguing architectural geometries and physicochemical properties. The obtained coordination assemblies were employed as efficient catalyst precursors in a wide range of reactions, including cross-couplings, reductions, substitutions, and hydroadditions. The correlations established between the structure of well-defined complexes and their catalytic efficiency enabled the identification of factors contributing to the enhancement of catalytic activity, which can be fundamental for the rational design of new high-performance catalytic systems. Since the presented thesis addresses a variety of aspects, it represents a valuable contribution to the areas of coordination and metallosupramolecular chemistry, as well as catalysis.

The main achievements presented in each of the six individual reports are as follows:

- A1** The effect of nuclearity was demonstrated in a model Suzuki-Miyaura reaction catalyzed by mono- and oligonuclear Pd^{II} complexes, revealing that the enhancement in catalytic activity is correlated with an increased number of catalytic sites *per* catalyst molecule.
- A2** The effects of substituents in the heterocyclic ring were defined for a broad range of pyridine complexes with Pd^{II} ions, showcasing their impact on coordination behavior and spectro-structural properties, specifically NMR shifts and interactions within the crystal lattice. These coordination compounds were also demonstrated to be efficient catalyst precursors in the Suzuki-Miyaura and Heck cross-coupling reactions, with performance depending on the specific functional groups present and the overall nature of the complexes.
- A3** An effective strategy for coordination-driven structural switching was developed for a series of complexes based on a pyridyl- β -diketonate ligand, resulting in the creation of new heterometallic polymers. The differences in composition and morphology between these heteronuclear aggregates were crucial for their varied catalytic efficiency in the Heck reaction.
- A4-A5** The flexidentate nature of pyridyl- β -diketonate ligands **HL16–HL18** enabled the formation of structurally diverse Pd^{II} and Pt^{II} species, with metal centers coordinated through β -diketonate units and simple pyridine-*N*-donors, as well as through unprecedented *N,O*- and *N,C*(η^3)-chelates, depending on the position of the *N*-atom in the heterocyclic ring. The significant application potential of these Pd^{II} and Pt^{II} complexes was exhibited as

catalyst precursors in the Heck reaction and olefin hydrosilylation, respectively, highlighting the crucial role of the organometallic units in enhancing catalytic performance.

- A6** A proof-of-concept system capable of responding to multiple external stimuli and operating within an integrated network of mechanistically distinct reactions has been developed. Our approach enabled the performance of multiple multi-stage processes, controlled by specific triggers and catalyzed by a single heteronuclear Pd^{II}/Pt^{II} complex, which consequently led to the preferential synthesis of various products with high efficiency and selectivity.

References

1. S. De, K. Mahata and M. Schmittel, *Chem. Soc. Rev.*, 2010, **39**, 1555-1575.
2. E. C. Constable and C. E. Housecroft, *Chem. Soc. Rev.*, 2013, **42**, 1429-1439.
3. X.-Z. Li, C.-B. Tian and Q.-F. Sun, *Chem. Rev.*, 2022, **122**, 6374-6458.
4. L.-J. Chen, H.-B. Yang and M. Shionoya, *Chem. Soc. Rev.*, 2017, **46**, 2555-2576.
5. Y. Sun, C. Chen, J. Liu and P. J. Stang, *Chem. Soc. Rev.*, 2020, **49**, 3889-3919.
6. E. G. Percástegui, T. K. Ronson and J. R. Nitschke, *Chem. Rev.*, 2020, **120**, 13480-13544.
7. W. Wang, Y.-X. Wang and H.-B. Yang, *Chem. Soc. Rev.*, 2016, **45**, 2656-2693.
8. W.-H. Fang and G.-Y. Yang, *Acc. Chem. Res.*, 2018, **51**, 2888-2896.
9. S. Kitagawa, R. Kitaura and S. i. Noro, *Angew. Chem. Int. Ed.*, 2004, **43**, 2334-2375.
10. J. Duan, W. Jin and S. Kitagawa, *Coord. Chem. Rev.*, 2017, **332**, 48-74.
11. R. A. Agarwal and N. K. Gupta, *Coord. Chem. Rev.*, 2017, **332**, 100-121.
12. A. Brzechwa-Chodzyńska, W. Drożdż, J. Harrowfield and A. R. Stefankiewicz, *Coord. Chem. Rev.*, 2021, **434**, 213820.
13. M. Castellano, R. Ruiz-Garcia, J. Cano, J. Ferrando-Soria, E. Pardo, F. R. Fortea-Perez, S.-E. Stiriba, W. P. Barros, H. O. Stumpf and L. Canadillas-Delgado, *Coord. Chem. Rev.*, 2015, **303**, 110-138.
14. M. Avinash and T. Govindaraju, *Acc. Chem. Res.*, 2018, **51**, 414-426.
15. N. C. Gianneschi, M. S. Masar and C. A. Mirkin, *Acc. Chem. Res.*, 2005, **38**, 825-837.
16. M. Kremer and U. Englert, *Z. Kristallogr. Cryst. Mater.*, 2018, **233**, 437-452.
17. T. M. Harris, *Encyclopedia of Reagents for Organic Synthesis*, 2001.
18. M. Seco, *J. Chem. Educ.*, 1989, **66**, 779.
19. W. Urbaniak, K. Jurek, K. Witt, A. Goraczko, B. Staniszewski and A. Mickiewicz, *Chemik*, 2011, **65**, 273.
20. A. Camerman, D. Mastropaolo and N. Camerman, *J. Am. Chem. Soc.*, 1983, **105**, 1584-1586.
21. J. M. Sprague, L. J. Beckham and H. Adkins, *J. Am. Chem. Soc.*, 1934, **56**, 2665-2668.
22. G. d. Gonzalo Calvo and A. R. Alcántara, *Pharmaceuticals*, 2021, **14**, 1043.
23. H. Siegel and M. Eggersdorfer, *Ullmann's Encyclopedia of Industrial Chemistry*, 2000.
24. W. Caminati and J.-U. Grabow, *J. Am. Chem. Soc.*, 2006, **128**, 854-857.
25. G. Allen and R. A. Dwek, *J. Chem. Soc. B*, 1966, 161-163.
26. Z. Yoshida, H. Ogoshi and T. Tokumitsu, *Tetrahedron*, 1970, **26**, 5691-5697.
27. K. A. Manbeck, N. C. Boaz, N. C. Bair, A. M. Sanders and A. L. Marsh, *J. Chem. Educ.*, 2011, **88**, 1444-1445.
28. J. L. Burdett and M. T. Rogers, *J. Am. Chem. Soc.*, 1964, **86**, 2105-2109.
29. R. G. Pearson, *J. Chem. Educ.*, 1968, **45**, 581.
30. T.-L. Ho, *Chem. Rev.*, 1975, **75**, 1-20.
31. M. Kolodziejcki, A. Walczak, Z. Hnatejko, J. Harrowfield and A. R. Stefankiewicz, *Polyhedron*, 2017, **137**, 270-277.
32. Y. Nakamura, K. Isobe, H. Morita, S. Yamazaki and S. Kawaguchi, *Inorg. Chem.*, 1972, **11**, 1573-1578.
33. R. C. Fay and T. Piper, *Inorg. Chem.*, 1964, **3**, 348-356.
34. E. Arslan, R. A. Lalancette and I. Bernal, *Struct. Chem.*, 2017, **28**, 201-212.
35. S. A. De Pascali, P. Papadia, S. Capoccia, L. Marchiò, M. Lanfranchi, A. Ciccarese and F. P. Fanizzi, *Dalton Trans.*, 2009, 7786-7795.
36. V. Isakova, I. Baidina, N. Morozova and I. Igumenov, *Polyhedron*, 2000, **19**, 1097-1103.
37. F. P. Pruchnik, P. Smoleński and K. Wajda-Hermanowicz, *J. Organomet. Chem.*, 1998, **570**, 63-69.
38. D. J. Otway and W. S. Rees Jr, *Coord. Chem. Rev.*, 2000, **210**, 279-328.
39. G. Aromí, P. Gamez and J. Reedijk, *Coord. Chem. Rev.*, 2008, **252**, 964-989.
40. V. V. Skopenko, V. M. Amirhanov, T. Y. Sliva, I. S. Vasilchenko, E. Anpilova and A. D. Garnovskii, *Russ. Chem. Rev.*, 2004, **73**, 737-752.
41. M. B. Hursthouse, M. A. Laffey, P. T. Moore, D. B. New, P. R. Raithby and P. Thornton, *J. Chem. Soc., Dalton Trans.*, 1982, 307-312.
42. K. AbduláMalik, *J. Chem. Soc., Dalton Trans.*, 1993, 2883-2890.
43. J. Lewis and C. Oldham, *J. Chem. Soc. A*, 1966, 1456-1462.
44. B. E. Buitendach, E. Erasmus, J. Conradie, J. Niemantsverdriet, H. Lang and J. C. Swarts, *Organometallics*, 2024.
45. M. Moro, P. Zardi, M. Rossi and A. Biffis, *Catalysts*, 2022, **12**, 307.
46. M. M. Jones, *J. Am. Chem. Soc.*, 1959, **81**, 3188-3189.
47. D. J. Bray, J. K. Clegg, L. F. Lindoy and D. Schilter, *Adv. Inorg. Chem.*, 2006, **59**, 1-37.
48. R. West, *J. Am. Chem. Soc.*, 1958, **80**, 3246-3249.
49. O. Onawumi, O. Faboya, O. Odunola, T. Prasad and M. Rajasekharan, *Polyhedron*, 2008, **27**, 113-117.

50. Y. Hoshino, M. Eto, T. Fujino, Y. Yukawa, T. Ohta, A. Endo, K. Shimizu and G. Sato, *Inorg. Chem. Acta*, 2004, **357**, 600-604.
51. V. Panyushkin, N. Achrimenko and A. Khachatryan, *Polyhedron*, 1998, **17**, 3053-3058.
52. V. I. Saloutin, Y. O. Edilova, Y. S. Kudyakova, Y. V. Burgart and D. N. Bazhin, *Molecules*, 2022, **27**, 7894.
53. A. Dalal, K. Nehra, A. Hooda, D. Singh, P. Kumar, S. Kumar, R. S. Malik and B. Rathi, *Inorganica Chim. Acta*, 2023, **550**, 121406.
54. K. Nehra, A. Dalal, A. Hooda, S. Bhagwan, R. K. Saini, B. Mari, S. Kumar and D. Singh, *J. Mol. Struct.*, 2022, **1249**, 131531.
55. S. G. Bott, B. D. Fahlman, M. L. Pierson and A. R. Barron, *J. Chem. Soc., Dalton Trans.*, 2001, 2148-2147.
56. A. Purdy, A. Berry, R. Holm, M. Fatemi and D. Gaskill, *Inorg. Chem.*, 1989, **28**, 2799-2803.
57. A. T. Larson, A. S. Crossman, S. M. Krajewski and M. P. Marshak, *Inorg. Chem.*, 2019, **59**, 423-432.
58. E. J. Hopkins, S. M. Krajewski, A. S. Crossman, F. D. Maharaj, L. T. Schwanz and M. P. Marshak, *Eur. J. Inorg. Chem.*, 2020, **2020**, 1951-1959.
59. A. S. Crossman, A. T. Larson, J. X. Shi, S. M. Krajewski, E. S. Akturk and M. P. Marshak, *J. Org. Chem.*, 2019, **84**, 7434-7442.
60. E. S. Akturk, S. J. Scappaticci, R. N. Seals and M. P. Marshak, *Inorg. Chem.*, 2017, **56**, 11466-11469.
61. S. M. Krajewski, A. S. Crossman, E. S. Akturk, T. Suhrbier, S. J. Scappaticci, M. W. Staab and M. P. Marshak, *Dalton Trans.*, 2019, **48**, 10714-10722.
62. F. Masero and V. Mougél, *Chem. Commun.*, 2023, **59**, 4636-4639.
63. J. L. Gorzynski, J. Chen and C. L. Fraser, *J. Am. Chem. Soc.*, 2005, **127**, 14956-14957.
64. C. Freund, W. Porzio, U. Giovanella, F. Vignali, M. Pasini, S. Destri, A. Mech, S. Di Pietro, L. Di Bari and P. Mineo, *Inorg. Chem.*, 2011, **50**, 5417-5429.
65. R. H. Elattar, S. F. El-Malla, A. H. Kamal and F. R. Mansour, *Coord. Chem. Rev.*, 2024, **501**, 215568.
66. S. K. Langley, N. F. Chilton, B. Moubaraki and K. S. Murray, *Inorg. Chem.*, 2013, **52**, 7183-7192.
67. J. K. Clegg, F. Li and L. F. Lindoy, *Coord. Chem. Rev.*, 2022, **455**, 214355.
68. A. J. Brock, J. K. Clegg, F. Li and L. F. Lindoy, *Coord. Chem. Rev.*, 2018, **375**, 106-133.
69. J. K. Clegg, F. Li and L. F. Lindoy, *Coord. Chem. Rev.*, 2013, **257**, 2536-2550.
70. P. A. Vigato, V. Peruzzo and S. Tamburini, *Coord. Chem. Rev.*, 2009, **253**, 1099-1201.
71. J. K. Clegg, F. Li, K. A. Jolliffe, G. V. Meehan and L. F. Lindoy, *Chem. Commun.*, 2011, **47**, 6042-6044.
72. M. Kolodziejski, A. J. Brock, G. Kurpiak, A. Walczak, F. Li, J. K. Clegg and A. R. Stefankiewicz, *Inorg. Chem.*, 2021, **60**, 9673-9679.
73. S. Pal, *Pyridine*, 2018, **57**, 57-74.
74. J. A. Joule, *Heterocyclic chemistry*, CRC Press, 2020.
75. J. A. Joule and K. Mills, *Heterocyclic chemistry at a glance*, John Wiley & Sons, 2012.
76. C. D. Johnson, I. Roberts and P. G. Taylor, *J. Chem. Soc.*, 1981, 409-413.
77. E. F. Scriven and R. Murugan, *Kirk-Othmer Encyclopedia of Chemical Technology*, 2000.
78. S. M. Soliman, *Comput. Theor. Chem.*, 2012, **994**, 105-111.
79. A. Blas, *J. Chem. Soc., Dalton Trans.*, 1996, 1493-1497.
80. R. Ilmi, I. Juma Al-busaidi, A. Haque and M. S. Khan, *J. Coord. Chem.*, 2018, **71**, 3045-3076.
81. O. Mamula and A. von Zelewsky, *Coord. Chem. Rev.*, 2003, **242**, 87-95.
82. N. Ségaud, J.-N. Rebilly, K. Sénéchal-David, R. Guillot, L. Billon, J.-P. Baltaze, J. Farjon, O. Reinaud and F. Banse, *Inorg. Chem.*, 2013, **52**, 691-700.
83. R. M. Wexler, M. C. Tsai, C. Friend and E. Muetterties, *J. Am. Chem. Soc.*, 1982, **104**, 2034-2036.
84. N. A. Lewis, S. Pakhomova, P. A. Marzilli and L. G. Marzilli, *Inorg. Chem.*, 2017, **56**, 9781-9793.
85. A. Krogul, J. Skupińska and G. Litwinienko, *J. Mol. Catal. A Chem.*, 2014, **385**, 141-148.
86. K. Nakano, N. Suemura, K. Yoneda, S. Kawata and S. Kaizaki, *Dalton Trans.*, 2005, 740-743.
87. M. L. Dell'Arciprete, C. J. Cobos, J. P. Furlong, D. O. Mártire and M. C. Gonzalez, *ChemPhysChem*, 2007, **8**, 2498-2505.
88. A. Krogul and G. Litwinienko, *Org. Process Res. Dev.*, 2015, **19**, 2017-2021.
89. A. Krogul and G. Litwinienko, *J. Mol. Catal. A Chem.*, 2015, **407**, 204-211.
90. M. Zafar, A. Atif, M. Nazar, S. Sumrra and R. Paracha, *Russ. J. Coord. Chem.*, 2016, **42**, 1-18.
91. G. Tseberlidis, D. Intrieri and A. Caselli, *Eur. J. Inorg. Chem.*, 2017, **2017**, 3589-3603.
92. A. Lannes, M. Intissar, Y. Suffren, C. Reber and D. Luneau, *Inorg. Chem.*, 2014, **53**, 9548-9560.
93. G. M. Rakić, S. Grgurić-Šipka, G. N. Kaluđerović, S. Gómez-Ruiz, S. K. Bjelogrić, S. S. Radulović and Ž. L. Tešić, *Eur. J. Med. Chem.*, 2009, **44**, 1921-1925.
94. A. Togni and L. M. Venanzi, *Angew. Chem. Int. Ed.*, 1994, **33**, 497-526.
95. A. J. Pardey and C. Longo, *Coord. Chem. Rev.*, 2010, **254**, 254-272.
96. A. Krogul, J. Cedrowski, K. Wiktorska, W. P. Ozimiński, J. Skupińska and G. Litwinienko, *Dalton Trans.*, 2012, **41**, 658-666.
97. C. Kaes, A. Katz and M. W. Hosseini, *Chem. Rev.*, 2000, **100**, 3553-3590.
98. A. Gorczynski, J. M. Harrowfield, V. Patroniak and A. R. Stefankiewicz, *Chem. Rev.*, 2016, **116**, 14620-14674.
99. N. B. Debata, D. Tripathy and D. K. Chand, *Coord. Chem. Rev.*, 2012, **256**, 1831-1945.

100. D. M. Peloquin and T. A. Schmedake, *Coord. Chem. Rev.*, 2016, **323**, 107-119.
101. G. de Ruiter, M. Lahav and M. E. van der Boom, *Acc. Chem. Res.*, 2014, **47**, 3407-3416.
102. B. Chen, J. J. Holstein, S. Horiuchi, W. G. Hiller and G. H. Clever, *J. Am. Chem. Soc.*, 2019, **141**, 8907-8913.
103. B. Happ, A. Winter, M. D. Hager and U. S. Schubert, *Chem. Soc. Rev.*, 2012, **41**, 2222-2255.
104. A. Rajput and R. Mukherjee, *Coord. Chem. Rev.*, 2013, **257**, 350-368.
105. C. R. Glasson, L. F. Lindoy and G. V. Meehan, *Coord. Chem. Rev.*, 2008, **252**, 940-963.
106. K. Biradha, M. Sarkar and L. Rajput, *Chem. Commun.*, 2006, 4169-4179.
107. L. Lindoy, E. Lee, S. S. Lee and S. Seo, 2017.
108. B. J. Holliday and C. A. Mirkin, *Angew. Chem. Int. Ed.*, 2001, **40**, 2022-2043.
109. C. J. Elsevier, J. Reedijk, P. H. Walton and M. D. Ward, *Dalton Trans.*, 2003, 1869-1880.
110. R. D. Mukhopadhyay and A. Ajayaghosh, *Chem. Soc. Rev.*, 2023.
111. S.-L. Lee, F.-L. Hu, X.-J. Shang, Y.-X. Shi, A. L. Tan, J. Mizera, J. K. Clegg, W.-H. Zhang, D. J. Young and J.-P. Lang, *New J. Chem.*, 2017, **41**, 14457-14465.
112. P.-D. Mao, N.-T. Yao, H.-Y. Sun, F.-F. Yan, Y.-Q. Zhang, Y.-S. Meng and T. Liu, *Cryst. Growth Des.*, 2022, **23**, 450-464.
113. A. Walczak and A. R. Stefankiewicz, *Inorg. Chem.*, 2018, **57**, 471-477.
114. M. Vakili, V. Darugar, F. S. Kamounah, P. E. Hansen, M. Hermann and M. Pittelkow, *J. Mol. Liq.*, 2023, **383**, 122074.
115. A. Walczak, G. Kurpik and A. R. Stefankiewicz, *Int. J. Mol. Sci.*, 2020, **21**, 6171.
116. M. J. Mayoral, P. Cornago, R. M. Claramunt and M. Cano, *New J. Chem.*, 2011, **35**, 1020-1030.
117. J.-T. Tan, W.-J. Zhao, S.-P. Chen, X. Li, Y.-L. Lu, X. Feng and X.-W. Yang, *Chem. Pap.*, 2012, **66**, 47-53.
118. A. Walczak, H. Stachowiak, G. Kurpik, J. Kaźmierczak, G. Hreczycho and A. R. Stefankiewicz, *J. Catal.*, 2019, **373**, 139-146.
119. S. Sanz, H. M. O'Connor, V. Martí-Centelles, P. Comar, M. B. Pitak, S. J. Coles, G. Lorusso, E. Palacios, M. Evangelisti and A. Baldansuren, *Chem. Sci.*, 2017, **8**, 5526-5535.
120. S. Sanz, H. M. O'Connor, P. Comar, A. Baldansuren, M. B. Pitak, S. J. Coles, H. Weihe, N. F. Chilton, E. J. McInnes and P. J. Lusby, *Inorg. Chem.*, 2018, **57**, 3500-3506.
121. D. Blasi, V. Nicolai, R. M. Gomila, P. Mercandelli, A. Frontera and L. Carlucci, *Chem. Commun.*, 2022, **58**, 9524-9527.
122. M. Wang, V. Vajpayee, S. Shanmugaraju, Y.-R. Zheng, Z. Zhao, H. Kim, P. S. Mukherjee, K.-W. Chi and P. J. Stang, *Inorg. Chem.*, 2011, **50**, 1506-1512.
123. H. O'Connor, S. Sanz, M. Pitak, S. Coles, G. Nichol, S. Piligkos, P. Lusby and E. Brechin, *CrystEngComm*, 2016, **18**, 4914-4920.
124. C. J. McMonagle, P. Comar, G. S. Nichol, D. R. Allan, J. González, J. A. Barreda-Argüeso, F. Rodríguez, R. Valiente, G. F. Turner and E. K. Brechin, *Chem. Sci.*, 2020, **11**, 8793-8799.
125. K. V. Domasevitch, V. D. Vreshch, A. B. Lysenko and H. Krautscheid, *Acta Crystallogr., Sect. C: Cryst. Struct. Commun.*, 2006, **62**, m443-m447.
126. H. B. Wu and Q. M. Wang, *Angew. Chem. Int. Ed.*, 2009, **48**, 7343-7345.
127. F. Liu and Y. Zhou, *Inorg. Chem. Commun.*, 2010, **13**, 1410-1413.
128. P. Slepukhin, N. Boltacheva, V. Filyakova and V. Charushin, *Russ. Chem. Bull.*, 2019, **68**, 1213-1218.
129. H. M. O'Connor, S. Sanz, A. J. Scott, M. B. Pitak, W. T. Klooster, S. J. Coles, N. F. Chilton, E. J. McInnes, P. J. Lusby and H. Weihe, *Molecules*, 2021, **26**.
130. S. Sanz, H. M. O'Connor, E. M. Pineda, K. S. Pedersen, G. S. Nichol, O. Mønsted, H. Weihe, S. Piligkos, E. J. McInnes and P. J. Lusby, *Angew. Chem. Int. Ed.*, 2015, **54**, 6761-6764.
131. D.-J. Wang, Y.-F. Kang, B.-P. Xu, J. Zheng and X.-H. Wei, *Spectrochim. Acta - A: Mol. Biomol. Spectrosc.*, 2013, **104**, 419-422.
132. D.-J. Wang, Y.-F. Kang, L. Fan, Y.-J. Hu and J. Zheng, *Opt. Mater.*, 2013, **36**, 357-361.
133. L. Wu, Y. Fang, W. Zuo, J. Wang, J. Wang, S. Wang, Z. Cui, W. Fang, H.-L. Sun and Y. Li, *J. Am. Chem. Soc.*, 2022, **2**, 853-864.
134. M. Dudek, J. K. Clegg, C. R. Glasson, N. Kelly, K. Gloe, K. Gloe, A. Kelling, H.-J. r. Buschmann, K. A. Jolliffe and L. F. Lindoy, *Cryst. Growth Des.*, 2011, **11**, 1697-1704.
135. G.-G. Hou, Y. Liu, Q.-K. Liu, J.-P. Ma and Y.-B. Dong, *Chem. Commun.*, 2011, **47**, 10731-10733.
136. G.-J. Chen, H.-C. Ma, W.-L. Xin, X.-B. Li, F.-Z. Jin, J.-S. Wang, M.-Y. Liu and Y.-B. Dong, *Inorg. Chem.*, 2017, **56**, 654-660.
137. F.-Z. Jin, C.-Q. Chen, Q. Zhao, J.-L. Kan, Y. Zhou and G.-J. Chen, *Catal. Commun.*, 2018, **111**, 84-89.
138. K. Jeremy, *J. Chem. Soc.*, 1995, 2269-2273.
139. V. D. Vreshch, A. N. Chernega, J. A. Howard, J. Sieler and K. V. Domasevitch, *Dalton Trans.*, 2003, 1707-1711.
140. A. M. Tous-Granados and A. J. Hernandez-Maldonado, *Chem. Commun.*, 2023, **59**, 10020-10023.
141. K. Jeremy, *J. Chem. Soc., Chem. Commun.*, 1992, 43-44.
142. S. Turner and F. Mabbs, *J. Chem. Soc., Dalton Trans.*, 1997, 1117-1118.
143. B. Chen, F. R. Fronczek and A. W. Maverick, *Chem. Commun.*, 2003, 2166-2167.

144. V. D. Vreshch, A. B. Lysenko, A. N. Chernega, J. A. Howard, H. Krautscheid, J. Sieler and K. V. Domasevitch, *Dalton Trans.*, 2004, 2899-2903.
145. T. E. Knight, D. Guo, J. P. Claude and J. K. McCusker, *Inorg. Chem.*, 2008, **47**, 7249-7261.
146. K.-N. Truong, C. Merckens and U. Englert, *Acta Crystallogr. C Struct. Chem.*, 2017, **73**, 724-730.
147. V. D. Vreshch, A. B. Lysenko, A. N. Chernega, J. Sieler and K. V. Domasevitch, *Polyhedron*, 2005, **24**, 917-926.
148. C. Merckens, F. Pan and U. Englert, *CrystEngComm*, 2013, **15**, 8153-8158.
149. D.-J. Li, L.-Q. Mo and Q.-M. Wang, *Inorg. Chem. Commun.*, 2011, **14**, 1128-1131.
150. B. Chen, F. R. Fronczek and A. W. Maverick, *Inorg. Chem.*, 2004, **43**, 8209-8211.
151. Y. Zhang, B. Chen, F. R. Fronczek and A. W. Maverick, *Inorg. Chem.*, 2008, **47**, 4433-4435.
152. C. Merckens, K.-N. Truong and U. Englert, *Acta Crystallogr. B Struct. Sci. Cryst. Eng. Mater.*, 2014, **70**, 705-713.
153. K.-N. Truong, C. Merckens and U. Englert, *Acta Crystallogr. B Struct. Sci. Cryst. Eng. Mater.*, 2017, **73**, 981-991.
154. D. Guo, T. E. Knight and J. K. McCusker, *Science*, 2011, **334**, 1684-1687.
155. G.-L. Wang, Y.-J. Lin, H. Berke and G.-X. Jin, *Inorg. Chem.*, 2010, **49**, 2193-2201.
156. D. Simond, S. E. Clifford, A. F. Vieira, C. Besnard and A. F. Williams, *RSC Adv.*, 2014, **4**, 16686-16693.
157. T. Banerjee, A. K. Biswas, T. S. Sahu, B. Ganguly, A. Das and H. N. Ghosh, *Dalton Trans.*, 2014, **43**, 13601-13611.
158. T.-J. Won, J. K. Clegg, L. F. Lindoy and J. C. McMurtrie, *Cryst. Growth Des.*, 2007, **7**, 972-979.
159. A. S. Dinca, S. Shova, A. E. Ion, C. Maxim, F. Lloret, M. Julve and M. Andruh, *Dalton Trans.*, 2015, **44**, 7148-7151.
160. A. E. Ion, S. Nica, A. M. Madalan, C. Maxim, M. Julve, F. Lloret and M. Andruh, *CrystEngComm*, 2014, **16**, 319-327.
161. T. Shiga, T. Nakanishi, M. Ohba and H. Ōkawa, *Polyhedron*, 2005, **24**, 2732-2736.
162. T. Shiga, M. Ohba and H. Ōkawa, *Inorg. Chem.*, 2004, **43**, 4435-4446.
163. T. Shiga, M. Ohba and H. Ōkawa, *Inorg. Chem. Commun.*, 2003, **6**, 15-18.
164. R. W. Saalfrank, V. Seitz, D. L. Calder, K. N. Raymond, M. Teichert and D. Stalke, *Eur. J. Inorg. Chem.*, 1998, **1998**, 1313-1317.
165. D. E. Fenton, J. R. Tate, U. Casellato, S. Tamburini, P. A. Vigato and M. Vidali, *Inorg. Chem. Acta*, 1984, **83**, 23-31.
166. A. Brock, J. C. McMurtrie and J. Clegg, *CrystEngComm*, 2019, **21**, 4786-4791.
167. R. W. Saalfrank, A. Scheurer, R. Puchta, F. Hampel, H. Maid and F. W. Heinemann, *Angew. Chem. Int. Ed.*, 2007, **46**, 265-268.
168. R. W. Saalfrank, V. Seitz, F. W. Heinemann, C. Göbel and R. Herbst-Irmer, *J. Chem. Soc., Dalton Trans.*, 2001, 599-603.
169. W. X. Gao, Q. J. Fan, Y. J. Lin and G. X. Jin, *Chin. J. Chem.*, 2018, **36**, 594-598.
170. Q.-J. Fan, Y.-J. Lin, F. E. Hahn and G.-X. Jin, *Dalton Trans.*, 2018, **47**, 2240-2246.
171. A. D. Burrows, M. F. Mahon, C. L. Renouf, C. Richardson, A. J. Warren and J. E. Warren, *Dalton Trans.*, 2012, **41**, 4153-4163.
172. Y. Y. Zhang, L. Zhang, Y. J. Lin and G. X. Jin, *Chem. Eur. J.*, 2015, **21**, 14893-14900.
173. A. D. Burrows, C. G. Frost, M. F. Mahon, P. R. Raithby, C. L. Renouf, C. Richardson and A. J. Stevenson, *Chem. Commun.*, 2010, **46**, 5067-5069.
174. K. Banerjee and K. Biradha, *New J. Chem.*, 2016, **40**, 1997-2006.
175. J. F. Wunsch, L. Eberle, J. P. Mullen, F. Rominger, M. Rudolph and A. S. K. Hashmi, *Inorg. Chem.*, 2022, **61**, 3508-3515.
176. P. D. Mao, S. H. Zhang, N. T. Yao, H. Y. Sun, F. F. Yan, Y. Q. Zhang, Y. S. Meng and T. Liu, *Chem. Eur. J.*, 2023, **29**, e202301262.
177. M. C. Pfrunder, A. J. Brock, J. J. Brown, A. Grosjean, J. Ward, J. C. McMurtrie and J. K. Clegg, *Chem. Commun.*, 2018, **54**, 3974-3976.
178. G. Fernandez Garcia, D. Guettas, V. Montigaud, P. Larini, R. Sessoli, F. Totti, O. Cador, G. Pilet and B. Le Guennic, *Angew. Chem. Int. Ed.*, 2018, **130**, 17335-17339.
179. K. R. Vignesh and G. Rajaraman, *ACS Omega*, 2021, **6**, 32349-32364.
180. P. C. Andrews, G. B. Deacon, R. Frank, B. H. Fraser, P. C. Junk, J. G. MacLellan, M. Massi, B. Moubaraki, K. S. Murray and M. Silberstein, *Eur. J. Inorg. Chem.*, 2009, **2009**, 744-751.
181. A. Béziau, S. A. Baudron and M. W. Hosseini, *Dalton Trans.*, 2012, **41**, 7227-7234.
182. L. Carlucci, G. Ciani, D. M. Proserpio and M. Visconti, *CrystEngComm*, 2011, **13**, 5891-5902.
183. D. Guettas, V. Montigaud, G. F. Garcia, P. Larini, O. Cador, B. Le Guennic and G. Pilet, *Eur. J. Inorg. Chem.*, 2018, **2018**, 333-339.
184. J. Li and R. Suo, *Spectrochim. Acta - A: Mol. Biomol. Spectrosc.*, 2023, **291**, 122357.
185. C. Caporale, A. N. Sobolev, W. Phonsri, K. S. Murray, A. Swain, G. Rajaraman, M. I. Ogden, M. Massi and R. O. Fuller, *Dalton Trans.*, 2020, **49**, 17421-17432.
186. V. Kondaparthi, A. Shaik, K. B. Reddy and D. D. Manwal, *Chem. Data Collect.*, 2019, **20**, 100203.
187. S. L. Nongbri, B. DASb and M. R. Kollipara, *J. Chem. Sci.*, 2012, **124**, 1365-1375.

References

188. J.-P. Tong, F. Shao, J. Tao, R.-B. Huang and L.-S. Zheng, *Inorg. Chem.*, 2011, **50**, 2067-2069.
189. M. Visconti, S. Maggini, G. Ciani, P. Mercandelli, B. Del Secco, L. Prodi, M. Sgarzi, N. Zaccheroni and L. Carlucci, *Cryst. Growth Des.*, 2019, **19**, 5376-5389.
190. S. L. Nongbri, B. Das and K. M. Rao, *J. Coord. Chem.*, 2012, **65**, 875-890.
191. S. K. Langley, N. F. Chilton, M. Massi, B. Moubaraki, K. J. Berry and K. S. Murray, *Dalton Trans.*, 2010, **39**, 7236-7249.
192. M. Kercher, B. König, H. Zieg and L. De Cola, *J. Am. Chem. Soc.*, 2002, **124**, 11541-11551.
193. G. Yu, Y. Xing, F. Chen, R. Han, J. Wang, Z. Bian, L. Fu, Z. Liu, X. Ai and J. Zhang, *ChemPlusChem*, 2013, **78**, 852-859.
194. H.-C. Lin, H. Kim, S. Barlow, J. M. Hales, J. W. Perry and S. R. Marder, *Chem. Commun.*, 2011, **47**, 782-784.
195. I. Borilovic, O. Roubeau, I. Fernández Vidal, S. J. Teat and G. Aromí, *Magnetochemistry*, 2015, **1**, 45-61.
196. V. Velasco, D. Aguilà, L. Barrios, I. Borilovic, O. Roubeau, J. Ribas-Ariño, M. Fumanal, S. J. Teat and G. Aromí, *Chem. Sci.*, 2015, **6**, 123-131.
197. J. Salinas-Uber, L. A. Barrios, O. Roubeau and G. Aromí, *Polyhedron*, 2013, **54**, 8-12.
198. L. A. Barrios, D. Aguilà, O. Roubeau, K. S. Murray and G. Aromí, *Aust. J. Chem.*, 2009, **62**, 1130-1136.
199. D. Aguilà, L. A. Barrios, O. Roubeau, S. J. Teat and G. Aromí, *Chem. Commun.*, 2011, **47**, 707-709.
200. L. Wolf and H. Hennig, *Z. Anorg. Allg. Chem.*, 1964, **329**, 301-308.
201. G. Kurpik, A. Walczak, I. Lukasik, Z. Matela and A. R. Stefankiewicz, *ChemCatChem*, 2024, **16**, e202301465.
202. C. A. Gunawardana, A. S. Sinha, J. Desper, M. Đaković and C. B. Aakeröy, *Cryst. Growth Des.*, 2018, **18**, 6936-6945.
203. Y. Huang and P. Yang, *Polyhedron*, 2019, **158**, 47-54.
204. Z. Xi, F. Liu, Y. Zhou and W. Chen, *Tetrahedron*, 2008, **64**, 4254-4259.
205. R. A. A. Abdine, G. Kurpik, A. Walczak, S. A. A. Aesh, A. R. Stefankiewicz, F. Monnier and M. Taillefer, *J. Catal.*, 2019, **376**, 119-122.
206. J.-H. Olivier, J. Harrowfield and R. Ziessel, *Chem. Commun.*, 2011, **47**, 11176-11188.
207. G. Kurpik, A. Walczak, M. Gilski, J. Harrowfield and A. R. Stefankiewicz, *J. Catal.*, 2022, **411**, 193-199.
208. S. Gonell and J. N. Reek, *ChemCatChem*, 2019, **11**, 1458-1464.
209. P. Scrimin, M. A. Cardona, C. M. L. Prieto and L. J. Prins, *Multivalency: Concepts, Research & Applications*, 2018, 153-176.
210. B. Helms and J. M. Fréchet, *Adv. Synth. Catal.*, 2006, **348**, 1125-1148.
211. D. Méry and D. Astruc, *Coord. Chem. Rev.*, 2006, **250**, 1965-1979.
212. R. Gramage-Doria, J. Hessels, S. H. Leenders, O. Tröppner, M. Dürr, I. Ivanović-Burmazović and J. N. Reek, *Angew. Chem. Int. Ed.*, 2014, **126**, 13598-13602.
213. G. Jayamurugan and N. Jayaraman, *Advanced Synthesis & Catalysis*, 2009, **351**, 2379-2390.
214. D. Astruc and F. Chardac, *Chem. Rev.*, 2001, **101**, 2991-3024.
215. F. Fu, J. Xiang, H. Cheng, L. Cheng, H. Chong, S. Wang, P. Li, S. Wei, M. Zhu and Y. Li, *ACS Catal.*, 2017, **7**, 1860-1867.
216. D. Astruc, E. Boisselier and C. Ornelas, *Chem. Rev.*, 2010, **110**, 1857-1959.
217. H.-K. Luo and H. Schumann, *J. Mol. Catal. A Chem.*, 2005, **227**, 153-161.
218. I. Bratko and M. Gómez, *Dalton Trans.*, 2013, **42**, 10664-10681.
219. G. Zhang, G. Proni, S. Zhao, E. C. Constable, C. E. Housecroft, M. Neuburger and J. A. Zampese, *Dalton Trans.*, 2014, **43**, 12313-12320.
220. R. S. Bagul and N. Jayaraman, *J. Organomet. Chem.*, 2012, **701**, 27-35.
221. G. E. Oosterom, J. N. Reek, P. C. Kamer and P. W. van Leeuwen, *Angew. Chem. Int. Ed.*, 2001, **40**, 1828-1849.
222. F. Yu, D. Poole III, S. Mathew, N. Yan, J. Hessels, N. Orth, I. Ivanović-Burmazović and J. N. Reek, *Angew. Chem. Int. Ed.*, 2018, **130**, 11417-11421.
223. M. Shibasaki and Y. Yamamoto, *Multimetallic catalysts in organic synthesis*, John Wiley & Sons, 2006.
224. E. C. Constable, G. Zhang, C. E. Housecroft, M. Neuburger, S. Schaffner and W.-D. Woggon, *New J. Chem.*, 2009, **33**, 1064-1069.
225. N. Krittametaporn, T. Chantarojsiri, A. Virachotikul, K. Phomphrai, N. Kuwamura, T. Kojima, T. Konno and P. Sangtrirutnugul, *Dalton Trans.*, 2020, **49**, 682-689.
226. N. E. Shepherd, H. Tanabe, Y. Xu, S. Matsunaga and M. Shibasaki, *J. Am. Chem. Soc.*, 2010, **132**, 3666-3667.
227. G. Kurpik, A. Walczak, M. Goldyn, J. Harrowfield and A. R. Stefankiewicz, *Inorg. Chem.*, 2022, **61**, 14019-14029.
228. M. Palusiak, *J. Organomet. Chem.*, 2007, **692**, 3866-3873.
229. K. Jaju, D. Pal, A. Chakraborty and S. Chakraborty, *Chem. Phys. Lett.*, 2019, **737**, 100031.
230. A. Kimura and T. Ishida, *Inorganics*, 2017, **5**, 52.
231. B. G. Tehan, E. J. Lloyd, M. G. Wong, W. R. Pitt, J. G. Montana, D. T. Manallack and E. Gancia, *Estimation of pKa using semiempirical molecular orbital methods. Part 1: Application to phenols and carboxylic acids*, 2002.
232. M. Chatzopoulou, E. Kotsampasakou and V. J. Demopoulos, *Synthetic Communications*, 2013, **43**, 2949-2954.

233. G. Kurpik, A. Walczak, G. Markiewicz, J. Harrowfield and A. R. Stefankiewicz, *Nanoscale*, 2023, **15**, 9543-9550.
234. A. Walczak, G. Kurpik, M. Zaranek, P. Pawluć and A. R. Stefankiewicz, *J. Catal.*, 2022, **405**, 84-90.
235. C.-L. Chen, Y.-H. Liu, S.-M. Peng and S.-T. Liu, *Tetrahedron Lett.*, 2005, **46**, 521-523.
236. E. M. Beccalli, E. Borsini, S. Brenna, S. Galli, M. Rigamonti and G. Broggin, *Chem. Eur. J.*, 2010, **16**, 1670-1678.
237. A. Shiota and H. C. Malinakova, *J. Organomet. Chem.*, 2012, **704**, 9-16.
238. G. Kurpik, A. Walczak, P. Dydio and A. R. Stefankiewicz, *Angew. Chem. Int. Ed.*, 2024, e202404684.
239. R. Peters, *Cooperative catalysis: designing efficient catalysts for synthesis*, John Wiley & Sons, 2015.
240. H. Li, C. C. Johansson Seechurn and T. J. Colacot, *ACS Catal.*, 2012, **2**, 1147-1164.
241. K. Nicolaou, P. G. Bulger and D. Sarlah, *Angew. Chem. Int. Ed.*, 2005, **44**, 4442-4489.
242. T. K. Meister, K. Riener, P. Gigler, J. r. Stohrer, W. A. Herrmann and F. E. Kühn, *ACS Catal.*, 2016, **6**, 1274-1284.
243. N. Kambe, T. Iwasaki and J. Terao, *Chem. Soc. Rev.*, 2011, **40**, 4937-4947.
244. L. D. de Almeida, H. Wang, K. Junge, X. Cui and M. Beller, *Angew. Chem. Int. Ed.*, 2021, **60**, 550-565.
245. A. Biffis, P. Centomo, A. Del Zotto and M. Zecca, *Chem. Rev.*, 2018, **118**, 2249-2295.
246. S. McCarthy, D. C. Braddock and J. D. Wilton-Ely, *Coord. Chem. Rev.*, 2021, **442**, 213925.

Reprints of publications



Contents lists available at ScienceDirect

Journal of Catalysis

journal homepage: www.elsevier.com/locate/jcat

Effect of the nuclearity on the catalytic performance of a series of Pd(II) complexes in the Suzuki-Miyaura reaction



Gracjan Kurpik^{a,b}, Anna Walczak^{a,b}, Mirosław Gilski^a, Jack Harrowfield^c, Artur R. Stefankiewicz^{a,b,*}

^a Faculty of Chemistry, Adam Mickiewicz University in Poznań, Uniwersytetu Poznańskiego 8, 61-614 Poznań, Poland

^b Center for Advanced Technology, Adam Mickiewicz University in Poznań, Uniwersytetu Poznańskiego 10, 61-614 Poznań, Poland

^c ISIS, Université de Strasbourg, 8 allée Gaspard Monge, 67083 Strasbourg, France

ARTICLE INFO

Article history:

Received 29 March 2022

Revised 10 May 2022

Accepted 24 May 2022

Available online 29 May 2022

Keywords:

Nuclearity effect

β -diketonate ligands

Pd(II) complexes

Homogeneous catalysis

Suzuki-Miyaura coupling

ABSTRACT

Development of well-defined multivalent systems with densely packed multiple functional groups located within a single molecular structure provides an excellent opportunity to generate catalysts of enhanced activity. A series of mono-, di- and trinuclear Pd(II) complexes based on polyketonate ligands allied with 2,2'-bipyridine has been designed, synthesized and fully characterized in both solution and solid state. The mono-, di- and tritopic β -diketonate molecules serve as scaffolds for Pd(II) active sites which, in the two latter cases, are forced into close proximity. Application of the complexes as catalysts in Suzuki-Miyaura cross-coupling as a model reaction has revealed significant differences in reaction yields and a trend in reactivity reflecting their nuclearity.

© 2022 The Author(s). Published by Elsevier Inc. This is an open access article under the CC BY license (<http://creativecommons.org/licenses/by/4.0/>).

1. Introduction

Investigation of factors influencing catalyst activity underlie the rational design of new, efficient catalysts to improve reaction yields and/or selectivity [1]. In that respect, multivalent systems, where multiple potentially active sites are present, constitute an important path in the unremitting struggle to reduce the costs of catalytic processes [2]. Clear evidence of a multivalency effect is the increasing importance of nanoparticles, polymers and dendrimers for catalytic applications [3]. In the majority of catalysed processes, a growing number of active centres in the individual molecule of a catalyst induces a positive effect observed as increase in efficiency, although there are cases in which a negative impact has also been seen [4]. The origin of the reactivity enhancement has been investigated and significant roles attributed to increased local concentration enabling more efficient substrate binding and cooperative effects connected with assistance of nearby centres in catalytic cycles [3b,5]. A successful example is provided in a series of dendrimers functionalized by phosphine-Pd(II) moieties where a positive dendritic effect in both Suzuki-Miyaura and Heck cross-coupling reactions has been demonstrated [6]. Nevertheless, multi-step covalent synthesis of dendritic systems and nanoparticles can lead to numerous problems associated with

yields, purification and reproducibility, providing undefined aggregates diversified in terms of size, shape, distribution of metal, and as a result of that, catalytic effectiveness [2,7]. Due to these aspects their considerable potential has not yet been fully exploited, especially in industry.

In general, there are numerous examples of both homo- and hetero-metallic polynuclear units applied as multivalent catalysts, primarily dendrimers and nanoparticles, that have been widely explored in various organic reactions [8]. In heterometallic systems, the focus has been largely on cooperativity between different roles in catalysis for the different metals, not upon any effects of nuclearity, and even in homonuclear systems other than dendrimers, systematic studies of the effects of nuclearity are lacking. Hence, the present study was undertaken to characterise the catalytic efficiency of structurally related mono-, di- and tri-nuclear Pd(II) complexes as opposed to larger entities, in part with the expectation that any effects should be most obvious at this end of the nuclearity scale. Despite a number of systems based on dendritic architectures having exhibited a positive effect in catalysis, molecular systems displaying this phenomenon are very limited [9]. In fact, we have observed marked differences in the yields of reactions catalysed by these relatively small oligonuclear Pd(II) coordination compounds. For the same absolute concentration of Pd, an increase in the number of metal ions in a single molecule of catalyst resulted in higher yields in the Suzuki-Miyaura cross-coupling reactions examined herein. This has defined a significant

* Corresponding author.

E-mail address: ars@amu.edu.pl (A.R. Stefankiewicz).

<https://doi.org/10.1016/j.jcat.2022.05.021>

0021-9517/© 2022 The Author(s). Published by Elsevier Inc.

This is an open access article under the CC BY license (<http://creativecommons.org/licenses/by/4.0/>).

positive effect on catalytic effectiveness for the complexes as a function of increasing nuclearity (Fig. 1). Thus, it provides a basis for regarding simple coordination compounds with a well-defined structure as an alternative to macromolecular systems, through a significant enhancement of catalytic activity of individual units due to the embedding several active centres on a properly designed multivalent core without increasing the catalyst metal loading.

2. Results and discussion

This work was based on the set of metallosupramolecular Pd(II) complexes **C1–C4** derived from mono- and poly-topic β -diketonate and 2,2'-bipyridine coligands. The four ligands **L1–L4**, involved syntheses where 1, 2 (two examples that differ in the location of the chelating group on the ring) or 3 diketone units were attached to a benzene core. To block polymerisation reactions involving purely diketonate species, the complexes **C1–C4** were formed by employing 2,2'-bipyridine to occupy two coordination sites on square-planar Pd(II), thus producing different oligonuclear species where each Pd(II) had an N_2O_2 coordination sphere. The complexation reactions between the ligands and a stoichiometric amount of $[Pd(bpy)(NO_3)_2]$ (1 equiv. for **L1**, 2 equiv. for **L2** and **L3**, 3 equiv. for **L4**) were performed in H_2O /acetone mixture (1:1, v/v) at 50 °C over 24 h without base being added to deprotonate the diketones (Fig. 2). The complexes were isolated by adding a 6-fold excess of NH_4PF_6 , which resulted in immediate deposition of an orange precipitate. The generation and purity of the ligands and cationic complexes were confirmed in solution via 1H NMR spectroscopy and ESI-MS spectrometry, and in the case of **C1**, **C3** and **C4** in the solid state using single-crystal X-ray diffraction.

The structure of the complexes **C1–C4** in solution was established using 1H NMR spectroscopy with d_6 -DMSO as solvent. The absence of enol proton signals near 16.5 ppm in comparison to the 1H NMR spectra of the ligands showed complexation to have resulted in deprotonation of the polyketone ligands. There were also noticeable shifts of the signals for *tert*-butyl protons H^5 and more minor shifts in the methine H^6 and aromatic proton H^{7-9} signals (see SI, Table S1). The unsymmetrical nature of the bound

diketonate units was reflected in the loss of twofold symmetry of the peaks due to the 2,2'-bipyridine units (Fig. 3 and see in SI, Figs. S7, S10, S13, S18). ESI-MS spectrometry also confirmed the successful generation of desired mono- and polynuclear complexes. All the peaks were in good agreement with their calculated theoretical distribution, allowing the molecularity of the coordination compounds to be unambiguously established (Figs. S9, S12, S17, S20).

The complexes **C1**, **C3** and **C4** were also characterized in the solid state (Fig. 4). Slow evaporation of DMF (**C1**, **C3**) or $MeNO_2$ (**C4**) solutions provided orange crystals suitable for single-crystal X-ray diffraction measurements. All the compounds, crystallizing in the triclinic space group $P\bar{1}$, showed the square planar geometry of Pd(II) ions coordinated by a β -diketonate chelate on one side and a bipyridine unit on the other (Fig. 4abd). Except for the *tert*-butyl groups, the molecules are very close to planar and devoid of steric hindrance to the axial coordination sites which could be involved in any catalytic function. Note that **C3** occurs as a dimer in the crystal (Fig. 4c), where two molecules are linked by a weak metal–metal interaction $Pd\cdots Pd$ (3.25 Å). As a result of the distorted symmetry of **C3**, which was not evident in solution spectra, half the Pd(II) ions adopted an elongated tetragonal pyramidal geometry. All crystal and structure refinement data are given in Table S2.

Assuming that the Pd(II) coordination compounds **C1–C4** would show catalytic activity in coupling reactions, their stability was investigated under basic as well as acidic conditions. The changes were followed via NMR spectroscopy through gradual addition of stoichiometric amounts of an acidic or basic titrant. Figs. S22 and S23 in SI show the 1H NMR spectra of a DMSO solution of complex **C1** after adding sequential portions of a base (triethylamine, TEA) and an acid (methanesulfonic acid, MSA), respectively. In both cases, no shifts of signals were detected. The complex **C1** was stable in basic as well as acidic environments, not undergoing any obvious reaction even after several days. The same behaviour was observed for **C2–C4**, indicating similar stability of these oligonuclear species (see SI, Figs. S24–S29). In comparison to previously reported Pd(II) complexes based on ambidentate pyridyl- β -diketonate ligands, their behaviour was quite different [10]. The

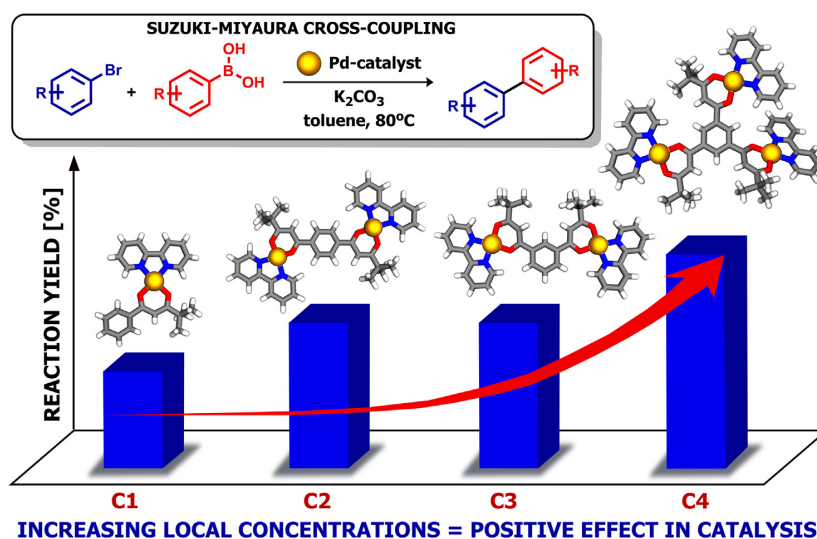


Fig. 1. The effect of local concentrations in the Suzuki-Miyaura cross-coupling catalysed by mono- and polynuclear Pd(II) complexes (the same Pd loading was provided in each reaction).

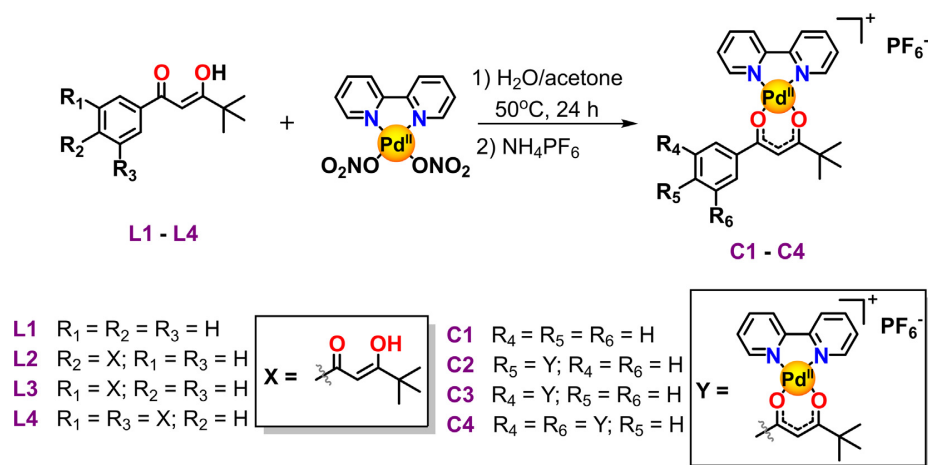
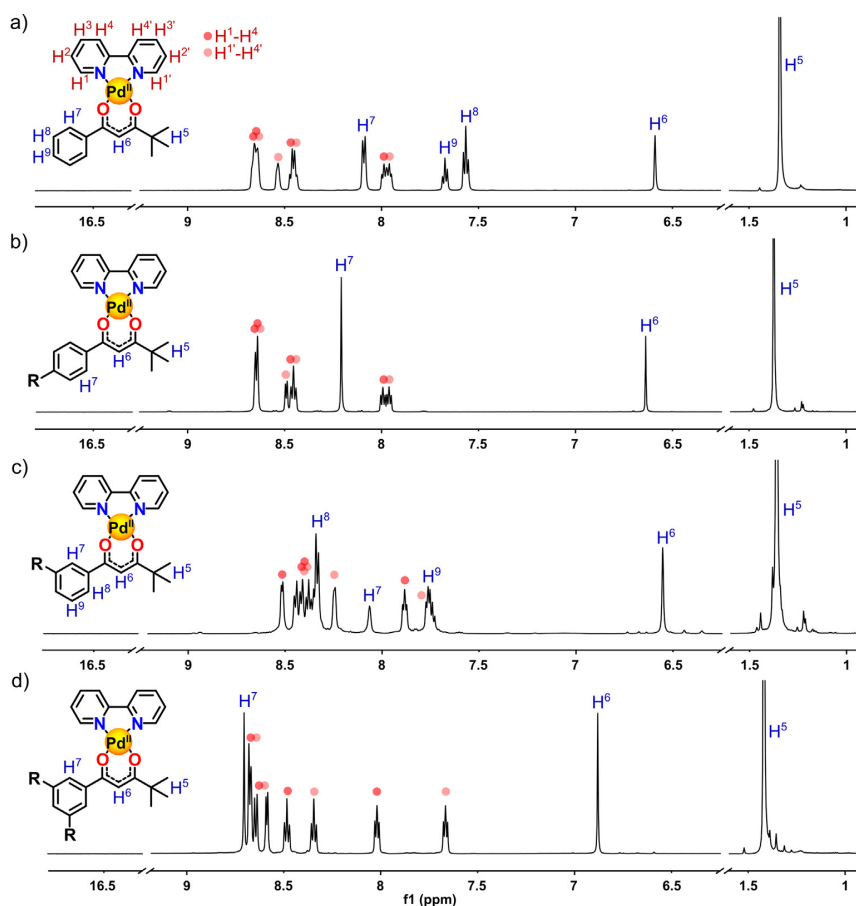


Fig. 2. General reaction scheme for synthesis of the complexes C1 – C4.

Fig. 3. Parts of ^1H NMR spectra (600 MHz, d_6 -DMSO) of the Pd(II) complexes: a) C1; b) C2; c) C3 and d) C4.

latter can be easily interconverted between *N*- and *O*-bound forms with 100% efficiency by appropriate pH control. Addition of base to the cationic *N*-bound complex led to linkage rearrangement and

formation of neutral *O,O*-chelated counterparts, a reaction which could be reversed by addition of acid. Such switching was not obviously possible for the compounds examined in this work, but the

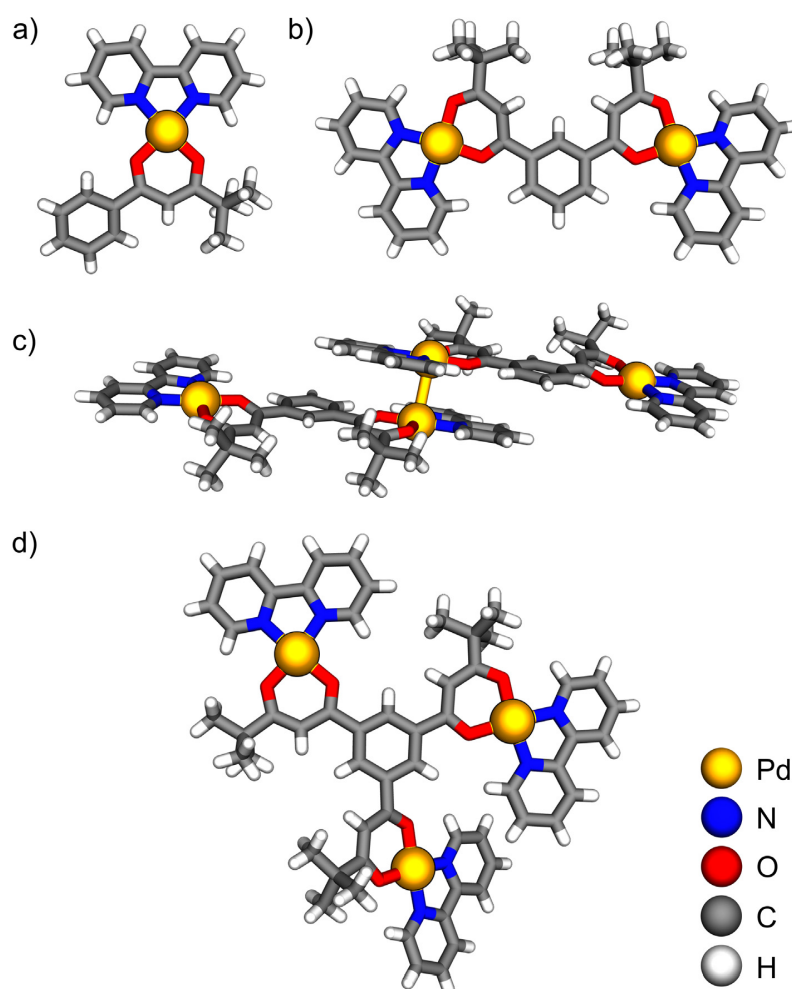


Fig. 4. X-ray structures of: a) **C1**, b) and c) **C3** in monomer and dimer forms, d) **C4**. The counterions and solvent molecules were omitted for clarity.

complexes **C1–C4** did appear to be less sensitive to acid, possibly because the bipyridine ligand rendered each complex entity cationic. The neutral complex $[\text{Pd}(\mathbf{L1})_2]$ derived from the monotopic ligand **L1**, in contrast, retained its form only under basic conditions, whereas the addition of acid led to its progressive decomposition and ultimately, as a result of a redox reaction, to the precipitation of metallic Pd (Figs. S30–S31).

To assess the influence of the differences in charge, composition and morphology between the complexes **C1–C4** on their catalytic activity, their use as catalyst precursors for the well-known Suzuki–Miyaura cross-coupling was chosen as a model reaction. While their actual catalytic efficiency was of interest, our major focus was primarily upon how this depended upon their compositional differences.

Conditions were firstly optimized for the Suzuki–Miyaura cross-coupling of 4'-bromoacetophenone and phenylboronic acid in the presence of base (K_2CO_3). All the optimization procedures are summarized in the SI, Table S3. From these experiments, it was found that the complexes **C1–C4** had their highest catalytic activity in toluene at 80 °C using 0.1 mol% Pd loading, enabling the synthesis of the expected 4-acetylbiphenyl in excellent yields (88–100% after just 4 h). To place the effects of each catalyst on an equal footing,

the polynuclear complexes **C2–C4** with more than one Pd(II) ion per complex molecule were considered simply in terms of the number of catalytic sites in each. Hence, the same molar percentage of Pd (not the complex) was employed in all the catalysed reactions and the various yields were not a consequence of different Pd loadings. Thus, any changes in catalytic activity can be directly related to the valency of the complex.

Groups of functionalized substrates were reacted to explore the capabilities of the reaction system in terms of functional group tolerance. As shown in Table 1, the complexes **C1–C4** allowed efficient coupling of aryl bromides with phenylboronic acid and the synthesis of a large scope of structurally distinct biphenyl derivatives. A range of different substrates bearing electron-donating as well as electron-withdrawing groups was investigated. All the reactions were performed without the need to exclude air or water, using the catalyst in the form of a DMF solution. The yields were determined via gas chromatography (GC) and the structures of products were confirmed using GC–MS analysis and NMR spectroscopy. The desired biphenyls were obtained in good to excellent yields and the cross-coupling reaction was clearly preferred. It is worth emphasizing that the catalysts **C1–C4** also enabled the coupling of pyridine or amine derivatives (**5a–7a**) which often lead to cata-

Table 1
The valency effect of catalysts **C1–C4** applied in the Suzuki-Miyaura coupling of functionalised ArBr with phenylboronic acid.^{a,c}

Substrate	Catalyst	Yield [%]
1a	C1	88
	C2	91
	C3	93
	C4	98 (95) ^d
2a	C1	70
	C2	79
	C3	70
	C4	92 (85) ^d
3a	C1	54
	C2	80
	C3	81
	C4	93 (86) ^d
4a	C1	53
	C2	70
	C3	79
	C4	92 (86) ^d
5a	C1	68
	C2	75
	C3	58
	C4	97 (94) ^d
6a	C1	49
	C2	56
	C3	60
	C4	70 (51) ^d
7a^b	C1	35
	C2	47
	C3	51
	C4	54 (46) ^d
8a	C1	57
	C2	68
	C3	76
	C4	89 (77) ^d
9a^b	C1	76
	C2	86
	C3	84
	C4	99 (82) ^d
10a^b	C1	23
	C2	61
	C3	32
	C4	73 (70) ^d

^a Reaction conditions: aryl bromide (1 mmol **1–6**, 0.5 mmol **7–8**, 0.33 mmol **9**, 0.25 mmol **10**), phenylboronic acid (1.2 mmol), K₂CO₃ (2.4 mmol) and Pd(II) complex (0.1 mol% Pd) were placed in a Schlenk flask under air atmosphere in toluene and heated at 80 °C over 4 h.

^b The reactions were performed over 24 h.

^c GC yields [%].

^d Isolated yields [%].

lyst poisoning [11] as well as aromatic polybromides (**7a–10a**), for which the GC conversion of aryl bromide was almost 100% [12]. The more important observation, however, is that trivalent catalyst **C4** performed more than three times better in the case of polyaromatic structures (e.g. **10a**), than its monovalent analogue. These results provide unequivocal proof that the significant enhancement in catalyst performance is a general nuclearity-related phenomenon. However, in order to obtain the multi-coupling products in high yields, it was necessary to extend the reaction time to 24 h (for instance, the GC yields were equal to 44% and 99% for the product **9a** using **C4**, respectively after 4 h and 24 h). Furthermore, the comparative experiments for substrates **1–10** demonstrated considerable differences between the individual catalysts in some cases. Overall, GC yields were the highest for **C4**, whereas **C1** exhibited the lowest catalytic activity in the majority of reactions. It indicated unequivocally that the catalyst efficiency is dependent on the composition of complexes, and actually the number of metal centres in each catalyst molecule for the same Pd loading. Regarding **C2** and **C3**, incorporating two catalytic sites in the structure in different positions, their catalytic activity was generally similar. Hence, the main factor responsible for the diversified efficiency of **C1–C4** seems to be their nuclearity, and other structural differences e.g. position of functional group on the aromatic ring, do not have a major impact on the catalytic efficiency.

A series of functionalised aryl boronic acids was also reacted with bromobenzene to further support and confirm the previous results and the evidence of an analogy to the dendritic effect. The same reaction conditions were maintained except for the coupling

between bromobenzene and 3-cyanophenylboronic acid **13**, which was carried out in ethanol due to the low solubility of the acid in toluene. Monitoring of the reactions via GC–MS analysis showed that a longer reaction time was required to reach acceptable yields (24 h). Most of the cross-coupling products were obtained in high yields > 70% (**1a**, **4a**, **8a**, **11a**, **12a**, **13a**), although we also noted poor yields in some cases (**14a**, **15a**), indicating a limitation of this procedure (Table 2). Despite low effectiveness in the latter examples, the nuclearity effect was still observed, e.g. by doubling the yield of **15a** in the reaction catalysed by **C4**. These tests with the variously substituted boronic acids nonetheless provided further evidence of the influence of the complex nuclearity on the catalytic activity. As in the initial study, significant differences in effectiveness were apparent, the mononuclear complex **C1** being the least active and the trinuclear **C4** the most.

Under identical reaction conditions (base, solvent, temperature, reaction time) and the same catalyst loading, the simple complexes [Pd(bpy)Cl₂], [Pd(bpy)(NO₃)₂], and [Pd(L1)₂] incorporating elements of **C1–C4** were significantly less active as catalysts (Table S4). Much lower GC yields, respectively 39%, 36% and 53% in comparison to 98% for **C4** in the reaction between 4-bromoacetophenone and phenylboronic acid, illustrated the importance of two different ligands on Pd(II) in the structures of **C1–C4**: bipyridine and β-diketone. Unambiguous indication of the role of each unit is difficult to determine at this stage of our investigations. However, of the very numerous Pd(II) complexes reported in the literature to effectively catalyse the Suzuki-Miyaura cross-coupling reaction [13], complex **C4** compares particularly well with the commonly employed commercial species such as [Pd(PPh₃)₂Cl₂] and [Pd(PPh₃)₄] (Table S4). Thus, **C4** can be considered as an effective catalyst for Suzuki-Miyaura coupling and possibly many related processes, constituting a useful addition to the catalyst family.

Any multinuclear metal complex can be regarded as a species where there is a high local concentration of the metal ion. Thus,

Table 2
The scope of the Suzuki-Miyaura coupling of bromobenzene with functionalised ArB(OH)₂.^{a,c}

Substrate	Catalyst	Yield [%]
1a	C1	89
	C2	95
	C3	96
	C4	98
4a	C1	38
	C2	44
	C3	63
	C4	79
8a	C1	43
	C2	70
	C3	72
	C4	74
11a	C1	47
	C2	53
	C3	54
	C4	70 (61) ^d
12a	C1	46
	C2	50
	C3	48
	C4	72 (59) ^d
13a^b	C1	79
	C2	82
	C3	86
	C4	94 (87) ^d
14a	C1	32
	C2	29
	C3	36
	C4	40 (31) ^d
15a	C1	9
	C2	18
	C3	12
	C4	19 (14) ^d

^a Reaction conditions: bromobenzene (1 mmol), boronic acid (1.2 mmol **1, 4, 11–15**, 0.6 mmol **8**), K₂CO₃ (2.4 mmol) and Pd(II) complex (0.1 mol% Pd) were placed in a Schlenk flask under air atmosphere in toluene and heated at 80 °C over 24 h.

^b The reactions were performed in ethanol.

^c GC yields [%].

^d Isolated yields [%].

for a catalytic metal where substrate binding is reversible, any dissociated substrate has relatively high probability of recapture due to the proximity of another site. This consequence of local concentration enhancement is one possible explanation of the observation of more effective reaction performance without increasing the catalyst loading [8c,14] considered to be especially noticeable in systems such as dendrimers, polymers and nanoparticles that contain many active centres attached to a multivalent scaffold [3c,15]. What is evident in the present results is that similar behaviour is apparent in much simpler and better defined oligonuclear species. These coordination units of a well-defined structure are obtained in a one-step synthesis which allows avoidance of potential problems including product losses, purification difficulties and irreproducibility. Even just a threefold difference in local concentration of Pd in the complexes **C1–C4** is sufficient to lead to significant differences in their effectiveness as catalysts of Suzuki-Miyaura coupling reactions at a common catalyst loading. While the exact nature of effects due to local concentration enhancement remains a matter of some speculation [16], increased Lewis acidity of a given metal site due to the proximity of others is one that is favoured [17]. For this reason, multivalent complexes would have more acidic catalytic sites than those of lower nuclearity, resulting in enhanced binding of substrates of a basic nature, and thus beneficially influencing the catalytic cycle and the observed reaction yields. To elucidate the observed positive effect in the reactions catalysed by **C1–C4**, our further research will focus on more detailed kinetic studies aimed at the establishment of a mechanism.

3. Conclusions

In this work we have described a series of new, mono- and oligonuclear metallosupramolecular compounds with Pd(II) centres bound in a heteroleptic environment of diketonate and bipyridine chelate units. These compounds differ significantly in terms of charge, composition and catalytic properties. They show enhanced stability under basic and acidic conditions in comparison to related diketonate complexes lacking the bipyridine coligand. All have been found to be efficient catalysts in Suzuki-Miyaura cross-coupling, as demonstrated in a number of experiments for a broad scope of structurally different aryl bromides and boronic acids. A significant trend in all these results is that the catalytic efficiency increases with the nuclearity of the catalyst. Thus, under the same reaction conditions and an identical total Pd(II) loading, the reaction yields were significantly enhanced as the number of Pd(II) ions per complex molecule increased. This is considered as new example of the nuclearity effect demonstrated on a simple, highly-stable and well-defined catalysts.

4. Experimental section

4.1. Materials and methods

All chemicals and solvents were obtained from commercial sources (mainly Sigma-Aldrich) and used without further purification. THF was dried using benzophenone/sodium procedure prior to use. The ^1H NMR and ^{13}C NMR spectra were acquired on Bruker Fourier 300 and 600 MHz spectrometers equipped with $^1\text{H}/^{13}\text{C}$ 5 mm probe, and referenced to the solvent residual peaks. All spectra were acquired at 298 K. The NMR solvents were purchased from Euriso-Top or Deutero GmbH, and used as received. GC-MS analysis was performed on a Bruker Scion SQ using a toluene method. ESI-MS spectra were recorded on a Bruker Impact HD Q-TOF spectrometer in positive-ion mode.

4.2. X-ray crystallography

The data have been deposited in the Cambridge Crystallographic Data Collection (CCDC), deposition numbers CCDC **2144898**, **2150458** and **2150450**. These data can be obtained free of charge via https://www.ccdc.cam.ac.uk/data_request/cif, or by emailing data_request@ccdc.cam.ac.uk, or by contacting The Cambridge Crystallographic Data Centre, 12, Union Road, Cambridge CB2.

4.3. General procedure for synthesis of Pd(II) complexes

To a mixture of H_2O /acetone (1:1, v/v, 10 mL) a ligand (0.1 mmol) was added. In case of the ligands **L2–L4** they were previously dissolved in chloroform (2 mL). After, $[\text{Pd}(\text{bpy})(\text{NO}_3)_2]$ (0.1 mmol for **L1**, 0.2 mmol for **L2** and **L3**, 0.3 mmol for **L4**) was added and the solution was stirred at 50 °C for 24 h. The complexes were obtained by adding a 6-fold excess of NH_4PF_6 to the above aqueous solution at 60 °C, which resulted in the immediate deposition of product. The precipitate was centrifuged off from the hot suspension, washed with cold water and diethyl ether, and then dried under vacuum.

4.4. General procedure for the Suzuki-Miyaura coupling

The reaction was performed in a Schlenk flask equipped with a magnetic stirring bar under air atmosphere. The tube was charged with aryl bromide (1.0 mmol, 1.0 equiv.), phenylboronic acid (1.2 mmol, 1.2 equiv.) and toluene as a solvent (10 mL). After, the complex **C4** (0.00033 mmol, 0.00033 equiv.) in the form of solution in DMF (0.1 mL) and K_2CO_3 (2.4 mmol, 2.4 equiv.) dissolved in H_2O (0.2 mL) were added. The Schlenk flask was sealed and the mixture was heated for 4 h at 80 °C. After, the solution was cooled to room temperature, diluted with dichloromethane (20 mL) and washed with water (10 mL). Gathered aqueous phase was extracted with dichloromethane (3×20 mL). The organic layers were collected, dried over Na_2SO_4 , filtered and the solvent was removed under vacuum. The residue was purified by column chromatography on silica gel.

Declaration of Competing Interest

The authors declare that they have no known competing financial interests or personal relationships that could have appeared to influence the work reported in this paper.

Acknowledgments

We thank the National Science Center (grant SONATA BIS 2018/30/E/ST5/00032 – ARS) for financial support.

Author contributions

The manuscript was written through contributions of all authors. All authors have given approval to the final version of the manuscript.

Appendix A. Supplementary material

Supplementary data to this article can be found online at <https://doi.org/10.1016/j.jcat.2022.05.021>.

References

- [1] (a) X. Wang, G. Zhang, L. Yang, E. Sharman, J. Jiang, Material descriptors for photocatalyst/catalyst design, *Wiley Interdisc. Rev.: Computational Mol. Sci.* **8** (5) (2018) 1369;

- (b) W. Tu, Y. Xu, S. Yin, R. Xu, Rational design of catalytic centers in crystalline frameworks, *Adv. Mater.* 1707582 (2018);
- (c) A. Thomas, M. Driess, Bridging the materials gap in catalysis: entrapment of molecular catalysts in functional supports and beyond, *Angew. Chem. Int. Ed.* 48 (11) (2009) 1890–1892;
- (d) S.J. Li, Y.T. Zhou, X. Kang, D.X. Liu, L. Gu, Q.H. Zhang, J.M. Yan, Q. Jiang, A Simple and Effective Principle for a Rational Design of Heterogeneous Catalysts for Dehydrogenation of Formic Acid, *Adv. Mater.* 31 (15) (2019) 1806781;
- (e) S. Alerasool, C.P. Kelkar, R.J. Farrauto, Rational Design Strategies for Industrial Catalysts. In: *Design of Heterogeneous Catalysts*, Ozkan, U. S., Ed. 2009.;
- (f) A. Walczak, H. Stachowiak, G. Kurpik, G. Hreczycho, A.R. Stefankiewicz, High catalytic activity and selectivity in hydrosilylation of new Pt(II) metallocene complexes based on ambidentate ligands, *J. Catal.* 373 (2019) 139–146;
- (g) R.A.A. Abdine, G. Kurpik, A. Walczak, S.A.A. Aeahs, A.R. Stefankiewicz, F. Monnier, M. Taillefer, Mild temperature amination of aryl iodides and aryl bromides with aqueous ammonia in the presence of CuBr and pyridyl-diketone ligands, *J. Catal.* 376 (2019) 119–122;
- (h) A. Walczak, G. Kurpik, M. Zaranek, P. Pawluć, A.R. Stefankiewicz, N palladacyclic complexes bearing flexidentate ligands as efficient (pre)catalysts for Heck ofenation of aryl halides, *J. Catal.* 405 (2022) 84–90.
- [2] P. Scrimin, M.A. Cardona, C.M.L. Prieto, L.J. Prins, Multivalency as a design criterion in catalyst development, *Multivalency* (2018) 153–176.
- [3] (a) D. Wang, D. Astruc, Dendritic catalysis—Basic concepts and recent trends, *Coord. Chem. Rev.* 257 (15–16) (2013) 2317–2334;
- (b) B. Helms, J.M.J. Fréchet, The dendrimer effect in homogeneous catalysis, *Adv. Synth. Catal.* 348 (10–11) (2006) 1125–1148;
- (c) D. Méry, D. Astruc, Dendritic catalysis: major concepts and recent progress, *Coord. Chem. Rev.* 250 (15–16) (2006) 1965–1979;
- (d) D. Astruc, E. Boisselier, C. Ornelas, Dendrimers designed for functions: from physical, photophysical, and supramolecular properties to applications in sensing, catalysis, molecular electronics, photonics, and nanomedicine, *Chem. Rev.* 110 (4) (2010) 1857–1959;
- (e) S. Kitagawa, R. Kitaura, S.-I. Noro, Functional porous coordination polymers, *Angew. Chem. Int. Ed.* 43 (18) (2004) 2334–2375.
- [4] (a) K. Heuze, D. Méry, D. Gauss, J.C. Blais, D. Astruc, Copper-free monomeric and dendritic palladium catalysts for the Sonogashira reaction: substituent effects, synthetic applications, and the recovery and re-use of the catalysts, *Chem.—A Eur. J.* 10 (16) (2004) 3936–3944;
- (b) R.S. Bagul, N. Jayaraman, Multivalent dendritic catalysts in organometallic catalysis, *Inorg. Chim. Acta* 409 (2014) 34–52;
- (c) N. Mketi, J.H.L. Jordaan, A. Jordaan, A.J. Swarts, S.F. Mapolie, Synthesis, characterization, and catalytic application of mononuclear and dendritic cationic cuiminopyridine-ligated complexes in aryl iodide hydroxylation, *Eur. J. Inorg. Chem.* 2016 (23) (2016) 3781–3790;
- (d) P. Neumann, H. Dib, A.M. Caminade, E. Hey-Hawkins, Redox control of a dendritic ferrocenyl-based homogeneous catalyst, *Angew. Chem. Int. Ed.* 54 (1) (2015) 311–314.
- [5] (a) K. Goren, J. Karabline-Kuks, Y. Shiloni, E. Barak-Kulbak, S.J. Miller, M. Portnoy, Multivalency as a key factor for high activity of selective supported organocatalysts for the Baylis-Hillman reaction, *Chem.—A Eur. J.* 21 (3) (2015) 1191–1197;
- (b) E. Delort, T. Darbre, J.-L. Reymond, A strong positive dendritic effect in a peptide dendrimer-catalyzed ester hydrolysis reaction, *J. Am. Chem. Soc.* 126 (2004) 15642–15643.
- [6] G. Jayamurugan, N. Jayaraman, Increased efficacies of an individual catalytic site in clustered multivalent dendritic catalysts, *Adv. Synth. Catal.* 351 (14–15) (2009) 2379–2390.
- [7] (a) M.V. Walter, M. Malkoch, Simplifying the synthesis of dendrimers: accelerated approaches, *Chem. Soc. Rev.* 41 (13) (2012) 4593–4609;
- (b) A. Sharma, A. Kakkar, Designing dendrimer and miktoarm polymer based multi-tasking nanocarriers for efficient medical therapy, *Molecules* 20 (9) (2015);
- (c) M. Fischer, F. Vögtle, Dendrimers: from design to application—A progress report, *Angew. Chem. Int. Ed.* 38 (7) (1999) 884–905.
- [8] (a) D. Astruc, F. Chardac, Dendritic catalysts and dendrimers in catalysis, *Chem. Rev.* 101 (9) (2001) 2991–3024;
- (b) D. Astruc, *Nanoparticles and Catalysis*, Wiley-VCH Weinheim (2007);
- (c) R.S. Bagul, N. Jayaraman, Efficacies of multivalent vs monovalent poly(ether imine) dendritic catalysts within a generation in multiple C-C bond forming reactions, *J. Organomet. Chem.* 701 (2012) 27–35;
- (d) F. Fu, J. Xiang, H. Cheng, L. Cheng, H. Chong, S. Wang, P. Li, S. Wei, M. Zhu, Y. Li, A Robust and efficient Pd3 cluster catalyst for the Suzuki reaction and its odd mechanism, *ACS Catal.* 7 (3) (2017) 1860–1867.
- [9] (a) H.-K. Luo, H. Schumann, New bi-nuclear and multi-nuclear α -diimine/nickel catalysts for ethylene polymerization, *J. Mol. Catal. A: Chem.* 227 (1–2) (2005) 153–161;
- (b) Z. Xi, F. Liu, Y. Zhou, W. Chen, Cu/L (L=pyridine-functionalized 1,3-diketones) catalyzed C-N coupling reactions of aryl halides with NH-containing heterocycles, *Tetrahedron* 64 (19) (2008) 4254–4259;
- (c) I. Bratko, M. Gomez, Polymetallic complexes linked to a single-frame ligand: cooperative effects in catalysis, *Dalton Trans.* 42 (30) (2013) 10664–10681.
- [10] A. Walczak, A.R. Stefankiewicz, pH-induced linkage isomerism of Pd(II) complexes: a pathway to air- and water-stable Suzuki-Miyaura-reaction catalysts, *Inorg. Chem.* 57 (1) (2018) 471–477.
- [11] (a) R.H. Crabtree, Deactivation in homogeneous transition metal catalysis: causes, avoidance, and cure, *Chem. Rev.* 115 (1) (2015) 127–150;
- (b) M. Kadri, J. Hou, V. Dorcet, T. Roisnel, L. Bechki, A. Miloudi, C. Bruneau, R. Gramage-Doria, Palladium-catalyzed cross-coupling reactions controlled by noncovalent ZnN interactions, *Chem.—A Eur. J.* 23 (21) (2017) 5033–5043.
- [12] (a) J. Tong, H. Wang, X. Cai, Q. Zhang, H. Ma, Z. Lei, Suzuki coupling reaction catalyzed heterogeneously by Pd(salen)/polyoxometalate compound: another example for synergistic effect of organic/inorganic hybrid, *Appl. Organomet. Chem.* 28 (2) (2014) 95–100;
- (b) J.B. Shaik, V. Ramkumar, B. Varghese, S. Sankararaman, Synthesis and structure of trans-bis(1,4-dimesityl-3-methyl-1,2,3-triazol-5-ylidene)palladium(II) dichloride and diacetate. Suzuki-Miyaura coupling of polybromoarenes with high catalytic turnover efficiencies, *Beilstein J. Org. Chem.* 9 (2013) 698–704.
- [13] R. Rossi, F. Bellina, A. Carpita, Palladium catalysts for the Suzuki cross-coupling reaction: an overview of recent advances, *Synthesis* 2004 (15) (2004) 2419–2440.
- [14] (a) S. Gonell, J.N.H. Reek, Gold-catalyzed Cycloisomerization Reactions within Guanidinium M(12)L(24) Nanospheres: the Effect of Local Concentrations, *ChemCatChem* 11 (5) (2019) 1458–1464;
- (b) R. Gramage-Doria, J. Hessels, S.H.A.M. Leenders, O. Tröppner, M. Dürr, I. Ivanović-Burmazović, J.N.H. Reek, Gold(I) Catalysis at Extreme Concentrations Inside Self-Assembled Nanospheres, *Angew. Chem. Int. Ed.* 53 (49) (2014) 13380–13384;
- (c) M. Kołodziejewski, A.J. Brock, G. Kurpik, A. Walczak, F. Li, J.K. Clegg, A.R. Stefankiewicz, Charge Neutral [Cu2L2] and [Pd2L2] Metalloclusters: Self-Assembly, Aggregation, and Catalysis, *Inorg. Chem.* 60 (13) (2021) 9673–9679;
- (d) F. Yu, D. Poole III, S. Mathew, N. Yan, J. Hessels, N. Orth, I. Ivanović-Burmazović, J.N.H. Reek, Control over Electrochemical Water Oxidation Catalysis by Preorganization of Molecular Ruthenium Catalysts in Self-Assembled Nanospheres, *Angew. Chem. Int. Ed.* 57 (35) (2018) 11247–11251.
- [15] (a) F. Manea, L. Pasquato, L.J. Prins, P. Scrimin, Multivalent catalysts for the cleavage of nucleic acids and their models, *Nucleic Acids Symp. Ser.* 51 (1) (2007) 67–68;
- (b) G.E. Oosterom, J.N.H. Reek, P.C.J. Kamer, P.W.N.M. van Leeuwen, Transition metal catalysis using functionalized dendrimers, *Angew. Chem. Int. Ed.* 40 (10) (2001) 1828–1849.
- [16] Y. Yamamoto, M. Shibasaki, *Multimetallic Catalysis in Organic Synthesis*, Wiley-VCH, Weinheim, 2004.
- [17] (a) G. Zhang, G. Proni, S. Zhao, E.C. Constable, C.E. Housecroft, M. Neuburger, J. A. Zampese, Chiral tetranuclear and dinuclear copper(II) complexes for TEMPO-mediated aerobic oxidation of alcohols: are four metal centres better than two?, *Dalton Trans.* 43 (32) (2014) 12313–12320;
- (b) E.C. Constable, G. Zhang, C.E. Housecroft, M. Neuburger, S. Schaffner, W.-D. Woggon, In search of enantioselective catalysts for the Henry reaction: are two metal centres better than one?, *New J Chem.* 33 (5) (2009) 1064–1069;
- (c) N. Krittametaporn, T. Chantarojsiri, A. Virachotikul, K. Phomphrai, N. Kuwamura, T. Kojima, T. Konno, P. Sangtrirutnugul, Influence of catalyst nuclearity on copper-catalyzed aerobic alcohol oxidation, *Dalton Trans.* 49 (3) (2020) 682–689;
- (d) N.E. Shepherd, H. Tanabe, Y. Xu, S. Matsunaga, M. Shibasaki, Direct Catalytic Asymmetric Vinylogous Mannich-Type and Michael Reactions of an α , β -Unsaturated γ -Butyrolactam under Dinuclear Nickel Catalysis, *J. Am. Chem. Soc.* 132 (11) (2010) 3666–3667.



Pd(II) Complexes with Pyridine Ligands: Substituent Effects on the NMR Data, Crystal Structures, and Catalytic Activity

Gracjan Kurpiak, Anna Walczak, Mateusz Goldyn, Jack Harrowfield, and Artur R. Stefankiewicz*

Cite This: *Inorg. Chem.* 2022, 61, 14019–14029

Read Online

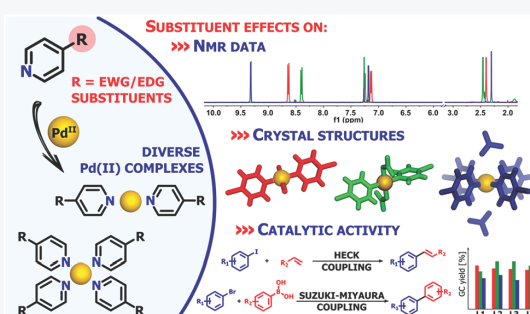
ACCESS |

Metrics & More

Article Recommendations

Supporting Information

ABSTRACT: A wide range of functionalized pyridine ligands have been employed to synthesize a variety of Pd(II) complexes of the general formulas $[\text{PdL}_4](\text{NO}_3)_2$ and $[\text{PdL}_2\text{Y}_2]$, where L = 4-X-py and Y = Cl^- or NO_3^- . Their structures have been unambiguously established via analytical and spectroscopic methods in solution (NMR spectroscopy and mass spectrometry) as well as in the solid state (X-ray diffraction). This in-depth characterization has shown that the functionalization of ligand molecules with groups of either electron-withdrawing or -donating nature (EWG and EDG) results in significant changes in the physicochemical properties of the desired coordination compounds. Downfield shifts of signals in the ^1H NMR spectra were observed upon coordination within and across the complex families, clearly indicating the relationship between NMR chemical shifts and the ligand basicity as estimated from $\text{p}K_a$ values. A detailed crystallographic study has revealed the operation of a variety of weak interactions, which may be factors explaining aspects of the solution chemistry of the complexes. The Pd(II) complexes have been found to be efficient and versatile precatalysts in Suzuki–Miyaura and Heck cross-coupling reactions within a scope of structurally distinct substrates, and factors have been identified that have contributed to efficiency improvement in both processes.



INTRODUCTION

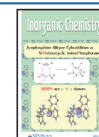
Since its discovery by Thomas Anderson in 1849, pyridine has been one of the most popular heterocyclic compounds used in chemistry. Despite the many similarities between pyridine and benzene, the introduction of an electronegative N atom to the aromatic ring significantly differentiates their physicochemical properties.¹ The presence of a pair of nonbonding electrons in the valence shell of the N atom enables pyridine derivatives to act as Lewis bases toward a wide variety of metal ions.² Both pyridine and polypyridine ligands are good neutral donors of mono- or multidentate nature, and their coordination properties can be relatively easily altered by substitution with electron-donating or -withdrawing groups.³ The structural and electronic modifications achieved by the functionalization of heterocyclic rings enable modulation of the metal coordination sphere, which can lead to improvement of the desired properties and potential applicability.⁴ Furthermore, pyridine and its derivatives can be utilized as model units for research on important biomolecules such as nicotine, pyridoxine, or nicotinamide adenine dinucleotide phosphate (NADP).^{4a,5} A wide variety of transition-metal complexes with pyridine-based ligands having both academic and industrial importance have been successfully generated, as reflected in the rich literature in this field.⁶ Notably, coordination structures based on pyridyl

units have shown real application potential as catalysts,⁷ compounds of cytotoxic activity,⁸ and molecule magnets.⁹

Where direct complexation equilibrium measurements of the Lewis basicity of a ligand are unavailable, the Brønsted basicity, measured as $\text{p}K_a$ values, usually rather readily obtained for pyridine derivatives, has been widely applied as a measure of the effect of any substituent on pyridine donor behavior.¹⁰ In a recent study of Pt(II) complexes of 4-substituted pyridines having some parallels with the present study of Pd(II) species,¹¹ it was found that the ^1H NMR chemical shifts of the 2/6 protons showed a same linear dependence on the $\text{p}K_a$ for the coordinated as well as free ligands, consistent with protonation being a useful guide to coordination behavior. Pd(II) complexes with pyridine derivatives have been used as efficient catalysts in reactions such as the carbonylation of nitro compounds,¹² reduction of nitro compounds to amines,¹³ or carbonylation of aniline derivatives by CO/O_2 .¹⁴ A successful example of the correlation between the catalytic efficiency and

Received: June 10, 2022

Published: August 19, 2022



ligand basicity is provided in the conversion of nitrobenzene to ethyl *N*-phenylcarbamate catalyzed by a series of $[\text{PdL}_2\text{Cl}_2]$ complexes, where L = various di- and monosubstituted pyridines.^{12a} An increase in the reaction yield was observed when Pd(II) complexes based on more basic ligands were used as catalysts, although steric effects were also apparent in species with 2/6 substituents, leading to the conclusion that 3 or 4 substitution provided the best correlation with basicity.

In this work, we have employed a series of 4-substituted pyridine ligands, **L1–L12** (Scheme 1), to generate an array of coordination compounds with Pd(II) cations of a square-planar geometry. The particular reaction conditions employed provided di- and tetrasubstituted complexes diversified in terms of their charge and composition. We anticipated that the properties of such complexes could be tuned by modifying the nature of the ligand substituents, and our efforts to prove this are presented below. Detailed analyses have been made of the structures and ^1H NMR spectra of the complexes in relation to substituent effects, and we have extended this investigation to that of functionality by employing the complexes as catalyst precursors in Suzuki–Miyaura and Heck cross-coupling reactions involving a range of organic reagents.

RESULTS AND DISCUSSION

Synthesis of Complexes. The substituents on the 4 position of ligands **L1–L12** span a range of both electron-withdrawing and -donating groups, but pyridine-N-bound complexes of all of the ligands can be isolated under the appropriate reaction conditions. While, in principle, mono, bis,

tris, and tetrakis species are possible, the use of an exact 2:1 L/Pd(II) reaction stoichiometry enabled the isolation of neutral $[\text{PdL}_2\text{Y}_2]$, where $\text{Y} = \text{Cl}^-$ or NO_3^- , whereas the use of a large excess of the ligand [10:1 L/Pd(II)] was required to shift the reaction equilibrium toward the exclusive generation of tetrasubstituted compounds, allowing for the ready isolation of cationic complexes $[\text{PdL}_4]^{2+}$ as their nitrate salts. The synthetic procedures are outlined in Scheme 1 and described in detail in the SI. On the basis of their ^1H NMR spectra [see the Supporting Information (SI) and Figure 1b] allied to the X-ray structural results (see below), all of the $[\text{PdL}_2\text{Cl}_2]$ products (**1a–12a**) appeared to contain only the trans isomer, whereas the $[\text{PdL}_2(\text{NO}_3)_2]$ products (**1b–12b**) contained minor but detectable amounts of the cis isomer. This preference for the trans configuration mimics that known for various Pt(II) analogues.¹¹ The use of PdCl_2 or $[\text{Pd}(\text{DMSO})_2\text{Cl}_2]$ (DMSO = dimethyl sulfoxide) as reactants for the formation of $[\text{PdL}_4]^{2+}$ cations (**1c–12c**) was efficient but required the elimination of chloride from the reaction mixtures by the addition of AgNO_3 . The ease of formation of the $[\text{PdL}_4]^{2+}$ cations appeared to increase with the basicity of the ligand, and this may explain why a pure species **6b** could not be isolated with the most strongly basic unit **L6**. The substituents of ligands **L10–L12** involve good coordinating sites that appeared, probably through competition with nitrate, to divert the formation of products **10b–12b** into that of inseparable mixtures.

Mass Spectrometry (MS) Analysis. The successful generation of the desired mononuclear Pd(II) compounds

Scheme 1. Synthetic Routes for the Pd(II) Complexes Based on the Pyridine Ligands L1–L12

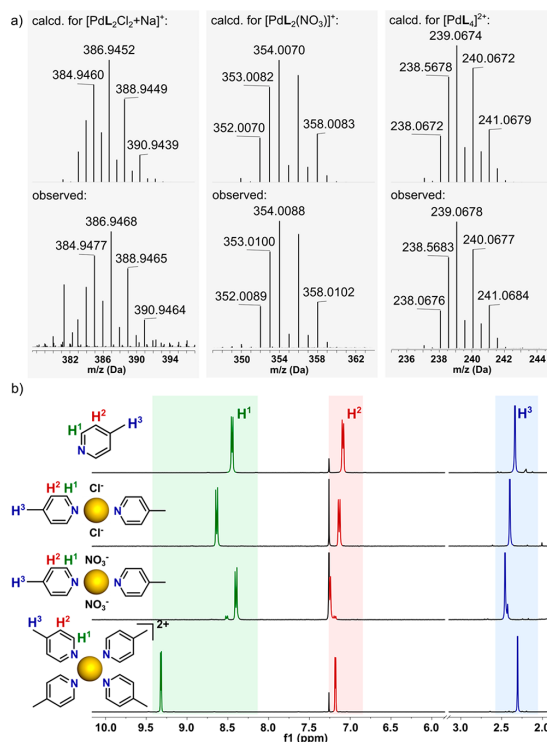
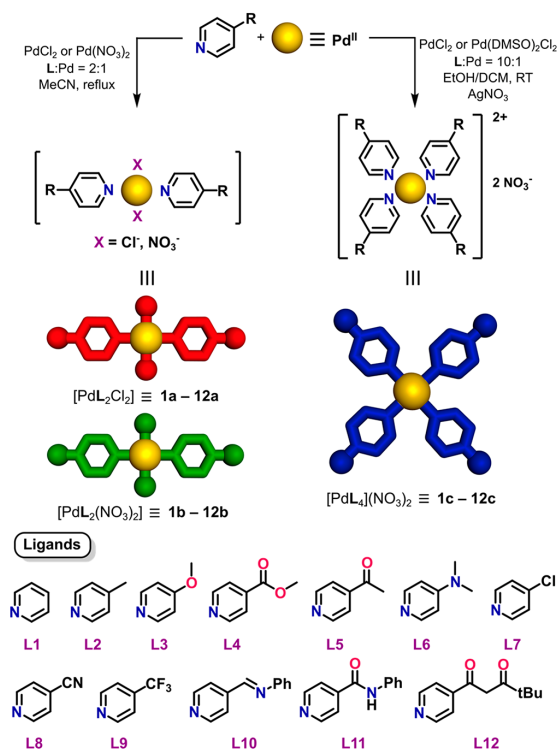


Figure 1. (a) ESI-MS spectra of Pd(II) complexes **2a–2c**, showing the calculated isotopic model (top) and observed data (bottom). (b) ^1H NMR spectra (300 MHz, CDCl_3) of compounds **2a–2c**.

was confirmed via electrospray ionization mass spectrometry (ESI-MS). As shown in Figure 1a, with the example of complexes with L2, isotopically resolved peaks were generally found for $[M + Na]^+$, $[M - NO_3]^-$, and $[M - 2NO_3]^{2+}$, where M represents the intact assembly for units of the general formulas $[PdL_2Cl_2]$ (2a), $[PdL_2(NO_3)_2]$ (2b), and $[PdL_4](NO_3)_2$ (2c), respectively. All of the peaks were in good agreement with their calculated distribution, allowing the molecularity to be unambiguously established and to distinguish the specific types of complexes. The MS data for all of the units are available in the SI.

NMR Spectroscopy. Apart from signals due to different substituents, the 1H NMR spectra were all very similar, with the 2-fold symmetry of the free ligands retained in all of the complexes and all ligand units in any particular complex being equivalent. In general, a greater sensitivity to the composition and structure of the complexes was seen in the chemical shifts of the H^1 protons (on C adjacent to N) rather than in those of the H^2 protons, and the presence of small amounts of cis isomer in the products 1b–12b, <10% in all cases, was readily discerned on this basis. Spectra typical of the whole group are shown for the complexes of L2 in Figure 1b, with the results for all other species being included in the SI. A comparison of the various *trans*- $[PdL_2(NO_3)_2]$ (1b–12b) and *trans*- $[PdL_2Cl_2]$ (1a–12a) pairs shows that the H^1 chemical shifts are sensitive to the nature of the adjacent donor atom, and this is presumably a contributor to the very large downfield shifts (~0.5–1 ppm relative to those of the free ligands) for the H^1 proton signals of complexes 1c–12c, although the dominant effect here may be that of ion pairing involving $C-H^1 \cdots ONO_2$ bonding, as proposed to explain similar observations on Pt(II) analogues.¹¹ Again, as observed for Pt(II), the H^1 chemical shifts (Table 1) show a close-to-linear dependence on the pK_a values of the protonated ligands (Figure 2), indicating that the substituent effects remain operative along with any effects of Pd(II) coordination.

Solution Complexation Equilibria. In regard to ligand substitution processes, Pd(II) is classified as a labile metal ion and its substitution reaction rates are typically orders of magnitude faster than those of Pt(II).¹⁷ This lability was readily observed for complexes 2a–2c by using 1H NMR spectroscopy to follow titrations with acid (methanesulfonic acid, MSA) and base (triethylamine, Et_3N). Results typical of what was observed generally are shown in Figure 3. Thus, the equilibrium mixture of *cis*- and *trans*-2b reacted with Et_3N to give ultimately some 2c, while no intermediates such as $[PdL_3Y]^+$ were detected via NMR. Because of the ligand deficiency after the altered L/Pd(II) complex stoichiometry, species 2c were necessarily accompanied by unidentifiable Pd(II) species to which L2 was not coordinated. Neutralization of the reaction mixture with MSA did not return the original complex, retaining the structure of tetrakis(pyridine) units (Figures 3a and S33). In another experiment, the 1H NMR titration of complex 2c with sequential portions of MSA led to changes indicative of the dissociation and protonation of L2 and probably some substitution of nitrate by methanesulfonate, which resulted in the complete disappearance of signals from 2c. Although the bis(ligand) units were identified as one of the decomposition products, their content decreased with increasing acid concentration. Neutralization of the mixture allowed regeneration of the tetrakis ions 2c (Figures 3b and S36).

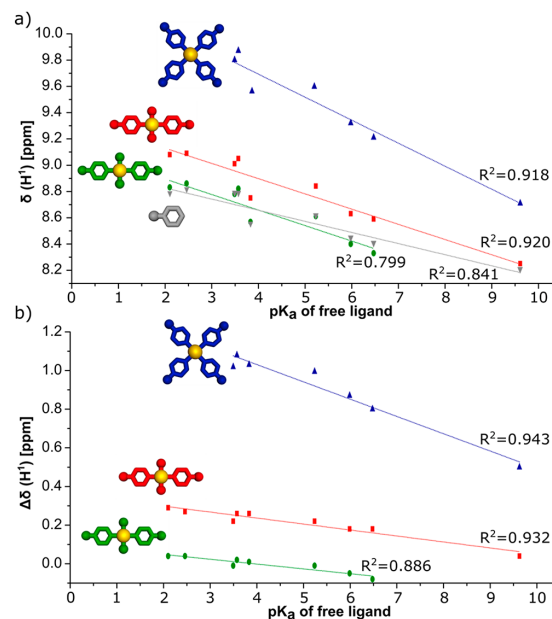


Figure 2. (a) Relationships between the chemical shifts (δ , ppm) of the signal H^1 in the 1H NMR spectra ($CDCl_3$, 25 °C) and pK_a values of free ligands for the Pd(II) complexes. (b) Relationships between the chemical shift changes ($\Delta\delta$, ppm) of the signal H^1 in the 1H NMR spectra ($CDCl_3$, 25 °C) and pK_a values of free ligands for the Pd(II) complexes. Only ligands of known pK_a values are included in the graphs.

Table 1. 1H NMR Chemical Shifts (δ , ppm) in $CDCl_3$ of H^1 Protons for Pd(II) Complexes Based on Ligands L1–L12

	$pK_a^{b,c}$	$\delta(H^1)$ [ppm]			
		L	PdL_2Cl_2 (1a–12a)	$PdL_2(NO_3)_2$ (1b–12b)	$PdL_4(NO_3)_2$ (1c–12c)
L1	5.23	8.62	8.84	8.61	9.63
L2	5.98	8.45	8.63	8.40	9.32
L3	6.47	8.41	8.59	8.33	9.21
L4	3.49	8.79	9.01	8.78	9.80
L5	3.57	8.79	9.05	8.82	9.87
L6	9.61	8.21	8.25		8.71
L7	3.83	8.49	8.75	8.50	9.52
L8	2.10	8.79	9.08	8.83	
L9	2.46	8.82	9.09	8.86	
L10	3.07	8.77	8.97		9.79
L11 ^a	3.12	8.79	8.99		9.44
L12	2.86	8.75	8.95		9.75

^aThe spectra of L11 and its complexes were recorded in $DMSO-d_6$.

^bFor ligands L1–L9, the experimental pK_a values are provided in the literature.^{11,15} For ligands L10–L12, the predicted pK_a values are provided by SciFinder.¹⁶

Conversely, no significant changes were observed during the 1H NMR titrations of 2b and 2c with MSA and Et_3N , respectively (Figures S34 and S35). Moreover, 2a turned out to be completely insensitive in both the basic and acidic environments (Figures S31 and S32).

In contrast to the series of $[PtL_4]Cl_2$ units obtained by Marzilli et al.,¹¹ the Pd(II) analogues have not been isolated despite many synthetic attempts. All experiments led to the

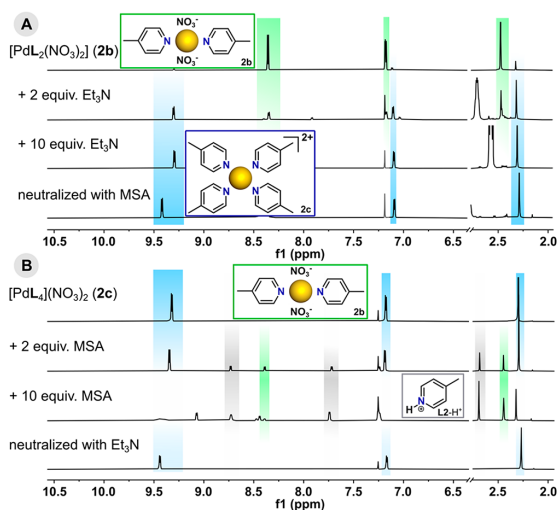


Figure 3. Parts of the ¹H NMR spectra (600 MHz, CDCl₃) showing the transformations of (a) 2b upon the addition of Et₃N and (b) 2c upon the addition of MSA.

formation of disubstituted species 1a–12a even if a significant excess of ligand was used. To explain the distinct behavior of Pd(II) and Pt(II) complexes, we investigated the influence of Cl[−] anions on the stability of the tetrakis(ligand) unit 2c. During ¹H NMR titration with triethylamine hydrochloride (Et₃N·HCl) as the chloride source, complete disappearance of the signals from 2c was noticed just after the addition of 2 equiv of the organic salt (Figures 4a and S29). Thus, in the presence of chloride, complete decomposition of 2c and finally conversion to 2a was observed along with the release of noncoordinated ligand molecules, as evidenced by the full consistency of NMR chemical shifts. Additionally, 2a was titrated with sequential portions of ligand in an attempt to form the tetrakis species. Its structure remained initially intact,

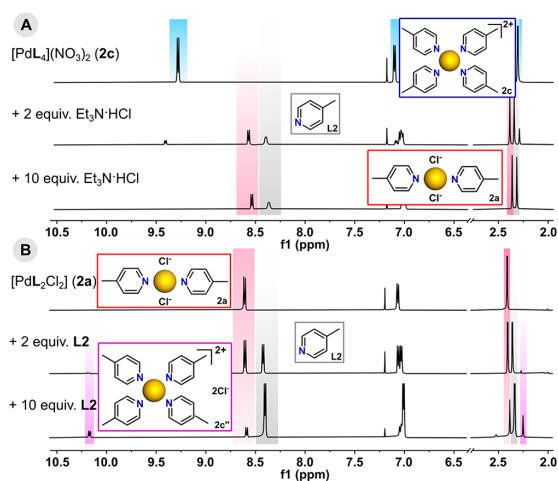


Figure 4. Parts of the ¹H NMR spectra (600 MHz, CDCl₃) showing the transformations of (a) 2c into 2a with Et₃N·HCl and (b) 2a upon the addition of L2.

but unusually high downfield signals [$\Delta\delta(\text{H}^1) = \sim 1.8$ ppm compared to that of free ligand] were found to appear with increasing ligand concentration (Figures 4b and S30). These signals could signify the replacement of chloride anions by L2 and generation of the target [PdL₄]Cl₂ (2c''), but the bis(pyridine) complex 2a was still the dominant form even with a large excess of ligand (10 equiv). All attempts to isolate tetrakis units were unsuccessful.

X-ray Crystallography. Slow diffusion of *n*-hexane vapor into saturated solutions of the complexes in chloroform afforded a number of crystals of Pd(II) units from three different families. Single-crystal X-ray structure determinations have been performed on 13 complexes: 2b, 2c, 3a, 3b, 4a–4c, 5b, 6a, 6c, and 7a–7c. Separation of the trans isomers of 2b, 3b, 4b, 5b, and 7b was achieved by selective crystallization from the mixture of geometrical isomers. All of the ORTEP representations with atom-labeling schemes are presented in Figures S40–S52. Selected geometric parameters are summarized in Table S18. These structure determinations establish the trans configuration of all of the [PdL₂Y₂] (Y = Cl[−] or NO₃[−]) species and the unidentate N coordination of the pyridine ligands in all cases, basic features that, along with the bond lengths and bond angles, are important but in no way exceptional (Tables S14–S17). What a single-crystal X-ray structure determination can add to this information is a definition of the weak interactions that occur within the crystal, and one convenient method to achieve this is to consider the Hirshfeld surfaces of components involving primary bonding interactions, as defined through the use of the program *CrystalExplorer*.¹⁸

The crystal structure of 6a·2CHCl₃ contains by far the most strongly basic ligand L6 in the present series, and thus the complex provides a reference point of one extreme of the bis(ligand) species. In the crystals of metal-ion complexes of aza-aromatic ligands, it is common to find that the aza-aromatic units lie in parallel planes, forming arrays described as involving “ π - π stacking”,¹⁹ although this may be a misleading or at least inadequate term as a description of the actual interactions occurring²⁰ and they may well be only part of a panoply of weak associative effects.²¹ Indeed, the L6 units in the crystal of 6a do form stacks, but the Hirshfeld surface shows that the interactions involved are purely dispersive and that the only interactions that exceed dispersion are those involving the solvent molecules. These interactions involve both C–H···Cl and Cl···Cl (halogen bonding²²) contacts and provide a model for solvation of the complex by chloroform as well as possibly explaining why the pyridine units are tilted with respect to the PdN₂Cl₂ plane (Figure 5a).

Passage to a complex of a much less basic ligand L2 and the replacement of chloride by nitrate in 2b lead to a much more complicated array of interactions exceeding dispersion. They derive exclusively, however, from the nitrate ligands and involve both O···H–C and O···C(aromatic) bonding, here perhaps indicating how an association between molecules might occur in solution, with the absence of solvent in the crystal indicating that solvation involves weaker interactions. Note that the L2 units do lie in parallel planes but with a centroid···centroid separation of 4.78 Å and no overlap in the projection perpendicular to the planes, so that they do not constitute a “stacked” array (Figure S53).

A more direct comparison of the consequences of replacing chloride by nitrate is possible through examination of the structures of 3a and 3b. Ligand L3 is again much less basic

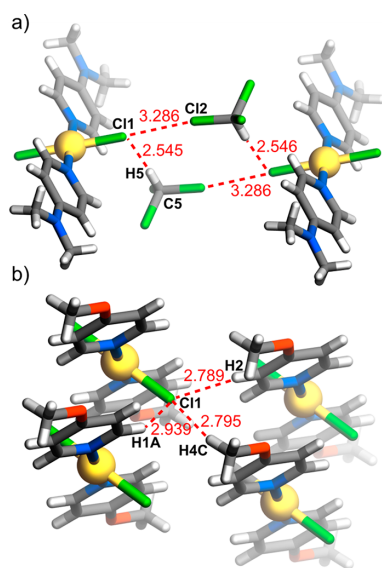


Figure 5. Weak interactions within the crystal structures of (a) 6a-2CHCl₃ and (b) 3a.

than L6, although slightly more basic than L2, and the methoxyl O is now an important point of interaction in both structures. In both, it is possible to find stacked arrays of the pyridine units, but again any interaction does not exceed dispersion in either case. In complex 3a, where the molecular unit has 2-fold symmetry, the chloride ligands are involved in interactions exceeding dispersion with both aromatic and aliphatic H, and these are complemented by O(methoxyl)⋯H–C(methoxyl), O(methoxyl)⋯H–C(pyridine) and C(methoxyl)–H⋯Cl interactions (Figures 5b and S54). In the crystal of complex 3b, the two pyridine ligands of each molecule are not equivalent and only one methoxyl group is involved in interactions exceeding dispersion. The polyatomic nature of the nitrate ligands means that they have multiple sites for interaction, but just like the chloride ligands of 3a, they serve to link molecules through interactions with both aromatic and aliphatic HC (Figure S55).

Pyridine (L1) itself is, of course, the parent ligand of all of the derivatives considered here, so that the nature of its complexes provides another reference point for the present series. Its consideration at this stage is appropriate in that it is less basic than L2, L3, or L6 but more so than any of the other ligands presently employed. Complex 1a has particular significance in that it has been structurally characterized in three different polymorphs, space groups $C2/c$,²³ $P\bar{1}$,²⁴ and $P2_1/n$.²⁵ This polymorphism can be understood in that the Hirshfeld surfaces show dispersion interactions to be dominant, completely for the $P\bar{1}$ polymorph and in association with limited reciprocal C–H⋯Cl interactions for the other two. Only in the $P2_1/n$ polymorph can it be said that there is an approach to a stacked array of pyridine units, but the centroid⋯centroid separation is 3.9159(2) Å and no indication of ring atom interactions beyond dispersion are apparent. Given the nondirectional nature of dispersion interactions, it is understandable that subtle differences in the conditions of crystallization might well give rise to the occupation of different local energy minima.

Another direct comparison of the consequences of replacing chloride by nitrate is provided in the structures of 7a and 7b. In complex 7a, each coordinated chloride has two interactions with pyridine-CH units and one barely discernible interaction with a pyridine-4-Cl unit (Figure 6a). While in complex 7b each bound nitrate is involved in O⋯H–C(pyridine) interactions analogous to the Cl⋯H–C interactions in 7a, one is also bound (through separate O atoms) to aromatic C and, as is clearly evident, to pyridine-4-Cl, and the other has just an additional O⋯Cl(pyridine) interaction (Figure 6b). In both complexes, these local interactions are associated with limited stacking of the pyridine units, but these involve centroid⋯centroid separations near 4.8 Å, with no evidence of any interaction outside dispersion. As a different polymorph (but also $P\bar{1}$), complex 7a has been structurally characterized previously as part of an investigation of halogen bonding within crystals of complexes of the $[M(X-py)_2(\text{halogen})_2]$ type.²⁶ The Hirshfeld surface for this polymorph is very similar to that of complex 7a, although the Cl⋯Cl interactions are somewhat more prominent. The centroid⋯centroid separation of the closest parallel pyridine ring pairs is also shorter at 3.9039(8) Å, although still with no indication of interactions exceeding dispersion.

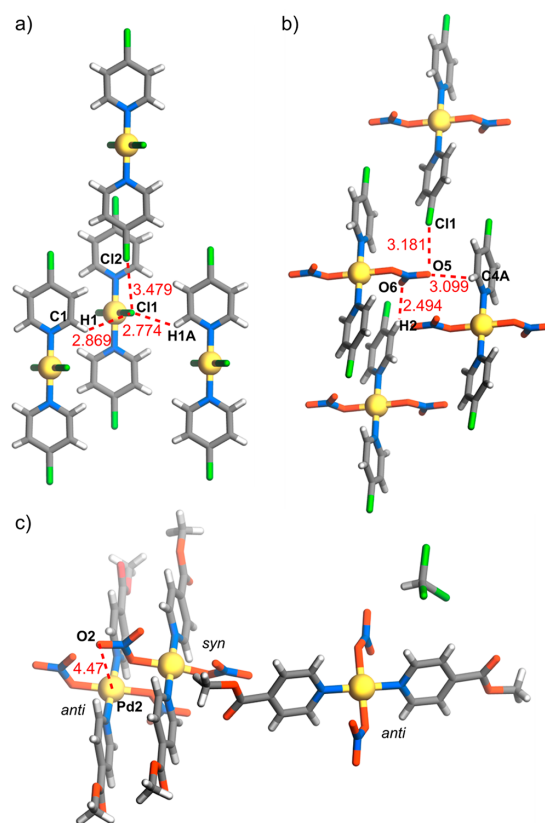


Figure 6. Weak interactions within the crystal structures of (a) 7a and (b) 7b. (c) Syn and anti orientations of nitrate ligands in the structure of 4b.

Ligand **L4** is appreciably less basic than pyridine, implying a significant electron-withdrawing effect of the methoxycarbonyl group on the pyridine ring, but in the structure of both complexes **4a** and **4b**, there is no indication on the Hirshfeld surfaces of a change in face-to-face pyridine ring interactions from that of dispersion. Instead, as observed in the structures already described, it is the coordinated anions and pyridine substituent that are involved in all interactions that exceed dispersion. The chloride ligands of the centrosymmetric complex **4a** are involved in interactions with both pyridine and ester methyl CH atoms of adjacent molecules of the ester substituent interacting with pyridine C, again a reciprocated case (Figure S56). Complex **4b** was in fact crystallized as a hemisolvate, $4b_2 \cdot \text{CHCl}_3$, and the presence of three inequivalent Pd sites as well as the presence of the solvent makes a description of the weak interactions in the crystal rather complicated. What is particularly interesting here, though, is the fact that while two of the three inequivalent Pd centers can be considered to have a square-planar coordination sphere, the third (Pd1) is square-pyramidal because of axial binding to nitrate O. Axial binding of a reaction substrate can, of course, be one of the initial steps in a catalytic mechanism, and while five coordination of Pd(II) is a well-understood occurrence,²⁷ it does not appear to be particularly favored in the present systems. The Pd1 environment in complex **4b** is unique in the present series in that, perhaps in order to accommodate the axial interaction, the two nitrate ligands have a syn orientation relative to the PdN_2O_2 plane, while in all other cases, it is anti (Figure 6c).

Ligand **L5** has Brønsted basicity very similar to that of **L4**, but the Hirshfeld surface for the centrosymmetric complex **5b** indicates that the acetyl substituent produces more significant charge relocation in the pyridine ring than does the methyl ester group. Thus, nitrate O is involved in interactions not only with both aromatic and aliphatic H, as in complexes **2b**, **3b**, **4b**, and **7b**, but also with the carbonyl C of the substituent and the pyridine C adjacent to it (Figure S57). Unlike complex **4b**, complex **5b** shows no evidence of an axial interaction with Pd exceeding dispersion, but as for Pd2 and Pd3 in complex **4b**, two O atoms are located, here, 3.776(6) Å above and below the PdN_2O_2 plane in a line with the Pd, indicating again that an axial approach could be a minimum energy pathway to binding an extra ligand. (In complex **4b**, the O atoms are 3.141(3) Å from Pd2 and 3.252(3) Å from Pd3.)

The application of Hirshfeld surface analysis to complexes **2c**, **4c**, **6c**, and **7c** is limited by the disorder present in the structures of **4c** and **7c**, so that a detailed analysis has been applied to the structures of complexes **2c** and **6c** only. All four complexes do, however, have a structure in which all four pyridine units lie close to perpendicular to the PdN_4 plane, a feature well-known in various tetrakis(pyridine) complexes and commonly ascribed to its enabling of the minimization of repulsion between the ligands,²⁸ with such a repulsion also being considered the reason for the difficulty in obtaining hexakis(pyridine) complexes of octahedral metal ions.²⁹ For $[\text{PtL}_4]^{2+}$ cations, where the same conformation is observed, an alternative explanation based on the observation of specific interactions of cations with counteranions has, however, been offered.¹¹ In the structure of complex **6c**, it is possible to discern a degree of interlocking of the cations with a resemblance to what is found in instances of the “terpyridine embrace”,^{19b} but as is seen in the bis(ligand) species **6a**, the Hirshfeld surface provides no evidence for interactions

exceeding dispersion between **L6** units. What is evident on the Hirshfeld surface is the versatility of nitrate in forming $\text{O} \cdots \text{H}-\text{C}$ bonds involving both aromatic and aliphatic H atoms. One result of this is that nitrate anions do form “caps” to each cation, as seen with the Pt(II) analogues,¹¹ by the interaction of O1 with three aromatic CH atoms (H1A, H6, and H6A) of adjacent ligands (Figure 7). The additional interactions of O2

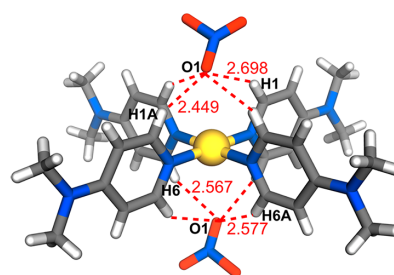


Figure 7. Nonbonding C–H···O interactions between $[\text{PdL}_4]^{2+}$ and nitrate counterions in the structure of complex **6c**.

with methyl CH (H9B and H9AB) and aromatic CH (H2) atoms serve to link cations into sheets parallel to (010) from which **L6** units project so that the sheets are linked through dispersion interactions. In the structure of complex **2c**, there is disorder of the anions, which complicates the interpretation of their interactions, but the Hirshfeld surface of the cations shows that the chains of cations running along [001] are, in fact, linked by C(aromatic)–H···C(aromatic) interactions, providing an example of where changing the substituent on pyridine results in the generation of pyridine···pyridine interactions exceeding dispersion, a feature not apparent in any of the other comparisons of the present work. Regardless of their disorder, the nitrate anions do appear to occupy capping regions of the cations, as seen in complex **6c**, and this is true also for the nondisordered anions associated with the disordered cations in complexes **4c** and **7c**.

What is observed in the solid state through crystal structure determinations does not necessarily apply to solutions, but the rarity of solvent incorporation in the structures presently described indicates that solvation interactions can be in competition with a variety of other forces determined by the particular nature of the solute. What has not been overtly considered in the discussion above of the tetrakis(pyridine) complexes is the fact that they are considered to be ionic species and thus that there should be an electrostatic factor to be allowed for in the cation···anion interactions. The calculation of Hirshfeld surfaces with neutral-atom wave functions may therefore be misleading in regard to the intensity of interactions but not their directionality, so that the cation capping by nitrate seen in the structures of complexes **2c**, **4c**, **6c**, and **7c** can still be seen as a consequence of $\text{O} \cdots \text{H}-\text{C}$ interactions. As argued in the case of Pt(II) analogues,¹¹ the preservation of such interactions in solution could explain why strong downfield shifts are also observed in the ^1H NMR spectra of complexes **2c**, **4c**, **6c**, and **7c**, although it is also important to note that the environment of the pyridine protons in the bis(pyridine) complexes is quite varied and quite different from that in the tetrakis species. In regard to catalysis by $[\text{PdL}_n\text{Y}_m]$, the interactions of different substituents and counteranions indicate possible structural features of a

Table 2. GC Yields [%]^a in Suzuki–Miyaura and Heck Cross-Coupling Reactions Catalyzed by Pd(II) Complexes Based on Ligands L1–L12

	pK _a of L	GC yield [%] in Suzuki–Miyaura coupling ^b			GC yield [%] in Heck coupling ^c		
		PdL ₂ Cl ₂ (1a–12a)	PdL ₂ (NO ₃) ₂ (1b–12b)	PdL ₄ (NO ₃) ₂ (1c–12c)	PdL ₂ Cl ₂ (1a–12a)	PdL ₂ (NO ₃) ₂ (1b–12b)	PdL ₄ (NO ₃) ₂ (1c–12c)
L1	5.23	97	93	95	85	88	90
L2	5.98	93	92	98	90	91	94
L3	6.47	93	91	91	86	82	76
L4	3.49	78	72	64	89	92	79
L5	3.57	86	87	88	80	92	75
L6	9.61	93		90	86		83
L7	3.83	82	74	75	90	92	80
L8	2.10	88	66		91	93	
L9	2.46	87	70		81	91	
L10	3.07	98		90	93		88
L11	3.12	86		79	88		90
L12	2.86	83		92	92		77

^aReaction yields were determined by GC–MS measurement of 4'-bromoacetophenone or iodobenzene decay as the average of three results.

^bReaction conditions: 4'-bromoacetophenone (0.2 mmol, 1 equiv), phenylboronic acid (0.24 mmol, 1.2 equiv), K₃PO₄ (0.4 mmol, 2 equiv), and Pd(II) complex (0.1 mol %) were stirred in toluene (2 mL) at 80 °C for 2 h. ^cReaction conditions: iodobenzene (0.2 mmol, 1 equiv), styrene (0.24 mmol, 1.2 equiv), Et₃N (1.0 mmol, 5 equiv), and Pd(II) complex (0.1 mol %) were stirred in DMSO (2 mL) at 120 °C for 2 h.

substrate that might enhance its binding to the catalyst, but this, of course, is one step in what must be a more complicated process.

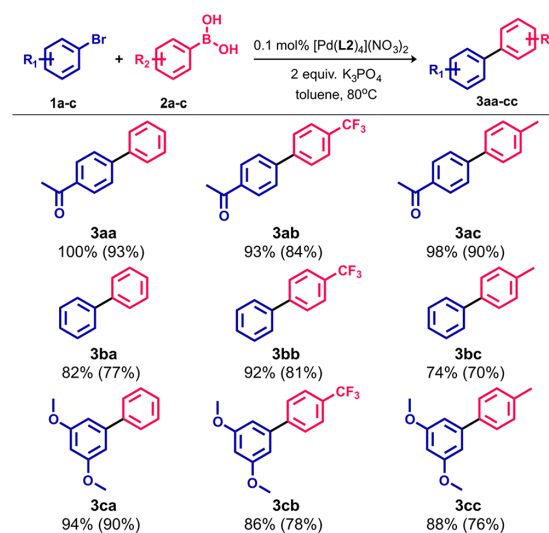
Catalytic Studies. Because of the structural differences between Pd(II) complexes with pyridine ligands, catalytic studies were undertaken in order to investigate their activity in Pd-catalyzed cross-coupling reactions and explore their diversity in functionality as well. Thus, their catalytic properties were tested and compared in both the Suzuki–Miyaura and Heck reactions.

Suzuki–Miyaura Coupling. Complex 2c was selected as a model catalyst precursor for which the reaction conditions were optimized in the coupling between 4'-bromoacetophenone and phenylboronic acid (Table S22). Among the tested bases (K₂CO₃, K₃PO₄, NaOH, and Et₃N) and solvents (chloroform, toluene, 1,4-dioxane, and *N,N*-dimethylformamide), the combination of K₃PO₄ and toluene allowed formation of the expected 4-acetylbiphenyl in the highest gas chromatography (GC) yield. The catalytic reactions were performed at 80 °C and, importantly, without the need to exclude air or water. Taking economic and environmental considerations into account, the optimal catalyst concentration was 0.1 mol %, which resulted in an almost quantitative conversion just after 2 h.

Subsequently, the catalytic activity of the full range of structurally diversified Pd(II) complexes with pyridine ligands was tested under the same optimized reaction conditions. The majority of the catalyst precursors provided the cross-coupling product in excellent yields of >90% (Table 2). Only minor differences were observed between bis and tetrakis complexes of a given ligand, so it appears that the nature of the complex and the different counterions does not directly influence the effectiveness of the catalyzed reaction. Nevertheless, some differences could be noted depending on the ring substituent. The lowest GC yields were observed for the complexes based on L4 (64–78%). Better GC yields (>70%) were achieved for the complexes based on L5, L7–L9, and L11, while those of L1–L3, L6, and L10 showed the highest activity in Suzuki–Miyaura coupling. Although no simple correlation was observed between GC yields and pK_a values of the ligands

(Figure S93), Pd(II) complexes with more basic pyridine ligands generally showed slightly greater catalytic effectiveness.

Complex 2c, as one of the most effective systems, was selected to explore the capabilities in the Suzuki–Miyaura cross-coupling in terms of functional-group tolerance. Under the optimized reaction conditions, a set of functionalized aryl bromides and arylboronic acids were reacted together. The 2c unit enabled the synthesis of scope of structurally distinct biphenyl derivatives 3aa–3cc in high-to-excellent yields (74–100%; Scheme 2). The high efficiency was observed regardless of the presence of electron-donating (–Me and –OMe) or electron-withdrawing (–CF₃ and –COMe) substituents in the

Scheme 2. Scope of the Suzuki–Miyaura Cross-Coupling Reaction between Aryl Bromides and Arylboronic Acids^a

^aThe GC yields were determined by GC–MS measurement of aryl bromide decay. The yields in parentheses are for the isolated compounds.

substrate molecules, highlighting the catalyst precursor versatility.

Heck Coupling. For an initial assessment of the efficacy of the complexes as catalyst precursors for the Heck reaction, the cross-coupling of iodobenzene with styrene catalyzed by **2c** was chosen as a model reaction to develop the reaction conditions (Table S24). Under the conditions optimized for the Suzuki–Miyaura reaction, only traces of the Heck coupling product were observed. For this reason, different variations in terms of solvents and bases were tested using a 1 mol % Pd(II) complex. The reaction did not proceed successfully in the presence of inorganic bases (K_3PO_4 and K_2CO_3) or nonpolar solvent (toluene). The pair of Et_3N and DMSO represented the best combination to reach high yields because almost quantitative conversion was achieved at 120 °C just after 2 h. Additional experiments showed that the catalyst loading could be reduced to 0.1 mol %. This concentration was sufficient to guarantee good conversion at the same time, whereas using 0.01 mol % significantly extended the reaction time. With these results in hand, subsequent catalytic reactions were performed in DMSO at 120 °C using Et_3N as a base and 0.1 mol % Pd(II) complex. Note that the Pd(II) complexes essentially retain their structure under the reaction conditions, as indicated by the 1H NMR spectra recorded after heating in DMSO at 120 °C (Figures S37–S39).

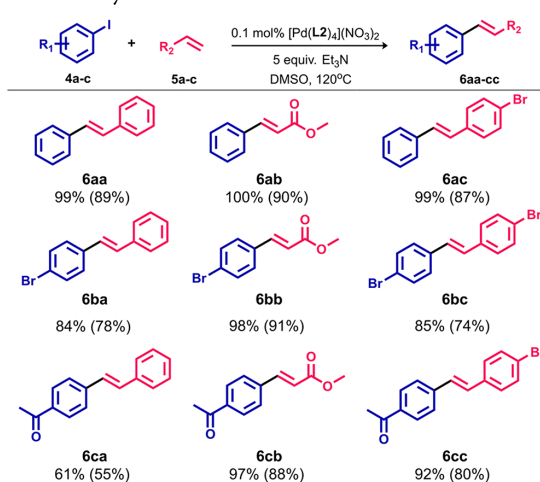
A comparison of the catalytic activities for a number of the other Pd(II) complexes was performed for the Heck reaction as well. As with the Suzuki–Miyaura cross-coupling, potential catalyst precursors were examined to evaluate the substituent effect on the efficiency in catalyzed reactions. Under the same conditions, very high GC yields (>90%) were obtained in most of the reactions, and yields of <80% were observed in only a few cases (Table 2). Overall, the tetrakis(pyridine) complexes, especially with ligands L3–L5 and L12, provided lower GC yields (75–79%) in comparison to neutral bis(ligand) species. Any ring substituent effect was negligible, and no clear relationship between the ligand basicity and catalytic activity of the Pd(II) complexes was apparent (Figure S95). In all cases, the selectivity in the (*E*)-stilbene formation was very high, ranging from 89% to 99%, and was completely independent of the catalyst precursor structure.

To investigate the scope of the Heck cross-coupling reaction, the catalytic properties of complex **2c** were further studied by using a set of functionalized substrates under the conditions described above. As shown in Scheme 3, **2c** showed good catalytic activity and selectivity in the reactions between aryl iodides and olefins, giving GC yields in the range of 61–100%. It is noteworthy that an excellent conversion was accomplished for acrylate derivatives (97–100%). The reaction system exhibited also great chemoselectivity toward iodoarenes because no cross-coupling involving bromoarene moieties, as either olefin or haloarene coupling partners, was observed.

Complex **2c** as a representative of the multiple family of Pd(II) complexes with pyridyl ligands has been extensively investigated with respect to catalytic properties that demonstrated high catalytic activity in the Suzuki–Miyaura and Heck cross-coupling reactions. On the basis of the experiments carried out, it can be concluded that all of the units presented herein constitute a group of versatile precatalysts that can be successfully applied in Pd-catalyzed reactions.

Because of the multitude of literature reports on the mechanism of both Suzuki–Miyaura and Heck cross-coupling,

Scheme 3. Scope of the Heck Cross-Coupling Reaction between Aryl Iodides and Olefins^a



^aThe GC yields were determined by GC–MS measurement of aryl iodide decay. The yields in parentheses are for the isolated compounds.

profound studies have not been conducted in this area. We assume that the bis- and tetrakis(pyridine) complexes considered in this paper play the precatalyst role. According to the generally accepted mechanism, the reduction of Pd(II) to Pd(0) occurs at the beginning of the catalytic cycle, leading to the generation of active species. The process then proceeds in a typical manner for Pd-catalyzed transformations, through the sequence of three consecutive stages involving oxidative addition, transmetalation or carbometalation, and reductive elimination, as described in numerous works.³⁰ The precatalyst was degraded during the cycle that was observed as precipitation of metallic Pd; therefore, it could not be regenerated and then reused.

CONCLUSIONS

In summary, a series of Pd(II) complexes based on a wide range of functionalized pyridine derivatives have been successfully generated and analyzed in solution via NMR spectroscopy and MS as well as in the solid state via X-ray diffraction. This work has been based on two sets of complexes of the general formulas $[PdL_4](NO_3)_2$ and $[PdL_2Y_2]$, where $Y = Cl^-$ or NO_3^- . Their properties have been examined in light of the ligand basicity as a factor of influence, although the results obtained have shown that this is just one of several factors that may be important. The complexes have been found to be of practical utility as simple and efficient catalyst precursors for both the Suzuki–Miyaura and Heck cross-coupling reactions for a scope of substrates under relatively mild conditions.

EXPERIMENTAL SECTION

General Procedures. All reagents were purchased from commercial suppliers (mainly Merck or Fluorochem) and used without further purification. High-purity solvents were purchased from VWR. NMR solvents were purchased from Deutero GmbH (Germany) and used as received. NMR spectra were acquired on Bruker Fourier 300 MHz, Bruker Avance IIIHD 400 MHz, and Bruker Avance IIIHD 600 MHz spectrometers at 25 °C and

referenced to a tetramethylsilane signal or solvent residual peaks. All NMR data were processed with Mestrelab Research *MNova* software. ESI-MS spectra were recorded on Bruker HD Impact and ABSciex QTOF 5600 spectrometers in positive-ion mode. Theoretical MS spectra were predicted using Mestrelab Research *MNova* software. GC-MS analyses were performed on a Bruker 450-GC spectrometer with a 30 m Varian DB-5 0.25 mm capillary column and a Scion SQ-MS detector.

X-ray Crystallography. X-ray measurements were performed using an Oxford Diffraction SuperNova diffractometer with monochromatic Cu $K\alpha$ radiation for **2c**, **3a**, **5b**, and **6a**. The diffraction data were collected on a Rigaku XtaLAB Synergy diffractometer equipped with a rotating anode as a Cu $K\alpha$ radiation source for **4a**. The remaining compounds were subjected to X-ray measurements on an Oxford Diffraction Xcalibur diffractometer with Mo $K\alpha$ radiation. Data collection and data reduction for all Pd(II) complexes were carried out using the *CrysAlisPRO* software.³¹ Using *OLEX2*, the intrinsic phasing method (*ShelXT*) was used for crystal structure solution.³² The exception is the **4a** structure, which was solved with direct methods (*ShelXS*).³³ The refinement process was performed with anisotropic displacement parameters for non-H atoms with the full-matrix least-squares method based on F^2 (*ShelXL*).^{32b} In all structures, except for **7a** and **7b**, the H atoms were placed in calculated positions and refined using a riding model. The high quality of the obtained single crystals of complexes **7a** and **7b** made it possible to carry out high-resolution X-ray measurements. Therefore, the H atoms have been derived from the difference Fourier map and refined without constraints. Crystallographic data, details on the refinement, twin structures, and disordered fragments in the crystal structures are included in the SI.

Synthesis of Ligands. Ligands L1–L9 were purchased from commercial suppliers and used as received. Ligands L10–L12 were prepared according to the previously described procedures.^{7e,34}

Synthesis of [PdL₂Cl₂] Complexes (1a–12a). One of the ligands L1–L12 (~0.2 mmol, 2 equiv) was added to an acetonitrile (MeCN) solution of PdCl₂ (~0.1 mmol, 1 equiv in 5 mL of MeCN). Then the resulting mixture was heated under reflux for 12 h. The precipitate that formed was centrifuged off, washed with MeCN (10 mL) and diethyl ether (Et₂O; 2 × 10 mL), and dried under vacuum. Specific details on the synthetic procedures and analytical data (quantities used, yields, NMR and MS data, etc.) can be found in the SI.

Synthesis of [PdL₂(NO₃)₂] Complexes (1b–12b). One of the ligands L1–L12 (0.2 mmol, 2 equiv) was added to an MeCN solution of Pd(NO₃)₂·2H₂O (0.1 mmol, 1 equiv in 5 mL of MeCN). Then, the resulting mixture was heated under reflux for 12 h. The solvent was then evaporated under reduced pressure. The crude product was redissolved in MeCN (1 mL) and reprecipitated by the addition of Et₂O (10 mL). The precipitate was centrifuged off, washed with Et₂O (2 × 10 mL), and dried under a vacuum. Specific details on the synthetic procedures and analytical data (quantities used, yields, NMR and MS data, etc.) can be found in the SI.

Synthesis of [PdL₄](NO₃)₂ Complexes (1c–12c). To a suspension of PdCl₂ or Pd(DMSO)₂Cl₂ (~0.1 mmol, 1 equiv) in ethanol (5 mL) was added a solution of one of the ligands L1–L12 (~1.0 mmol, 10 equiv) in dichloromethane (DCM; 5 mL), and the resulting mixture was stirred at room temperature for 1 h. Then, AgNO₃ (~0.2 mmol, 2 equiv) in 0.5 mL of H₂O was added, and the resulting suspension was stirred for an additional 12 h excluding light. The reaction mixture was filtered to remove AgCl, and then the filtrate was evaporated under reduced pressure. The crude product was redissolved in DCM (1 mL) and reprecipitated by the addition of *n*-hexane (10 mL). The precipitate was centrifuged off, washed with *n*-hexane (2 × 10 mL), and dried under a vacuum. Specific details on the synthetic procedures and analytical data (quantities used, yields, NMR and MS data, etc.) can be found in the SI.

Suzuki–Miyaura Coupling. A reaction vessel equipped with a stirring bar was charged with aryl bromide (1.0 mmol, 1.0 equiv) and arylboronic acid (1.2 mmol, 1.2 equiv) dissolved in toluene (10 mL). Then, the Pd(II) precatalyst (0.001 mmol, 0.001 equiv) as a solution

in chloroform (0.05 mL) and solid K₃PO₄ (2.0 mmol, 2.0 equiv) was added. The vial was sealed, and the reaction mixture was heated for 2 h at 80 °C. Then, the resulting solution was cooled to room temperature, diluted with DCM (50 mL), and washed with distilled water (40 mL). The collected aqueous phase was extracted with DCM (2 × 50 mL). The organic layers were gathered, dried over Na₂SO₄, and filtered, and the solvent was removed under reduced pressure. The residue was purified by column chromatography on silica gel to obtain the desired products **3aa–3cc**. The full characterization of the coupling products is available in the SI.

Heck Reaction. A reaction vessel equipped with a stirring bar was charged with aryl iodide (1.0 mmol, 1.0 equiv) and olefin (1.2 mmol, 1.2 equiv) dissolved in DMSO (10 mL). Then, the Pd(II) precatalyst (0.001 mmol, 0.001 equiv) as a solution in DMSO (0.05 mL) and Et₃N (5.0 mmol, 5.0 equiv) was added. The vial was sealed, and the reaction mixture was heated for 2 h at 120 °C. Then, the resulting solution was cooled to room temperature, diluted with ethyl acetate (50 mL), and washed with icy distilled water (40 mL). The collected aqueous phase was extracted with ethyl acetate (2 × 50 mL). The organic layers were gathered, dried over Na₂SO₄, and filtered, and the solvent was removed under reduced pressure. The residue was purified by column chromatography on silica gel to obtain the desired products **6aa–6cc**. The full characterization of the coupling products is available in the SI.

■ ASSOCIATED CONTENT

Supporting Information

The Supporting Information is available free of charge at <https://pubs.acs.org/doi/10.1021/acs.inorgchem.2c01996>.

Additional experimental details, materials and methods, NMR and ESI-MS spectra for all compounds, NMR titration experiments, crystal data and structure refinement for Pd(II) complexes, reaction development for catalytic tests, and characterization of cross-coupling products (PDF)

Accession Codes

CCDC 2175520–2175532 contain the supplementary crystallographic data for this paper. These data can be obtained free of charge via www.ccdc.cam.ac.uk/data_request/cif, or by emailing data_request@ccdc.cam.ac.uk, or by contacting The Cambridge Crystallographic Data Centre, 12 Union Road, Cambridge CB2 1EZ, UK; fax: +44 1223 336033.

■ AUTHOR INFORMATION

Corresponding Author

Artur R. Stefankiewicz – Faculty of Chemistry, Adam Mickiewicz University in Poznań, Poznań 61-614, Poland; Center for Advanced Technology, Adam Mickiewicz University in Poznań, Poznań 61-614, Poland; orcid.org/0000-0002-6177-358X; Email: ars@amu.edu.pl

Authors

Gracjan Kurpiak – Faculty of Chemistry, Adam Mickiewicz University in Poznań, Poznań 61-614, Poland; Center for Advanced Technology, Adam Mickiewicz University in Poznań, Poznań 61-614, Poland

Anna Walczak – Faculty of Chemistry, Adam Mickiewicz University in Poznań, Poznań 61-614, Poland; Center for Advanced Technology, Adam Mickiewicz University in Poznań, Poznań 61-614, Poland

Mateusz Goldyn – Faculty of Chemistry, Adam Mickiewicz University in Poznań, Poznań 61-614, Poland; orcid.org/0000-0003-2282-9816

Jack Harrowfield – Institut de Science et d'Ingénierie
Supramoléculaires, Université de Strasbourg, Strasbourg
67083, France

Complete contact information is available at:
<https://pubs.acs.org/10.1021/acs.inorgchem.2c01996>

Author Contributions

All authors have approved the final version of the manuscript.

Notes

The authors declare no competing financial interest.

ACKNOWLEDGMENTS

We thank the National Science Center (Grant SONATA BIS 2018/30/E/ST5/00032 to A.R.S.) for financial support.






REFERENCES

- (1) (a) Pal, S. *Pyridine: A Useful Ligand in Transition Metal Complexes*; IntechOpen, 2018. (b) Joule, J. A.; Mills, K.; Smith, G. F. *Heterocyclic Chemistry*, 3rd ed.; CRC Press, 1995.
- (2) Jensen, W. B. The Lewis acid-base definitions: a status report. *Chem. Rev.* **1978**, *78* (1), 1–22.
- (3) (a) Patroniak, V.; Kubicki, M.; Stefankiewicz, A. R.; Grochowska, A. M. Preparation of new heterotopic ligands. *Tetrahedron* **2005**, *61* (23), 5475–5480. (b) Stefankiewicz, A. R.; Wałęsa-Chorab, M.; Harrowfield, J.; Kubicki, M.; Hnatejko, Z.; Korabik, M.; Patroniak, V. Self-assembly of transition metal ion complexes of a hybrid pyrazine–terpyridine ligand. *Dalton Trans.* **2013**, *42* (5), 1743–1751. (c) Gorczyński, A.; Harrowfield, J. M.; Patroniak, V.; Stefankiewicz, A. R. Quaterpyridines as Scaffolds for Functional Metallosupramolecular Materials. *Chem. Rev.* **2016**, *116* (23), 14620–14674. (d) Brzechwa-Chodzyńska, A.; Zieliński, M.; Gilski, M.; Harrowfield, J. M.; Stefankiewicz, A. R. Dynamer and Metallo-dynamer Interconversion: An Alternative View to Metal Ion Complexation. *Inorg. Chem.* **2020**, *59* (12), 8552–8561. (e) Čonková, M.; Drozd, W.; Milosz, Z.; Cecot, P.; Harrowfield, J.; Lewandowski, M.; Stefankiewicz, A. R. Influencing prototropy by metal ion coordination: supramolecular transformation of a dynamer into a Zn-based toroidal species. *J. Mater. Chem. C* **2021**, *9* (9), 3065–3069.
- (4) (a) Krogul, A.; Cedrowski, J.; Wiktorska, K.; Ozimiński, W. P.; Skupińska, J.; Litwinienko, G. Crystal structure, electronic properties and cytotoxic activity of palladium chloride complexes with monosubstituted pyridines. *Dalton Trans.* **2012**, *41* (2), 658–666. (b) Bugarčić, Ž. D.; Petrović, B.; Zangrando, E. Kinetics and mechanism of the complex formation of [Pd(NNN)Cl]⁺ with pyridines in methanol: synthesis and crystal structure of [Pd(terpy)(py)](ClO₄)₂. *Inorg. Chim. Acta* **2004**, *357* (9), 2650–2656.
- (5) (a) Schlosser, M.; Mongin, F. Pyridine elaboration through organometallic intermediates: regiochemical control and completeness. *Chem. Soc. Rev.* **2007**, *36* (7), 1161–1172. (b) Dell'arciprete, M. L.; Cobos, C. J.; Furlong, J. P.; Mártire, D. O.; Gonzalez, M. C. Reactions of sulphate radicals with substituted pyridines: a structure-reactivity correlation analysis. *ChemPhysChem* **2007**, *8* (17), 2498–505.
- (6) (a) Debata, N. B.; Tripathy, D.; Chand, D. K. Self-assembled coordination complexes from various palladium(II) components and bidentate or polydentate ligands. *Coord. Chem. Rev.* **2012**, *256* (17), 1831–1945. (b) Peloquin, D. M.; Schmedake, T. A. Recent advances in hexacoordinate silicon with pyridine-containing ligands: Chemistry and emerging applications. *Coord. Chem. Rev.* **2016**, *323*, 107–119. (c) Pazderski, L.; Szyk, E.; Sitkowski, J.; Kamiński, B.; Kozerski, L.; Toušek, J.; Marek, R. Experimental and quantum-chemical studies of 15N NMR coordination shifts in palladium and platinum chloride complexes with pyridine, 2,2'-bipyridine and 1,10-phenanthroline. *Magn. Reson. Chem.* **2006**, *44* (2), 163–170. (d) Happ, B.; Winter, A.; Hager, M. D.; Schubert, U. S. Photogenerated avenues in macromolecules containing Re(i), Ru(ii), Os(ii), and Ir(iii) metal complexes of pyridine-based ligands. *Chem. Soc. Rev.* **2012**, *41* (6), 2222–2255. (e) Kristiansson, O. Bis(4-aminopyridine)silver(I) nitrate and tris(2,6-diaminopyridine)silver(I) nitrate. *Acta Crystallogr. C* **2000**, *56* (2), 165–167. (f) Webb, M. I.; Wu, B.; Jang, T.; Chard, R. A.; Wong, E. W. Y.; Wong, M. Q.; Yapp, D. T. T.; Walsby, C. J. Increasing the Bioavailability of Ru(III) Anticancer Complexes through Hydrophobic Albumin Interactions. *Chem. Eur. J.* **2013**, *19* (50), 17031–17042.
- (7) (a) Pardey, A. J.; Longo, C. Catalysis by rhodium complexes bearing pyridine ligands: Mechanistic aspects. *Coord. Chem. Rev.* **2010**, *254* (3), 254–272. (b) Togni, A.; Venanzi, L. M. Nitrogen Donors in Organometallic Chemistry and Homogeneous Catalysis. *Angew. Chem., Int. Ed.* **1994**, *33* (5), 497–526. (c) Walczak, A.; Stachowiak, H.; Kurpiak, G.; Kaźmierczak, J.; Hreczycho, G.; Stefankiewicz, A. R. High catalytic activity and selectivity in hydrosilylation of new Pt(II) metallosupramolecular complexes based on ambidentate ligands. *J. Catal.* **2019**, *373*, 139–146. (d) Abdine, R. A. A.; Kurpiak, G.; Walczak, A.; Aesh, S. A. A.; Stefankiewicz, A. R.; Monnier, F.; Taillefer, M. Mild temperature amination of aryl iodides and aryl bromides with aqueous ammonia in the presence of CuBr and pyridyldiketone ligands. *J. Catal.* **2019**, *376*, 119–122. (e) Walczak, A.; Stefankiewicz, A. R. pH-Induced Linkage Isomerism of Pd(II) Complexes: A Pathway to Air- and Water-Stable Suzuki–Miyaura-Reaction Catalysts. *Inorg. Chem.* **2018**, *57* (1), 471–477.
- (8) (a) Rakić, G. M.; Grgurić-Šipka, S.; Kaluderović, G. N.; Gómez-Ruiz, S.; Bjelogrić, S. K.; Radulović, S. S.; Tešić, Ž. L. Novel trans-dichloridoplatinum(II) complexes with 3- and 4-acetylpyridine: Synthesis, characterization, DFT calculations and cytotoxicity. *Eur. J. Med. Chem.* **2009**, *44* (5), 1921–1925. (b) Holford, J.; Sharp, S. Y.; Murrer, B. A.; Abrams, M.; Kelland, L. R. In vitro circumvention of cisplatin resistance by the novel sterically hindered platinum complex AMD473. *Br. J. Cancer* **1998**, *77* (3), 366–373.
- (9) (a) Lannes, A.; Intissar, M.; Suffren, Y.; Reber, C.; Luneau, D. Terbium(III) and Yttrium(III) Complexes with Pyridine-Substituted Nitronyl Nitroxide Radical and Different β-Diketone Ligands. Crystal Structures and Magnetic and Luminescence Properties. *Inorg. Chem.* **2014**, *53* (18), 9548–9560. (b) Alexandropoulos, D. I.; Cunha-Silva, L.; Pham, L.; Bekiari, V.; Christou, G.; Stamatatos, T. C. Tetranuclear Lanthanide(III) Complexes with a Zigzag Topology from the Use of Pyridine-2,6-dimethanol: Synthetic, Structural, Spectroscopic, Magnetic and Photoluminescence Studies. *Inorg. Chem.* **2014**, *53* (6), 3220–3229.
- (10) (a) Palusiak, M. Substituent effect in para substituted Cr(CO)₅-pyridine complexes. *J. Organomet. Chem.* **2007**, *692* (18), 3866–3873. (b) Nakano, K.; Suemura, N.; Yoneda, K.; Kawata, S.; Kaizaki, S. Substituent effect of the coordinated pyridine in a series of pyrazolato bridged dinuclear diiron(ii) complexes on the spin-crossover behavior. *Dalton Trans.* **2005**, No. 4, 740–743. (c) Jaju, K.; Pal, D.; Chakraborty, A.; Chakraborty, S. Electronic substituent effect on Se–H⋯N hydrogen bond: A computational study of para-substituted pyridine–SeH₂ complexes. *Chem. Phys. Lett.* **2019**, *737*, 100031. (d) Kimura, A.; Ishida, T. Pybox-Iron(II) Spin-Crossover Complexes with Substituent Effects from the 4-Position of the Pyridine Ring (Pybox = 2,6-Bis(oxazolin-2-yl)pyridine). *Inorganics* **2017**, *5* (3), 52.
- (11) Lewis, N. A.; Pakhomova, S.; Marzilli, P. A.; Marzilli, L. G. Synthesis and Characterization of Pt(II) Complexes with Pyridyl Ligands: Elongated Octahedral Ion Pairs and Other Factors Influencing 1H NMR Spectra. *Inorg. Chem.* **2017**, *56* (16), 9781–9793.
- (12) (a) Krogul, A.; Skupińska, J.; Litwinienko, G. Tuning of the catalytic properties of PdCl₂(XnPy)₂ complexes by variation of the basicity of aromatic ligands. *J. Mol. Catal. A Chem.* **2014**, *385*, 141–148. (b) Krogul, A.; Skupińska, J.; Litwinienko, G. Catalytic activity of PdCl₂ complexes with pyridines in nitrobenzene carbonylation. *J. Mol. Catal. A Chem.* **2011**, *337* (1), 9–16.
- (13) Krogul, A.; Litwinienko, G. Application of Pd(II) Complexes with Pyridines as Catalysts for the Reduction of Aromatic Nitro

- Compounds by CO/H₂O. *Org. Process Res. Dev.* **2015**, *19* (12), 2017–2021.
- (14) Krogul, A.; Litwinienko, G. One pot synthesis of ureas and carbamates via oxidative carbonylation of aniline-type substrates by CO/O₂ mixture catalyzed by Pd-complexes. *J. Mol. Catal. A Chem.* **2015**, *407*, 204–211.
- (15) (a) Tehan, B. G.; Lloyd, E. J.; Wong, M. G.; Pitt, W. R.; Gancia, E.; Manallack, D. T. Estimation of pK_a Using Semiempirical Molecular Orbital Methods. Part 2: Application to Amines, Anilines and Various Nitrogen Containing Heterocyclic Compounds. *Quant. Struct.-Act. Rel.* **2002**, *21* (5), 473–485. (b) Brivio, M.; Schlosrich, J.; Ahmad, M.; Tolond, C.; Bugg, T. D. Investigation of acid-base catalysis in the extradiol and intradiol catechol dioxygenase reactions using a broad specificity mutant enzyme and model chemistry. *Org. Biomol. Chem.* **2009**, *7* (7), 1368–73. (c) Iyehara Ogawa, H.; Liu, S.-Y.; Sakata, K.; Niyitani, Y.; Tsuruta, S.; Kato, Y. Inverse correlation between combined mutagenicity in Salmonella typhimurium and strength of coordinate bond in mixtures of cobalt(II) chloride and 4-substituted pyridines. *Mutat. Res. Genet. Toxicol.* **1988**, *204* (2), 117–121. (d) Uwai, K.; Konno, N.; Kitamura, S.; Ohta, S.; Takeshita, M. Purification and characterization of rat liver enzyme catalyzing stereoselective reduction of acetylpyridines. *Chirality* **2005**, *17* (8), 494–500. (e) Honda, H. ¹H-MAS-NMR Chemical Shifts in Hydrogen-Bonded Complexes of Chlorophenols (Pentachlorophenol, 2,4,6-Trichlorophenol, 2,6-Dichlorophenol, 3,5-Dichlorophenol, and *p*-Chlorophenol) and Amine, and H/D Isotope Effects on ¹H-MAS-NMR Spectra. *Molecules* **2013**, *18* (4), 4786. (f) Chatzopoulou, M.; Kotsampasakou, E.; Demopoulos, V. J. Clauson–Kaas-Type Synthesis of Pyrrolyl-phenols, from the Hydrochlorides of Aminophenols, in the Presence of Nicotinamide. *Synth. Commun.* **2013**, *43* (21), 2949–2954. (g) Stilinović, V.; Kaitner, B. Salts and Co-Crystals of Genticic Acid with Pyridine Derivatives: The Effect of Proton Transfer on the Crystal Packing (and Vice Versa). *Cryst. Growth Des.* **2012**, *12* (11), 5763–5772.
- (16) <https://scifinder.cas.org> Calculated using Advanced Chemistry Development (ACD/Labs) Software V11.02 (© 1994–2022 ACD/Labs).
- (17) Helm, L.; Merbach, A. E. Inorganic and Bioinorganic Solvent Exchange Mechanisms. *Chem. Rev.* **2005**, *105* (6), 1923–1960.
- (18) Spackman, P. R.; Turner, M. J.; McKinnon, J. J.; Wolff, S. K.; Grimwood, D. J.; Jayatilaka, D.; Spackman, M. A. CrystalExplorer: a program for Hirshfeld surface analysis, visualization and quantitative analysis of molecular crystals. *J. Appl. Crystallogr.* **2021**, *54* (3), 1006–1011.
- (19) (a) Janiak, C. A critical account on π – π stacking in metal complexes with aromatic nitrogen-containing ligands. *J. Chem. Soc., Dalton Trans.* **2000**, No. 21, 3885–3896. (b) Scudder, M. L.; Goodwin, H. A.; Dance, I. G. Crystal supramolecular motifs: two-dimensional grids of terpy embraces in [ML₂] complexes (L = terpy or aromatic N₃-tridentate ligand). *New J. Chem.* **1999**, *23* (7), 695–705.
- (20) (a) Gavezzotti, A. The “sceptical chymist”: intermolecular doubts and paradoxes. *CrystEngComm* **2013**, *15* (20), 4027–4035. (b) Martinez, C. R.; Iverson, B. L. Rethinking the term “ π -stacking”. *Chem. Sci.* **2012**, *3* (7), 2191–2201. (c) Bloom, J. W. G.; Wheeler, S. E. Taking the Aromaticity out of Aromatic Interactions. *Angew. Chem., Int. Ed.* **2011**, *50* (34), 7847–7849. (d) Grimme, S. Do Special Noncovalent π – π Stacking Interactions Really Exist? *Angew. Chem., Int. Ed.* **2008**, *47* (18), 3430–3434. (e) Ehrlich, S.; Moellmann, J.; Grimme, S. Dispersion-Corrected Density Functional Theory for Aromatic Interactions in Complex Systems. *Acc. Chem. Res.* **2013**, *46* (4), 916–926.
- (21) (a) Tiekink, E. R. T. Supramolecular assembly based on “emerging” intermolecular interactions of particular interest to coordination chemists. *Coord. Chem. Rev.* **2017**, *345*, 209–228. (b) Meyer, E. A.; Castellano, R. K.; Diederich, F. Interactions with Aromatic Rings in Chemical and Biological Recognition. *Angew. Chem., Int. Ed.* **2003**, *42* (11), 1210–1250.
- (22) Cavallo, G.; Metrangolo, P.; Milani, R.; Pilati, T.; Priimagi, A.; Resnati, G.; Terraneo, G. The Halogen Bond. *Chem. Rev.* **2016**, *116* (4), 2478–2601.
- (23) Viostat, B.; Dung, N.-H.; Robert, F. Structure du trans-dichlorobis(pyridine)palladium(II). *Acta Crystallogr. C* **1993**, *49* (1), 84–85.
- (24) Liao, C.-Y.; Lee, H. M. trans-Dichlorodipyridinepalladium(II). *Acta Crystallogr. E* **2006**, *62* (4), m680–m681.
- (25) Lee, H. M.; Liao, C.-Y. A new monoclinic polymorph of trans-dichlorodipyridinepalladium(II). *Acta Crystallogr. E* **2008**, *64* (11), m1447.
- (26) Zordan, F.; Brammer, L. M–X···X–C Halogen-Bonded Network Formation in MX₂(4-halopyridine)₂ Complexes (M = Pd, Pt; X = Cl, I; X' = Cl, Br, I). *Cryst. Growth Des.* **2006**, *6* (6), 1374–1379.
- (27) Maresca, L.; Natile, G. Five-Coordination in Platinum(II) and Palladium(II) Chemistry. *Comments Inorg. Chem.* **1993**, *14* (6), 349–366.
- (28) Zhang, Y.; Woods, T. J.; Rauchfuss, T. B. Homoleptic Rhodium Pyridine Complexes for Catalytic Hydrogen Oxidation. *J. Am. Chem. Soc.* **2021**, *143* (27), 10065–10069.
- (29) Templeton, J. L. Hexakis(pyridine)ruthenium(II) tetrafluoroborate. Molecular structure and spectroscopic properties. *J. Am. Chem. Soc.* **1979**, *101* (17), 4906–4917.
- (30) (a) Miyaura, N.; Suzuki, A. Palladium-catalyzed cross-coupling reactions of organoboron compounds. *Chem. Rev.* **1995**, *95* (7), 2457–2483. (b) Miyaura, N.; Yamada, K.; Sugimoto, H.; Suzuki, A. Novel and convenient method for the stereo- and regioselective synthesis of conjugated alkenes and alkyne via the palladium-catalyzed cross-coupling reaction of 1-alkenylboranes with bromoalkenes and bromoalkynes. *J. Am. Chem. Soc.* **1985**, *107* (4), 972–980. (c) Knowles, J. P.; Whiting, A. The Heck–Mizoroki cross-coupling reaction: a mechanistic perspective. *Org. Biomol. Chem.* **2007**, *5* (1), 31–44. (d) Matos, K.; Soderquist, J. A. Alkylboranes in the Suzuki–Miyaura Coupling: Stereochemical and Mechanistic Studies. *J. Org. Chem.* **1998**, *63* (3), 461–470. (e) Braga, A. A. C.; Morgon, N. H.; Ujaque, G.; Lledós, A.; Maseras, F. Computational study of the transmetalation process in the Suzuki–Miyaura cross-coupling of aryls. *J. Organomet. Chem.* **2006**, *691* (21), 4459–4466. (f) Heck, R. F.; Nolley Jr, J. Palladium-catalyzed vinylic hydrogen substitution reactions with aryl, benzyl, and styryl halides. *J. Org. Chem.* **1972**, *37* (14), 2320–2322.
- (31) *CrysAlisPRO*; Rigaku Oxford Diffraction Ltd.: Yarnton, Oxfordshire, England, 2019.
- (32) (a) Dolomanov, O. V.; Bourhis, L. J.; Gildea, R. J.; Howard, J. A. K.; Puschmann, H. OLEX2: a complete structure solution, refinement and analysis program. *J. Appl. Crystallogr.* **2009**, *42* (2), 339–341. (b) Sheldrick, G. Crystal structure refinement with SHELXL. *Acta Crystallogr. C* **2015**, *71* (1), 3–8.
- (33) (a) Parsons, S.; McCall, K.; Robertson, N. CSD Communication (Private Communication), CCDC, Cambridge, England, 2015. (b) Sheldrick, G. A short history of SHELX. *Acta Crystallogr. A* **2008**, *64* (1), 112–122.
- (34) (a) Martins, F. J.; Mol Lima, R.; Alves dos Santos, J.; de Almeida Machado, P.; Soares Coimbra, E.; David da Silva, A.; Rezende Barbosa Raposo, N. Biological Properties of Heterocyclic Pyridinylimines and Pyridinylhydrazones. *Lett. Drug. Des. Discovery* **2015**, *13*, 107–114. (b) Beck, D. E.; Reddy, P. V. N.; Lv, W.; Abdelmalak, M.; Tender, G. S.; Lopez, S.; Agama, K.; Marchand, C.; Pommier, Y.; Cushman, M. Investigation of the Structure–Activity Relationships of Aza-A-Ring Indenoisoquinoline Topoisomerase I Poisons. *J. Med. Chem.* **2016**, *59* (8), 3840–3853.

Cite this: *Nanoscale*, 2023, 15, 9543

Enhanced catalytic performance derived from coordination-driven structural switching between homometallic complexes and heterometallic polymeric materials†

 Gracjan Kurpik, ^{a,b} Anna Walczak, ^{a,b} Grzegorz Markiewicz, ^{a,b}
 Jack Harrowfield ^c and Artur R. Stefankiewicz ^{*a,b}

A bifunctional ligand 4,4-dimethyl-1-(pyridin-4-yl)pentane-1,3-dione (HL) able to provide two distinct coordination sites, *i.e.* anionic β -diketonate (after deprotonation) and neutral pyridine, has been used in the synthesis of Ag(I), Pd(II) and Pt(II) complexes that then have been applied as metalloligands for the construction of new heterometallic polymeric materials. The ambidentate nature of L^- enables switching between different modes of coordination within mononuclear complexes or their conversion into polymeric species in a fully controllable way. The coordination-driven processes can be triggered by various stimuli, *i.e.* a metal salt addition or acid–base equilibria, and presents an efficient strategy for the generation of metallosupramolecular materials. As a consequence of self-assembly, new multimetallic coordination aggregates have been synthesized and characterized in depth in solution (1H NMR, ESI-MS) as well as in the solid state (XPS, SEM-EDS, FTIR, pXRD, TGA). Furthermore, the Pd-based assemblies have been found to be efficient catalyst precursors in the Heck cross-coupling reaction, demonstrating a direct impact of compositional and morphological differences on their catalytic activity.

Received 21st March 2023.
Accepted 1st May 2023

DOI: 10.1039/d3nr01298k

rsc.li/nanoscale

Introduction

Metal–ligand interactions are the primary driving force in the generation of simple coordination compounds, as well of metallosupramolecular architectures with a high degree of complexity and a precisely defined structure.¹ Taking into account the character of a coordinate bond, *i.e.* its high strength but commonly dynamic nature, coordination-driven self-assembly processes are characterized by high controllability at the molecular level with respect to directionality, reversibility and post-synthetic switchability.² The supramolecular transformations induced by different external physicochemical stimuli, *e.g.* changes in concentration,^{3,4} acid–base equilibria,^{5,6} stoichiometry,^{7,8} cation/anion exchange,^{9,10} or radiation,^{11,12} lead to entirely new systems of diverse chemical

composition, structure, topology and properties. Thus, externally driven interconversion processes and other structural modifications play an increasingly important role in the design and construction of functional materials that constitute a competitive approach to classical synthesis.^{2,13}

Ambidentate pyridyl- β -diketonate ligands derived from pyridyl-1,3-diketones are an interesting class of organic species commonly used as building blocks in coordination and metallosupramolecular chemistry.^{14–16} Such units are capable of binding metal-ion centers in more than one way through different donor-atom combinations. The distinct nature of coordination sites, *i.e.* anionic β -diketonate and neutral pyridine, makes them good donors for a wide range of metal cations, both hard and soft acids according to HSAB theory.^{17,18} In most cases, they act as *O,O*-chelates or as simple N-donors through the pyridine ring, but other coordination modes can be achieved.^{19,20} Due to this structural variety they have found a number of applications in the construction of sophisticated coordination assemblies, including complex compounds,^{21–24} macrocycles,¹⁴ multimetallic polymers,^{20,25,26} metal–organic frameworks (MOFs)^{27,28} and metallocages.^{29–31}

Although a number of reports on metallosupramolecular assemblies based on pyridyl- β -diketonate-derived ligands are available in the literature, we focused on an unexplored aspect, namely the switchable nature of species with such units as

^aCenter for Advanced Technology, Adam Mickiewicz University in Poznań, Uniwersytetu Poznańskiego 10, 61-614 Poznań, Poland. E-mail: ars@amu.edu.pl

^bFaculty of Chemistry, Adam Mickiewicz University in Poznań, Uniwersytetu Poznańskiego 8, 61-614 Poznań, Poland

^cInstitut de Science et d'Ingénierie Supramoléculaires, Université de Strasbourg, 8 allée Gaspard Monge, 67083 Strasbourg, France

†Electronic supplementary information (ESI) available. CCDC 2244267. For ESI and crystallographic data in CIF or other electronic format see DOI: <https://doi.org/10.1039/d3nr01298k>

well as conducting studies on the application potential of new heterometallic aggregates. In this work the ditopic molecule 4,4-dimethyl-1-(pyridin-4-yl)pentane-1,3-dione (HL) was employed to synthesize a series of Ag(I), Pd(II) and Pt(II) coordination compounds which were further converted into more complex metallosupramolecular assemblies. Particular efforts have been undertaken to ensure an efficient strategy for multi-stage supramolecular transformations between the resultant systems triggered by external stimuli. The present work describes coordination-driven structural switching between a variety of mononuclear complexes based on the ligand HL/L⁻ and Ag(I), Pd(II) and Pt(II) cations. As a consequence of metallosupramolecular self-assembly, new heterometallic polymeric materials have been obtained and their physicochemical characterization is described ahead. Additionally, the diversity in their functionality has been illustrated by their use as catalyst precursors in the Heck cross-coupling reaction.

Results and discussion

Synthesis and characterization of complexes

As shown in Fig. 1, the pyridyl-β-diketone ligand HL acts as the starting material and main building block for all coordination species presented. Its ambidentate nature was used to design, obtain and convert a series of complexes with Ag(I), Pd(II) and Pt(II) cations. All the coordination compounds presented herein can be directly synthesized by complexation reactions between HL and appropriate metal salts. Pd(II) and Pt(II) complexes, *i.e.* [Pd(HL)₄](NO₃)₂ (C3), [Pt(HL)₄](NO₃)₂ (C4) and [PdL₂] (C6) were synthesized according to literature procedures.^{22,23} The compound [Ag(HL)₂]NO₃ (C1) was synthesized by the reaction of HL (2 equiv.) with AgNO₃ (1 equiv.) carried out in DCM/EtOH (1 : 1, v/v) at room temperature for 18 h. The generation and purity of the desired complex were

confirmed in solution *via* ¹H NMR spectroscopy and ESI-MS spectrometry (Fig. S1 and S2†). Moreover, slow evaporation of the methanol solution provided crystals, suitable for single-crystal X-ray diffraction measurements. The complex C1 crystallizes in the monoclinic space group *P2₁/n* and has an almost ideal linear geometry of Ag(I) coordination where the N–Ag–N angle is equal to 170.53°. It is worth emphasizing that C1 occurs as a dimer in the crystal (Fig. S13†), where two molecules are linked by a weak metal–metal interaction Ag...Ag (3.08 Å),^{32,33} but this was not confirmed in solution. The β-diketone units remained in their protonated enol form and were not involved in the formation of coordinate bonds. The crystal and structure refinement data are given in the ESI, Table S1.†

Two structurally distinct Pd(II) complexes of the ligand HL and ethylenediamine (en) co-ligand were observed in solution *via* ¹H NMR spectroscopy but neither could be isolated in pure form. The reaction of [Pd(en)(NO₃)₂] with 2 equiv. of HL in CD₃CN resulted in the formation of [Pd(en)(HL)₂](NO₃)₂ (C2) whereas the deprotonation of HL (1 equiv.) with Et₃N prior to the addition of metal salt gave [Pd(en)L]NO₃ (C5). Hence, depending on the reaction conditions applied one or two molecules of the ligand HL occupy two available positions in Pd(II) sphere and coordinate by *O,O*-chelate or *N*-donors, respectively. ¹H NMR spectroscopy as well as ESI-MS spectrometry allowed unequivocal determination of the structures and molecularity of the new compounds generated (Fig. S3–S6†).

Structural switching

In addition to their direct syntheses, the complexes can be converted into other species by addition of either appropriate metal salts or acid/base, as shown by ¹H NMR spectroscopy (Fig. 2 and see ESI, Fig. S14–S19†). As previously mentioned, the ligand HL reacted with AgNO₃ to give the disubstituted

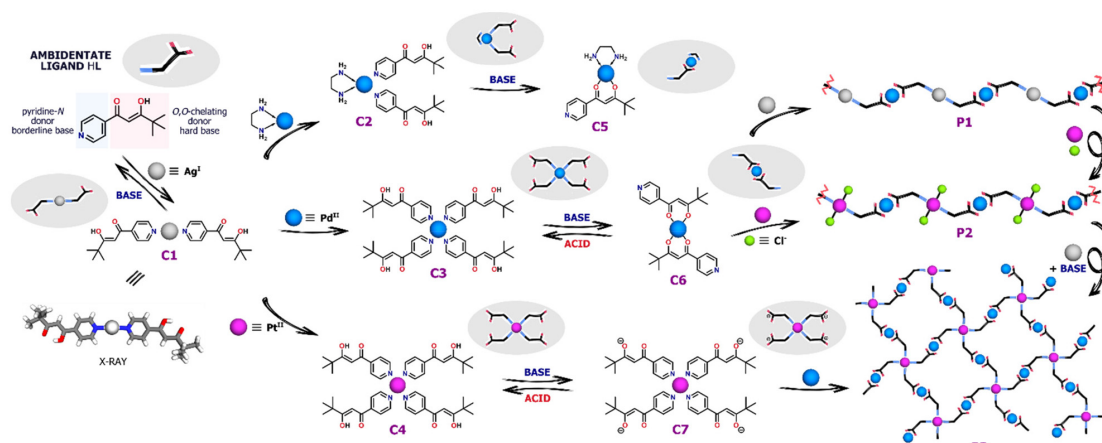


Fig. 1 General scheme showing the supramolecular transformations within coordination-driven assemblies based on Ag(I), Pd(II) and Pt(II) ions and the pyridyl-β-diketone ligand HL.

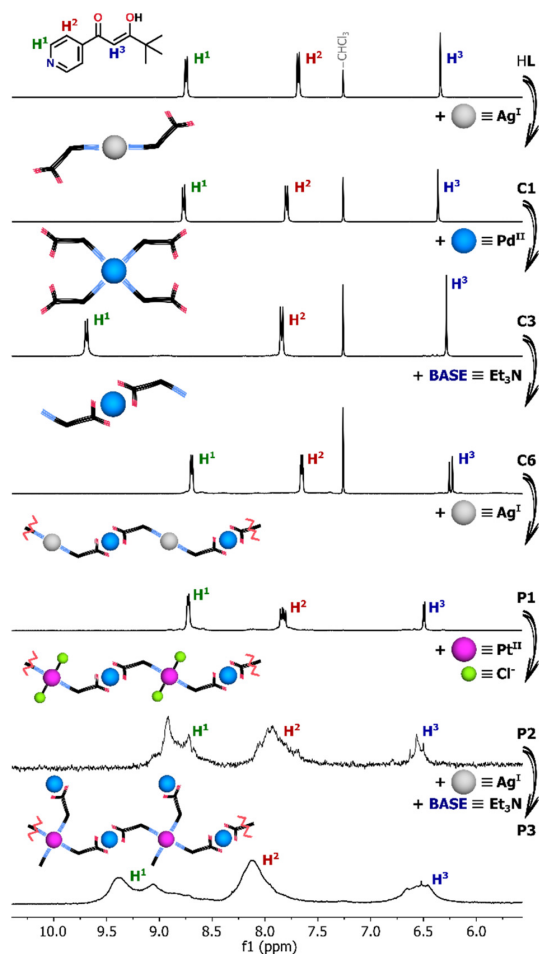


Fig. 2 Parts of ^1H NMR spectra (600 MHz, CDCl_3 or $\text{DMSO}-d_6$ for P1–P3) showing the coordination-driven transformations triggered by the addition of metal salt or base.

coordination compound C1 although it decomposes under the influence of base (Fig. S14†). After addition of 0.5 equiv. of Et_3N only upfield shifted signals from the deprotonated ligand L^- were observed. Therefore, the instability of C1 under basic conditions excluded its further coordination through O,O -chelation requiring prior deprotonation.

Nevertheless, the $\text{Ag}(\text{I})$ complex C1 can be completely transformed into $\text{Pd}(\text{II})$ or $\text{Pt}(\text{II})$ species upon addition of the appropriate metal salt. As a result of $\text{Pd}(\text{NO}_3)_2$ addition, gradual disappearance of the C1 signals was observed, along with the emergence of new intense signals for the $\text{Pd}(\text{II})$ compound, which was found to be the four-coordinate complex C3 (Fig. S15†). As shown by ^1H NMR titration experiments, the change in the coordination number from 2 to 4 was clearly illustrated by the significantly downshifted signal ($\Delta\delta = \sim 0.8$ ppm) from the protons near pyridine-N atoms (H^1).

Similar behavior was observed when C1 was titrated with $[\text{Pd}(\text{en})(\text{NO}_3)_2]$. Two molecules of the ligand HL derived from the degradation of the $\text{Ag}(\text{I})$ complex completed the coordination sphere of $\text{Pd}(\text{II})$ leading to the formation of the heteroleptic compound C2 (Fig. S16†).

In contrast, no additional signals or shifts were initially detected during the transformation of C1 triggered by $\text{Pt}(\text{II})$ ions. The $\text{Ag}(\text{I})$ complex appeared to be stable as $\text{Pt}(\text{NO}_3)_2$ was added, not undergoing any obvious reaction. The generation of the desired complex C4 was noticed only after several days due to the greater kinetic inertness of $\text{Pt}(\text{II})$ ion in comparison to $\text{Pd}(\text{II})$, for which no kinetic hysteresis was observed during the experiment (Fig. S17 and S18†).

The $\text{Pd}(\text{II})$ and $\text{Pt}(\text{II})$ coordination compounds generated by these metal ion exchange reactions of C1 were subjected to the addition of base (Et_3N). $\text{Pd}(\text{II})$ complexes C3 and C6 can be easily interconverted between N- and O,O -donor forms with 100% efficiency by deprotonation/protonation of the enolic centre.²² Addition of base to the cationic N-bound complex C3 leads to linkage rearrangement and formation of neutral O,O -chelated counterparts, a reaction which can be reversed by addition of methanesulfonic acid (MSA). Similarly, titration of the heteroleptic species C2 with Et_3N caused a change in the coordination mode *via* release of one N-bound ligand molecule and the formation of monocharged complex C5 (Fig. S19†). No further transformation into the homoleptic complex C6 coordinated by two β -diketonate units occurred despite the addition of a large excess of Et_3N (10 equiv.), consistent with the high stability of the $\text{Pd}(\text{en})$ unit. In contrast to its $\text{Pd}(\text{II})$ analogue, the $\text{Pt}(\text{II})$ complex C4 does not undergo any conversion under basic conditions even after several days. The switching between cationic and neutral species is completely retarded by the kinetic inertness of $\text{Pt}(\text{II})$. Addition of a stoichiometric amount of Et_3N results only in deprotonation of the uncoordinated enol units and formation of anions $[\text{PtL}_4]^{2-}$ (C7), while the N-bound complex structure remains essentially intact.²³

Synthesis of heterometallic polymers

Due to the presence of accessible coordination sites capable of reacting with metal cations, the complexes C6 and C7 (the deprotonated form of C4) can act as metalloligands. As a pyridine-N donor, $\text{Pd}(\text{II})$ complex C6 was expected to be a good ligand for $\text{Ag}(\text{I})$ and for this reason C6 was reacted with AgOTf (or AgNO_3) in anticipation of the formation of a new multimetallic aggregate $[\text{PdAg}_x\text{L}_2]_n^{x+}$ (P1), where $x \approx 1$. In this structure, the O,O -chelating and pyridine-N donors were expected to be involved in coordination with $\text{Pd}(\text{II})$ and $\text{Ag}(\text{I})$, respectively, with $\text{Ag}(\text{I})$ being two-coordinate, as in complex C1. During a ^1H NMR titration of C6 with AgOTf , a progressive decrease in signal intensity was observed as a result of the precipitation of a new product (Fig. S20–S21†) along with minor downfield chemical shifts that could be attributed to the coordination of $\text{Ag}(\text{I})$ cations by pyridine-N. Full disappearance of ^1H NMR signals from the $\text{Pd}(\text{II})$ metalloligand C6 and complete product

precipitation (**P1**) were observed after the addition of 1 equiv. of Ag(I), corresponding to the expected reaction stoichiometry.

Next, **C6** was reacted with an equimolar amount of PtCl₂ in the expectation that retention of the chlorido ligands would favor formation of Pt(II) centers involving just two pyridine-N donors.^{34,35} The reaction was performed in MeCN at 80 °C for 24 h, giving an orange precipitate, consistent with the formation of a coordination polymer **P2**. In order to verify the composition of the aggregate, we synthesized an analogue of the complex **C6** – [Pd(bpm)₂],³⁶ which lacks pyridyl donors. In the control experiment, Pt(II) salt was added to the solution of [Pd(bpm)₂] under the reaction conditions, but no clear changes were observed in the ¹H NMR spectra (Fig. S23†). Thus, the Pd/Pt exchange could be unambiguously excluded in the structure of the monomer **C6**, confirming the preservation of *O,O*-coordination for Pd(II) ions. The isolated material **P2** was highly insoluble in most common solvents and only in DMSO-*d*₆ it was possible to record ¹H NMR spectrum which showed severely broadened signals, indicative of the generation of the complex metalloaggregates in this solvent (Fig. S9†).

The capacity to deprotonate the enol units of **C4** without causing complex decomposition or isomerization prompted us to react **C7** with Pd(NO₃)₂ under basic conditions. The formation of a new species (**P3**) was observed and again broad and highly overlapped set of signals for all of the aromatic and methine protons were observed in the ¹H NMR spectrum (Fig. S11†). This broadening is characteristic of and consistent with the presence of complex metallosupramolecular assemblies. The spectrum contained no signal from the enol group of a diketone moiety (≈16 ppm), indicating complete coordination between this group and Pd(II), possibly as a result of the creation of a complex branched oligomeric structure. The control experiment carried out for a simple Pt(II) complex with pyridine ligands also excluded the exchange of inert Pt(II) ions with Pd(II). As indicated by the ¹H NMR spectra (Fig. S24†), its structure was retained in the reaction environment, which showed that only deprotonated *O,O*-chelates could be involved in the Pd(II) coordination.

The coordination-driven switching strategies developed for the mononuclear complexes **C1**–**C7** were successfully adapted to the transformations of the coordination polymers **P1**–**P3** as well. In order to exchange Ag(I) cations with Pt(II), PtCl₂ was added to the solution of **P1** in DMSO-*d*₆, which resulted in the precipitation of AgCl and a clear color change. The transformation, followed by ¹H NMR spectroscopy, indicated the formation of a new coordination complex, as illustrated by the significant broadening of downshifted signals in a spectrum consistent with that of **P2**. Furthermore, the polymer **P2** was converted into **P3** in a two-step process by adding AgNO₃ and, subsequently, Et₃N. First, a counterion exchange from Cl[–] to NO₃[–] was carried out by removing chlorido co-ligands, followed by rearrangement of the structure in a basic environment.³⁴ The labile NO₃[–] anions in the coordination sphere of Pt(II) can be readily replaced under basic conditions, leading to the generation of a two-dimensional lattice with Pt(II) ions

bound by four pyridine-N donors, which was demonstrated by strong downfield shifts in the ¹H NMR spectrum after this conversion.

Characterization of heterometallic materials

As expected for coordination polymers, their solubility in most solvents was very limited, which effectively hampered their full characterization in solution. Although the ¹H NMR spectra for **P1**–**P3** described above are not readily interpreted, their profiles are consistent with the formation of larger aggregates. High-resolution ESI-MS spectrometry also confirmed the successful generation of the desired heteronuclear complexes. The mass spectra recorded for **P1**–**P3** demonstrated the presence of the expected fragmentary constituents consisting of chains of successive monomers connected by additional metal ions. All of the identified peaks were in good agreement with their calculated theoretical distribution, allowing the composition and heterometallic nature of the aggregates to be established (Fig. S8, S10 and S12†).

The metal content of the polymeric materials **P1**–**P3** was determined *via* ICP-MS analysis, which enabled confirmation of the presence of the two different metals expected, *i.e.* Ag and Pd for **P1**; Pd and Pt for **P2**, **P3** (Table S2†). The percentage contribution of individual metal ions corresponds well to the values calculated for each polymer, with minor deviations perhaps attributable to the lack of any means of ensuring sample purity. XPS spectroscopy confirmed the identity of the different metal mixtures in the three heterometallic polymers (Fig. S25–S27†). The XPS spectra of **P1**–**P3** showed signals indicating the presence of Ag(I), Pd(II), and Pt(II) ions, as well as elements from the organic unit: C, O, N.

To further investigate the complex formation, ATR-FTIR analysis was performed in order to confirm the involvement of specific chemical groups in coordination (Fig. S28–S34†). The absorption bands in the structure of the ligand HL have been assigned by the comparison of its spectrum with the spectra of the reference compounds containing the indicative fragments, *i.e.* pinacolone, acetylacetone, pyridine and methyl isonicotinate (Fig. S35†). It resulted in the identification of characteristic band at 1611 cm^{–1} related to the stretching vibration of the C=O bond of β-diketonate unit ($\nu_{C=O}$) and four bands in the region 1585–1427 cm^{–1} from C=N and C=C bond vibrations of the heterocyclic ring (ν_{py}). With regard to the coordination assemblies, their recorded IR spectra were consistent with the assumed bonding modes.³⁷ For the mononuclear compounds, the shifts of the absorption bands to lower wavenumbers corresponding to β-diketonate (**C6**) or pyridine ring (**C2**, **C4**) demonstrate the existence of the metal coordination bonding and confirm the complexation reaction of the ligand HL with the appropriate metal ions, whereas the other bands are observed almost in the same position (Fig. S36†). FTIR spectra show that the generation of the heterometallic polymers **P1**–**P3** results in the clear red shifts of the bands characteristic of both $\nu_{C=O}$ and ν_{py} vibrations of the ligand functional groups (Fig. 3). Furthermore, in the spectra of **C2**, **C4** and **P1**, we observed the appearance of an additional

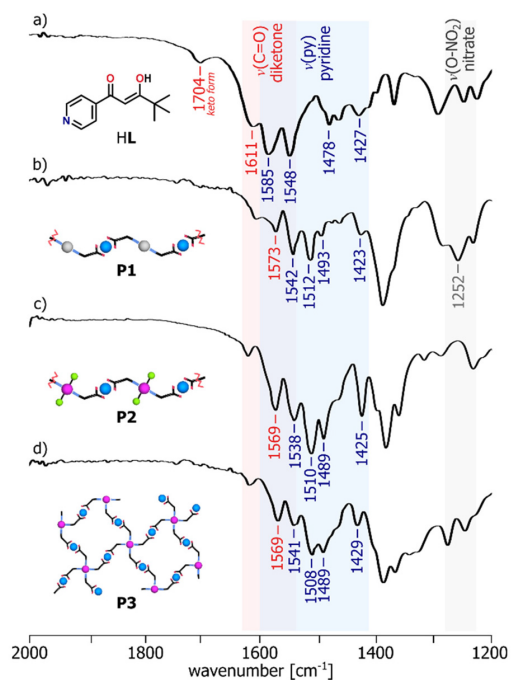


Fig. 3 ATR-FTIR spectra in the 2000–1200 cm^{-1} region of: the ligand HL (a) and the polymers P1–P3 (b–d), showing the involvement of the functional groups in metal binding.

band in the region of 1250–1300 cm^{-1} , originating from the stretching vibrations of the O–NO₂ bond due to the presence of NO₃[−] counterions in the complex structures.

The bimetallic materials were also characterized *via* scanning electron microscopy (SEM) to establish their morphology (Fig. S43, S45 and S47[†]). The images were recorded with an accelerating voltage of 10 kV and magnification up to $\times 30\,000$ using an LFD in solid state. The morphologies of the coordination polymer aggregates P1–P3 indicate the existence of irregular polymer networks depending on their one- or two-dimensional structure. The SEM images of P1–P3 illustrate the formation of quasi-spherical particles of various sizes in the nanometer range. As shown in Fig. 4, all the species show a tendency to agglomerate into larger clusters and the one-dimensional polymers P1–P2 intertwine with each other, creating rounded, disordered shapes. For comparison, SEM images were also recorded for the metalloligands C1, C4 and C6 (Fig. S49–S51[†]). In contrast to P1–P3, the mononuclear complexes appear as single microcrystals with regular shapes. The SEM results are consistent with the data obtained *via* powder X-ray diffraction (pXRD) studies. The pXRD patterns with a set of sharp and intense reflections indicate the crystallinity of the samples C1, C4 and C6 (Fig. S37–S39[†]). In contrast, the diffractograms recorded for P1–P3 established their amorphous character (Fig. S40–S42[†]), which, however, can be advantageous with regard to their use as (pre) catalysts, facilitating dispersion in the reaction medium.

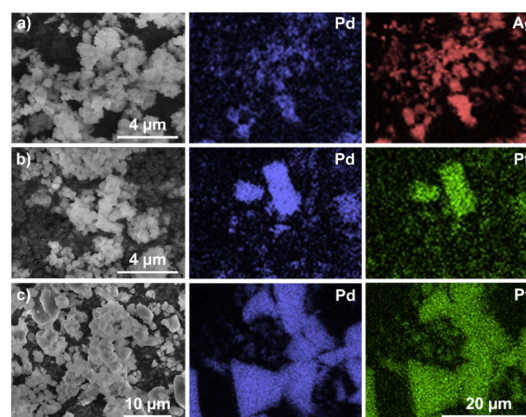


Fig. 4 SEM images and EDS elemental mapping of the sample composition for (a) P1; (b) P2 and (c) P3. The same magnification indicated in the graphic was used for all EDS images.

EDS mapping provided the topographic distribution of individual elements in the samples (Fig. 4 and S44, S46, S48[†]). Comparison of the false-color EDS mapping images demonstrated the uniform and common location of the metal pairs in each solid, consistent with their identity as heterometallic coordination polymers.

Thermogravimetric analysis (TGA) was conducted to study the thermal stability of the compounds P1–P3 and compare their properties with the metalloligands C4 and C6 used as building blocks in their synthesis. The experiments were performed in the temperature range 30–600 °C under N₂ with a heating rate of 10 °C min^{−1}. The TGA curves of the polymeric materials P1–P3 have similar profiles and show higher stability than the mononuclear analogues C4 and C6 (Fig. S52–S57[†]). In the DTG curves (Fig. S58[†]), the main peaks which indicate the rate of decomposition are always shifted towards higher temperatures when P1–P3 are compared to the corresponding mononuclear units, attributed to the retardation of volatilization within the polymers. The heterometallic aggregates show no weight loss of up to ~ 250 °C, whereas C4 and C6 begin to decompose at 160 and 210 °C, respectively. The stepwise decomposition *via* gradual removal of organic components from the structure of compounds P2–P3 leads to the formation of the mixture of appropriate metal oxides – PdO and PtO₂ as the residue (calcd. 44.76% and found 47.01% for P2; calcd. 38.53% and found 35.21% for P3). The polymer P1 turned out to be the most stable, as illustrated by the very gentle course of the TGA curve. In the tested temperature range, it underwent thermal degradation only partially, because the weight loss was equal to 24.44% whereas the mixture of thermal decomposition products, *i.e.* PdO and metallic silver in the final residue should constitute 29.84% of the sample mass.

Catalytic studies

The ability to combine in close and ordered proximity different catalytically active metal ions in the polymers pre-

sently described renders them of particular interest for evaluation of the influence of one metal on the activity of another. The remarkable utility of Pd complexes as catalysts for cross-coupling reactions led us to choose familiar reactions of this kind for an initial assessment of the catalytic properties of the polymers and their precursors. The reaction screening revealed a high potential of the polymeric species **P1–P3** to be applied as precatalysts in various Pd-catalyzed C–C coupling reactions, such as the Heck, Suzuki–Miyaura and Sonogashira reactions. Considering the most promising results in the former process, we decided to assess the influence of the compositional differences between homometallic complexes and heterometallic materials on their catalytic activity in this reaction. Thus, the Heck cross-coupling between iodobenzene and styrene catalyzed by **P2** was chosen as a model reaction for the development of reaction conditions. All the optimization procedures are summarized in the ESI, Table S3.† The percentage of Pd in all the structures was determined *via* ICP-MS analysis and the results were used to calculate the catalyst loading. Different variations in terms of solvents and bases were tested using a 0.1 mol% Pd. Of all the combinations, the pair of Et₃N and DMSO gave the expected (*E*)-stilbene in the highest GC yield after 18 h. Further experiments revealed that the catalyst loading could be reduced to relatively low concentration – 0.05 mol%. This concentration was sufficient to guarantee an

almost quantitative conversion along with excellent selectivity achievable after 6 h, whereas the use of 0.01 mol% significantly extended the reaction time to 18 h. Taking economic and environmental considerations into account, subsequent catalytic reactions were carried out in DMSO at 100 °C for 6 h using Et₃N (2 equiv.) as a base and 0.05 mol% Pd. Importantly, the reactions were performed without the need to exclude air or water. Furthermore, the metalloaggregates **P1–P3** showed high stability under ambient conditions exceeding several months of storage without any decomposition or loss of catalytic activity, which is beneficial in terms of their utility as catalyst precursors.

A series of catalytic tests was performed to evaluate and compare the performance of other coordination assemblies containing Pd(II) ions in the Heck cross-coupling reaction. For the selected set of aryl iodides and olefins (Fig. 5a), the complex **C6**, a building block of all the coordination polymers, had a lower efficiency under the same total Pd loading (GC yields in the range of 60–68%). Roughly the same results (55–70%) were obtained using a mixture of [Pd(bpm)₂] and PtCl₂, *i.e.* the constituents of the polymer **P2**, lacking the pyridine units and thus unable to unite under the catalytic reaction conditions. In both cases, the lower GC yields are possibly due to the absence of neighboring metal ions compared to the heterometallic aggregates. A number of catalytic centers in a

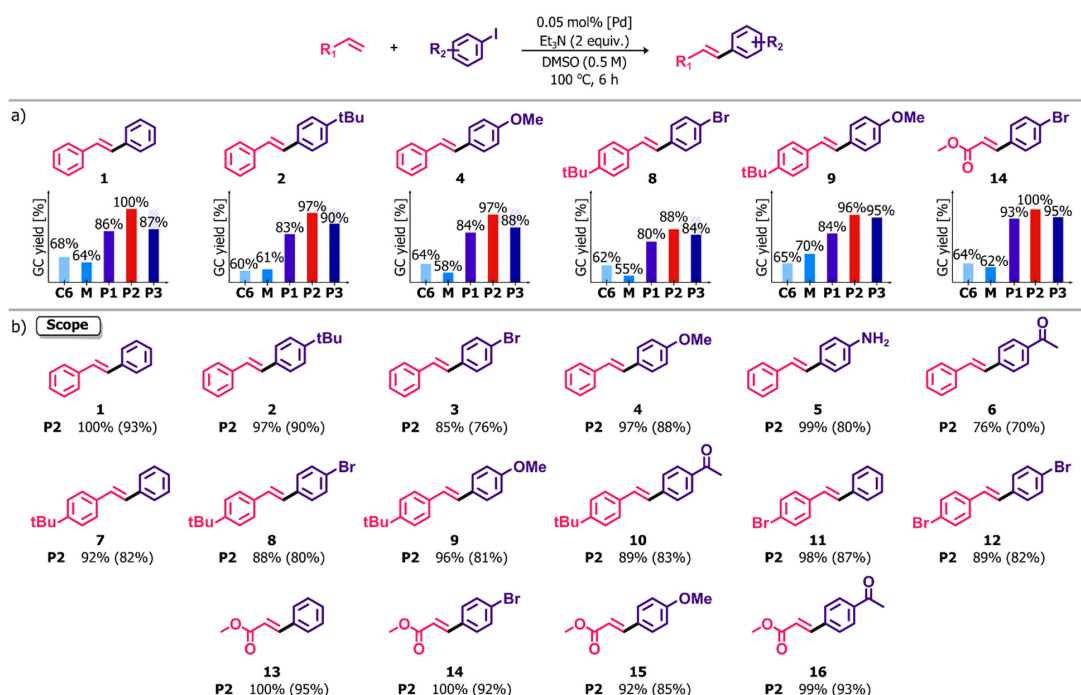


Fig. 5 (a) Comparative tests showing different catalytic activity of the complex **C6**, a mixture of [Pd(bpm)₂] and PtCl₂ (**M**), and the coordination polymers **P1–P3** in the Heck cross-coupling reaction. (b) Scope of the Heck cross-coupling catalyzed by **P2**. Reaction conditions: aryl iodide (0.5 mmol, 1 equiv.), olefin (0.5 mmol, 1 equiv.), Et₃N (1.0 mmol, 2 equiv.) and the Pd(II) complex (0.05 mol% Pd) were stirred in DMSO (1 mL) at 100 °C for 6 h. Yields determined by GC-MS measurements of aryl iodide decay. The yields in parentheses are those of the isolated compounds.

single molecule significantly increases catalytic activity through a higher local concentration of Pd which is demonstrated in considerably enhanced effectiveness in the reactions catalyzed by **P1–P3**. This positive effect, defined in the literature for dendrimers,^{38–41} coordination polymers,^{42,43} and recently for polynuclear complexes,⁴⁴ was also observed in this case and provides an explanation of the apparent differences between mononuclear units and **P1–P3**. The results of the comparative tests for **P1–P3** demonstrated high efficiency of all the species, slightly variable as indicated by the different reaction yields. The lower catalytic activity of **P3** might be explained due to its morphology since the catalytic sites in the structure of the two-dimensional polymer **P3** might be less accessible compared to its linear counterparts **P1–P2**. Nevertheless, the extension of the reaction time to 12 h allowed attainment of yields comparable to those with the pre-catalyst **P2**. The local concentration enhancement could possibly be weaker in the case of reactions catalyzed by **P1**. The presence of labile Ag(I) ions as linkers between Pd(II) units might promote polymer fragmentation under reaction conditions that limits the influence of the nuclearity effect. On the other hand, very inert Pt(II) ions are able to retain the polymer structure of **P2** more effectively. Thus, a number of differences between the mononuclear complexes and coordination polymers **P1–P3**, *i.e.* varied nuclearity, composition, dimensionality and morphology, had a significant impact on the course of catalytic reactions and, consequently, on the obtained reaction yields.

With these optimized conditions in hand, we undertook studies of the scope and limitations of this system in the Heck cross-coupling reaction between a series of structurally diversified substrates. The investigations were carried out with the use of **P2** as a catalyst precursor, identified to be the most effective among the investigated. As shown in Fig. 5b, the high efficiency of **P2** was revealed regardless of the presence of electron donating (–OMe, –NH₂, –*t*Bu) or electron withdrawing (–COMe, –Br) functional groups in the reactant molecules. In all cases, the stilbene derivatives were formed in high-to-excellent isolated yields, ranging from 70% to 93%. Moreover, the reaction of methyl acrylate with a set of aryl iodides enabled the synthesis of coupling products in excellent yields (85–95%). It is noteworthy that the reaction system exhibited great chemoselectivity towards aryl iodides because no cross-coupling involving bromoarene moieties, as either olefin or haloarene coupling partners, was observed. In all cases, the selectivity in the generation of reaction products with the (*E*)-configuration of double bond was very high and completely independent of the nature of substrates since (*Z*)-isomers never exceeded 10% as determined *via* GC-MS distribution of both isomers.

Conclusions

In summary, the ambidentate nature of the ligand HL and its conjugate base L[–] allows the generation of distinct complex

compounds with modifiable structure and tunable properties. The availability of free coordination sites enables their utilization as metalloligands in further complexation reactions. The work also defines an effective strategy of coordination-driven structural switching processes for a specific group of coordination systems based on pyridyl- β -diketone ligands. As a consequence, we have successfully synthesized and analyzed new polymeric materials based on precious metals. The structural features, morphology and stability of these coordination assemblies were determined *via* NMR, ESI-MS ICP-MS, XPS, FTIR, SEM-EDS and TG analyses, which unambiguously confirmed their heterometallic character. Furthermore, the coordination polymers reported in this paper exhibit not only structural variety but, more importantly, diverse functionality, as reflected in their catalytic activity. The polymers have been found to be efficient and versatile precatalysts in the Heck cross-coupling reaction within a scope of structurally distinct substrates.

Author contributions

The manuscript was written through contributions of all authors. All authors have given approval to the final version of the manuscript.

Conflicts of interest

There are no conflicts to declare.

Acknowledgements

This research was funded by the National Science Centre in Poland (grant SONATA BIS 2018/30/E/ST5/00032 – ARS).

References

- 1 E. C. Constable and C. E. Housecroft, *Chem. Soc. Rev.*, 2013, **42**, 1429–1439.
- 2 W. Wang, Y.-X. Wang and H.-B. Yang, *Chem. Soc. Rev.*, 2016, **45**, 2656–2693.
- 3 K. Uehara, K. Kasai and N. Mizuno, *Inorg. Chem.*, 2010, **49**, 2008–2015.
- 4 S. Tashiro, M. Tominaga, T. Kusukawa, M. Kawano, S. Sakamoto, K. Yamaguchi and M. Fujita, *Angew. Chem., Int. Ed.*, 2003, **42**, 3267–3270.
- 5 J. Beswick, V. Blanco, G. De Bo, D. A. Leigh, U. Lewandowska, B. Lewandowski and K. Mishiho, *Chem. Sci.*, 2015, **6**, 140–143.
- 6 V. Blanco, A. Carlone, K. D. Hänni, D. A. Leigh and B. Lewandowski, *Angew. Chem., Int. Ed.*, 2012, **51**, 5166–5169.
- 7 Q.-F. Sun, S. Sato and M. Fujita, *Nat. Chem.*, 2012, **4**, 330–333.

- 8 S. Hiraoka, T. Yi, M. Shiro and M. Shionoya, *J. Am. Chem. Soc.*, 2002, **124**, 14510–14511.
- 9 O. Jurček, P. Bonakdarzadeh, E. Kalenius, J. M. Linnanto, M. Groessl, R. Knochenmuss, J. A. Ihalainen and K. Rissanen, *Angew. Chem., Int. Ed.*, 2015, **54**, 15462–15467.
- 10 H. T. Chifotides and K. R. Dunbar, *Acc. Chem. Res.*, 2013, **46**, 894–906.
- 11 S. Chen, L.-J. Chen, H.-B. Yang, H. Tian and W. Zhu, *J. Am. Chem. Soc.*, 2012, **134**, 13596–13599.
- 12 M. Han, R. Michel, B. He, Y.-S. Chen, D. Stalke, M. John and G. H. Clever, *Angew. Chem., Int. Ed.*, 2013, **52**, 1319–1323.
- 13 V. Blanco, D. A. Leigh and V. Marcos, *Chem. Soc. Rev.*, 2015, **44**, 5341–5370.
- 14 A. D. Burrows, M. F. Mahon, C. L. Renouf, C. Richardson, A. J. Warren and J. E. Warren, *Dalton Trans.*, 2012, **41**, 4153–4163.
- 15 C. J. McMonagle, P. Comar, G. S. Nichol, D. R. Allan, J. González, J. A. Barreda-Argüeso, F. Rodríguez, R. Valiente, G. F. Turner, E. K. Brechin and S. A. Moggach, *Chem. Sci.*, 2020, **11**, 8793–8799.
- 16 G.-L. Wang, Y.-J. Lin, H. Berke and G.-X. Jin, *Inorg. Chem.*, 2010, **49**, 2193–2201.
- 17 R. G. Pearson, *J. Chem. Educ.*, 1968, **45**, 581–587.
- 18 T.-L. Ho, *Chem. Rev.*, 1975, **75**(1), 1–20.
- 19 M. J. Mayoral, P. Cornago, R. M. Claramunt and M. Cano, *New J. Chem.*, 2011, **35**, 1020–1030.
- 20 A. Walczak, G. Kurpik and A. R. Stefankiewicz, *Int. J. Mol. Sci.*, 2020, **21**(17), 6171.
- 21 S.-L. Lee, F.-L. Hu, X.-J. Shang, Y.-X. Shi, A. L. Tan, J. Mizera, J. K. Clegg, W.-H. Zhang, D. J. Young and J.-P. Lang, *New J. Chem.*, 2017, **41**, 14457–14465.
- 22 A. Walczak and A. R. Stefankiewicz, *Inorg. Chem.*, 2018, **57**, 471–477.
- 23 A. Walczak, H. Stachowiak, G. Kurpik, J. Kaźmierczak, G. Hreczycho and A. R. Stefankiewicz, *J. Catal.*, 2019, **373**, 139–146.
- 24 R. A. A. Abdine, G. Kurpik, A. Walczak, S. A. A. Aeash, A. R. Stefankiewicz, F. Monnier and M. Taillefer, *J. Catal.*, 2019, **376**, 119–122.
- 25 M. Dudek, J. K. Clegg, C. R. K. Glasson, N. Kelly, K. Gloe, K. Gloe, A. Kelling, H.-J. Buschmann, K. A. Jolliffe, L. F. Lindoy and G. V. Meehan, *Cryst. Growth Des.*, 2011, **11**, 1697–1704.
- 26 P. C. Andrews, G. B. Deacon, R. Frank, B. H. Fraser, P. C. Junk, J. G. MacLellan, M. Massi, B. Moubaraki, K. S. Murray and M. Silberstein, *Eur. J. Inorg. Chem.*, 2009, **2009**, 744–751.
- 27 G.-G. Hou, Y. Liu, Q.-K. Liu, J.-P. Ma and Y.-B. Dong, *Chem. Commun.*, 2011, **47**, 10731–10733.
- 28 B. Chen, F. R. Fronczek and A. W. Maverick, *Inorg. Chem.*, 2004, **43**, 8209–8211.
- 29 S. Sanz, H. M. O'Connor, V. Martí-Centelles, P. Comar, M. B. Pitak, S. J. Coles, G. Lorusso, E. Palacios, M. Evangelisti, A. Baldansuren, N. F. Chilton, H. Weihe, E. J. L. McInnes, P. J. Lusby, S. Piligkos and E. K. Brechin, *Chem. Sci.*, 2017, **8**, 5526–5535.
- 30 H.-B. Wu and Q.-M. Wang, *Angew. Chem., Int. Ed.*, 2009, **48**, 7343–7345.
- 31 S. Sanz, H. M. O'Connor, P. Comar, A. Baldansuren, M. B. Pitak, S. J. Coles, H. Weihe, N. F. Chilton, E. J. L. McInnes, P. J. Lusby, S. Piligkos and E. K. Brechin, *Inorg. Chem.*, 2018, **57**, 3500–3506.
- 32 H.-L. Zhu, X.-M. Zhang, X.-Y. Liu, X.-J. Wang, G.-F. Liu, A. Usman and H.-K. Fun, *Inorg. Chem. Commun.*, 2003, **6**, 1113–1116.
- 33 E. M. Njogu, B. Omondi and V. O. Nyamori, *J. Coord. Chem.*, 2015, **68**, 3389–3431.
- 34 G. Kurpik, A. Walczak, M. Goldyn, J. Harrowfield and A. R. Stefankiewicz, *Inorg. Chem.*, 2022, **61**, 14019–14029.
- 35 N. A. Lewis, S. Pakhomova, P. A. Marzilli and L. G. Marzilli, *Inorg. Chem.*, 2017, **56**, 9781–9793.
- 36 M. Kołodziejski, A. Walczak, Z. Hnatejko, J. Harrowfield and A. R. Stefankiewicz, *Polyhedron*, 2017, **137**, 270–277.
- 37 K. Nakamoto, *Infrared Spectra of Inorganic and Coordination Compounds*, Wiley-Interscience, 1970.
- 38 B. Helms and J. M. J. Fréchet, *Adv. Synth. Catal.*, 2006, **348**, 1125–1148.
- 39 R. S. Bagul and N. Jayaraman, *J. Organomet. Chem.*, 2012, **701**, 27–35.
- 40 E. Delort, T. Darbre and J.-L. Reymond, *J. Am. Chem. Soc.*, 2004, **126**, 15642–15643.
- 41 D. Wang and D. Astruc, *Coord. Chem. Rev.*, 2013, **257**, 2317–2334.
- 42 M. Kołodziejski, A. J. Brock, G. Kurpik, A. Walczak, F. Li, J. K. Clegg and A. R. Stefankiewicz, *Inorg. Chem.*, 2021, **60**, 9673–9679.
- 43 S. Kitagawa, R. Kitaura and S.-I. Noro, *Angew. Chem., Int. Ed.*, 2004, **43**, 2334–2375.
- 44 G. Kurpik, A. Walczak, M. Gilski, J. Harrowfield and A. R. Stefankiewicz, *J. Catal.*, 2022, **411**, 193–199.



Contents lists available at ScienceDirect

Journal of Catalysis

journal homepage: www.elsevier.com/locate/jcat

C(sp³),N palladacyclic complexes bearing flexidentate ligands as efficient (pre)catalysts for Heck olefination of aryl halides



Anna Walczak^{a,b}, Gracjan Kurpik^{a,b}, Maciej Zaranek^b, Piotr Pawluć^{a,b}, Artur R. Stefankiewicz^{a,b}

^a Faculty of Chemistry, Adam Mickiewicz University in Poznań, Uniwersytetu Poznańskiego 8, 61-614 Poznań, Poland

^b Centre for Advanced Technologies, Adam Mickiewicz University, Uniwersytetu Poznańskiego 10, 61-614 Poznań, Poland

ARTICLE INFO

Article history:

Received 26 October 2021

Accepted 24 November 2021

Available online 30 November 2021

Dedicated to Dr Christian Bruneau for his outstanding contribution to organometallic chemistry and catalysis.

Keywords:

Pd(II) complexes
Supramolecular chemistry
Flexidentate ligands
Catalysis
Heck
Olefination of aryl halides

ABSTRACT

C,N-cyclopalladated complexes are among the most robust and widely used (pre)catalysts of cross-coupling reactions, combining long shelf life with high catalytic activity. In this report, we describe synthesis and properties of new Pd(II) complexes of a flexidentate ligand – 2,2-dimethyl-5-(2-pyridyl)pentane-3,5-dione (HL). Its coordinating properties resulted in the formation of two stereoisomeric *cis*- and *trans*-PdL₂ complexes each with one ligand in *O,O'*- and the other in *N,C(sp³)*-coordination modes. The solid-state structures have been established by means of single-crystal X-ray diffraction methods and are retained in solution as indicated by NMR spectroscopy. Both these isomers proved to be efficient (pre)catalysts of phosphine-free Heck cross-coupling of iodoarenes with olefins.

© 2021 The Author(s). Published by Elsevier Inc. This is an open access article under the CC BY license (<http://creativecommons.org/licenses/by/4.0/>).

1. Introduction

Palladacyclic complexes are a group of species of notably broad potential application as (pre)catalysts of cross-coupling reactions [1,2]. Amid the widespread research in the latter field, the Heck cross-coupling of aryl halides with alkene C(sp²)-H bonds has become an area of particular importance because of its unrivalled usefulness in preparation of π -conjugated systems [3]. As Heck reaction catalysts, *N,C(sp³)*-cyclopalladated species provide examples of unprecedented reactivity. While still not as well-known and explored as their C(sp²) counterparts, they are generally considered more active, thermally stable and easier to fine-tune by ligand modification [4]. Some examples of *N,C(sp³)*-cyclopalladated complexes of documented catalytic activity are presented in Fig. 1 [5–7].

Flexidentate pyridyl- β -diketones are well-known organic ligands, which have found many applications in different fields [8–10]. Their versatility results from their various coordination modes of bonding to metal ions in anionic, neutral and zwitterionic forms depending on the reaction conditions [11,12]. This feature means that in addition to forming simple mononuclear coordination compounds, other more sophisticated homo- and

heterometallic architectures, including polymers, cages or metal-organic frameworks can be generated [12–18,33,34]. Recently, we have successfully utilized ambidentate ligands of this type in complexes with Pd(II), Pt(II), Cu(I) and Cu(II) to provide a series of metallosupramolecular complexes with different levels of dynamicity and high catalytic activity in important processes such as the Suzuki-Miyaura, alkene hydrosilylation and Ullmann reactions [12,19–21]. There, the coordination to the metal ion has involved either *O,O'*-chelation of the β -diketone moiety or pyridyl-*N* donation or a combination of both. Linkage *via* the central C(sp³) carbon of acetylacetonate complexes is known for Pt(II) and Pd(II) ions [22–25], but no example of Pd(II) complexes based on pyridyl- β -diketonate ligands where bonding occurs both *via O,O'*-chelation and pyridyl-*N* and C(sp³) donation has yet been reported.

In this work, we have employed the 2,2-dimethyl-5-(2-pyridyl)pentane-3,5-dione ligand (HL) in which donor atoms are arranged in such a way that not only can they act as either an *O,O'*-donor or a simple *N*-donor but also as an *N,O*-donor and, after methylene deprotonation, as an *N,C*-donor [11,26]. To assess the prospect of the adoption of this last mode to give an organometallic species, a reaction of HL with Pd(II) was examined under basic conditions. In fact, this resulted in the formation of new PdL₂ coordination assembly of a unique organometallic nature as two geometric

E-mail address: ars@amu.edu.pl (A.R. Stefankiewicz)

<https://doi.org/10.1016/j.jcat.2021.11.033>

0021-9517/© 2021 The Author(s). Published by Elsevier Inc.

This is an open access article under the CC BY license (<http://creativecommons.org/licenses/by/4.0/>).

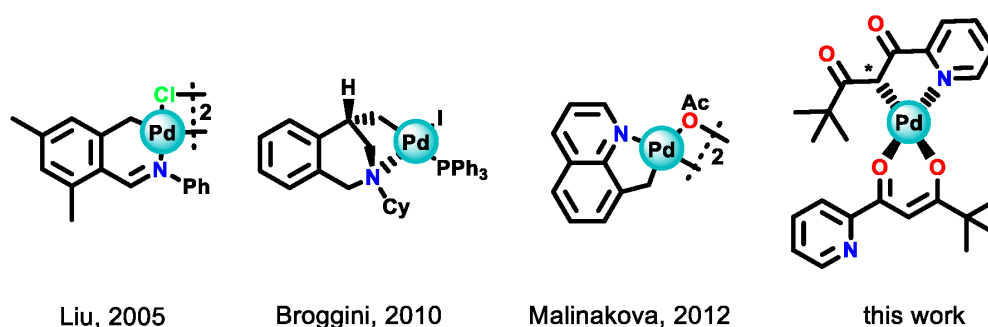


Fig. 1. Examples of catalytically active $N,C(sp^3)$ -cyclopalladated complexes [5–7].

isomers where one ligand L^- is bound as an O,O' -chelate and another as an $N,C(sp^3)$ -chelate in a single complex molecule. Their full structural and spectroscopic characterization in solid state as well as in solution and their physicochemical properties are described ahead. Establishment of their organometallic nature in conjunction with their high stability prompted us to evaluate their catalytic activity.

2. Results and discussion

The ligand HL was synthesized by a Claisen condensation involving the reaction of methyl picolinate with pinacolone in the presence of NaH [19–21]. Subsequently, HL was reacted with $PdCl_2$ in a 2:1 molar ratio in an environment of Na_2CO_3 , resulting in the formation of organometallic PdL_2 -type complexes in the form of *cis* and *trans* geometric isomers. Separation of these has been achieved by selective crystallization of the *trans* form and mechanical separation of the crystals in the case of the *cis* isomer (Fig. 2a). Slow evaporation of an *n*-hexane solution led to deposition of pure *trans*- PdL_2 . However, addition of small volume of chlorinated solvent (e.g. $CHCl_3$ or DCM) to the crystallization solution resulted in deposition of a mixture of *cis/trans* geometrical isomers. As yet, the pure form of *cis*- PdL_2 has not been isolated in quantities that could allow its full characterization in solution, despite a num-

ber of attempts. That basic reaction conditions do not lead to exclusive adoption of the O,O' -chelation mode by the deprotonated ligand L^- as seen with its 3- and 4-pyridyl isomers is presumably a consequence of the stability of the 5-membered C,N -chelate ring, which can be formed in this case [19]. The ease of formation of the L^- anion and its proximity to the pyridyl- N donor appear to favor the formation of a palladacyclic unit within the complexes. The structure of the two isomeric compounds was first established in the solid state *via* single crystal X-ray diffraction. Measurements based on NMR spectroscopy and mass spectrometry were used subsequently to characterize their composition and behavior in solution.

Crystals suitable for the X-ray structure determinations were obtained through slow evaporation from appropriate solutions, as indicated in Fig. 2bc. The *trans* isomer was the sole product isolated from *n*-hexane solution. This complex, crystallizing in the monoclinic space group $C2/c$, has a clearly distorted pseudo square-planar geometry of $Pd(II)$, with both ligand anions being chelated but in either N,C - or O,O' -modes, generating 5- or 6-membered rings respectively (Fig. 2b). While the $PdCNO_2$ unit is essentially planar, the differences between the donor atoms result in the coordination sphere showing a significant trapezoidal distortion from a square array. The $Pd-C$ distance (2.01 Å) is typical of such a bond [27,28]. The distal location of the *t*-butyl substituents

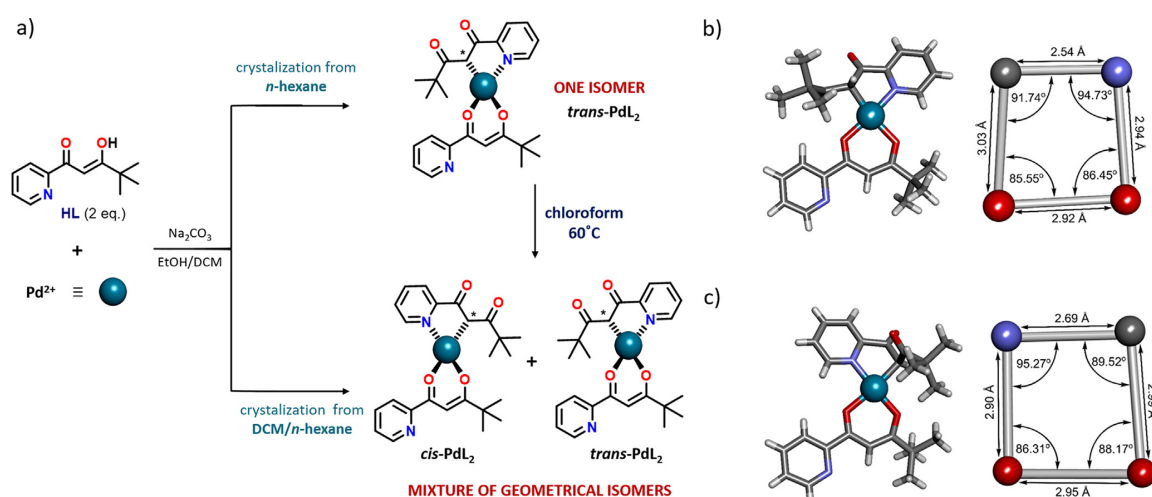


Fig. 2. a) Synthetic routes for the preparation of complexes: *cis*- and *trans*- PdL_2 ; X-ray structures and schematic representation of $Pd(II)$ coordination spheres for two isomers: b) *trans*- PdL_2 and c) *cis*- PdL_2 . The solvent molecule was omitted for clarity.

is the basis of its designation as the *trans* isomer. The carbon bound to Pd is asymmetric, meaning that the complex exists as two enantiomers, both of which are present in one crystal, as required by the space group designation. However, both enantiomeric forms are distributed over the one Pd site, creating disorder in the structure.

Single crystals of *cis*-PdL₂ could be selected mechanically from the mixture resulting from slow evaporation of an *n*-hexane/DCM solution. The complex crystallizes in the triclinic space group *P*-1 along with one *n*-hexane molecule in the unit cell. The coordination sphere of Pd(II) is almost the same as for *trans*-PdL₂, except that now the *t*-butyl substituents are proximal. Significant deviations from a true square planar geometry are again evident, as illustrated in Fig. 2c.

In solution, the complexes were characterized as pure *trans*-PdL₂ and the mixture of *cis/trans*-PdL₂. The molecular nature of the complexes has been unambiguously established via ESI-MS spectrometry (Fig. S6 and S10). All observed peaks are in good agreement with the theoretical isotope distribution, clearly indicating the protonation of the complex molecules of general formula PdL₂ (calcd. for [M+H]⁺: *m/z* = 515.1166; observed: *m/z* = 515.1186 and *m/z* = 515.1169, respectively for *trans*-PdL₂ and the mixture of *cis*- and *trans*-PdL₂). More specific characterization has been accomplished via NMR measurements (Fig. S1-S5 and S7-S9). As shown in the ¹H NMR spectra (Fig. 3), the structure established via XRD was retained in solution. In the case of *trans*-PdL₂, the duplication of aromatic signals H¹⁻⁴ is consistent with different coordination modes for the two ligand molecules, i.e. as *O,O'*- and *N,C*-chelates. The absence of an enol proton H⁸ signal in comparison to the ¹H NMR spectrum of non-coordinated ligand is consistent with the binding of one ligand unit in its enolate form (Fig. 3ab), while the residual methylene proton signal H⁶ of the

N,C-bound ligand is apparent near $\delta = 4.9$. The *trans* geometry was further confirmed by means of 1D NOESY spectra (Fig. S4-S5). The ¹H NMR spectrum of the *cis/trans* mixture showed two sets of signals of similar intensity, but subtraction of those due to the *trans* isomer enabled those of the *cis* to be readily identified. As both isomers have C₁ symmetry, the *t*-butyl groups in both are inequivalent and four distinct signals for these groups are apparent in the spectrum of the mixture, while signals due to the methylene protons of the two isomers (Fig. 3c and S7) are also clearly resolved. Signal integration showed that the *cis* and *trans* isomers, obtained as a result of crystallization from an DCM/*n*-hexane solution, were formed in a nearly 1:1 molar ratio (Fig. S7).

Equilibration of the isomeric complexes can be readily observed by heating a chloroform solution of *trans*-PdL₂ at 60 °C for 1 h (Fig. 3c and S11). Thus, the molar ratio at equilibrium at 60 °C was found to be close to 2:3 (*cis* to *trans*) and remains unchanged after cooling to room temperature. To explore the *cis/trans* isomerization, *trans*-PdL₂ was gradually heated and the changes were observed via ¹H NMR spectroscopy (Fig. S12). The percentage of *cis* isomer increased with temperature over the range 25 - 60 °C. At all times, the spectra could be interpreted in terms of contributions from just the two isomers and no intermediates were detected.

In view of the fact that cross-coupling reactions often require the presence of a base in the catalytic cycle, before undertaking research on the catalytic activity of these organometallic Pd(II) complexes, their stability in a basic medium was explored. An ¹H NMR titration was performed by sequentially adding portions of triethylamine (TEA). The cationic *N*-bound complexes of the 3- and 4-pyridyl isomers of HL are known to undergo rapid transformation to the *O,O'*-chelates on addition of base [19], but here, the

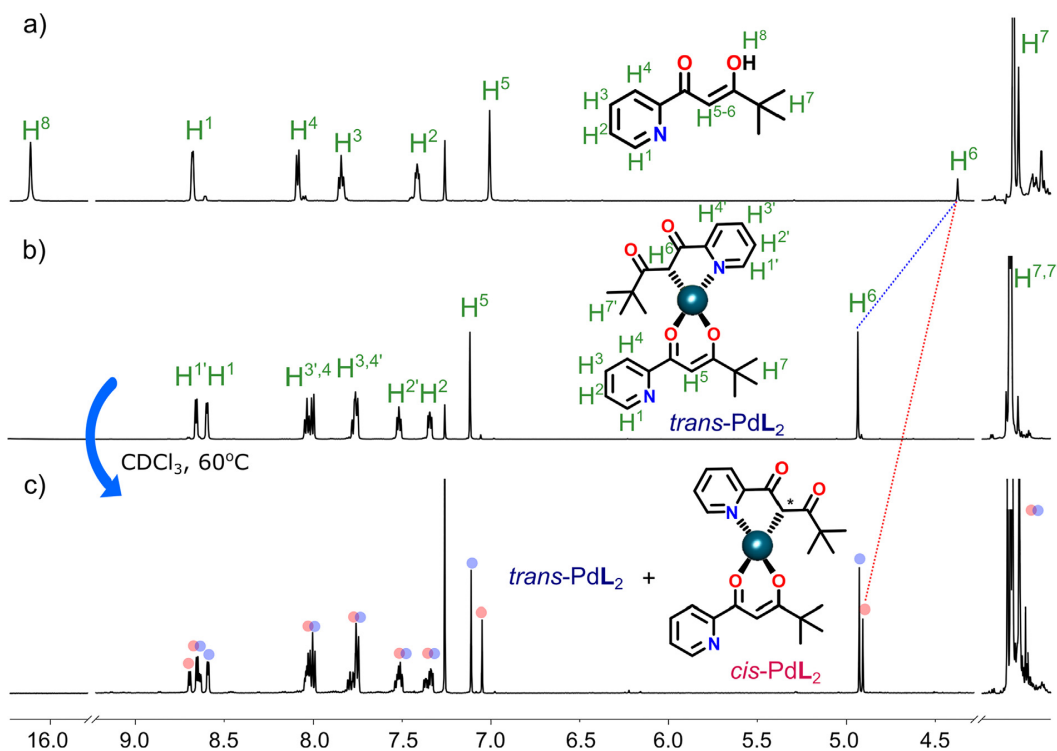


Fig. 3. The stacked ¹H NMR spectra (CDCl₃, 600 MHz) of: a) ligand HL; b) *trans*-PdL₂; c) the mixture of two isomers *cis*- and *trans*-PdL₂ (marked red and blue, respectively) after 1 h of heating.

N,C-bound ligand was completely unaffected, even after the addition of 6 equivalents of TEA (Fig. S13 and S14). Further, no evidence for the decomposition or transformation was found after heating the samples and storage for 7 days, demonstrating a considerable stability of both isomeric forms *cis*- and *trans*-PdL₂ in a basic environment. Furthermore, these palladacyclic complexes show high water and air stability exceeding two years of storage without any decomposition or loss of catalytic activity, which is beneficial in terms of their practical utility as catalyst precursors.

Thus, both the organometallic character of the complexes and their stability in the presence of a base were a premise of potential catalytic activity of PdL₂ in cross-coupling reactions. The Heck cross-coupling was chosen as a model reaction. The reaction system was comprised of equimolar amounts of 4-iodotoluene and styrene, PdL₂ catalyst and a base. 4-Bromotoluene did not undergo any transformation and thus, all further experiments were carried out using aryl iodides. The process of initial screening and optimization of reaction conditions is summarized in Table 1. The results of optimization show a slightly variable but high selectivity of the catalytic system containing PdL₂ towards formation of *trans* product **3aa**.

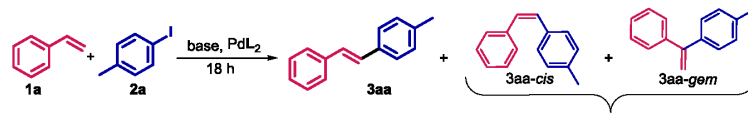
All bases that were used turned out to be effective, but Cs₂CO₃ and K₃PO₄ (entries 1 and 3, respectively) provided the best conversion and selectivity towards **3aa**, i.e. 4-methyl-*trans*-stilbene. The two minor products were identified as the other two possible isomers of **3aa**: the *cis* and the *gem* one. For further optimization, the latter was chosen, given its higher availability and much lower price, yet effectiveness comparable within the limits of measurement error. Out of curiosity, 1-aminopropan-2-ol was used as both a solvent and a base, but complete conversion of **2a** in such a system required the reaction to proceed for 18 h at 120 °C (entries 6 and 7). The two most suitable solvents were found to be 1,4-dioxane and *N,N*-dimethylformamide. Whereas in the case of reaction carried out in DMF it was possible to compensate for a decrease in the load of PdL₂ by increasing the overall concentration of the reaction mixture (entry 10), the same effect was not observed when 1,4-dioxane was used as a solvent (entry 9). Also,

the use of two alternative solvents, isopropanol (entry 11) and Cyrene™ (entry 12), lead to decrease in both conversion of styrene and selectivity towards the desired **3aa**. As a result, the conditions as in entry 10 were chosen for substrate scope determination. It is worth noting that no additive was needed to induce or maintain catalytic activity, however, reactions were successful only when dry solvents were used, although they did not require an inert gas atmosphere to proceed. It was also established that the mixture of PdL₂ isomers was catalytically active to the same extent as the pure *trans* isomer, which was not surprising given the observed thermal equilibration of both forms of this complex. Under the same conditions as established for PdL₂, the classical catalytic systems comprising of either 0.5 mol% Pd(dba)₂ / 2 mol% PPh₃ or 0.5 mol% [PdCl₂(PPh₃)₂] led to conversion of **3** of at most 80%. Similar effect was observed when PdCl₂ and **L** were used separately in an attempt to generate the PdL₂ (pre)catalyst in situ.

Next, groups of functionalized iodoarenes and olefins were reacted together to explore the capabilities of the PdL₂-based reaction system in terms of functional group tolerance.

Under the described conditions, it was possible to carry out successful Heck cross-coupling of all the reagents listed in Table 2. In all cases, selectivity of the formation of **3** was high to very high, ranging from 83% for **3ab** to 99% or more for **3ae**, **3ca** and **3da**. The reaction system exhibited also an excellent chemoselectivity towards iodoarenes, as no cross-coupling involving bromoarene moieties, both as olefin (**1e**) and haloarene (**2e**) coupling partners, was observed. Moreover, it was not hindered by either activating (**2a**, **2b**, **2f**) or deactivating (**2c**, **2d**, **2e**) substituents on the iodoarene molecules. The reaction of 2-vinylpyridine **1c**, despite very good selectivity, reached only a moderate conversion of 45% of its coupling partner **2a**, which was probably due to competitive formation of a stable palladacyclic intermediate with the pyridine *N*-atom coordinated to Pd(II) cation. In general, the unique properties of Pd(II) ions and the ligand **HL** engineering resulted in the formation of new *N,C*(sp³)-cyclopalladated complexes stable under air atmosphere and basic conditions, which allowed their application in catalysis. High reaction yields and excellent chemoselectivity

Table 1
Initial screening and optimization of the Heck cross-coupling reaction conditions using mixture of *cis* and *trans*-PdL₂.



	solvent	<i>c</i> _{1a} [M]	[Pd] [mol%]	byproducts Base (equiv.) ^a	<i>T</i> [°C]	conv. [%] ^b	3aa sel. [%] ^f
1	1,4-dioxane	0.5	1	Cs ₂ CO ₃ (2)	100	100	99
2	1,4-dioxane	0.5	1	K ₂ CO ₃ (2)	100	93	99
3	1,4-dioxane	0.5	1	K ₃ PO ₄ (2)	100	95	99
4	1,4-dioxane	0.5	1	Et ₃ N (2)	100	86	92
5	acetonitrile	0.5	1	K ₃ PO ₄ (2)	85	75	98
6	MIPA ^d	0.5	1	solvent	100	76	90
7	MIPA	0.5	1	solvent	120	100	89
8	DMF ^e	0.5	1	K ₃ PO ₄ (2)	100	100	94
9	1,4-dioxane	1	0.5	K ₃ PO ₄ (1)	100	54	99
10	DMF	1	0.5	K₃PO₄ (1)	100	100	98
11	<i>i</i> PrOH	1	0.5	K ₃ PO ₄ (1)	100 ^g	43	86
12	Cyrene™ ^g	1	0.5	K ₃ PO ₄ (1)	100	27	71
13	DMF	1	0.3	K ₃ PO ₄ (1)	100	53	97

^a relatively to **2a**.

^b determined by GC measurement of **2a** decay.

^c measured by GC-MS distribution of **3aa** isomers.

^d MIPA – 1-aminopropan-2-ol.

^e DMF – *N,N*-dimethylformamide.

^f reaction in a sealed Schlenk bomb flask.

^g Cyrene™ – dihydrolevoglucosenone.

Table 2
The substrate scope of the PdL₂-catalyzed Heck cross-coupling. Yields in parentheses are those of isolated compounds.

1	2	3	Conv. of 2	Yield of 3
Olefin 1	Aryl iodides 2	Product 3		
1			100%	98% (92%)
2			100%	83% (70%)
3			96%	86%
4			90%	85% (81%)
5			100%	99% (89%)
6			100%	93% (80%)
7			96%	86% (79%)
8			45%	44%
9			84%	84% (78%)
10			90%	86% (81%)
11			92%	88% (80%)
12			95%	92% (83%)
13			83%	91%

in cross-coupling reactions between olefins **1a–1f** and iodoarenes **2a–2f** revealed good catalytic properties of PdL₂ in the context of the literature [5–7].

3. Conclusions

In summary, we have synthesized two isomers of a novel Pd^{II}L₂ palladacyclic complex, in which two molecules of a flexidentate pyridyl β-diketonate ligand simultaneously coordinate to the metal center in two different modes – κ²O,O' and κ¹C,κ¹N. The *cis* and *trans*- forms of Pd^{II}L₂ were characterized spectroscopically in solution, as well as in the solid state by the means of XRD, although only the *trans* isomer has been isolated in pure form. A dependency

of *cis* to *trans* ratio on the selection of crystallization solvent has been also described. Both these N,C(sp³)-palladacyclic compounds were stable in basic environments and were applied as (pre)catalysts in the Heck cross-coupling reaction, which they have turned out to promote efficiently in loading as low as 0.5 mol% and without any auxiliary ligand additives. The Pd(II) complex described in this report is a great example of the unique family of catalytically active palladacyclic compounds and the first one in which a single flexidentate ligand provides sufficient stabilization of the Pd central atom throughout the whole catalytic cycle, leading to cross-coupling products obtained with excellent chemo- and stereoselectivity. Moreover, its straightforward preparation and bench-stability exceeding two years are a good premise of its prospective practical utility.

4. Experimental section

4.1. Materials and methods

Commercially available reagents, solvents and other chemicals were purchased from Sigma-Aldrich. NMR solvents were purchased from Deutero GmbH and used as received. The ^1H NMR and ^{13}C NMR spectra were acquired at 298 K on Bruker Fourier 300 MHz and Avance III HD 400 and 600 MHz spectrometers and referenced to the solvent residual peaks. All 2D NMR spectroscopic experiments were performed using standard pulse sequences from the Bruker pulse program library. ESI-MS spectra were recorded on Bruker Impact HD Q TOF spectrometer in positive ion mode. GC-MS analyses were performed on a Bruker Scion 436-GC with Scion SQ mass spectrometry detector. The ligand **HL** was prepared by Claisen condensation following a literature procedure [19,21].

4.2. X-ray crystallography

The structural studies for the complexes *cis*- and *trans*-PdL₂ were performed on an Oxford Diffraction SuperNova diffractometer equipped with a CCD detector and a Cryojet cooling system. X-ray data were collected at 130 K using graphite-monochromated Cu K α radiation source ($\lambda_{\alpha} = 1.54178 \text{ \AA}$) with the ω -scan technique. Data reduction, UB-matrix determination and absorption correction were performed with the CrysAlisPro software [29]. Using Olex2 [30], the structures were solved by direct methods with ShelXT [31] and refined by full-matrix least-squares against F² with the program SHELXL [32] refinement package based on Least Squares minimization. All non-hydrogen atoms were refined anisotropically. Some of the hydrogen atoms were located on a difference Fourier map and they were refined isotropically. The rest of the H-atoms were located in idealized positions by molecular geometry and refined as riding groups with $U_{\text{iso}}(\text{H}) = 1.2 U_{\text{eq}}(\text{C})$. Selected structural parameters are reported in Table S1. The data have been deposited in the Cambridge Crystallographic Data Collection (CCDC), deposition numbers CCDC 195840-195841. These data can be obtained free of charge via www.ccdc.cam.ac.uk/data_request/cif, or by emailing data_request@ccdc.cam.ac.uk, or by contacting The Cambridge Crystallographic Data Centre, 12, Union Road, Cambridge CB2.

4.3. Synthesis of complexes

***trans*-PdL₂**: Na₂CO₃ (31.8 mg, 0.3 mmol) dissolved in 0.5 mL H₂O was added to the solution of **HL** (41.2 mg, 0.2 mmol) in DCM/EtOH (1:1, v/v, 6 mL). The mixture was stirred for an hour at room temperature. Then, a suspension of PdCl₂ (17.7 mg, 0.1 mmol) in EtOH (6 mL) was added and the reaction was allowed to proceed for an additional 12 h. The resulting mixture was filtered and the filtrate was evaporated to dryness under reduced pressure. The crude product of *trans*-PdL₂ was redissolved in *n*-hexane (6 mL) and left for 12 h at room temperature. The crystals formed were centrifuged off, washed with *n*-hexane (10 mL) and dried in vacuo. Yield: 38.7 mg, 75%.

Mixture *cis*- and *trans*-PdL₂: The preparation of the mixed geometrical isomers *cis/trans* was analogous to the procedure described above. However, the crude product was redissolved in a mixture of DCM/*n*-hexane (1:1, v/v, 8 mL) and left for 12 h at room temperature. After, the resulting crystals were centrifuged off, washed with *n*-hexane (10 mL) and dried in vacuo. Yield: 42.3 mg, 82%.

4.4. General procedure of catalytic reactions

As a general remark, in a typical experiment, the (pre)catalyst was weighed first and the amounts of other components were adjusted accordingly. For initial experiments, new stirring bars were used for each reaction.

In a screw-cap vial, 2.3 mg (5 μmol) of PdL₂, 212.3 mg (1.0 mmol) of anhydrous K₃PO₄, and 1 mL of dry *N,N*-dimethylformamide were placed followed by 1.0 mmol of iodoarene and 1.0 mmol of alkene. A PTFE stirring bar was placed in the reaction mixture, the vial was closed tight and put in an oil bath. The reaction mixture was stirred for 18 h at 100 °C. Having cooled down, the reaction mixture was quenched with 1 mL of water and extracted with two 2 mL portions of *n*-hexane/chloroform (1:1 v/v). Gas chromatography samples were taken from combined organic phases which were next filtered through a bed of silica, evaporated and dried *in vacuo*. NMR analyses were carried out without further purification.

Declaration of Competing Interest

The authors declare that they have no known competing financial interests or personal relationships that could have appeared to influence the work reported in this paper.

Acknowledgements

The work was supported by the Polish National Centre grant: (A.R. S.) SONATA BIS 2018/30/E/ST5/00032. We thank Prof. Jack Harrowfield for helpful discussions during the manuscript preparations. AW and MZ are supported by the Foundation for Polish Science (FNP) START programme.

Author Contributions

The manuscript was written through contributions of all authors. All authors have given approval to the final version of the manuscript.

Appendix A. Supplementary material

Supplementary data to this article can be found online at <https://doi.org/10.1016/j.jcat.2021.11.033>.

References

- [1] P.Y. Choy, X. He, F.Y. Kwong, in: *Palladacycles*, Elsevier, 2019, pp. 21–173, <https://doi.org/10.1016/B978-0-12-815505-9.00003-2>.
- [2] W.A. Herrmann, V.P.W. Böhm, C.-P. Reisinger, *Application of palladacycles in heck type reactions*, *J. Organomet. Chem.* 576 (1–2) (1999) 23–41.
- [3] I.P. Beletskaya, A.V. Cheprakov, *The heck reaction as a sharpening stone of palladium catalysis*, *Chem. Rev.* 100 (8) (2000) 3009–3066.
- [4] G.C. Dickmu, I.P. Smoliakova, *Cyclopalladated complexes containing an (sp³)C–Pd bond*, *Coord. Chem. Rev.* 409 (2020) 213203, <https://doi.org/10.1016/j.ccr.2020.213203>.
- [5] C.-L. Chen, Y.-H. Liu, S.-M. Peng, S.-T. Liu, *An efficient catalyst for Suzuki–Miyaura coupling reaction in aqueous medium under aerobic conditions*, *Tetrahedron Lett.* 46 (3) (2005) 521–523.
- [6] E. Beccalli, E. Borsini, S. Brenna, S. Galli, M. Rigamonti, G. Broggin, σ -Alkylpalladium intermediates in intramolecular heck reactions: isolation and catalytic activity, *Chemistry – A European Journal* 16 (5) (2010) 1670–1678.
- [7] A. Shiota, H.C. Malinakova, *Palladacycles: effective catalysts for a multicomponent reaction with allylpalladium(II)-intermediates*, *J. Organomet. Chem.* 704 (2012) 9–16.
- [8] A.D. Burrows, M.F. Mahon, C.L. Renouf, C. Richardson, A.J. Warren, J.E. Warren, *Dipyridyl β -diketonate complexes and their use as metalloligands in the formation of mixed-metal coordination networks*, *Dalton Trans.* 41 (14) (2012) 4153–4163.
- [9] G.-L. Wang, Y.-J. Lin, H. Berke, G.-X. Jin, *Two-step assembly of multinuclear metallacycles with half-sandwich Ir, Rh, and Ru fragments for counteranion encapsulation*, *Inorg. Chem.* 49 (5) (2010) 2193–2201.

- [10] M. Dudek, J.K. Clegg, C.R.K. Glasson, N. Kelly, K. Gloe, A. Kelling, H.-J. Buschmann, K.A. Jolliffe, L.F. Lindoy, G.V. Meehan, Interaction of copper(II) with ditopic pyridyl- β -diketone ligands: dimeric, framework, and metallogel structures, *Cryst. Growth Des.* 11 (5) (2011) 1697–1704.
- [11] M. José Mayoral, P. Cornago, R.M. Claramunt, M. Cano, Pyridyl and pyridiniumyl β -diketones as building blocks for palladium(II) and allyl-palladium(II) isomers. Multinuclear NMR structural elucidation and liquid crystal behaviour, *New J. Chem.* 35 (5) (2011) 1020–1030.
- [12] A. Walczak, G. Kurpiak, A.R. Stefankiewicz, Intrinsic effect of pyridine-N-position on structural properties of Cu-based low-dimensional coordination frameworks, *Int. J. Mol. Sci.* 21 (17) (2020) 6171, <https://doi.org/10.3390/ijms21176171>.
- [13] G.-G. Hou, Y. Liu, Q.-K. Liu, J.-P. Ma, Y.-B. Dong, NbO lattice MOFs based on octahedral M(II) and ditopic pyridyl substituted diketone ligands: structure, encapsulation and guest-driven luminescent property, *Chemical Communication* 47 (38) (2011) 10731–10733.
- [14] H.-B. Wu, Q.-M. Wang, Construction of heterometallic cages with tripodal metallogel ligands, *Angew. Chem. Int. Ed.* 48 (40) (2009) 7343–7345.
- [15] P.C. Andrews, G.B. Deacon, R. Frank, B.H. Fraser, P.C. Junk, J.G. MacLellan, M. Massi, B. Mobaraki, K.S. Murray, M. Silberstein, Formation of HoIII trinuclear clusters and GdIII monodimensional polymers induced by ortho and para regioisomers of pyridyl-functionalised β -diketones: synthesis, structure, and magnetic properties, *Eur. J. Inorg. Chem.* 2009 (6) (2009) 744–751.
- [16] M. Wang, V. Vajpayee, S. Shanmugaraju, Y.-R. Zheng, Z. Zhao, H. Kim, P.S. Mukherjee, K.-W. Chi, P.J. Stang, Coordination-driven self-assembly of M3L2 trigonal cages from preorganized metallogel ligands incorporating octahedral metal centers and fluorescent detection of nitroaromatics, *Inorg. Chem.* 50 (4) (2011) 1506–1512.
- [17] K.V. Domasevitch, V.D. Vreshch, A.B. Lysenko, H. Krautscheid, Two-dimensional square-grid frameworks formed by self-associating copper(II) complexes with 1-(3-pyridyl)- and 1-(4-pyridyl)-substituted butane-1,3-diones, *Acta Crystallographica Section C* 62 (9) (2006) m443–m447.
- [18] M. Kotodziejski, A.J. Brock, G. Kurpiak, A. Walczak, F. Li, J.K. Clegg, A.R. Stefankiewicz, Charge neutral [Cu2L2] and [Pd2L2] metalocycles: self-assembly, aggregation, and catalysis, *Inorg. Chem.* 60 (13) (2021) 9673–9679.
- [19] A. Walczak, A.R. Stefankiewicz, pH-induced linkage isomerism of Pd(II) complexes: a pathway to air- and water-stable Suzuki–Miyaura-reaction catalysts, *Inorg. Chem.* 57 (1) (2018) 471–477.
- [20] A. Walczak, H. Stachowiak, G. Kurpiak, J. Kaźmierczak, G. Hreczycho, A.R. Stefankiewicz, High catalytic activity and selectivity in hydrosilylation of new Pt(II) metallocyclic complexes based on ambidentate ligands, *J. Catal.* 373 (2019) 139–146.
- [21] R.A.A. Abdine, G. Kurpiak, A. Walczak, S.A.A. Aeash, A.R. Stefankiewicz, F. Monnier, M. Taillefer, Mild temperature amination of aryl iodides and aryl bromides with aqueous ammonia in the presence of CuBr and pyridyldiketone ligands, *J. Catal.* 376 (2019) 119–122.
- [22] S. Baba, T. Ogura, S. Kawaguchi, Reactions of bis(acetylacetonato)palladium(II) with triphenylphosphine and nitrogen bases, *Bull. Chem. Soc. Jpn.* 47 (3) (1974) 665–668.
- [23] S.P. Khramenko, E.A. Bykova, S.A. Gromilov, M.R. Gallyamov, S.G. Kozlova, N.K. Moroz, S.V. Korenev, Novel mixed-ligand palladium complexes [Pd2(acac)3NO3] and [Pd(acac)NO3]n involving O- and γ -C-bonded acetylacetonate linkers, *Polyhedron* 31 (1) (2012) 272–277.
- [24] S.A. De Pascali, P. Papadia, A. Ciccarese, C. Pacifico, F.P. Fanizzi, First examples of β -diketonate platinum(II) complexes with sulfoxide ligands, *Eur. J. Inorg. Chem.* 2005 (4) (2005) 788–796.
- [25] S. Okeya, Y. Kawakita, S. Matsumoto, Y. Nakamura, S. Kawaguchi, N. Kanehisa, K. Miki, N. Kasai, C. O-chelates of the trifluoroacetylacetonate dianion with palladium(II), Molecular structure of [Pd(tfac(2-)-C, O)(PPh3)(2,6-Me2-py)], *Bull. Chem. Soc. Jpn.* 55 (7) (1982) 2134–2142.
- [26] S. Maggini, P.S. White, [μ -1,3-Dioxo-1,3-bis(pyridin-2-yl)propane-2,2-diido- κ N, C; κ C, N']bis[(1,3-diphenylpropane-1,3-dionato- κ O, O')palladium(II)](Pd-Pd), *Acta Crystallographica Section E, Structure reports online* 67 (Pt 6) (2011) m749–50.
- [27] J. Spencer, M. Pfeffer, N. Kyritsakas, J. Fischer, Regioselectivity of the insertion of 4,4-dimethyl-2-pentyne into the Pd-C bond of cyclopalladated complexes, *Organometallics* 14 (5) (1995) 2214–2224.
- [28] Y. Wang, Y.u. Chen, Z. Jiang, F. Liu, F. Liu, Y. Zhu, Y. Liang, Z. Wu, Halogen effects on phenylethynyl palladium(II) complexes for living polymerization of isocyanides: a combined experimental and computational investigation, *Sci. China Chem.* 62 (4) (2019) 491–499.
- [29] O.D. CrysAlisPRO, P.R.O. Agilent CrysAlis, A.T. Ltd, Yarnton, Oxfordshire, England, 2014.
- [30] O.V. Dolomanov, L.J. Bourhis, R.J. Gildea, J.A.K. Howard, H. Puschmann, OLEX2: a complete structure solution, refinement and analysis program, *J. Appl. Crystallogr.* 42 (2) (2009) 339–341.
- [31] G. Sheldrick, SHELXT - Integrated space-group and crystal-structure determination, *Acta Crystallographica Section A* 71 (1) (2015) 3–8.
- [32] G. Sheldrick, Crystal structure refinement with SHELXL, *Acta Crystallographica Section C* 71 (1) (2015) 3–8.
- [33] A. Brzechwa-Chodzyńska, W. Drożdż, J. Harrowfield, A.R. Stefankiewicz, *Coord. Chem. Rev.* 434 (2021) 2138202.
- [34] A. Brzechwa-Chodzyńska, M. Zieliński, M. Gilski, J.M. Harrowfield, A.R. Stefankiewicz, *Inorg. Chem.* 59 (2020) 8552–8561.

Crafting Versatile Modes of Pt(II) Complexes with Flexidentate Pyridyl- β -diketones: Synthesis, Structural Characterization, and Catalytic Behavior in Olefin Hydrosilylation

Gracjan Kurpik,^[a, b] Anna Walczak,^[a, b] Igor Łukasik,^[a, b] Zuzanna Matela,^[a, b] and Artur R. Stefankiewicz*^[a, b]

Cycloplatinated complexes, with their high reactivity, combined with the capability to tailor ligands for specific catalytic processes, play a pivotal role in materials science and coordination chemistry, serving as versatile catalysts for applications in the organic synthesis of industrially relevant processes. In this report, we describe the synthesis and characterization of a new family of Pt(II) complexes based on three isomeric pyridyl- β -diketones diversified in terms of *N*-atom location in the heterocyclic ring. By appropriate control of the reaction conditions, we were able to generate distinct coordination

species, featuring ligands arranged as *N,C*(*sp*³)- and *N,O*-chelates, as well as simple pyridyl-*N* donors. Various analytical techniques, including X-Ray diffraction, NMR spectroscopy and ESI-MS spectrometry enabled the characterization of different coordination modes of the central atoms and unambiguously established the complex structures. Furthermore, all the Pt(II) coordination units have been found to be highly active and selective catalyst precursors in the hydrosilylation reactions within a broad scope of olefins with hydrosilanes.

Introduction

The coordination chemistry of platinum offers unique opportunities for the design of novel mononuclear complexes and more sophisticated architectures for prospective practical applications.^[1] The ability to access a wide range of redox states, coordination numbers, and geometries of the central atom leads to structural diversity within these systems, resulting in a broad spectrum of physicochemical properties.^[2] In its divalent oxidation state, platinum is classified as one of the softest metal centers, displaying a preference for bonding with soft bases, e.g. phosphines, thiolates or alkyl ligands.^[3] Pt(II) complexes are most commonly associated with a square-planar geometry, known for their high kinetic inertness.^[4] They have attracted considerable attention due to their remarkable properties, which include cytotoxicity, catalytic activity and luminescence. These attributes render them valuable in various real-world

applications.^[5] For instance, Pt-based compounds, notably cisplatin, carboplatin and multiple derivatives, have proven to be effective chemotherapeutic drugs widely used in the treatment of various cancers.^[6] Additionally, several Pt(II) complexes have been shown to have high catalytic activity in industrially important processes,^[7] including hydrosilylation, hydrogenation, and hydroformylation.^[8] Nonetheless, a range of disadvantages of Pt(II) catalysts, such as low stability, sensitivity to environmental conditions, susceptibility to catalyst poisoning, or a lack of selectivity in specific reactions, still limit their significant application potential.^[6c,9] To overcome these drawbacks, new design strategies are essential for crafting compounds with desirable properties and specific activity. In the realm of modern catalysis using precious metals, the quest is to reduce noble metal consumption, eliminate by-products in catalytic processes, simplify catalyst preparation, and, above all, facilitate the transition from a laboratory scale to industrial production.

In this work, we employed pyridyl- β -diketones HL1-HL3, differentiated by the location of pyridine-*N* donors with respect to the β -diketone moiety, to generate a new series of Pt(II) complexes C1-C6. We utilized both the neutral and deprotonated (diketonate) forms of HL1-HL3. Given their heterotopic nature and the unique characteristics of Pt(II), we expected these ligands to adopt coordination modes distinct from those seen with lighter transition metals.^[10] The influence of the pyridine-*N*-position on physicochemical properties and catalytic activity has already been demonstrated for Pd(II) and Cu(II) complexes. This results in diverse coordination assemblies in terms of charge, composition, and dimensionality, albeit with a common preference for either the deprotonated pyridyl-diketone binding as an *O,O*-chelate, or the neutral ligand binding via *N*-donors.^[10a-b] Here, we have found that while all

[a] G. Kurpik, A. Walczak, I. Łukasik, Z. Matela, Prof. A. R. Stefankiewicz
Center for Advanced Technology
Adam Mickiewicz University
Uniwersytetu Poznańskiego 10, 61-614 Poznań (Poland)
E-mail: ars@amu.edu.pl

[b] G. Kurpik, A. Walczak, I. Łukasik, Z. Matela, Prof. A. R. Stefankiewicz
Faculty of Chemistry
Adam Mickiewicz University in Poznań
Uniwersytetu Poznańskiego 8, 61-614 Poznań (Poland)

Supporting information for this article is available on the WWW under <https://doi.org/10.1002/cctc.202301465>

© 2023 The Authors. ChemCatChem published by Wiley-VCH GmbH. This is an open access article under the terms of the Creative Commons Attribution Non-Commercial License, which permits use, distribution and reproduction in any medium, provided the original work is properly cited and is not used for commercial purposes.

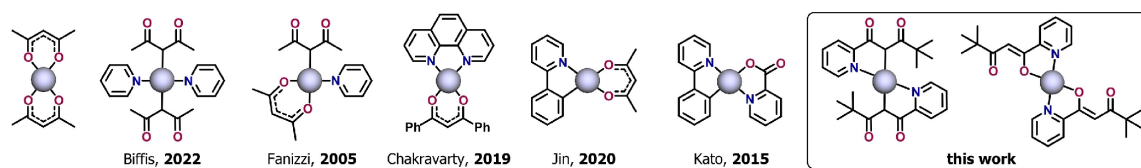


Figure 1. Different variants of coordination in Pt(II) complexes with *N*- and *O*-donor ligands incorporating acetylacetonate and pyridine moieties.^[11a–d,12]

three ligands can be used in their neutral forms to give *N*-bound complexes, in their deprotonated forms the coordination chemistry becomes more complex. Even in the case of simple ligands, such as derivatives of acetylacetonate and pyridine (constituents of the investigated ligands), Pt(II) ions show a tendency to create unconventional combinations, including organometallic bonding, which leads to uncommon entities (Figure 1).^[11] Thus, the incorporation of distinct coordination sites within a single ligand structure results in the formation of unique *N,C(sp³)*- and *N,O*-chelates, a possibility exclusive to $L1^-$. In contrast to heteroleptic complexes, they represent the first examples of such an arrangement achieved within homoleptic species. Their structures have been unequivocally established in solution by means of NMR spectroscopy and ESI-MS spectrometry, and, in the case of **C1**, in the solid state via X-ray diffraction. With the expectation that the compositional and structural differences could directly affect chemical properties, we assessed their catalytic activity in the olefin hydrosilylation reaction, resulting in the development of a new family of efficient and selective catalyst precursors suitable for a broad scope of substrates. Despite using the same components to construct the Pt(II) complexes, we have demonstrated how to achieve enhanced catalytic efficiency through controllable manipulations of the coordination mode.

Results and Discussion

Synthesis

The ligands HL1–HL3, 2,2-dimethyl-5-(2-, 3- or 4-pyridyl)pentane-3,5-dione, were prepared via a Claisen condensation between methyl esters of appropriate pyridinecarboxylic acids and pinacolone in the presence of a strong base (NaH) by adapting a previously reported procedure.^[10b,13] Due to the different positions of the *N*-donor atoms, complexation reactions with Pt(II) cations were expected to yield different coordination modes. Indeed, the reaction of the ligands HL1–HL3 with PtCl₂ resulted in a variety of species with unlike coordination environments (Figure 2). To achieve specific coordination modes, synthetic procedures, varied in regard to stoichiometry, pH, solvent and temperature, were employed. The complexes **C1**–**C2**, based on HL1, were synthesized after prior ligand deprotonation under basic conditions (Na₂CO₃). These species, of a common formula Pt(L1)₂, were obtained but the use of different reaction media led to the formation of *N,C(sp³)*- or *N,O*-chelates in the mixed solvent EtOH/DCM or

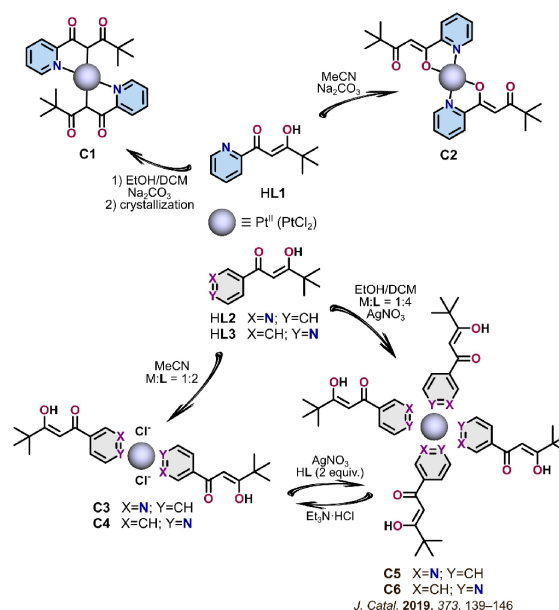


Figure 2. General reaction scheme for the synthesis of the Pt(II) complexes **C1**–**C6** based on pyridyl- β -diketonate ligands HL1–HL3.

pure MeCN, respectively. The complex **C1**, due to its isolation by fractional crystallization, was obtained in a yield of only 17%, whereas **C2** was isolated with a much higher yield of 64%. Interestingly, these 5-membered chelate ring coordination modes were only possible for the ligand $L1^-$ and appeared to be favored over 6-membered diketonate ring formation, previously observed for the Pd analogues.^[10b] The neutral ligands HL2 and HL3 readily provided complexes [Pt(HL)₂Cl₂] and [Pt(HL)₄](NO₃)₂, coordinated exclusively by the pyridyl-*N* donors (Figure 2). To obtain the disubstituted neutral species **C3**–**C4**, the complexation reactions were carried out in MeCN at 90 °C using ligand HL2 or HL3 and PtCl₂ in an exact 2:1 molar ratio, giving the desired species in 81% and 67% yields, respectively. In both cases, only *trans* products were isolated. As previously reported,^[14] the cationic compounds **C5**–**C6** were prepared by reacting PtCl₂ with 4 equiv. of either HL2 or HL3 in EtOH/DCM, with the addition of AgNO₃ to displace chlorido ligands. These two species are readily interconvertible, as the reaction of the tetrakis complexes with chloride ions leads to the bis species, which can be converted back to the tetrakis form by reaction with an additional portion of free ligand in the

presence of AgNO_3 (see SI, Figure S11–12). Despite considerable effort, the complexes obtained from reactions of PtCl_2 with HL2 and HL3 under basic conditions have not been fully characterized. The products appear to be inseparable mixtures and are certainly not *O,O*-diketonate chelates. It has long been known that, while it is possible to prepare the diketonate complex $[\text{Pt}(\text{acac})_2]$ (acac = 2,4-pentanedionate) where the ligand binds as an *O,O*-chelate, it readily converts to species where the diketonate is bound through the central C-donor,^[12,15] reaction with pyridine, for example, providing an equilibrium mixture of $[\text{Pt}(\gamma\text{-acac})_2(\text{py})_2]$ and $[\text{Pt}(\text{O},\text{O}'\text{-acac})(\gamma\text{-acac})(\text{py})]$.^[16] Presuming that similar chemistry could arise with both L2^- and L3^- , this raises the prospect that the ligands might function as bridging species, giving rise to oligomeric mixtures.

X-ray structure determination

The reaction of PtCl_2 with HL1 carried out in the mixed solvent EtOH/DCM produced a crude mixture of **C1** and **C2** (see SI, Figure S1) and isolation of pure **C1** proved challenging, with fractional crystallization being the only effective method. High-quality single crystals of **C1** suitable for the X-ray structural determination were successfully obtained by slow diffusion of *n*-hexane vapors into a solution of crude mixture in DCM. Detailed crystal and structure refinement data are presented in the SI (see Table S1). In **C1**, which crystallizes in the triclinic space group *P*-1, Pt(II) exhibits a distorted square-planar coordination geometry, with two ligand anions chelated in an *N,C*(sp^3)-mode, forming 5-membered rings (Figure 3a). The complexation reaction resulted in the generation of two stereogenic centers but in the solid state, only one stereoisomer of **C1** was detected, likely due to the bulky nature of the substituents on the ligand, forcing their positions to be in opposing orientations, ultimately giving the *meso* form. The PtC_2N_2 unit displays a *trans* configuration and is nearly planar, although significant deviations from the ideal square geometry of the

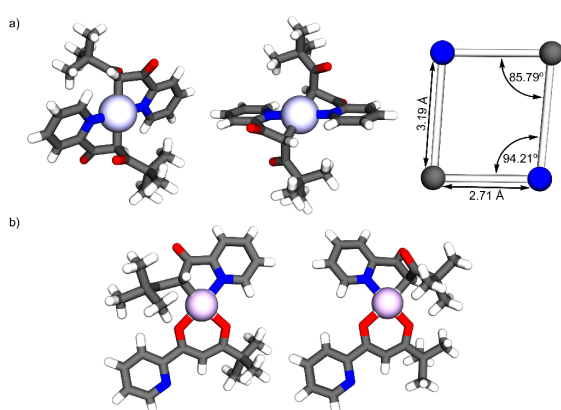


Figure 3. The X-ray structures of the organometallic species based on HL1: a) Pt(II) complex **C1**; b) analogous Pd(II) compounds in the form of *cis* and *trans* geometric isomers reported previously.^[10c] The solvent molecules were omitted for clarity.

Pt(II) ion are observed, resulting from differences in Pt–N and Pt–C bond lengths, as well as the spanning of two edges by chelation. These deviations are apparent in both edge dimensions ($2.71 \times 3.19 \text{ \AA}$), as well as N–C–N and C–N–C angles (85.79° and 94.21°). The crystal structure of **C1** reveals the flexidentate nature of HL1, as evidenced by the orientation of the β -diketone units perpendicular to the complex plane. It is worth emphasizing that, in contrast to **C1**, the ligand HL1 adopts quite different arrangements in the structure of Pd(II) analogues, serving as both *O,O'*- and *N,C*(sp^3)-chelating units within a single complex molecule.^[10c] This arrangement results in the formation of two stereoisomeric *cis*- and *trans*-Pd(L1)₂ complexes of PdCNO₂ coordination environment (Figure 3b).

NMR spectroscopy

Due to keto-enol tautomerism, the pyridyl- β -diketonate ligands HL1–HL3 can exist in two forms in solution.^[10a–b,14] For instance, in the ¹H NMR spectrum of HL1 recorded in CDCl₃ (Figure 4a), the dominant form in this solvent is the enol tautomer (~92%), while the presence of diketone is indicated by the weak signal H⁵ near 4.4 ppm. Given the significant contribution of the enol tautomer, any shift changes in the spectra of the complexes have been attributed solely to the corresponding signals of ligands in this form.

The complex **C1** has been characterized in solution via NMR spectroscopy and ESI-MS spectrometry. As seen in the ¹H NMR spectrum (Figure 4b), the structure of the complex established by XRD measurement was retained in solution. A single set of signals indicates the symmetrical arrangement consistent with the same coordination mode of two ligand molecules. The absence of the enol proton signal H⁷, in comparison to the ¹H

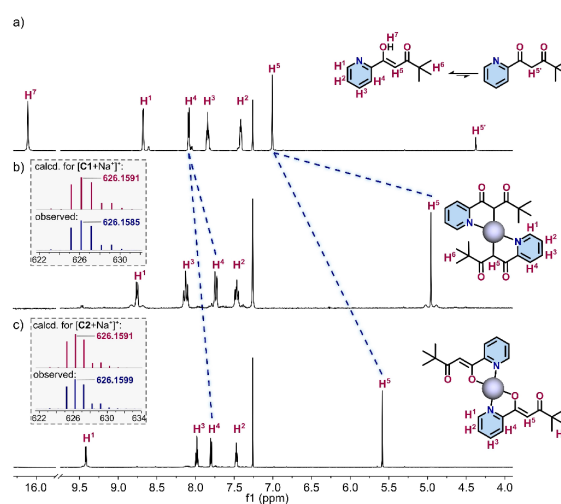


Figure 4. The stacked part of ¹H NMR spectra (600 MHz, CDCl₃) of the ligand HL1 (a) and its Pt(II) complexes coordinated in different modes – **C1** (b) and **C2** (c). Inset: ESI-MS spectra of **C1** (b) and **C2** (c), showing the calculated isotope model (top) and observed data (bottom).

NMR spectrum of the free ligand (Figure 4a), reflects the ligand's coordination after deprotonation. Additionally, the methine proton signal H^5 is significantly upfield shifted by ~ 2.0 ppm compared to the corresponding signal of HL1. Notable shifts in the aromatic proton signals H^{1-4} are also observed, particularly well-marked in the positions of the protons H^3 and H^4 , which appear in the spectrum of **C1** in the reverse order compared to HL1. Considering the crystal structure and the high symmetry of the ^1H NMR spectrum, the exclusive presence of the complex **C1** in the *meso* form could be confirmed, thus excluding the existence of other stereoisomers in solution.

The ^1H NMR spectrum of the bulk product obtained from the synthesis in EtOH/DCM (see SI, Figure S1) revealed the presence of two dominant species, subsequently identified as **C1** and **C2** after the fractional crystallization of the mixture and independent synthesis of **C2**. In the ^1H NMR spectrum of **C2**, the absence of the enol proton signal H^7 near 16.0 ppm indicated that Pt(II) complexation had led to the deprotonation of the diketone moiety (Figure 4c). Notably, there were clear shifts in the signals, particularly evident for the methine proton H^5 , which was up-shifted by 1.5 ppm in comparison to the corresponding signal of uncoordinated HL1. A significant downfield shift of ~ 0.7 ppm in the aromatic proton signal H^1 , relative to that of the free ligand, established the involvement of the pyridine-*N* in Pt(II) complexation. Given the proximity of the keto-enolate moiety to the pyridyl-*N* donor atom, these observations are consistent with *N,O*-chelation in this case. ESI-MS analysis also confirmed the successful generation of the desired complexes with the general formula $\text{Pt}(\text{L1})_2$ (Figure S3 and S6). All the observed peaks were in good agreement with the calculated isotope distribution, allowing the composition of the complexes to be unambiguously established (calcd. for $[\text{M} + \text{Na}]^+$: $m/z = 626.1591$; observed: $m/z = 626.1585$ and $m/z = 626.1599$, respectively for **C1** and **C2**).

The ^1H NMR spectra of the bis- and tetrakis complexes **C3**–**C6** were relatively straightforward to assign, the data for **C5**–**C6** being consistent with those previously reported.^[14] In the spectra of the complexes derived from HL3, for example (Figure 5), it was evident that the β -diketonate units remained non-coordinated, as indicated by the presence of the signal for the enol protons H^5 . While the shifts in the signals for the protons H^{2-5} were minor, the coordination of pyridine-*N* was evident in the pronounced downfield shifts for H^1 and the significant shift differences compared to the spectrum of the free ligand ($\Delta\delta = 0.35$ and 1.05 ppm, respectively for **C4** and **C6**). Similar effects were observed in the spectra of complexes **C3** and **C5**, derived from ligand HL2 (see SI, Figure S7). ESI-MS spectrometry also confirmed the successful generation of the desired mononuclear units (Figure S9–S10). All the observed peaks were in good agreement with the theoretical isotope distribution, providing explicit evidence for the formation of the complex molecules of general formulas $[\text{Pt}(\text{HL})_2\text{Cl}_2]$ and $[\text{Pt}(\text{HL})_4](\text{NO}_3)_2$.

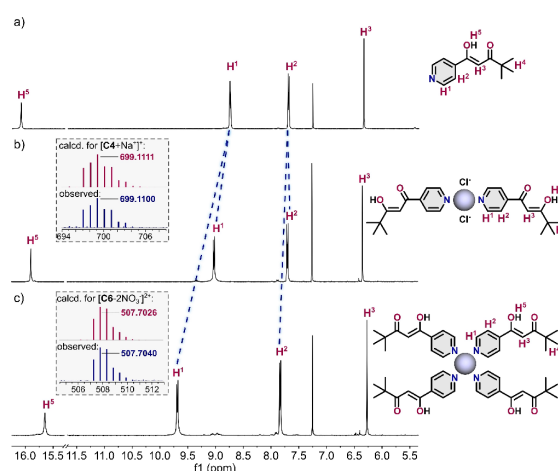


Figure 5. Part of the stacked ^1H NMR spectra (600 MHz, CDCl_3) of the ligand HL3 (a) and its di- and tetra-substituted Pt(II) complexes – **C4** (b) and **C6** (c). Inset: ESI-MS spectra of **C4** (b) and **C6** (c), showing the calculated isotope model (top) and observed data (bottom).

Catalytic studies

Complexes **C5**–**C6** have demonstrated their potential as precursors for active and highly selective precatalysts in olefin hydrosilylation with a broad range of substrates.^[14] They constitute the first example of Pt(II) compounds based on pyridyl- β -diketonate ligands ever applied in this catalytic reaction. The high efficiency of **C5**–**C6**, comparable to commonly used Pt species such as Karstedt's catalyst, prompted us to expand this family with new complexes featuring ambidentate units. It was anticipated that these new complexes, involving a new type of organometallic system, might exhibit even greater catalytic activity in the hydrosilylation reaction. Thus, this study was undertaken to assess and compare the catalytic properties of **C1**–**C6**, with the expectation that the variations in structure and composition could lead to further improvement in catalyst performance.

Initial studies utilized the organometallic complex **C1** to determine the optimal conditions for catalyzing the hydrosilylation reaction between dimethylphenylsilane and 1-octene in equimolar amounts. The highest catalytic activity was achieved in toluene at 80 °C, using a Pt(II) complex loading of 0.001 mol%. All attempts to reduce the catalyst concentration or lower the reaction temperature resulted in decreased conversions, though always with high regioselectivity for the β -addition product. The process of initial screening and optimization of reaction conditions is summarized in Table S2.

Under these optimal conditions, successful hydrosilylation reactions were carried out with 1-octene and styrene, representing aliphatic and aromatic olefins, using various structurally distinct hydrosilanes. The bulk of our experiments were based on complexes **C1**, **C2**, **C4**, and **C6** applied as precatalysts. **C3** was of limited utility due to its very low solubility in toluene, resulting in significantly reduced reaction yields ($< 10\%$ in most

cases). Additionally, structural isomers **C5** and **C6** showed essentially identical reactivity, so only data for the latter are provided. In all cases, the hydrosilylation products were formed in good to excellent isolated yields, ranging from 60% to 97%, and not significantly dependent on the specific nature of the alkene or hydrosilane (Figure 6). High efficiency was noted for hydrosilanes functionalized with alkoxy groups (**1d**, **1e**, **2e**) or compounds containing more than one Si–H bond (**1g**, **1h**), with reaction times longer than an hour being necessary in only a few cases. All catalytic systems exhibited excellent regioselectivity toward *anti*-Markovnikov addition, as confirmed by GC-MS analysis and NMR spectroscopy. β -addition products were strongly favored, with α -addition products detected in only two cases, for **2e** and **2f**.

While all the Pt(II) precursors exhibited high catalytic activity, their structural diversity resulted in minor variations in the obtained reaction yields. Based on GC conversion or NMR

yields, the most efficient catalyst was found to be the organometallic complex **C1**, closely followed by **C2**. However, in several cases, a noticeable decrease in the activity of **C4** and **C6** was observed. The lower catalytic activity of these complexes might be attributed to the coordination of four ligands, potentially resulting in increased steric hindrance. Consequently, the catalytic sites within their structure are less accessible when compared to the disubstituted species. Furthermore, we considered the electronic environment of metal centers within the structures of **C1**–**C6**, proposing that the pivotal factor influencing the diverse catalytic properties could be the direct involvement or absence of the β -diketone moiety in the complexation of Pt(II) ions. In the case of **C1** and **C2**, the deprotonated β -diketonate units actively participate in coordination, whereas they remain non-coordinated for **C3**–**C6**. Additionally, due to the electron-withdrawing nature of this group, they weaken the bonds between Pt(II) and pyridine-*N* donors. Therefore, the electron density on the metal centers significantly increases upon complexation with **HL1**, leading to higher reactivity of **C1** and **C2** and contributing to the enhancement in their catalytic efficiency. Given the low catalyst loading, excellent reaction yields, and outstanding selectivity in comparison with the previously reported complexes like **C5**–**C6** and many other Pt catalysts,^[9,17] the exceptional performance of the new species based on **HL1**, specifically **C1** and **C2**, underscores their significant potential for broader applications in the hydrosilylation reaction.

Among the mechanisms proposed in the literature for the hydrosilylation reaction catalyzed by Pt(II) complexes, the Chalk-Harrod catalytic cycle, involving Pt(II/IV) species, is widely recognized and generally accepted.^[8a,17a,18] It proceeds through the oxidative addition of the Si–H bond to the metal center, followed by the insertion of olefin into the metal hydride. As a consequence, an active Pt(IV) species is generated as an intermediate, which then undergoes reductive elimination. This step results in the formation of an organosilicon compound as the final product and the regeneration of the Pt(II) complex. This mechanism adheres to the *anti*-Markovnikov rule, consistent with the obtained results.

Conclusions

In summary, we have successfully synthesized a novel family of complexes by harnessing Pt(II) in combination with three isomeric pyridyl- β -diketone ligands. These species were characterized through a variety of spectroscopic techniques, both in solution and, in the solid state, as exemplified by **C1**'s X-ray structure determination. This work demonstrates the profound impact that variations in the *N*-atom position within the heterocyclic ring can exert on the coordination modes adopted by the central metal atom. Through precise manipulation of reaction conditions, we successfully isolated various coordination species, wherein these versatile ambidentate ligands function as simple *N*-donors or *N,C*(*sp*²)- and *N,O*-chelates, which constitute the first examples of such coordination modes achieved within a single ligand. Most notably, all these

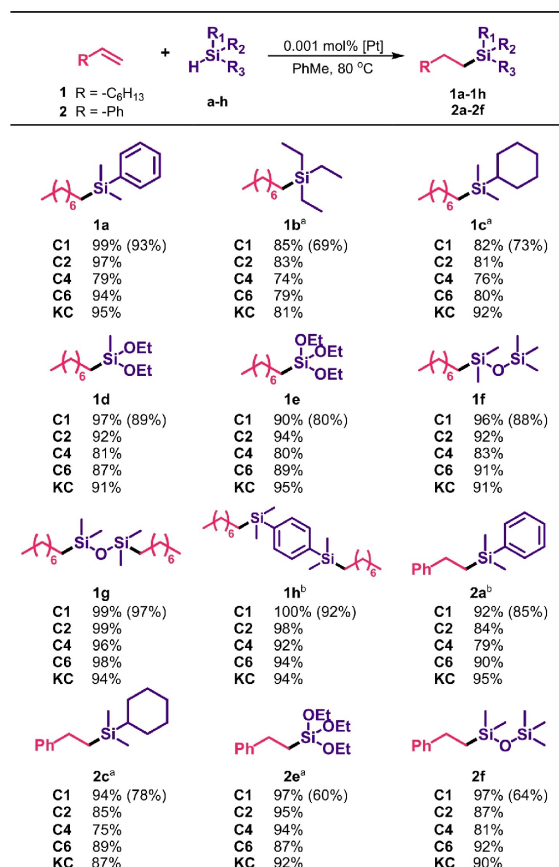


Figure 6. The scope of the olefin hydrosilylation reaction catalyzed by the complexes **C1**–**C6** and the Karstedt's catalyst (**KC**). Reaction conditions: olefin (0.5 mmol), hydrosilane (0.5 mmol), catalyst (0.001 mol%) in PhMe (1 mL) at 80 °C for 1 h. Yields determined by GC-MS measurements or NMR spectroscopy using 1,3,5-trimethoxybenzene as internal standard. The yields in parentheses are those of the isolated compounds. (a) The reactions were performed for 6 h. (b) 1.0 mmol of olefin was used.

complexes have proven to be exceptional catalysts for hydrosilylation reactions, exhibiting remarkable catalytic performance and regioselectivity. This is particularly pronounced in the case of C1 and C2, underscoring the significance of the organometallic nature or neutral character in catalytic enhancement. In comparison to numerous other Pt(II) catalysts reported in the literature, these complexes feature straightforward preparation, very low catalyst loading (0.001 mol%), and adaptability in combination with a wide range of structurally distinct reagents. These complex characteristics hold the promise of applications in materials chemistry, particularly in the production of intricate organosilicon compounds.

Supporting Information

The authors have cited additional references within the Supporting Information.^[19]

Deposition Number(s) 2304804 (for C1) contain(s) the supplementary crystallographic data for this paper. These data are provided free of charge by the joint Cambridge Crystallographic Data Centre and Fachinformationszentrum Karlsruhe Access Structures service.

Author Contributions

All authors have given approval to the final version of the manuscript.

Acknowledgements

The work was supported by the Polish National Centre (grant PRELUDIUM 2022/45/N/ST4/00518 – GK). GK is a scholarship holder of the Adam Mickiewicz University Foundation for the academic year 2023/2024.

Conflict of Interests

There are no conflicts to declare.

Data Availability Statement

The data that support the findings of this study are available from the corresponding author upon reasonable request.

Keywords: Pt(II) complexes · pirydył-β-diketones · coordination compounds · Pt catalysts · hydrosilylation

- [1] a) T. Sawada, M. Yoshizawa, S. Sato, M. Fujita, *Nat. Chem.* **2009**, *1*, 53–56; b) F. Ibukuro, T. Kusakawa, M. Fujita, *J. Am. Chem. Soc.* **1998**, *120*, 8561–8562; c) J. Brooks, Y. Babayan, S. Lamansky, P. I. Djurovich, I. Tsyba, R. Bau, M. E. Thompson, *Inorg. Chem.* **2002**, *41*, 3055–3066; d) L. Bai, C.

- Gao, Q. Liu, C. Yu, Z. Zhang, L. Cai, B. Yang, Y. Qian, J. Yang, X. Liao, *Eur. J. Med. Chem.* **2017**, *140*, 349–382.
 [2] V. Brabec, O. Hrabina, J. Kasparkova, *Coord. Chem. Rev.* **2017**, *351*, 2–31.
 [3] M. L. Clarke, *Polyhedron* **2001**, *20*, 151–164.
 [4] a) M. Melnik, C. E. Holloway, *Coord. Chem. Rev.* **2006**, *250*, 2261–2270; b) C. E. Holloway, M. Melnik, *Rev. Inorg. Chem.* **2004**, *24*, 135–299; c) C. Holloway, M. Melnik, *Open Chemistry* **2011**, *9*, 501–548.
 [5] a) P. Rios, A. Rodriguez, S. Conejero, *Chem. Commun.* **2020**, *56*, 5333–5349; b) Y.-X. Jia, B.-B. Li, Y. Li, S. A. Pullarkat, K. Xu, H. Hirao, P.-H. Leung, *Organometallics* **2014**, *33*, 6053–6058; c) A. E. Patterson, J. J. Miller, B. A. Miles, E. L. Stewart, J.-M. E. J. Melanson, C. M. Vogels, A. M. Cockshutt, A. Decken, P. Morin, S. A. Westcott, *Inorg. Chim. Acta* **2014**, *415*, 88–94; d) X. Zheng, H. Wang, Y. Li, *RSC Adv.* **2016**, *6*, 88174–88178; e) M.-Y. Yuen, V. A. L. Roy, W. Lu, S. C. F. Kui, G. S. M. Tong, M.-H. So, S. S.-Y. Chui, M. Muccini, J. Q. Ning, S. J. Xu, C.-M. Che, *Angew. Chem. Int. Ed.* **2008**, *47*, 9895–9899; f) I. Eryazici, C. N. Moorefield, G. R. Newkome, *Chem. Rev.* **2008**, *108*, 1834–1895; g) X. Mou, Y. Wu, S. Liu, M. Shi, X. Liu, C. Wang, S. Sun, Q. Zhao, X. Zhou, W. Huang, *J. Mater. Chem.* **2011**, *21*, 13951–13962.
 [6] a) S. J. Berners-Price, *Angew. Chem. Int. Ed.* **2011**, *50*, 804–805; b) L. Kelland, *Nat. Rev. Cancer* **2007**, *7*, 573–584; c) W. Villarreal, L. Colina-Vegas, C. Rodrigues de Oliveira, J. C. Tenorio, J. Ellena, F. C. Gozzo, M. R. Cominetti, A. G. Ferreira, M. A. B. Ferreira, M. Navarro, A. A. Batista, *Inorg. Chem.* **2015**, *54*, 11709–11720; d) I. Kostova, *Recent Pat. Anti-Cancer Drug Discovery* **2006**, *1*, 1–22.
 [7] Q. Liu, Z. Zhang, *Catalysis Science, Technology* **2019**, *9*, 4821–4834.
 [8] a) T. K. Meister, K. Riener, P. Gigler, J. Stohrer, W. A. Herrmann, F. E. Kühn, *ACS Catal.* **2016**, *6*, 1274–1284; b) B. Marciniak, J. Guliński, *J. Organomet. Chem.* **1993**, *446*, 15–23; c) X. Cui, K. Junge, X. Dai, C. Kreyenschulte, M.-M. Pohl, S. Wohlrab, F. Shi, A. Brückner, M. Beller, *ACS Cent. Sci.* **2017**, *3*, 580–585; d) A. Mehrban, D. Muhammad, M. Muhammad Ali, B. Sineen, M. Fareeha, *International Journal of Sciences: Basic and Applied Research (IJSBAR)* **2013**, *7*; e) J. Yang, J. Liu, Y. Ge, W. Huang, C. Schneider, R. Dühren, R. Franke, H. Neumann, R. Jackstell, M. Beller, *Chem. Commun.* **2020**, *56*, 5235–5238; f) J. Pospech, I. Fleischer, R. Franke, S. Buchholz, M. Beller, *Angew. Chem. Int. Ed.* **2013**, *52*, 2852–2872; g) K. Kuciński, J. Szudkowska-Frątczak, G. Hreczycho, *Chem. Eur. J.* **2016**, *22*, 13046–13049.
 [9] Y. Nakajima, S. Shimada, *RSC Adv.* **2015**, *5*, 20603–20616.
 [10] a) A. Walczak, G. Kurpiak, A. R. Stefankiewicz, *Int. J. Mol. Sci.* **2020**, *21*; b) A. Walczak, A. R. Stefankiewicz, *Inorg. Chem.* **2018**, *57*, 471–477; c) A. Walczak, G. Kurpiak, M. Zaranek, P. Pawluć, A. R. Stefankiewicz, *J. Catal.* **2022**, *405*, 84–90; d) G. Kurpiak, A. Walczak, G. Markiewicz, J. Harrowfield, A. R. Stefankiewicz, *Nanoscale* **2023**, *15*, 9543–9550.
 [11] a) M. Moro, P. Zardi, M. Rossi, A. Biffis, *Catalysts* **2022**, *12*, 307; b) A. Upadhyay, S. Gautam, V. Ramu, P. Kondaiah, A. R. Chakravarty, *Dalton Trans.* **2019**, *48*, 17556–17565; c) Y. Yan, Z. Yu, C. Liu, X. Jin, *Dyes Pigm.* **2020**, *173*, 107949; d) M. Ebina, A. Kobayashi, T. Ogawa, M. Yoshida, M. Kato, *Inorg. Chem.* **2015**, *54*, 8878–8880; e) K. Ohno, K. Shiraiishi, T. Sugaya, A. Nagasawa, T. Fujihara, *Inorg. Chem.* **2022**, *61*, 3420–3433; f) L. Zhang, L. Tian, M. Li, R. He, W. Shen, *Dalton Trans.* **2014**, *43*, 6500–6512; g) F. D. Lewis, G. D. Salvi, *Inorg. Chem.* **1995**, *34*, 3182–3189; h) L. Guijie, S. Yuanbin, in *Light-Emitting Diode* (Ed.: T. Jagannathan), IntechOpen, Rijeka **2018**, p. Ch. 5.
 [12] S. A. De Pascali, P. Papadia, A. Ciccarese, C. Pacifico, F. P. Fanizzi, *Eur. J. Inorg. Chem.* **2005**, *2005*, 788–796.
 [13] R. A. A. Abdine, G. Kurpiak, A. Walczak, S. A. A. Aeash, A. R. Stefankiewicz, F. Monnier, M. Taillefer, *J. Catal.* **2019**, *376*, 119–122.
 [14] A. Walczak, H. Stachowiak, G. Kurpiak, J. Kaźmierczak, G. Hreczycho, A. R. Stefankiewicz, *J. Catal.* **2019**, *373*, 139–146.
 [15] a) S. A. De Pascali, A. Muscella, C. Vetrugno, S. Marsigliante, F. P. Fanizzi, *Inorg. Chim. Acta* **2014**, *412*, 88–93; b) S. A. De Pascali, P. Papadia, S. Capoccia, L. Marchiò, M. Lanfranchi, A. Ciccarese, F. P. Fanizzi, *Dalton Trans.* **2009**, 7786–7795; c) A. Muscella, N. Calabriso, F. P. Fanizzi, S. A. De Pascali, L. Urso, A. Ciccarese, D. Migoni, S. Marsigliante, *Br. J. Pharmacol.* **2008**, *153*, 34–49.
 [16] a) T. Ito, T. Kiriya, Y. Nakamura, A. Yamamoto, *Bull. Chem. Soc. Jpn.* **1976**, *49*, 3257–3264; b) T. Ito, T. Kiriya, A. Yamamoto, *Bull. Chem. Soc. Jpn.* **1976**, *49*, 3250–3256.
 [17] a) H. Ogawa, M. Yamashita, *Dalton Trans.* **2013**, *42*, 625–629; b) M. B. Lachachi, T. Benabdallah, P. M. Aguiar, M. H. Youcef, A. C. Whitwood, J. M. Lynam, *Dalton Trans.* **2015**, *44*, 11919–11928; c) T. Iimura, N. Akasaka, T. Kosai, T. Iwamoto, *Dalton Trans.* **2017**, *46*, 8868–8874.
 [18] a) A. K. Roy, R. B. Taylor, *J. Am. Chem. Soc.* **2002**, *124*, 9510–9524; b) S. E. Parker, J. Börgel, T. Ritter, *J. Am. Chem. Soc.* **2014**, *136*, 4857–4860; c) S.

- Sakaki, N. Mizoe, M. Sugimoto, *Organometallics* **1998**, *17*, 2510–2523; d) A. Adamski, M. Kubicki, P. Pawluć, T. Grabarkiewicz, V. Patroniak, *Catal. Commun.* **2013**, *42*, 79–83.
- [19] a) Rigaku-Oxford Diffraction, CrysAlisPro Oxford Diffraction Ltd, Abingdon, England V 1. 171. 36. 2., England **2006**; b) O. V. Dolomanov, L. J. Bourhis, R. J. Gildea, J. A. Howard, H. Puschmann, *J. Appl. Crystallogr.* **2009**, *42*, 339–341; c) G. M. Sheldrick, *Acta Crystallogr. Sect. A* **2015**, *71*, 3–8; d) G. M. Sheldrick, *Acta Crystallogr. Sect. C* **2015**, *71*, 3–8; e) W. Xue, Z.-W. Qu, S. Grimme, M. Oestreich, *J. Am. Chem. Soc.* **2016**, *138*, 14222–14225; f) N. S. Abeynayake, J. Zamora-Moreno, S. Gorla, B. Donnadiou, M. A. Muñoz-Hernández, V. Montiel-Palma, *Dalton Trans.* **2021**, *50*, 11783–11792; g) J. R. Carney, B. R. Dillon, L. Campbell, S. P. Thomas, *Angew. Chem. Int. Ed.* **2018**, *57*, 10620–10624; h) D. Noda, A. Tahara, Y. Sunada, H. Nagashima, *J. Am. Chem. Soc.* **2016**, *138*, 2480–2483; i) M. Zhong, X. Pannecoucke, P. Jubault, T. Poisson, *Chem. Eur. J.* **2021**, *27*, 11818–11822; j) Y.-S. Song, B. R. Yoo, G.-H. Lee, I. N. Jung, *Organometallics* **1999**, *18*, 3109–3115.

Manuscript received: November 14, 2023

Revised manuscript received: November 30, 2023

Accepted manuscript online: December 5, 2023

Version of record online: December 18, 2023

Multi-Stimuli-Responsive Network of Multicatalytic Reactions using a Single Palladium/Platinum Catalyst

Gracjan Kurpik, Anna Walczak, Paweł Dydio,* and Artur R. Stefankiewicz*

Abstract: Given her unrivalled proficiency in the synthesis of all molecules of life, nature has been an endless source of inspiration for developing new strategies in organic chemistry and catalysis. However, one feature that remains thus far beyond chemists' grasp is her unique ability to adapt the productivity of metabolic processes in response to triggers that indicate the temporary need for specific metabolites. To demonstrate the remarkable potential of such stimuli-responsive systems, we present a metabolism-inspired network of multicatalytic processes capable of selectively synthesising a range of products from simple starting materials. Specifically, the network is built of four classes of distinct catalytic reactions—cross-couplings, substitutions, additions, and reductions, involving three organic starting materials—terminal alkyne, aryl iodide, and hydrosilane. All starting materials are either introduced sequentially or added to the system at the same time, with no continuous influx of reagents or efflux of products. All processes in the system are catalysed by a multifunctional heteronuclear Pd^{II}/Pt^{II} complex, whose performance can be controlled by specific additives and external stimuli. The reaction network exhibits a substantial degree of orthogonality between different pathways, enabling the controllable synthesis of ten distinct products with high efficiency and selectivity through simultaneous triggering and suppression mechanisms.

active molecules, crucial for sustaining various functions of living organisms.^[1] In living cells, a number of processes that generate mass, energy, and information transfer are seamlessly integrated into a complex network of dynamic interactions and sequences of multi-stage reactions.^[2] Due to the cooperativity in the action of multiple enzymes, each signal reaching the cell is processed to direct processes into specific pathways, accurately balancing cellular production.^[2–3] The maintenance of vital functions of each cell relies on a multi-stimuli-responsive system, which efficiently and simultaneously manages hundreds of catalytic reactions in concert, reflecting the vastness of metabolic processes that continuously produce all necessary metabolites at levels temporarily required by the cell.^[4] Therefore, to sustain cellular homeostasis, all metabolic pathways must fulfil certain criteria, such as orthogonality, controllability, and adaptability. Additionally, regulatory mechanisms are essential for optimising metabolite flow to ensure the overall system stability and integration with other cellular processes.^[5]

Nature has been a wellspring of inspiration for researchers and has provided the foundational framework for many discoveries across the realms of (bio)chemistry, (bio)engineering, and medicine.^[6] For chemists, it has become an aspiration to replicate the remarkable performance of metabolic processes in constructing molecules, thus driving the development of innovative concepts in synthetic chemistry and catalysis.^[7] This fascination has spurred the development of numerous catalytic systems, each striving to mimic the complex enzymatic machinery found in cells.^[8] Nevertheless, the enormous potential of bio-inspired catalytic systems, capable of dynamically responding to environmental changes and precisely crafting diverse compounds on demand, thus mirroring the finesse of natural systems in regulating metabolite flows as per temporal requirements, remains largely unexplored.^[9]

Introduction

Millions of years of evolution have enabled nature to develop intricate metabolic systems to achieve exceptionally effective processes for the synthesis of sophisticated bio-

[*] G. Kurpik, Dr. A. Walczak, Prof. A. R. Stefankiewicz
 Center for Advanced Technologies
 Adam Mickiewicz University in Poznań
 Uniwersytetu Poznańskiego 10, 61-614 Poznań, Poland
 G. Kurpik, Dr. A. Walczak, Prof. A. R. Stefankiewicz
 Faculty of Chemistry
 Adam Mickiewicz University in Poznań
 Uniwersytetu Poznańskiego 8, 61-614 Poznań, Poland
 Dr. P. Dydio
 Yusuf Hamied Department of Chemistry
 University of Cambridge
 Lensfield Road, CB21EW Cambridge, UK

Dr. P. Dydio
 University of Strasbourg, CNRS
 ISIS UMR 7006
 8 Allée Gaspard Monge, 67000 Strasbourg, France
 E-mail: pd552@cam.ac.uk
 ars@amu.edu.pl

© 2024 The Authors. Angewandte Chemie International Edition published by Wiley-VCH GmbH. This is an open access article under the terms of the Creative Commons Attribution License, which permits use, distribution and reproduction in any medium, provided the original work is properly cited.

Herein, we report a metabolism-inspired artificial system designed to respond to multiple stimuli, operating within an integrated network of mechanistically distinct reactions, effectively imitating the multi-responsive systems found in nature (Figure 1). While achieving a perfect replication of the intricacy and excellence of metabolic processes remains elusive, the aim of this study is to demonstrate that artificial networks can exhibit features inherent to natural metabolic systems. Specifically, our approach involves a strategic design for the efficient performance of multi-stage processes between three simple starting materials, terminal alkyne **S1**, aryl iodide **S2**, and hydrosilane **S3**, catalysed by a single multifunctional heteronuclear Pd^{II}/Pt^{II} cooperative catalyst. We demonstrate that due to a substantial degree of orthogonality between different transformations, the specific pathways within the network can be augmented by the sequences and nature of simple chemical reagents and physical triggers **T1–T9**. Such control of different catalytic activities enables the preferential synthesis of each product from a diverse range, denoted as **P1–P10**, as well as their temporal interconversions, as described below.

Results and Discussion

At the outset of these studies, we hypothesised that Pd and Pt complexes would serve as promising candidates for establishing a catalytic reaction network. We envisioned that combining these two metals would grant access to a broad range of available transformations due to their unique ability to mediate various catalytic processes, including myriads of cross-couplings, substitutions, additions, and reductions.^[10]

To develop potential multifunctional Pd and Pt catalytic systems, our approach involved constructing heteronuclear Pd^{II}/Pt^{II} complexes. Our rationale was that integrating both catalytic metal centres into a single molecular architecture would improve compatibility between individual catalytically active sites throughout the reaction sequence and

create an opportunity for cooperation between different metal centres.^[11] In addition, such a multifunctional catalyst would mirror enzymes bearing multiple active sites, with fatty acid synthase (FAS) constituting a prime example.^[12] As ligating structures, we selected two isomeric pyridyl- β -diketonate ligands, 2,2-dimethyl-5-(3- or 4-pyridyl)pentane-3,5-dione (**HL1** and **HL2**, respectively), commonly employed in metallosupramolecular chemistry,^[13] together with chelating *N*-donor coligands, 2,2'-bipyridine (bpy) and ethylenediamine (en).

A conventional hierarchical synthesis^[14] with metal precursors and selected ligands gave rise to a series of four heterometallic complexes **C1–C4** with Pd^{II} and Pt^{II}, having the N₂O₂ and N₄ coordination spheres, respectively (Figure 2a). The formation of **C1–C4** was confirmed by NMR spectroscopy, ESI-MS, and elemental analysis as summarised in Figure 2d and 2e and detailed in the Supporting Information (Figures S3–S10). Because **C1–C4** were of low crystallinity in the solid state, the crystal structures of [Pt(**HL1**)₄](NO₃)₂ (**C^{Pt}**) and [Pd(**L1**)(bpy)]PF₆ (**C^{Pd}**) were utilised to model the heterometallic structure, as shown for **C1** in Figure 2b and 2c.

We selected phenylacetylene **S1**, iodobenzene **S2**, and triethylsilane **S3** as model starting materials. In the presence of **C1–C4**, we expected the substrates to engage in a series of sequential and simultaneous processes. Specifically, the Sonogashira, Heck, and Hiyama cross-couplings, as well as the protodehalogenation reaction are known to be catalysed by structurally related Pd complexes.^[10f,13d,15] In turn, the hydrosilylation and silylation reactions can occur in the presence of similar Pt complexes.^[14a,16] Lastly, the semi- or complete reduction reactions can be catalysed by either Pd or Pt complexes.^[17] Consequently, a range of structurally distinct products, **P1–P10**, could be formed through different pathways, as depicted in Figure 3a. We envisioned that the preferential formation of particular products would depend on the order and relative rates of specific catalytic processes, which in turn could be controlled by the catalysts and the reaction conditions. Importantly, the activities and selectiv-

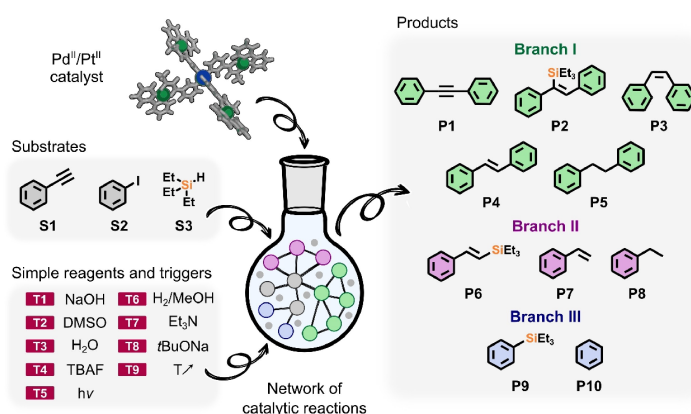


Figure 1. Multi-responsive performance triggered by various external stimuli within a bio-inspired network of multi-stage reactions catalysed by the heteronuclear Pd^{II}/Pt^{II} complex.

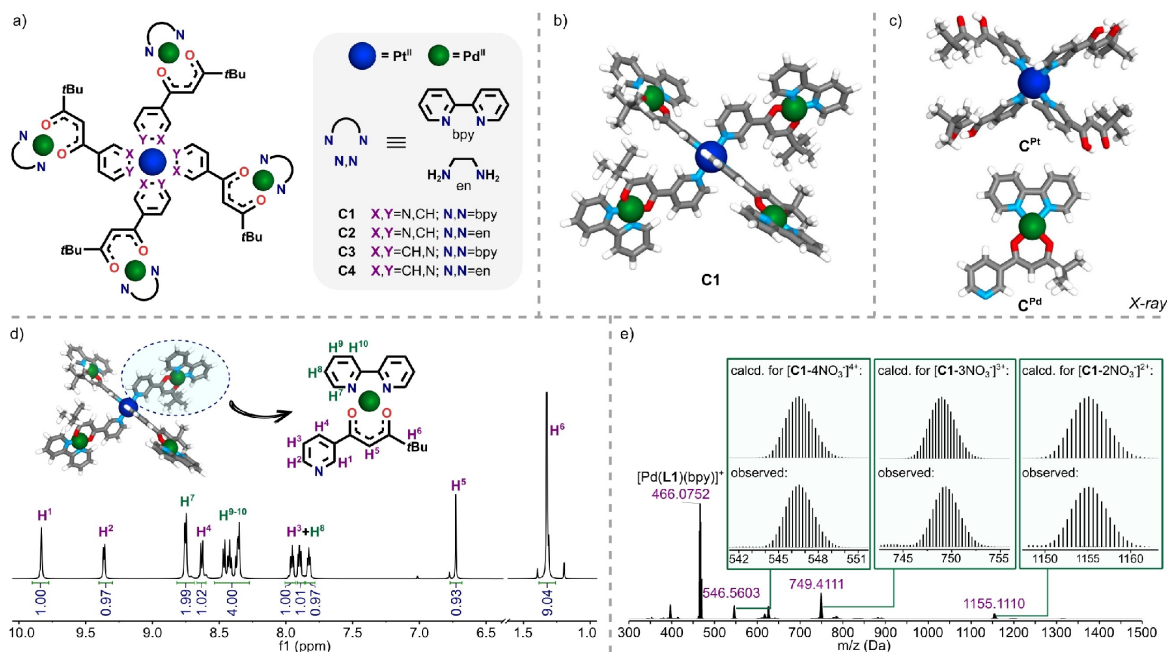


Figure 2. Heteronuclear Pd/Pt-complexes tested as catalysts for the reaction network. a) Structures of **C1–C4**. b) Model structure of heteronuclear complex **C1**. c) X-ray structures of the mononuclear constituents— C^{Pt} and C^{Pd} . d) Part of the 1H NMR spectrum (600 MHz, $DMSO-d_6$) of **C1**. e) ESI-MS spectrum of **C1** showing the calculated isotope model (top) and observed data (bottom).

ities of individual transformations depend not only on the catalysts but also on simple chemical reagents and physical stimuli, such as NaOH, TBAF, or DMSO and temperature or light, respectively.^[18] We surmised that such additives or reaction conditions could be strategically used in a sequential and controlled manner, acting as triggers to direct the network toward specific outcomes by promoting specific reaction pathways, resembling the regulation of natural metabolic systems through external stimuli.^[8b,19]

The topological analysis of the reaction network shown in Figure 3a reveals its three main branches (**I–III**), each utilising either two or all three starting materials. For instance, in branch **I**, **S1** undergoes the initial reaction with **S2** prior to any transformations involving **S3**, while in branch **II**, **S1** reacts first with **S3** prior to engaging **S2**. In turn, in branch **III**, **S2** reacts with **S3** without any role for **S1**. Interestingly, certain products within the network can be generated through multiple pathways, which may occur within the same branch or transpire across different branches, reflecting the system's capacity for convergence. For instance, all the pathways producing **P1–P4** within branch **I** may ultimately converge to **P5** as the final product. In turn, pathways leading to **P4** can occur via **P1**, **P2**, or **P3** as preceding intermediates within branch **I** or involve **P6** and **P7** as alternative intermediates formed in branch **II**, thereby connecting branches **I** and **II**.

The development of sequences of chemical and physical stimuli promoting the selective formation of each of products **P1–P10** and their subsequent interconversions

involved extensive experimentation conducted with all heteronuclear complexes **C1–C4** and different simple chemical reagents and physical triggers. The most efficient and selective pathways were observed to occur in the presence of **C1** as a catalyst and **T1–T9** as triggers, as schematically shown in Figure 3a and further detailed in Figure 3b. The sequences of triggers leading selectively to **P1–P10** are described and compared with other representative examples ahead. Further details, including experiments with **C2–C4** and a series of control experiments with model mononuclear complexes (C^{Pt} , C^{Pd}), are presented in the Supporting Information.

Branch I: S1 reacts with S2, prior to reacting with S3. We found that **S1** and **S2** readily underwent the Sonogashira reaction, forming **P1** in >99% yield, in the presence of NaOH (**T1**) as a trigger and **C1** as a catalyst. Then, **P1** in situ underwent a range of subsequent reactions with **S3**, resulting in the formation of **P2–P5**, with the selectivity being governed by the imposed triggers **T2–T4** (Figure 3). Specifically, in the absence of any additional triggers, **P1** reacted with **S3** in the hydrosilylation reaction, forming **P2** with an overall yield of 98%. However, when in the presence of either DMSO or water (**T2** and **T3**, respectively), **P1** and **S3** underwent alternative stereoselective semi-reductive processes, forming two distinct products, namely **P3** or **P4**, with overall yields of 90% and 62%, respectively. In addition, **P3** and **P4** could be interconverted between each other under UV light irradiation (**T5**). Irrespective of the starting point, i.e., **P3** or **P4**, the

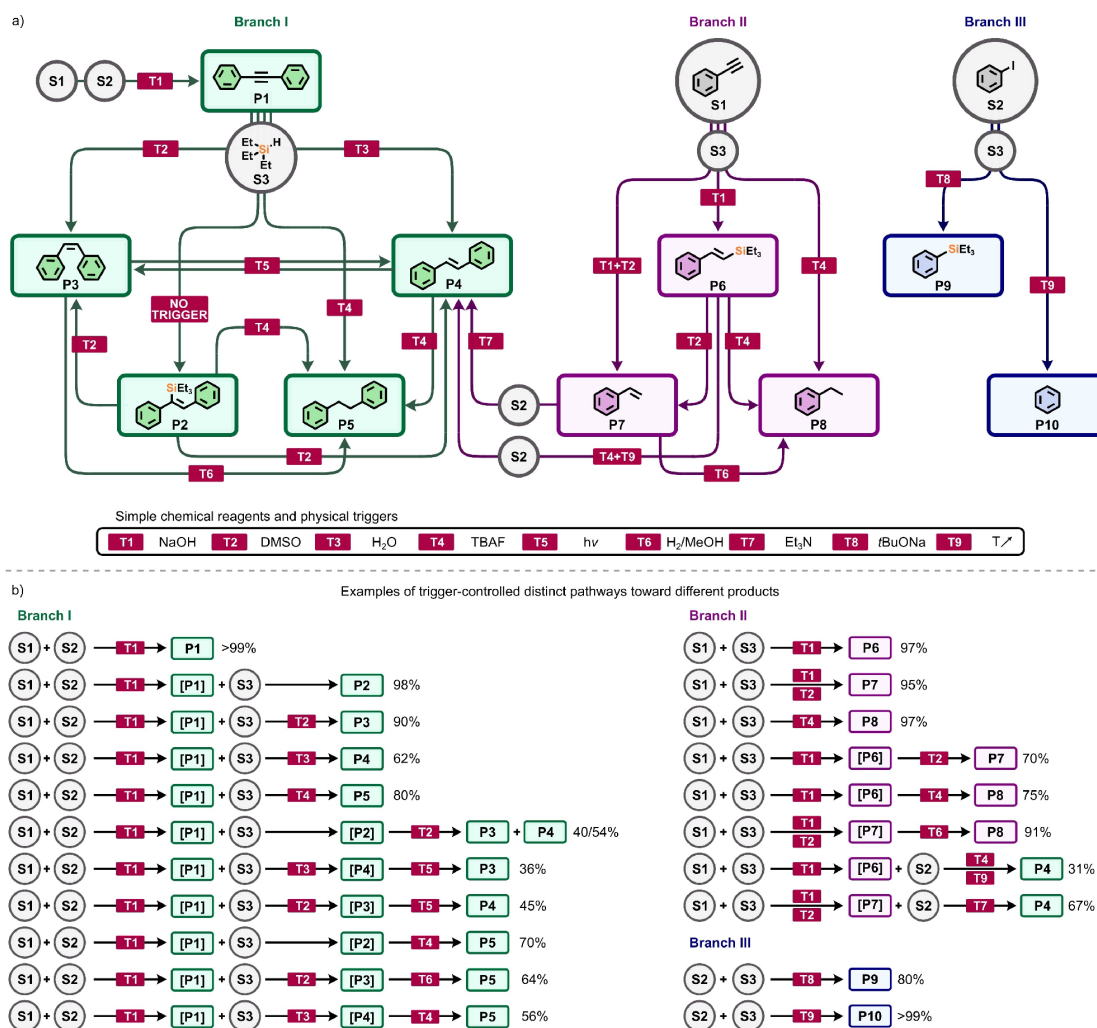


Figure 3. a) Multi-stimuli-responsive network of reactions between **S1–S3** added sequentially, catalysed by **C1** and controlled by **T1–T9**, and b) trigger-directed pathways toward distinct products within branches I–III.

irradiation process produced a nearly equimolar mixture of both stereoisomers, indicating that a dynamic equilibrium was reached under these conditions.^[20] In turn, in the presence of TBAF (**T4**), **P1** was converted into fully reduced **P5** in 80% yield.

We observed that thus-formed **P2–P4** could be further converted in situ to **P3–P5** when applying additional triggers. For instance, **P2** was converted into **P3** and **P4** (40% and 54% overall yields) when triggered by the addition of DMSO (**T2**). In turn, **P2** and **P4** converted to **P5** (70% and 56%, respectively) when TBAF (**T4**) was introduced. Finally, **P3** was transformed into **P5** (64%) when exposed to H₂ and methanol (**T6**).

Branch II: **S1** reacts with **S3**, prior to reacting with **S2**. Branch **II** is comprised of **S1** and **S3** reacting to generate three new products, **P6–P8**, some of which can undergo

subsequent transformations with **S2** (Figure 3a). We found that in the presence of **C1** and NaOH (**T1**), **S1** and **S3** reacted to form **P6**, the hydrosilylation product, in a nearly quantitative yield (97%). However, the same reaction in the additional presence of DMSO (**T2**) resulted in the selective semi-reduction, furnishing **P7** (95%). In turn, in the presence of TBAF (**T4**), fully reduced **P8** was formed instead (97%).

Like in branch **I**, when suitable triggers were applied, some initially formed products of branch **II** could be in situ converted into other products of the same branch or transposed into products of branch **I**. For instance, initially formed **P6** was converted in situ into **P7** or **P8**, in 70% or 75% overall yields, when triggered by the addition of DMSO (**T2**) or TBAF (**T4**). In turn, **P7** was transferred in situ into **P8** (91%) when exposed to H₂ and methanol (**T6**).

Alternatively, **P6** or **P7**, and **S2** underwent the Hiyama or Heck cross-coupling, respectively, when triggered by either TBAF (**T4**) and temperature (**T9**) or Et₃N (**T7**), forming **P4** (31% and 67%, respectively). These reaction pathways interconnect branches **I** and **II**.

Branch III: S2 reacts with S3. Devoid of **S1**, branch **III** involves the processes occurring for **S2** and **S3**, leading to products **P9** and **P10** (Figure 3a). In the presence of *t*BuONa (**T8**) and **C1**, **S2** and **S3** reacted to form **P9** in 80% yield. Alternatively, in the absence of any base yet at elevated temperature (**T9**), the reaction furnished **P10** in a nearly quantitative yield (>99%). Unlike branches **I** and **II**, branch **III** remains independent of the rest of the network.

Kinetic hierarchy and pathway orthogonality. In metabolic systems, the selective formation of specific products from all available substrates is governed by the kinetic hierarchy and orthogonality of processes, which are determined by the conditions and enzymes, i.e., sophisticated catalysts often exhibiting exquisite substrate and reaction selectivities. In

the experiments for the synthetic network presented above, in addition to the chemical additives and physical triggers that controlled the orthogonality of competitive pathways catalysed by **C1**, the kinetic hierarchy of processes was augmented by the sequential addition of building blocks **S1–S3**.

To evaluate the kinetic hierarchy and pathway orthogonality within this artificial system, we studied the performance of **C1** with all starting materials present in the reaction mixture from the start. We observed that, despite the potential complexities, a significant portion of the products within the network remains accessible when using the heteronuclear complex **C1** in combination with the same triggers **T1–T9**, as detailed below and shown in Figure 4. Nevertheless, some processes are inherently favoured by the current catalyst, outcompeting other pathways, preventing access to some products in the current system.

When **S1**, **S2**, and **S3** were all reacted together in the presence of **C1** and **T1**, the system favoured the generation

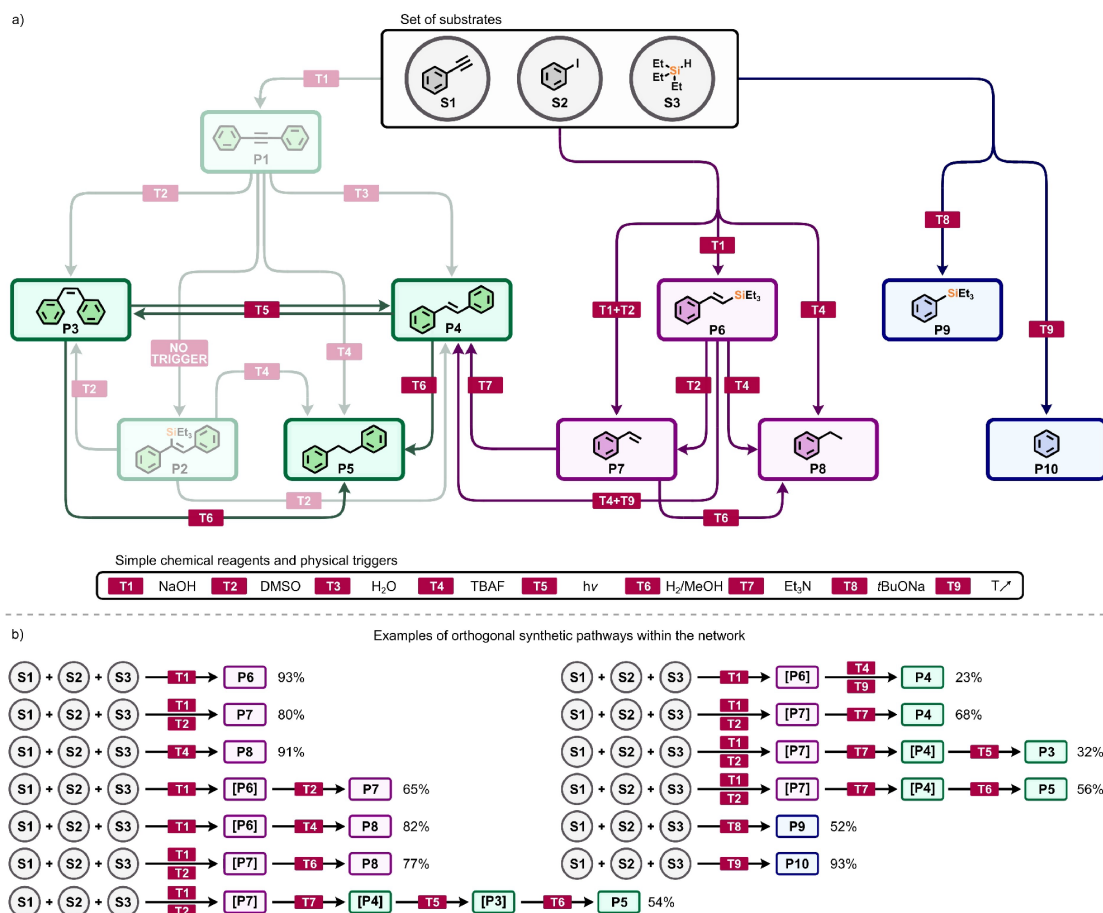


Figure 4. a) Multi-stimuli-responsive network of reactions between **S1–S3**, all present in the system at the same time, catalysed by **C1** and controlled by **T1–T9**, and b) trigger-directed pathways toward distinct products, illustrating the level of orthogonality between different processes in the system.

of **P6** (93%) over **P1** (<1%) and **P2** (<1%), which could be otherwise formed under these conditions. This selectivity profile reflects the kinetic preference of **C1** for the hydrosilylation reaction over the Sonogashira coupling under these conditions. Importantly, thus-formed **P6** could be in situ converted into **P7** (65%), **P8** (82%), or **P4** (23%), in subsequent reactions triggered by **T2**, **T4**, or **T4** with **T9**, respectively, using the reagents initially introduced into the system.

In turn, when the reaction between **S1**, **S2**, and **S3** was triggered by **T1** and **T2**, we observed selective semi-reduction, yielding **P7** (80%). When subsequently triggered by **T6** or **T7**, thus-formed **P7** could be reduced by remaining **S3** forming **P8** (77%) or cross-coupled with **S2** furnishing **P4** (68%). The latter could be further converted in situ to **P3** (32%) or **P5** (56%), when triggered by **T5** or **T6**, respectively.

Furthermore, the reaction between **S1**, **S2**, and **S3** triggered by **T4** led to **P8** (91%), leaving **S2** behind, showing that all products of branch **II** are accessible when all starting materials are present at the same time and the performance of **C1** is trigger-controlled. Similarly, both products of branch **III** can be formed in reactions with all substrates present, yielding **P9** (52%) or **P10** (93%), when triggered by **T8** or **T9**, respectively.

Overall, due to the kinetic preference for hydrosilylation and reduction reactions over the Sonogashira coupling by **C1**, the orthogonality in branch **I** is not complete when **S1**, **S2**, and **S3** are all present. However, upon the formation of **P1**, the individual synthetic pathways leading to **P2–P5** are fully orthogonal. Additionally, all the synthetic pathways in branches **II** and **III** can be considered orthogonal, with reactivity determined by the triggers employed.

Influence of triggers. As exemplified above, sequences of various triggers denoted as **T1–T9** play a central role in governing the overall selectivity of the network, guiding the progression of different reactions along distinct pathways within each of the three branches (**I–III**). For instance, among several bases tested, NaOH (**T1**) proved to be the most effective for the efficient performance of the Sonogashira coupling (Figure 5a). In turn, chemical additives, such as DMSO, water, TBAF, and H₂ (**T2–T4**, **T6**) inhibited the inherent hydrosilylation reactivity forming **P2** and **P6** within branches **I** and **II**, inducing the reductive processes instead. The type of additives controlled both the chemo- and stereoselectivity of these reductive processes, directing the reaction pathways between products **P3–P5** and **P7–P8**. For instance, the presence of DMSO (**T2**) in strictly defined proportions (Figure 5b) enabled the *cis*-selective semi-reduction of internal or terminal alkynes, furnishing **P3** and **P7**, respectively. In turn, water (**T3**) ensured the *trans*-selective semi-reduction, enabling the preferential generation of **P4**. In this case, the water content proved to be critical for the chemoselectivity, controlling the preferential formation of the hydrosilylation, semi-, or complete reduction products (Figure 5c). Also, TBAF and H₂ (**T4** and **T6**) facilitated the reactions toward the complete reduction products (**P5** and **P8**). In turn, exposure to UV light (**T5**) triggered the interconversions between **P3** and **P4** through

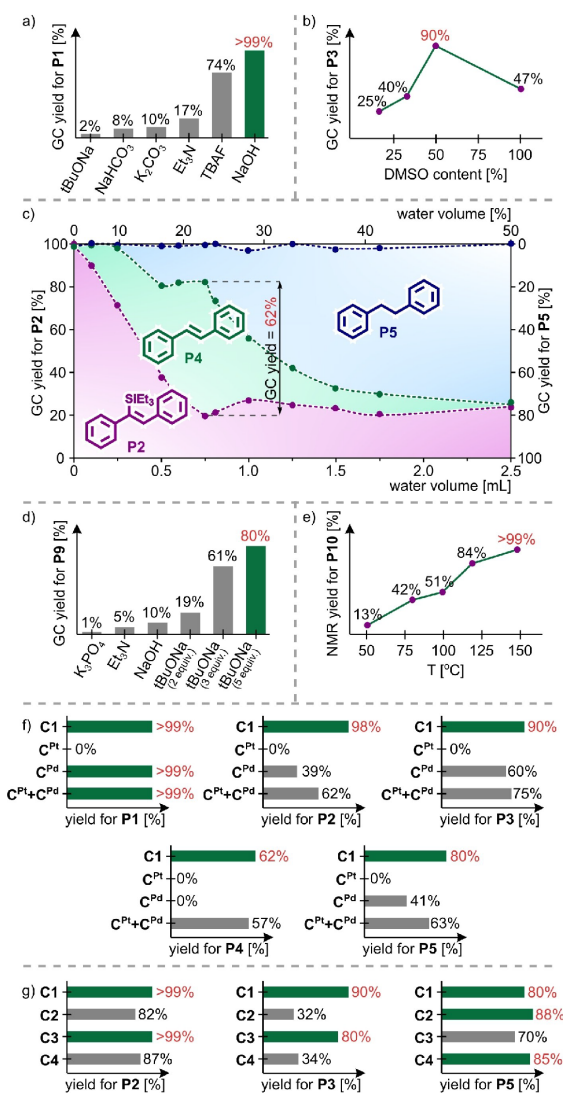


Figure 5. The effect of various triggers and catalysts for the catalytic reaction network. a) The effect of different bases on the Sonogashira coupling. b) The effect of the amount of DMSO (**T2**) on the *cis*-selective semi-reduction. c) The effect of the amount of water (**T3**) on the divergent product formation in the reaction of **P1** and **S3**. d) The effect of different bases on the silylation reaction. e) The effect of the temperature (**T9**) on the protodehalogenation reaction. f) Comparative tests demonstrating the enhanced catalytic activity of the complex **C1** in comparison to its mononuclear constituents: **C^{Pt}**, **C^{Pd}**, and their mixture, while maintaining a constant concentration of Pd and Pt. g) The comparison of catalytic efficiency between **C1–C4** in the selected transformations.

photomediated *cis/trans*-isomerisation. Alternative to the complete reduction, hydrosilylation and semi-reduction products (**P2** and **P6**) could enter the Hiyama and Heck cross-couplings triggered by TBAF (**T4**) at an elevated temperature (**T9**) and Et₃N (**T7**), respectively. Lastly, unlike

for the Sonogashira coupling, *t*BuONa (**T8**) proved to be the most effective base in the silylation reaction (Figure 5d vs. Figure 5a), while the elevated temperature (**T9**) enabled the protodehalogenation reaction (Figure 5e).

Influence of catalysts & their heteronuclearity. Despite the distinct roles of Pd^{II} and Pt^{II} centers in individual catalytic processes of the reaction network, their incorporation into a single complex structure proved to significantly enhance their overall performance. To illustrate the effect, the performance of **C1** was compared against the performance of its mononuclear constituents, namely **C^{Pt}** and **C^{Pd}**, or their mixture. As shown in Figure 5f, the yields of the processes within branch **I** in the presence of **C1** were superior to those in the presence of either mononuclear constituents or their mixture. Furthermore, the excellent catalytic activity of **C1** could also be traced back to its customised coordination arrangement. Despite the structural similarities of heteronuclear complexes **C1–C4**, **C1** turned out to be typically the most effective, selective, and versatile, as exemplified in Figure 5g and detailed in the Supporting Information. Consequently, the catalytic performance of **C1** within the reaction network can be associated with incorporating both metal centers in a single molecular structure supported with specific chelating ligands, creating a specific coordination environment for both neighboring metal sites suitable for efficient catalysis.

Conclusion

To conclude, inspired by the metabolic processes occurring in nature, we investigated a network of reactions comprising transition metal-catalysed synthetic processes between a set of starting materials either introduced sequentially or present in the system from the beginning. The model system was designed to enable a range of multi-stage transformations, including cross-coupling, substitution, addition, and reduction reactions. We demonstrated the feasibility of orchestrating these chemical processes within the system through meticulous control of the reaction environment. The interplay of the network and the specific temporal chemical additives and physical triggers governed the formation of a series of distinct products from simple starting materials with high efficiency and selectivity. Overall, the performance and stimuli-responsiveness of this model system resemble the remarkable features of metabolic networks, selectively producing various complex metabolites from simple building blocks as temporarily needed by the system. Although the presented system does not achieve complete orthogonality, which would require several advanced catalysts tailored to specific substrates, many of the synthetic pathways catalysed by single bimetallic catalyst **C1** in the network can be characterised as orthogonal. With these results as groundwork, the next stage would be to advance it into a more sophisticated system characterised by controllable, kinetically orchestrated, and fully orthogonal processes, operating under homeostatic conditions with a continuous flux of substrates, products, and energy. We hope the study will inspire further research merging complex

systems chemistry with practical organic chemistry toward the improved efficient and sustainable synthesis of fine chemicals and materials.

Supporting Information

The authors have cited additional references within the Supporting Information.^[21]

Acknowledgements

We thank M. Gołdyn (Adam Mickiewicz University) for X-ray crystallography. This research was funded by the National Science Centre in Poland (grant SONATA BIS 2018/30/E/ST5/00032—ARS), European Research Council (grant ERC StG 804106—PD), and Morrell Fund, Yusuf Hamied Department of Chemistry, University of Cambridge. GK is a scholarship holder of the Adam Mickiewicz University Foundation for the academic year 2023/2024.

Conflict of Interest

The authors declare no conflict of interest.

Data Availability Statement

The data that support the findings of this study are available in the supplementary material of this article.

Keywords: multicatalytic systems · heteronuclear complexes · cooperative catalysis · multi-stage reactions · transition metals

- [1] a) B. Ø. Palsson, *Systems biology: properties of reconstructed networks*, Cambridge university press, 2006; b) K. Ruiz-Mirazo, C. Briones, A. de la Escosura, *Chem. Rev.* **2014**, *114*, 285–366; c) R. Roszak, A. Wołos, M. Benke, Ł. Gleń, J. Konka, P. Jensen, P. Burgchardt, A. Żądło-Dobrowolska, P. Janiuk, S. Szymkuć, B. A. Grzybowski, *Chem* **2024**, *10*, 952–970.
- [2] a) N. Barkai, S. Leibler, *Nature* **1997**, *387*, 913–917; b) H. Jeong, B. Tombor, R. Albert, Z. N. Oltvai, A. L. Barabási, *Nature* **2000**, *407*, 651–654; c) L. H. Hartwell, J. J. Hopfield, S. Leibler, A. W. Murray, *Nature* **1999**, *402*, C47–C52; d) N. M. Ivanov, M. G. Baltussen, C. L. F. Regueiro, M. T. G. M. Derks, W. T. S. Huck, *Angew. Chem. Int. Ed.* **2023**, *62*, e202215759; e) J. E. Purvis, G. Lahav, *Cell* **2013**, *152*, 945–956.
- [3] U. S. Bhalla, R. Iyengar, *Science* **1999**, *283*, 381–387.
- [4] a) S. N. Semenov, A. S. Y. Wong, R. M. van der Made, S. G. J. Postma, J. Groen, H. W. H. van Roekel, T. F. A. de Greef, W. T. S. Huck, *Nat. Chem.* **2015**, *7*, 160–165; b) B. N. Kholodenko, *Nat. Rev. Mol. Cell Biol.* **2006**, *7*, 165–176; c) D. E. Koshland, A. Goldbeter, J. B. Stock, *Science* **1982**, *217*, 220–225.
- [5] a) J. Stelling, S. Klamt, K. Bettenbrock, S. Schuster, E. D. Gilles, *Nature* **2002**, *420*, 190–193; b) S. Schuster, T. Dandekar, D. A. Fell, S. Schuster, T. Dandekar, D. A. Fell, *Trends Biotechnol.* **1999**, *17*, 53–60; c) A. V. Pandit, S. Srinivasan, R. Mahadevan, *Nat. Commun.* **2017**, *8*, 15188; d) T. U. Chae, S. Y.

- Choi, J. W. Kim, Y.-S. Ko, S. Y. Lee, *Curr. Opin. Biotechnol.* **2017**, *47*, 67–82.
- [6] a) J. W. Lee, D. Na, J. M. Park, J. Lee, S. Choi, S. Y. Lee, *Nat. Chem. Biol.* **2012**, *8*, 536–546; b) B. A. Grzybowski, W. T. S. Huck, *Nat. Nanotechnol.* **2016**, *11*, 585–592; c) J. Nielsen, J. D. Keasling, *Cell* **2016**, *164*, 1185–1197; d) Z. P. Gerdtzen, P. Daoutidis, W. S. Hu, *Metab. Eng.* **2004**, *6*, 140–154; e) S. Zarra, D. M. Wood, D. A. Roberts, J. R. Nitschke, *Chem. Soc. Rev.* **2015**, *44*, 419–432.
- [7] a) G. Ashkenasy, T. M. Hermans, S. Otto, A. F. Taylor, *Chem. Soc. Rev.* **2017**, *46*, 2543–2554; b) P. van Duppen, E. Daines, W. E. Robinson, W. T. S. Huck, *J. Am. Chem. Soc.* **2023**, *145*, 7559–7568; c) A. Sharko, B. Spitzbarth, T. M. Hermans, R. Eelkema, *J. Am. Chem. Soc.* **2023**, *145*, 9672–9678; d) A. Wolos, R. Roszak, A. Żądło-Dobrowolska, W. Beker, B. Mikulak-Klucznik, G. Spólnik, M. Dygas, S. Szymkuć, B. A. Grzybowski, *Science* **2020**, *369*, eaaw1955; e) A. Galván, F. J. Fañanás, F. Rodríguez, *Eur. J. Inorg. Chem.* **2016**, *2016*, 1306–1313; f) C. M. R. Volla, I. Atodiressei, M. Rueping, *Chem. Rev.* **2014**, *114*, 2390–2431; g) R. C. Wende, P. R. Schreiner, *Green Chem.* **2012**, *14*, 1821–1849; h) J. Zhu, H. Bienaymé, *Multi-component reactions*, John Wiley & Sons, **2006**.
- [8] a) B. Helwig, B. van Sluijs, A. A. Pogodaev, S. G. J. Postma, W. T. S. Huck, *Angew. Chem. Int. Ed.* **2018**, *57*, 14065–14069; b) W. E. Robinson, E. Daines, P. van Duppen, T. de Jong, W. T. S. Huck, *Nat. Chem.* **2022**, *14*, 623–631; c) O. R. Maguire, W. T. S. Huck, *Emerg. Top. Life Sci.* **2019**, *3*, 517–527; d) H. Fanlo-Virgós, A.-N. R. Alba, S. Hamieh, M. Colomb-Delsuc, S. Otto, *Angew. Chem. Int. Ed.* **2014**, *53*, 11346–11350; e) S. G. J. Postma, I. N. Vialshin, C. Y. Gerritsen, M. Bao, W. T. S. Huck, *Angew. Chem. Int. Ed.* **2017**, *56*, 1794–1798.
- [9] For recent leading reviews on switchable catalysis and stimuli-responsive materials, see: a) S. Acosta-Calle, A. J. M. Miller, *Acc. Chem. Res.* **2023**, *56*, 971–981; b) M. J. Wiestner, P. A. Ulmann, C. A. Mirkin, *Angew. Chem. Int. Ed.* **2011**, *50*, 114–137; c) A. Ghorbani-Choghmarani, Z. Taherinia, *RSC Adv.* **2022**, *12*, 23595–23617; d) S. P. Ihrig, F. Eisenreich, S. Hecht, *Chem. Commun.* **2019**, *55*, 4290–4298; e) G. C. Thaggard, J. Haimerl, R. A. Fischer, K. C. Park, N. B. Shustova, *Angew. Chem. Int. Ed.* **2023**, *62*, e202302859; f) D. Lunic, E. Bergamaschi, C. J. Teskey, *Angew. Chem. Int. Ed.* **2021**, *133*, 20762–20773; g) J. Sheng, D. R. Pooler, B. L. Feringa, *Chem. Soc. Rev.* **2023**, *52*, 5875–5891; h) I. P. Beletskaya, C. Nájera, M. Yus, *Chem. Soc. Rev.* **2020**, *49*, 7101–7166; i) D. D. Díaz, D. Kühbeck, R. J. Koopmans, *Chem. Soc. Rev.* **2011**, *40*, 427–448; j) J. Wang, Z. Li, I. Willner, *Angew. Chem. Int. Ed.* **2023**, *135*, e202215332; k) E. Benchimol, B.-N. T. Nguyen, T. K. Ronson, J. R. Nitschke, *Chem. Soc. Rev.* **2022**, *51*, 5101–5135; l) C. Pezzato, C. Cheng, J. F. Stoddart, R. D. Astumian, *Chem. Soc. Rev.* **2017**, *46*, 5491–5507; m) C. D. Jones, J. W. Steed, *Chem. Soc. Rev.* **2016**, *45*, 6546–6596; n) R. Li, K. Landfester, C. T. Ferguson, *Angew. Chem. Int. Ed.* **2022**, *134*, e202211132; o) L. Zhang, H.-X. Wang, S. Li, M. Liu, *Chem. Soc. Rev.* **2020**, *49*, 9095–9120; p) G. Zhan, W. Du, Y.-C. Chen, *Chem. Soc. Rev.* **2017**, *46*, 1675–1692; q) A. C. Deacy, G. L. Gregory, G. S. Sulley, T. T. Chen, C. K. Williams, *J. Am. Chem. Soc.* **2021**, *143*, 10021–10040; r) V. Blanco, D. A. Leigh, V. Marcos, *Chem. Soc. Rev.* **2015**, *44*, 5341–5370.
- [10] a) H. Li, C. C. C. Johansson Seechurn, T. J. Colacot, *ACS Catal.* **2012**, *2*, 1147–1164; b) K. C. Nicolaou, P. G. Bulger, D. Sarlah, *Angew. Chem. Int. Ed.* **2005**, *44*, 4442–4489; c) T. K. Meister, K. Riener, P. Gigler, J. Stohrer, W. A. Herrmann, F. E. Kühn, *ACS Catal.* **2016**, *6*, 1274–1284; d) N. Kambe, T. Iwasaki, J. Terao, *Chem. Soc. Rev.* **2011**, *40*, 4937–4947; e) R. Chinchilla, C. Nájera, *Chem. Rev.* **2014**, *114*, 1783–1826; f) S. McCarthy, D. C. Braddock, J. D. E. T. Wilton-Ely, *Coord. Chem. Rev.* **2021**, *442*, 213925; g) X. Cui, K. Junge, X. Dai, C. Kreyenschulte, M.-M. Pohl, S. Wohlrab, F. Shi, A. Brückner, M. Beller, *ACS Cent. Sci.* **2017**, *3*, 580–585; h) L. D. de Almeida, H. Wang, K. Junge, X. Cui, M. Beller, *Angew. Chem. Int. Ed.* **2021**, *60*, 550–565.
- [11] R. Peters, *Cooperative Catalysis: Designing Efficient Catalysts for Synthesis* **2015**.
- [12] D. Giordano, D. Coppola, R. Russo, R. Denaro, L. Giuliano, F. M. Lauro, G. di Prisco, C. Verde, *Adv. Microb. Physiol.* **2015**, *66*, 357–428.
- [13] a) C. J. McMonagle, P. Comar, G. S. Nichol, D. R. Allan, J. González, J. A. Barreda-Argüeso, F. Rodríguez, R. Valiente, G. F. Turner, E. K. Brechin, S. A. Moggach, *Chem. Sci.* **2020**, *11*, 8793–8799; b) H.-B. Wu, Q.-M. Wang, *Angew. Chem. Int. Ed.* **2009**, *48*, 7343–7345; c) J. K. Clegg, F. Li, L. F. Lindoy, *Coord. Chem. Rev.* **2022**, *455*, 214355; d) G. Kurpik, A. Walczak, G. Markiewicz, J. Harrowfield, A. R. Stefankiewicz, *Nanoscale* **2023**, *15*, 9543–9550; e) A. Walczak, G. Kurpik, A. R. Stefankiewicz, *Int. J. Mol. Sci.* **2020**, *21*.
- [14] a) A. Walczak, H. Stachowiak, G. Kurpik, J. Kaźmierczak, G. Hreczycho, A. R. Stefankiewicz, *J. Catal.* **2019**, *373*, 139–146; b) Y. Li, Z. Gu, C. Zhang, S. Li, L. Zhang, G. Zhou, S. Wang, J. Zhang, *Eur. J. Med. Chem.* **2018**, *144*, 662–671.
- [15] a) A. Walczak, A. R. Stefankiewicz, *Inorg. Chem.* **2018**, *57*, 471–477; b) A. Walczak, G. Kurpik, M. Zaranek, P. Pawluć, A. R. Stefankiewicz, *J. Catal.* **2022**, *405*, 84–90; c) G. Kurpik, A. Walczak, M. Goldyn, J. Harrowfield, A. R. Stefankiewicz, *Inorg. Chem.* **2022**, *61*, 14019–14029; d) R. Chinchilla, C. Nájera, *Chem. Soc. Rev.* **2011**, *40*, 5084–5121; e) H. Doucet, J. C. Hierso, *Angew. Chem. Int. Ed.* **2007**, *46*, 834–871; f) M. Ashraf, M. S. Ahmad, Y. Inomata, N. Ullah, M. N. Tahir, T. Kida, *Coord. Chem. Rev.* **2023**, *476*, 214928; g) D. Mc Cartney, P. J. Guiry, *Chem. Soc. Rev.* **2011**, *40*, 5122–5150; h) M. Shimizu, T. Hiyama, *Angew. Chem. Int. Ed.* **2005**, *44*, 214–231.
- [16] a) G. Kurpik, A. Walczak, I. Łukasik, Z. Matela, A. R. Stefankiewicz, *ChemCatChem* **2024**, *16*, e202301465; b) C. Cheng, J. F. Hartwig, *Chem. Rev.* **2015**, *115*, 8946–8975; c) S. Liu, G. S. Girolami, *J. Am. Chem. Soc.* **2021**, *143*, 17492–17509; d) G. Pan, C. Hu, S. Hong, H. Li, D. Yu, C. Cui, Q. Li, N. Liang, Y. Jiang, L. Zheng, *Nat. Commun.* **2021**, *12*, 64; e) J. V. Obligacion, P. J. Chirik, *Nat. Rev. Chem.* **2018**, *2*, 15–34.
- [17] a) C. E. Garrett, K. Prasad, *Adv. Synth. Catal.* **2004**, *346*, 889–900; b) B. Li, P. H. Dixneuf, *Chem. Soc. Rev.* **2021**, *50*, 5062–5085; c) S. Cacchi, G. Fabrizi, *Chem. Rev.* **2005**, *105*, 2873–2920.
- [18] a) Y. Duan, G. Ji, S. Zhang, X. Chen, Y. Yang, *Catal. Sci. Technol.* **2018**, *8*, 1039–1050; b) M. Planellas, W. Guo, F. Alonso, M. Yus, A. Shafir, R. Pleixats, T. Parella, *Adv. Synth. Catal.* **2014**, *356*, 179–188; c) N. Iranpoor, H. Firouzabadi, R. Azadi, *J. Organomet. Chem.* **2010**, *695*, 887–890; d) A. Hamze, O. Provot, M. Alami, J.-D. Brion, *Org. Lett.* **2006**, *8*, 931–934; e) F. Luo, C. Pan, W. Wang, Z. Ye, J. Cheng, *Tetrahedron* **2010**, *66*, 1399–1403; f) L. A. Aronica, F. Morini, A. M. Caporusso, P. Salvadori, *Tetrahedron Lett.* **2002**, *43*, 5813–5815.
- [19] a) A. A. Pogodaev, C. L. Fernández Regueiro, M. Jakštaitė, M. J. Hollander, W. T. S. Huck, *Angew. Chem. Int. Ed.* **2019**, *58*, 14539–14543; b) N. Singh, G. J. M. Formon, S. De Piccoli, T. M. Hermans, *Adv. Mater.* **2020**, *32*, 1906834; c) M. Teders, A. A. Pogodaev, G. Bojanov, W. T. S. Huck, *J. Am. Chem. Soc.* **2021**, *143*, 5709–5716; d) B. A. Grzybowski, K. Fitzner, J. Paczesny, S. Granick, *Chem. Soc. Rev.* **2017**, *46*, 5647–5678.
- [20] Typically, isomer *E* is dominant under the photostationary state. However, the photostationary state can be impacted by various components of the reaction mixture, such as solvent, catalyst, by-products, or residual reagents; see: a) D. Schulte-Frohlinde, H. Blume, H. Güsten, *J. Phys. Chem.* **1962**, *66*, 2486–2491; b) J. M. Rodier, A. B. Myers, *J. Am. Chem. Soc.*

- 1993, 115, 10791–10795; c) H. Görner, H. J. Kuhn, *Advances in photochemistry* **1994**, 19, 1–117.
- [21] a) G. Kurpik, A. Walczak, M. Gilski, J. Harrowfield, A. R. Stefankiewicz, *J. Catal.* **2022**, 411, 193–199; b) *Rigaku Oxford Diffraction*, (2022), *CrysAlisPro Software system, version 1.171.42.85a*, Rigaku Corporation, Wroclaw, Poland; c) G. M. Sheldrick, *Acta Crystallogr. A: Found. Adv.* **2015**, 71, 3–8; d) G. M. Sheldrick, *Acta Crystallogr. C Struct. Chem.* **2015**, 71, 3–8; e) O. V. Dolomanov, L. J. Bourhis, R. J. Gildea, J. A. Howard, H. Puschmann, *J. Appl. Crystallogr.* **2009**, 42, 339–341.
- [22] Deposition number 2332008 contains the supplementary crystallographic data for this paper. These data are provided free of charge by the joint Cambridge Crystallographic Data Centre and Fachinformationszentrum Karlsruhe Access Structures service.

Manuscript received: March 7, 2024

Accepted manuscript online: June 15, 2024

Version of record online: August 1, 2024

Declaration letters of co-authors

M.Sc. Gracjan Kurpik
Laboratory of Functional Nanostructures
Center for Advanced Technologies
Adam Mickiewicz University in Poznań
e-mail: gracjan.kurpik@amu.edu.pl

Poznań, 20/09/2024

DECLARATION

I hereby declare that in the following publications:

- [A1] G. Kurpik, A. Walczak, M. Gilski, J. Harrowfield, A. R. Stefankiewicz
Effect of the nuclearity on the catalytic performance of a series of Pd^{II} complexes in the Suzuki-Miyaura reaction
Journal of Catalysis **2022**, *411*, 193–199; DOI: 10.1016/j.jcat.2022.05.021
- [A2] G. Kurpik, A. Walczak, M. Goldyn, J. Harrowfield, A. R. Stefankiewicz
Pd^{II} complexes with pyridine ligands: substituent effects on the NMR Data, crystal structures, and catalytic activity
Inorganic Chemistry **2022**, *61*, 14019–14029; DOI: 10.1021/acs.inorgchem.2c01996
- [A3] G. Kurpik, A. Walczak, G. Markiewicz, J. Harrowfield, A. R. Stefankiewicz
Enhanced catalytic performance derived from coordination-driven structural switching between homometallic complexes and heterometallic polymeric materials
Nanoscale **2023**, *15*, 9543–9550; DOI: 10.1039/D3NR01298K
- [A4] A. Walczak, G. Kurpik, M. Zaranek, P. Pawluć, A. R. Stefankiewicz
C(sp³),N palladacyclic complexes bearing flexidentate ligands as efficient (pre)catalysts for Heck olefination of aryl halides
Journal of Catalysis **2022**, *405*, 84–90; DOI: 10.1016/j.jcat.2021.11.033
- [A5] G. Kurpik, A. Walczak, I. Łukasik, Z. Matela, A. R. Stefankiewicz
Crafting versatile modes of Pt^{II} complexes with flexidentate pyridyl-β-diketones: synthesis, structural characterization, and catalytic behavior in olefin hydrosilylation
ChemCatChem **2024**, *16*, e202301465; DOI: 10.1002/cctc.202301465
- [A6] G. Kurpik, A. Walczak, P. Dydio, A. R. Stefankiewicz
Multi-stimuli-responsive network of multicatalytic reactions using a single palladium/platinum catalyst
Angewandte Chemie International Edition **2024**, *63*, e202404684; DOI: 10.1002/anie.202404684

my substantive contributions as a co-author include:

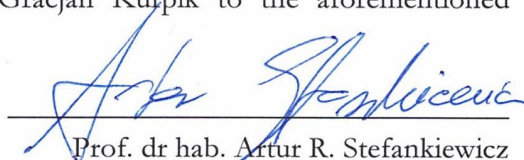
- in [A1]:
 - synthesis of the ligands and complexes **C1–C4**;
 - characterization of the complexes using NMR spectroscopy and mass spectrometry;
 - crystal growth for diffraction measurements;
 - design and preparation of acid-base titration experiments;
 - performance of all catalytic experiments, including the optimization of reaction conditions, investigation of the scope and limitations of the catalytic system, study of the nuclearity effect, purification and characterization of reaction products;

- co-creation of the study concept;
- co-interpretation of experimental data and discussion of the research results;
- preparation of supplementary materials for the manuscript;
- creation of all figures and schemes included in the manuscript and supplementary materials;
- co-authoring of the manuscript text;
- in [A2]:
 - synthesis of the ligands and all Pd^{II} complexes;
 - characterization of the complexes using NMR spectroscopy and mass spectrometry;
 - crystal growth for diffraction measurements;
 - design and preparation of titration experiments (switching between different forms of complexes);
 - performance of all catalytic experiments, including the optimization of reaction conditions, investigation of the scope and limitations of the catalytic system, comparative experiments between catalysts, purification and characterization of reaction products;
 - co-creation of the study concept;
 - co-interpretation of experimental data and discussion of the research results;
 - preparation of supplementary materials for the manuscript;
 - creation of all figures and schemes included in the manuscript and supplementary materials;
 - co-authoring of the manuscript text;
- in [A3]:
 - synthesis of the ligand and all coordination compounds;
 - characterization of the complexes using NMR spectroscopy and mass spectrometry;
 - obtaining crystals of the Ag^I complex for diffraction measurements;
 - development of the strategies for coordination-driven structural switching;
 - design and preparation of ¹H NMR titration experiments;
 - characterization of the heterometallic polymers using different analytical techniques;
 - performance of all catalytic experiments, including the optimization of reaction conditions, investigation of the scope and limitations of the catalytic system, comparison of different catalytic systems, purification and characterization of reaction products;
 - co-creation of the study concept;
 - co-interpretation of experimental data and discussion of the research results;
 - preparation of supplementary materials for the manuscript;
 - creation of all figures and schemes included in the manuscript and supplementary materials;
 - co-authoring of the manuscript text;
- in [A4]:
 - resynthesis of the complexes *cis*- and *trans*-[PdL₂];
 - characterization of the complexes *via* NMR spectroscopy;
 - co-interpretation of experimental data and discussion of the research results;

- preparation of supplementary materials for the manuscript;
- co-creation of figures and schemes for the manuscript and supplementary materials;
- co-authoring of the manuscript text;
- in [A5]:
 - synthesis of the ligands and Pt^{II} complexes;
 - characterization of the complexes using NMR spectroscopy and mass spectrometry;
 - crystal growth for diffraction measurements;
 - performance of all catalytic experiments, including the optimization of reaction conditions, investigation of the scope and limitations of the catalytic system, comparative experiments between catalysts, purification and characterization of reaction products;
 - creation of the study concept;
 - co-interpretation of experimental data and discussion of the research results;
 - preparation of supplementary materials for the manuscript;
 - creation of all figures and schemes included in the manuscript and supplementary materials;
 - co-authoring of the manuscript text;
- in [A6]:
 - synthesis of the ligands, mononuclear building blocks C^{Pt} and C^{Pd}, and heterometallic complexes C1–C4;
 - characterization of the complexes using NMR spectroscopy and mass spectrometry;
 - obtaining crystals of the complex C^{Pd} for diffraction measurements;
 - modelling of the structure of C1;
 - optimization of reaction conditions for all catalytic transformations;
 - identification of the physical and chemical triggers T1–T9;
 - development of various synthetic pathways within branches I-III;
 - purification and characterization of the reaction products P1–P10;
 - investigation of kinetic hierarchy and pathway orthogonality in the network;
 - study of the influence of catalyst heteronuclearity on multicatalytic performance;
 - co-interpretation of experimental data and discussion of the research results;
 - preparation of supplementary materials for the manuscript;
 - creation of all figures and schemes included in the manuscript and supplementary materials;
 - co-authoring of the manuscript text.


M.Sc. Gracjan Kurpik

I hereby certify the contribution of M.Sc. Gracjan Kurpik to the aforementioned publications, as described above.


Prof. dr hab. Artur R. Stefankiewicz

Prof. dr hab. Artur R. Stefankiewicz
Laboratory of Functional Nanostructures
Center for Advanced Technologies
Adam Mickiewicz University in Poznań
e-mail: ars@amu.edu.pl

Poznań, 20/09/2024

DECLARATION

I hereby declare that in the following publications:

- [A1] G. Kurpik, A. Walczak, M. Gilski, J. Harrowfield, A. R. Stefankiewicz
Effect of the nuclearity on the catalytic performance of a series of Pd^{II} complexes in the Suzuki-Miyaura reaction
Journal of Catalysis **2022**, *411*, 193–199; DOI: 10.1016/j.jcat.2022.05.021
- [A2] G. Kurpik, A. Walczak, M. Gołdyn, J. Harrowfield, A. R. Stefankiewicz
Pd^{II} complexes with pyridine ligands: substituent effects on the NMR Data, crystal structures, and catalytic activity
Inorganic Chemistry **2022**, *61*, 14019–14029; DOI: 10.1021/acs.inorgchem.2c01996
- [A3] G. Kurpik, A. Walczak, G. Markiewicz, J. Harrowfield, A. R. Stefankiewicz
Enhanced catalytic performance derived from coordination-driven structural switching between homometallic complexes and heterometallic polymeric materials
Nanoscale **2023**, *15*, 9543–9550; DOI: 10.1039/D3NR01298K
- [A4] A. Walczak, G. Kurpik, M. Zaranek, P. Pawluć, A. R. Stefankiewicz
C(sp³),N palladacyclic complexes bearing flexidentate ligands as efficient (pre)catalysts for Heck olefination of aryl halides
Journal of Catalysis **2022**, *405*, 84–90; DOI: 10.1016/j.jcat.2021.11.033
- [A5] G. Kurpik, A. Walczak, I. Łukasik, Z. Matela, A. R. Stefankiewicz
Crafting versatile modes of Pt^{II} complexes with flexidentate pyridyl-β-diketones: synthesis, structural characterization, and catalytic behavior in olefin hydrosilylation
ChemCatChem **2024**, *16*, e202301465; DOI: 10.1002/cctc.202301465
- [A6] G. Kurpik, A. Walczak, P. Dydio, A. R. Stefankiewicz
Multi-stimuli-responsive network of multicatalytic reactions using a single palladium/platinum catalyst
Angewandte Chemie International Edition **2024**, *63*, e202404684; DOI: 10.1002/anie.202404684

my substantive contributions as a co-author include:

- conceptualization, organization, and management of the work;
- co-interpretation of experimental data and discussion of the research results;
- co-authoring of the manuscript text;
- correspondence with editors and referees.



Prof. dr hab. Artur R. Stefankiewicz

Dr. Anna Walczak
Laboratory of Functional Nanostructures
Center for Advanced Technologies
Adam Mickiewicz University in Poznań
e-mail: aj69161@amu.edu.pl

Poznań, 19/09/2024

DECLARATION

I hereby declare that in the following publications:

- [A1]** G. Kurpik, A. Walczak, M. Gilski, J. Harrowfield, A. R. Stefankiewicz
Effect of the nuclearity on the catalytic performance of a series of Pd^{II} complexes in the Suzuki-Miyaura reaction
Journal of Catalysis **2022**, *411*, 193–199; DOI: 10.1016/j.jcat.2022.05.021
- [A2]** G. Kurpik, A. Walczak, M. Gołdyn, J. Harrowfield, A. R. Stefankiewicz
Pd^{II} complexes with pyridine ligands: substituent effects on the NMR Data, crystal structures, and catalytic activity
Inorganic Chemistry **2022**, *61*, 14019–14029; DOI: 10.1021/acs.inorgchem.2c01996
- [A3]** G. Kurpik, A. Walczak, G. Markiewicz, J. Harrowfield, A. R. Stefankiewicz
Enhanced catalytic performance derived from coordination-driven structural switching between homometallic complexes and heterometallic polymeric materials
Nanoscale **2023**, *15*, 9543–9550; DOI: 10.1039/D3NR01298K
- [A4]** A. Walczak, G. Kurpik, M. Zaranek, P. Pawluć, A. R. Stefankiewicz
C(sp³),N palladacyclic complexes bearing flexidentate ligands as efficient (pre)catalysts for Heck olefination of aryl halides
Journal of Catalysis **2022**, *405*, 84–90; DOI: 10.1016/j.jcat.2021.11.033
- [A5]** G. Kurpik, A. Walczak, I. Łukasik, Z. Matela, A. R. Stefankiewicz
Crafting versatile modes of Pt^{II} complexes with flexidentate pyridyl-β-diketones: synthesis, structural characterization, and catalytic behavior in olefin hydrosilylation
ChemCatChem **2024**, *16*, e202301465; DOI: 10.1002/cctc.202301465
- [A6]** G. Kurpik, A. Walczak, P. Dydio, A. R. Stefankiewicz
Multi-stimuli-responsive network of multicatalytic reactions using a single palladium/platinum catalyst
Angewandte Chemie International Edition **2024**, *63*, e202404684; DOI: 10.1002/anie.202404684

my substantive contributions as a co-author include:

- in **[A1]**:
 - XRD measurements, including the establishment and description of the structure of **C1**;
 - co-development of initial research concepts;
 - co-interpretation of experimental data and discussion of the research results;
 - co-authoring of the manuscript text;

- in [A2]:
 - co-development of initial research concepts;
 - development of the synthetic strategies for the tetrasubstituted Pd^{II} complexes;
 - co-interpretation of experimental data and discussion of the research results;
 - co-authoring of the manuscript text;
- in [A3]:
 - XRD measurements, including the establishment and description of the structure of **C1**;
 - co-development of initial research concepts;
 - co-interpretation of experimental data and discussion of the research results;
- in [A4]:
 - synthesis of the complexes *cis*- and *trans*-[PdL₂];
 - XRD measurements, including the establishment and description of the structures of Pd^{II} complexes;
 - characterization of the complexes *via* NMR spectroscopy and ESI-MS spectrometry;
 - co-creation of initial research concepts;
 - co-interpretation of experimental data and discussion of the research results;
 - creation of figures and schemes included in the manuscript;
 - preparation of the first draft of the manuscript and subsequent revisions;
- in [A5]:
 - crystal growth for diffraction measurements;
 - XRD measurements, including the establishment and description of the structure of the organometallic Pt^{II} complex;
 - co-interpretation of experimental data and discussion of the research results;
- in [A6]:
 - development of the synthetic strategies for the complexes **C1–C4**;
 - co-development of initial research concepts;
 - co-interpretation of experimental data and discussion of the research results.



Dr. Anna Walczak

Prof. Jack M. Harrowfield
Institut de Science et d'Ingénierie Supramoléculaires
Université de Strasbourg
8 allée Gaspard Monge, 67083 Strasbourg
e-mail: harrowfield@unistra.fr

Strasbourg, 25/09/2024

DECLARATION

I hereby declare that in the following publications:

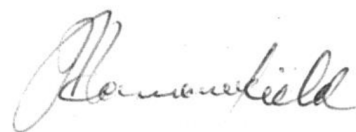
[A1] G. Kurpik, A. Walczak, M. Gilski, J. Harrowfield, A. R. Stefankiewicz
Effect of the nuclearity on the catalytic performance of a series of Pd^{II} complexes in the Suzuki-Miyaura reaction
Journal of Catalysis **2022**, *411*, 193–199; DOI: 10.1016/j.jcat.2022.05.021

[A2] G. Kurpik, A. Walczak, M. Goldyn, J. Harrowfield, A. R. Stefankiewicz
Pd^{II} complexes with pyridine ligands: substituent effects on the NMR Data, crystal structures, and catalytic activity
Inorganic Chemistry **2022**, *61*, 14019–14029; DOI: 10.1021/acs.inorgchem.2c01996

[A3] G. Kurpik, A. Walczak, G. Markiewicz, J. Harrowfield, A. R. Stefankiewicz
Enhanced catalytic performance derived from coordination-driven structural switching between homometallic complexes and heterometallic polymeric materials
Nanoscale **2023**, *15*, 9543–9550; DOI: 10.1039/D3NR01298K

my substantive contributions as a co-author include:

- assistance in the analysis of crystallographic data;
- co-interpretation of experimental data and discussion of the research results;
- assistance in the preparation of the final text.



Prof. Jack M. Harrowfield

Prof. UAM dr hab. Mirosław Gilski
Department of Crystallography
Faculty of Chemistry
Adam Mickiewicz University in Poznań
e-mail: mirek@amu.edu.pl

Poznań, 19/09/2024

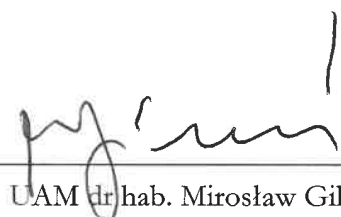
DECLARATION

I hereby declare that in the following publication:

[A1] G. Kurpik, A. Walczak, M. Gilski, J. Harrowfield, A. R. Stefankiewicz
Effect of the nuclearity on the catalytic performance of a series of Pd^{II} complexes in the Suzuki-Miyaura reaction
Journal of Catalysis **2022**, *411*, 193–199; DOI: 10.1016/j.jcat.2022.05.021

my substantive contributions as a co-author include:

- XRD measurements for the complexes **C3** and **C4**;
- establishment and description of the complex structures.



Prof. UAM dr hab. Mirosław Gilski

Dr. Mateusz Gołdyn
Laboratory of Functional Nanostructures
Center for Advanced Technologies
Adam Mickiewicz University in Poznań
e-mail: mateusz.goldyn@amu.edu.pl

Poznań, 20/09/2024

DECLARATION

I hereby declare that in the following publication:

[A2] G. Kurpik, A. Walczak, M. Gołdyn, J. Harrowfield, A. R. Stefankiewicz
Pd^{II} complexes with pyridine ligands: substituent effects on the NMR Data, crystal structures, and catalytic activity
Inorganic Chemistry **2022**, *61*, 14019–14029; DOI: 10.1021/acs.inorgchem.2c01996

my substantive contributions as a co-author include:

- XRD measurements of all crystals;
- establishment and description of the structures of the Pd^{II} complexes;
- analysis of crystallographic data.


Dr. Mateusz Gołdyn

Dr. Grzegorz Markiewicz
Laboratory of Functional Nanostructures
Center for Advanced Technologies
Adam Mickiewicz University in Poznań
e-mail: grzegorz.markiewicz@amu.edu.pl

Poznań, 20/09/2024

DECLARATION

I hereby declare that in the following publication:

[A3] G. Kurpik, A. Walczak, G. Markiewicz, J. Harrowfield, A. R. Stefankiewicz
Enhanced catalytic performance derived from coordination-driven structural switching between homometallic complexes and heterometallic polymeric materials
Nanoscale **2023**, 15, 9543–9550; DOI: 10.1039/D3NR01298K

my substantive contributions as a co-author include:

- performance of ^1H NMR titration experiments;
- design of FT-IR experiments;
- co-interpretation of experimental data and discussion of the research results;
- proofreading of the manuscript text.



Dr. Grzegorz Markiewicz

Dr. Maciej Zaranek
Laboratory of Organometallic Catalysis
Center for Advanced Technologies
Adam Mickiewicz University in Poznań
e-mail: m.zaranek@amu.edu.pl

Poznań, 19/09/2024

DECLARATION

I hereby declare that in the following publication:

[A4] A. Walczak, G. Kurpik, M. Zaranek, P. Pawluć, A. R. Stefankiewicz
C(sp³),N palladacyclic complexes bearing flexidentate ligands as efficient (pre)catalysts for Heck olefination of aryl halides
Journal of Catalysis **2022**, *405*, 84–90; DOI: 10.1016/j.jcat.2021.11.033

my substantive contribution as a co-author includes:

- performance of all catalytic experiments, including the optimization of reaction conditions, investigation of the scope and limitations of the catalytic system, characterization of reaction products;
- co-interpretation of experimental data and discussion of the research results;
- co-authoring of the manuscript text.



Dr. Maciej Zaranek

Prof. dr hab. Piotr Pawluć
Laboratory of Organometallic Catalysis
Faculty of Chemistry, Center for Advanced Technologies
Adam Mickiewicz University in Poznań
e-mail: piotrpaw@amu.edu.pl

Poznań, 20/09/2024

DECLARATION

I hereby declare that in the following publication:

[A4] A. Walczak, G. Kurpiak, M. Zaranek, P. Pawluć, A. R. Stefankiewicz
C(sp³),N palladacyclic complexes bearing flexidentate ligands as efficient (pre)catalysts for Heck olefination of aryl halides
Journal of Catalysis **2022**, 405, 84–90; DOI: 10.1016/j.jcat.2021.11.033

my substantive contributions as a co-author include:

- conceptualization, organization, and management of the work;
- co-interpretation of experimental data and discussion of the research results;
- co-authoring of the manuscript text.



Prof. dr hab. Piotr Pawluć

B.Sc. Igor Łukasik
Laboratory of Functional Nanostructures
Faculty of Chemistry
Adam Mickiewicz University in Poznań
e-mail: igoluk@st.amu.edu.pl

Montpellier, 19/09/2024

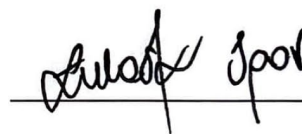
DECLARATION

I hereby declare that in the following publication:

[A5] G. Kurpiak, A. Walczak, I. Łukasik, Z. Matela, A. R. Stefankiewicz
Crafting versatile modes of Pt^{II} complexes with flexidentate pyridyl- β -diketones: synthesis, structural characterization, and catalytic behavior in olefin hydrosilylation
ChemCatChem **2024**, *16*, e202301465; DOI: 10.1002/cctc.202301465

my substantive contributions as a co-author include:

- resynthesis of Pt^{II} complexes;
- participation in catalytic studies.



Igor Łukasik

B.Sc. Zuzanna Matela
Laboratory of Functional Nanostructures
Faculty of Chemistry
Adam Mickiewicz University in Poznań
e-mail: zuzmat16@st.amu.edu.pl

Montpellier, 19/09/2024

DECLARATION

I hereby declare that in the following publication:

[A5] G. Kurpiak, A. Walczak, I. Łukasik, Z. Matela, A. R. Stefankiewicz
Crafting versatile modes of Pt^{II} complexes with flexidentate pyridyl-β-diketones: synthesis, structural characterization, and catalytic behavior in olefin hydrosilylation
ChemCatChem **2024**, 16, e202301465; DOI: 10.1002/cctc.202301465

my substantive contributions as a co-author include:

- resynthesis of Pt^{II} complexes;
- participation in catalytic studies.



Zuzanna Matela

Dr. Pawel Dydio
Yusuf Hamied Department of Chemistry
University of Cambridge
e-mail: pd552@cam.ac.uk

Cambridge, 19/09/2024

DECLARATION

I hereby declare that in the following publication:

[A6] G. Kurpik, A. Walczak, P. Dydio, A. R. Stefankiewicz
Multi-stimuli-responsive network of multicatalytic reactions using a single palladium/platinum catalyst
Angewandte Chemie International Edition **2024**, *63*, e202404684; DOI: 10.1002/anie.202404684

my substantive contributions as a co-author include:

- conceptualization, organization, and management of the work;
- co-interpretation of experimental data and discussion of the research results;
- co-authoring of the manuscript text;
- correspondence with the editor and referees.



Dr. Pawel Dydio